Superconvergence and Error Estimation of Finite Element Solutions to Fire-exposed Frame Problems

A thesis submitted for the degree of Doctor of Philosophy

by

James Alexander Kirby

Department of Mathematical Sciences, Brunel University

October 2000

Abstract

When a fire reaches the point of flashover the hot gases inside the burning room ignite resulting in furnace-like conditions. Thereafter, the building frame experiences temperatures sufficient to compromise its structural integrity. Physical and mathematical models help to predict when this will happen. This thesis looks at both the thermal and structural aspects of modelling a frame exposed to a post-flashover fire.

The temperatures in the frame are calculated by solving a 2D heat conduction equation over the cross-section of each beam. The solution procedure uses the finite element method with automatic mesh generation/adaption based on the Delaunay triangulation process and the recovered heat flux.

With the Euler-Bernoulli assumption that the cross-section of a beam remains plane and perpendicular to the neutral line and that strains are small, an error estimator, based on the work of Bank and Weiser [9], has been derived for finite element solutions to small-deformation, thermoelastic and thermoplastic frame problems. The estimator has been shown to be consistent for all finite element solutions and asymptotically exact when the solution involves appropriate higher degree polynomials. The asymptotic exactness is shown to be closely related to superconvergence properties of the approximate solution in these cases. Specifically, with coupled bending and compression, it is necessary to use quadratic approximations, instead of linear, for the compression and twisting terms to get a global $O(h^2)$ rate of convergence in the energy norm, some superconvergence properties and asymptotic exactness with the error estimator.

Acknowledgements

Completing this thesis has been far from a solo effort and so I take the opportunity here to express my gratitude to all at Brunel University who helped me along the way. In particular, I wish to thank my supervisors, Professor J. R. Whiteman and Dr. M. Warby for their guidance and hard work.

I would also like to thank the Building Research Establishment, particularly Tony Morris and Ray Connolly. My work with them was the motivation for the subject of this thesis.

Finally, on a personal note, I give a special thankyou to my parents, Jean and John, my brother, Andrew, and my girlfriend, Sue, for all their support and encouragement. My mother sadly passed away during my time spent on this work and I dedicate this thesis to her.

Contents

Chapter 1

Introduction

When a building is designed it must meet safety requirements that include provisions for fire protection. Although the building as a whole is considered the requirements apply to individual structural elements. The assumption is that if the individual elements are satisfactory then the whole building should perform at least as well [22].

The ultimate method of determining the performance of a structural element is the laboratory fire test as laid out in BS476 [1] and ISO834 [3]. Such testing is expensive and time consuming. The designer must be pretty sure that the structure will pass the test to avoid the repeated costs. Hence the need for physical and mathematical models that can help to predict the outcome. Furthermore, assemblies of structural elements may be modelled that would be just too impractical to test in the laboratory. As computer power increases the structures that can be modelled become more complex. The ultimate goal must be an 'all singing all dancing' computer program that simulates every aspect of a building's response to a real fire. This is not yet practical and we still rely on many mathematical idealogies that simplify the structural problem.

Always at the forefront of computational modelling has been the finite element method with its flexibility to cope with complex geometries and ease of application to any system of partial differential equations. Historically, engineers have led the way in finite elements, applying the method to a wide variety of thermal and structural problems. Meanwhile mathematicians have analysed the performance of the method and, more importantly, how to improve the results it provides. Chapter 3 of this thesis describes the finite element method and introduces some standard techniques in error analysis and error estimation.

The most important structural aspect of a building is its frame. The performance of the frame under the influence of fire exposure will dictate that of the building. The first simplification of the overall structural problem is to model the building structurally as its skeletal frame loaded with the weight of the walls and floors within. The frame is then modelled as an assembly of one-dimensional structures known as beams. The behaviour of each beam is governed by its cross-sectional properties, both geometric and physical (i.e. temperature and stiffness). It is this frame problem that is the focus of this thesis. The mathematical background was largely covered by Timoshenko [34] in

1934 although practical applications were limited until the development of the computer later in the 20th century. Since then authors like Berg and Da Deppo [10], Nigam [24] and Toridis and Khozeimeh [35] have pioneered the work in computational frame analysis. The paper by Toridis and Khozeimeh in 1971 [35] outlines a general finite element method for the elastic and plastic analysis of rigid frames under both static and dynamic loading. More recently, authors such as Terro [33] and Wang [37] have applied the finite element method to fire-exposed frame models. While the models have become quite sophisticated, allowing for large deformation and very realistic material models, these finite element solution procedures have not benefited from modern mathematical developments.

Essentially, the finite element method performs calculations on a discretization of the domain, called a mesh, which, for two-dimensional domains, is a tessellation of polygons, called elements. The method derives a piecewise polynomial that is continuous across the element sides and approximates the solution to the partial differential equations such that

$$\|e\| \leq Ch^p$$

where $\|e\|$ is a measure of the error in the energy norm, h is a measure of the element size, p is the order of the polynomial and C is a constant, independent of h but inversely proportional to the smallest element angle [44]. Since the error depends on h, a way of reducing the error is to reduce the size of the elements. As to where the mesh needs smaller elements, users of the finite element method have developed error indicators. These are numbers that are computable from the finite element solution and approximate $\|e\|$ or some other measure of the error such that, globally,

$$C_1 \|e\| \leq \eta \leq C_2 \|e\|$$

where η is the error indicator and C_1 and C_2 are constants. The calculation of η is performed on an element by element basis in such a way that

$$\eta^2 = \sum_{i=1}^{n} \eta_i^2$$

where n is the number of elements. In this relation the η_i's represent each element's contribution to the global error and are used to determine elements that need refining. A well known error indicator uses the method of gradient averaging. It compares the gradient of the finite element solution with that of a smoother function obtained by interpolating the average gradient at the nodes [20]. This smoother gradient function is an example of a recovered gradient. An error indicator using an alternative recovered gradient method is that of Zienkiewicz and Zhu [43]. Other error indicators have been developed based on the difference between the applied forces and those calculated from the finite element solution; see, for example, Babuska and Rheinboldt [8] and Bank and Weiser [9].

The aim of this thesis is to apply some of the recent developments in finite element error analysis to fire-exposed frame problems. There are two parts to this class of problem, thermal and structural, both of which are covered. The thermal problem is to calculate the temperature distribution throughout the frame structure. A typical simplification is

to assume that the temperatures are constant in the axial direction of each beam so that the temperature distribution is two-dimensional; i.e. across the beam cross-section. Hence, the thermal part is the solution of a 2D heat conduction problem for each beam in the frame. The finite element method performs heat conduction calculations on a mesh of triangular elements as illustrated in Figure 1.1. Reducing the size of the elements, while not allowing interior angles to become too small, reduces the error in the solution. Error indicators are used to identify elements that need refining. The refinement method adopted places new nodes along the element edges ensuring that the refined mesh is a Delaunay triangulation of the nodes. This is described in detail in Chapter 4 of this thesis. The structural problem is to calculate the deformation of the frame due to applied mechanical loads and thermal loads caused by the increase in temperature. The finite element method performs calculations on a mesh of one-dimensional elements. Again, error indicators are used to identify elements in the mesh that need refinement.

Structural modelling is introduced in Chapter 5. The stress and strain tensors are defined and equilibrium equations are derived for an elastic material from their integral forms. Chapter 6 describes the thermal effects and derives the heat conduction equation. Beam theory, that is used to simplify the structural frame problem, is introduced in Chapter 7 for thermoelastic frame problems. Equilibrium equations, based on Euler-Bernoulli assumptions, are derived from the integral equilibrium equations. A finite element method is derived which is shown to be superconvergent at the connecting nodes, and at mid-points in some cases, for sufficiently high order of polynomial approximation. Error estimates are obtained for the finite element frame and a Bank-Weiser type error estimator is analysed. This estimator is shown to be asymptotically exact for the superconvergent case. This work is extended in Chapter 8 for application to thermoplastic frames.

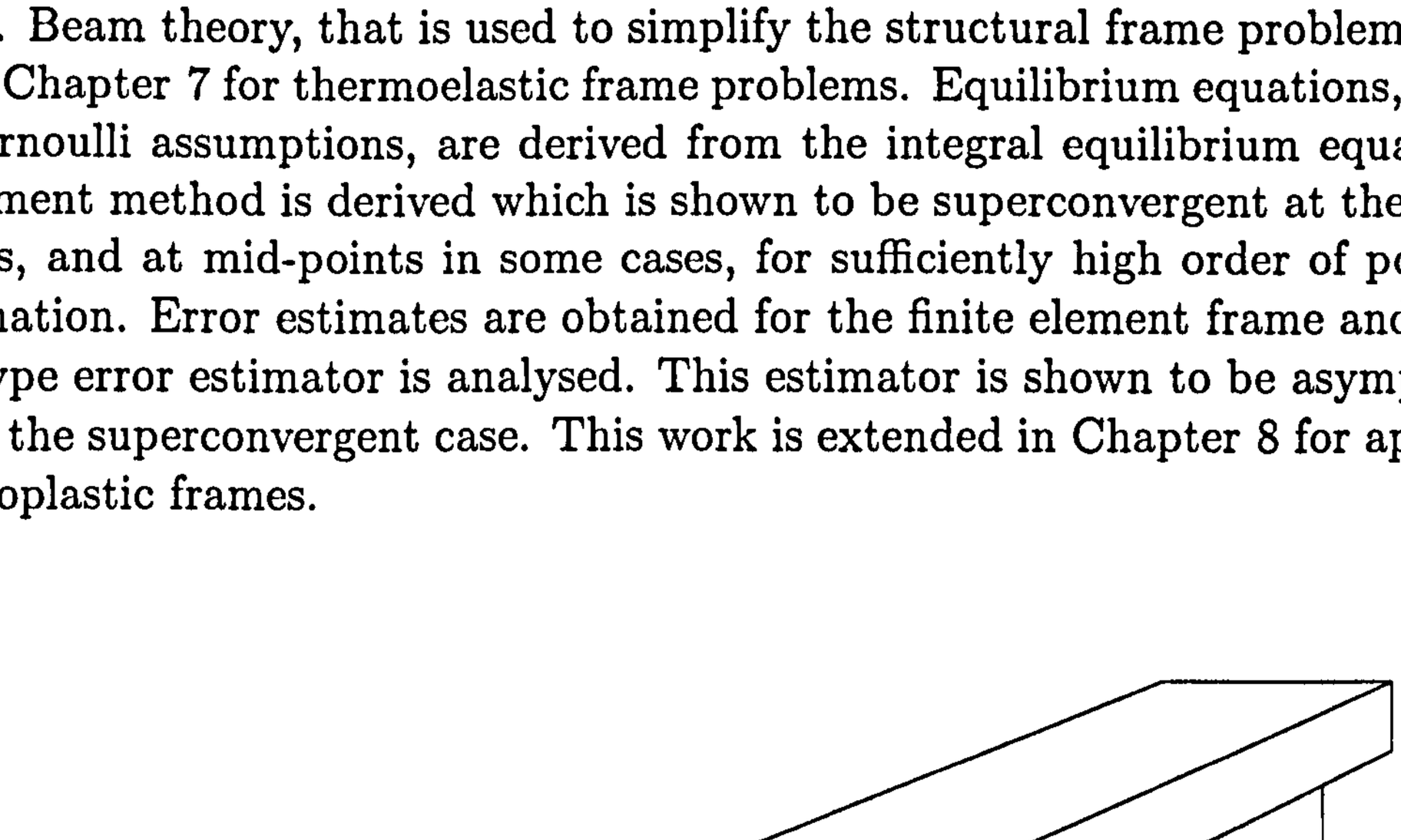

Figure 1.1 : Typical beam showing the discretized cross-section.

Chapter 2

Mathematical Preliminaries

2.1 Notation

2.1.1 Vectors, matrices and tensors

Vectors and matrices are printed in bold. Their components are printed in normal style with subscripts denoting the indices. For example,

$$\boldsymbol{A} = \begin{pmatrix} A_{11} & A_{12} & A_{13} \\ A_{21} & A_{22} & A_{23} \\ A_{31} & A_{32} & A_{33} \end{pmatrix}.$$

Unless otherwise stated matrices are denoted by capitals and vectors by lowercase characters. Where possible, expressions involving tensors are written in matrix form. On a few occasions where this is not possible the tensor expression is written in component form using the usual index notation where repeated indices imply summation; for example

$$a_{ii} = a_{11} + a_{22} + a_{33}.$$

Use of this notation shall be clearly indicated in the text.

2.1.2 Integrals

When a vector valued function, $\boldsymbol{f}(\boldsymbol{x})$, is to be integrated over a general domain, Ω, the integral is written

$$\int_{\boldsymbol{x}\in\Omega} \boldsymbol{f}(\boldsymbol{x})\,\mathrm{d}\boldsymbol{x}.$$

In the contexts considered in this thesis, $\Omega \subset \mathbb{R}$, $\Omega \subset \mathbb{R}^2$ or $\Omega \subset \mathbb{R}^3$.

2.1.3 Hilbert space

The n dimensional vector space $(L_2(\Omega))^n$ is the space of all function vectors defined over the domain Ω that are square integrable; i.e. the integral

$$\int_{x\in\Omega} u^T u \, \mathrm{d}x \tag{2.1}$$

is finite. The one dimensional space, L_2, is an example of Hilbert space[18] and is also denoted by H^0. Smaller Hilbert spaces are defined as those containing functions with derivatives in L_2. For example, in one dimension,

$$H^1 = \{v : v' \in L_2\}, \tag{2.2}$$
$$H^2 = \{v : v'' \in L_2\}, \tag{2.3}$$

and, in two dimensions,

$$H^1 = \left\{v : \frac{\partial v}{\partial x}, \frac{\partial v}{\partial y} \in L_2\right\}, \tag{2.4}$$
$$H^2 = \left\{v : \frac{\partial^2 v}{\partial x^2}, \frac{\partial^2 v}{\partial y^2}, \frac{\partial^2 v}{\partial x \partial y} \in L_2\right\}. \tag{2.5}$$

The L_2 inner product of two vector functions $\boldsymbol{u}$ and $\boldsymbol{v}$ in $(L_2(\Omega))^n$ is denoted by $(\boldsymbol{u}, \boldsymbol{v})_\Omega$ where

$$(\boldsymbol{u}, \boldsymbol{v})_\Omega := \int_{x\in\Omega} \boldsymbol{u}^T \boldsymbol{v} \, \mathrm{d}x. \tag{2.6}$$

When the context is clear we will abbreviate $(\boldsymbol{u}, \boldsymbol{v})_\Omega$ by $(\boldsymbol{u}, \boldsymbol{v})$.

The L_2 norm of a vector function $\boldsymbol{u}(\boldsymbol{x}) \in (L_2(\Omega))^n$ is denoted fully by $\|\boldsymbol{u}\|_{L_2(\Omega)}$ and defined *via* the relation

$$\|\boldsymbol{u}\|^2_{L_2(\Omega)} := (\boldsymbol{u}, \boldsymbol{u})_{L_2(\Omega)} = \int_{x\in\Omega} \boldsymbol{u}^T \boldsymbol{u} \, \mathrm{d}x. \tag{2.7}$$

In the case $\boldsymbol{u} : (a, b) \to \mathbb{R}^n$, i.e. $\boldsymbol{u}$ is a function of a single variable, the L_2 inner product and norm are defined by

$$(\boldsymbol{u}, \boldsymbol{v})_{(a,b)} := \int_a^b \boldsymbol{u}^T \boldsymbol{v} \, \mathrm{d}x \tag{2.8}$$
$$\|\boldsymbol{u}\|^2_{L_2(a,b)} := \int_a^b \boldsymbol{u}^T \boldsymbol{u} \, \mathrm{d}x. \tag{2.9}$$

When the context is clear we will abbreviate $\|\boldsymbol{u}\|_{L_2(\Omega)}$ by $\|\boldsymbol{u}\|_{L_2}$. The definition (2.7) is completely general with the particular form depending on its argument. For example, if $\boldsymbol{u}$ has three components, u_1, u_2 and u_3, we may write

$$\|\boldsymbol{u}\|^2_{L_2} = \|u_1\|^2_{L_2} + \|u_2\|^2_{L_2} + \|u_3\|^2_{L_2}.$$

2.2 Norm inequalities

The following results are used in Chapter 3. Let $u \in L_2(0,l)$ with either $u(0) = 0$ or $u(l) = 0$ then

$$|u(x)| \leq \sqrt{l}\,\|u'\|_{L_2} \tag{2.10}$$
$$\|u\|_{L_2} \leq l\,\|u'\|_{L_2} \tag{2.11}$$

Proof

If $u(0) = 0$ then we write

$$|u(x)| = |\int_0^x u'(x)\,dx| \leq \int_0^x |u'(x)|\,\mathrm{d}x \tag{2.12}$$

otherwise, if $u(l) = 0$, we write

$$|u(x)| = |\int_x^l u'(x)\,dx| \leq \int_x^l |u'(x)|\,\mathrm{d}x \tag{2.13}$$

In either case

$$|u(x)| \leq \int_0^l |u'(x)|\,\mathrm{d}x = (|u'|, 1) \tag{2.14}$$

and (2.10) follows using the Cauchy-Schwarz inequality. Equation (2.11) follows by writing

$$\|u\|_{L_2}^2 = \int_0^l |u(x)|^2\,\mathrm{d}x \leq \int_0^l l\,\|u'\|_{L_2}^2\,\mathrm{d}x = l^2\,\|u'\|_{L_2}^2\,. \tag{2.15}$$

2.3 The Dirac delta function

The analysis in Chapters 3 and 7 uses the Dirac delta function, denoted by δ, which is defined by the property that

$$\int_{-\infty}^{\infty} f(y)\delta(y)\,\mathrm{d}y = f(0) \tag{2.16}$$

for all piecewise continuous functions f. For (2.16) to be true for all such functions it can be shown that if δ is to be considered pointwise then $\delta(y) = 0$ for all $y \neq 0$ with $\delta(0)$ being infinite. Hence δ is not a function in the usual sense. Note that if $\mathcal{H}$ denotes the Heaviside function given by

$$\mathcal{H}(y) := \begin{cases} 0 & y < 0 \\ 1 & y \geq 0 \end{cases} \tag{2.17}$$

then $\mathcal{H}'$ also has these properties. Furthermore, as a consequence of (2.16), if $x \in \mathbb{R}$ is fixed and $f(y) = \mathcal{H}(x - y)$ then

$$\mathcal{H}(x) = \int_{-\infty}^{\infty} \delta(y) H(x - y)\, \mathrm{d}y = \int_{-\infty}^{x} \delta(y)\, \mathrm{d}y \tag{2.18}$$

and from this we interpret δ as the derivative of $\mathcal{H}$ which is the conclusion that would be obtained when the condition of the fundamental theorem of calculus applies.

A more general form of (2.16) is obtained by making the change of variable $y = z - x$ where x is independent of z. By letting $g(z) = f(z - x)$ and noting that $f(0) = f(x - x) = g(x)$ we have

$$\int_{-\infty}^{\infty} g(z)\delta(z - x)\, \mathrm{d}z = g(x). \tag{2.19}$$

2.4 Interpolation

Analysis of finite element methods makes use of results from interpolation theory. The analysis in Chapters 3 and 7 uses a particular result which we derive here. It bounds certain derivatives of the interpolation error in the L_2 norm using the Peano kernel theorem [27] and shows the order of convergence as the interpolation interval, h, is reduced.

Let f be a continuous function over the interval $[x_{i-1}, x_i]$ and let $\Pi_k f$ be a polynomial interpolant of degree k. For a fixed point x we define the functional $\mathcal{L}$ by

$$\mathcal{L}(f) := f(x) - \Pi_k f(x) \tag{2.20}$$

and we note that in the case that f is a polynomial of degree $\leq k$ we have $\mathcal{L}(f) = 0$. For a more general function f we have the Taylor series

$$f(x) = f(x_{i-1}) + f'(x_{i-1})(x - x_{i-1}) + \cdots + \frac{1}{k!} f^{(k)}(x_{i-1})(x - x_{i-1})^k + R_k(x), \tag{2.21}$$

where the remainder, $R_k(x)$, may be written, in integral form, as

$$R_k(x) = \frac{1}{k!} \int_{x_{i-1}}^{x} (x - y)^k f^{(k+1)}(y)\, \mathrm{d}y \tag{2.22}$$

$$= \frac{1}{k!} \int_{x_{i-1}}^{x_i} (x - y)_+^k f^{(k+1)}(y)\, \mathrm{d}y \tag{2.23}$$

where

$$(x - y)_+^k := \begin{cases} (x - y)^k, & x_{i-1} \leq y \leq x \\ 0, & x \leq y \leq x_i \end{cases}. \tag{2.24}$$

Applying $\mathcal{L}$ to (2.21) and using the remark above we have that

$$\mathcal{L}(f) = \mathcal{L}(R_{k-j}) \qquad \forall j = 0 \ldots k. \tag{2.25}$$

From the definition of an integral it can be shown that it is valid to interchange the $\mathcal{L}$ operator and the integral so that

$$\mathcal{L}(f) = \frac{1}{(k-j)!}\int_{x_{i-1}}^{x_i} f^{(k-j+1)}(y)K_j(x,y)\,\mathrm{d}y \qquad \forall j = 0\ldots k \tag{2.26}$$

where

$$K_j(x,y) := \mathcal{L}_x((x-y)_+^{k-j}). \tag{2.27}$$

The subscript x indicates that the interpolation must be carried out with respect to the x variable in $K_j(x,y)$. Equation (2.26) is known as the Peano Kernel theorem [27]. We may use it to derive bounds for the interpolation error and its derivatives. Differentiating (2.26) m times with respect to x we have

$$\frac{\mathrm{d}^m\mathcal{L}(f)}{\mathrm{d}x^m} = \frac{1}{(k-j)!}\int_{x_{i-1}}^{x_i} f^{(k-j+1)}(y)\frac{\partial^m K_j(x,y)}{\partial x^m}\,\mathrm{d}y \qquad \forall j = 0\ldots k-m. \tag{2.28}$$

Application of the Cauchy-Schwarz inequality gives us

$$\left|\frac{\mathrm{d}^m\mathcal{L}(f)}{\mathrm{d}x^m}\right|^2 \leq \frac{1}{(k-j)!}\left\|\frac{\partial^m K_j}{\partial x^m}\right\|^2_{L_2(x_{i-1},x_i)}\left\|f^{(k-j+1)}\right\|^2_{L_2(x_{i-1},x_i)} \qquad \forall j = 0\ldots k-m. \tag{2.29}$$

Now, with $h_i = x_i - x_{i-1}$, it can be shown for all the interpolants Π_k considered in this thesis that $K_j(x,y)$ is of order h_i^{k-j} and $\frac{\partial^m K_j}{\partial x^m}$ is of order h_i^{k-j-m} for $m = 0\ldots k-j$. In this thesis we have only the 2 point linear Lagrange interpolant, the cubic Hermite interpolant, the 3 point quadratic Lagrange interpolant and the quintic polynomial based on the function and derivatives at 3 distinct points. As an example we consider the case with the 2 point linear Lagrange interpolant so that $k = 1$ and, with $j = 0$,

$$(x-y)_+ := \begin{cases} x-y, & x_{i-1} \leq y \leq x \\ 0, & x \leq y \leq x_i \end{cases}. \tag{2.30}$$

The linear Lagrange interpolant to this, over the interval $[x_{i-1}, x_i]$, is

$$\Pi_1(x-y)_+ = \left(1 - \frac{x-x_{i-1}}{h_i}\right)(x_{i-1}-y) + \left(\frac{x-x_{i-1}}{h_i}\right)(x_i - y) = (x-y). \tag{2.31}$$

Hence

$$K(x,y) = \mathcal{L}((x-y)_+) = \begin{cases} 0, & x_{i-1} \leq y \leq x \\ y-x, & x \leq y \leq x_i \end{cases}. \tag{2.32}$$

which shows that $K_1(x,y)$ is of order h_i. Differentiating with respect to x we have

$$\frac{\partial K_1(x,y)}{\partial x} = \begin{cases} 0, & a \leq y \leq x \\ -1, & x \leq y \leq b \end{cases}. \tag{2.33}$$

which is of order 1.

Using the above information about $K_j(x,y)$ we now integrate $\left(\frac{\partial^m K_j}{\partial x^m}\right)^2$ with respect to x from x_{i-1} to x_i to give us

$$\left\|\frac{\partial^m K_j}{\partial x^m}\right\|^2_{L_2(x_{i-1},x_i)} \leq C h_i^{2(k-j-m)+1}. \tag{2.34}$$

Hence

$$\left|\frac{d^m \mathcal{L}(f)}{dx^m}\right|^2 \leq C h_i^{2(k-j-m)+1} \left\|f^{(k-j+1)}\right\|^2_{L_2(x_{i-1},x_i)} \tag{2.35}$$

from which it follows, after integrating $\left|\frac{d^m \mathcal{L}(f)}{dx^m}\right|^2$ over the interval, that

$$\left\|\frac{d^m}{dx^m}\Big(f(x) - \Pi_k f(x)\Big)\right\|^2_{L_2(x_{i-1},x_i)} \leq C h_i^{2(k-j-m+1)} \left\|f^{(k-j+1)}\right\|^2_{L_2(x_{i-1},x_i)} \qquad \forall\, j = 0 \ldots k-m. \tag{2.36}$$

Equation (2.36) shows the relation between h_i and f in bounding the interpolation error measured in the L_2 norm over the interval $[x_{i-1}, x_i]$. We now consider the case where $[x_{i-1}, x_i]$ is a subinterval of the interval $[a,b] \subset \mathbb{R}$ and obtain a similar result in $\|\cdot\|_{L_2(a,b)}$. Let

$$[a,b] = [x_0, x_1] \cup [x_1, x_2] \cup \cdots [x_{n-1}, x_n]$$

then

$$\left\|\frac{d^m}{dx^m}\Big(f(x) - \Pi_k f(x)\Big)\right\|^2_{L_2(a,b)} = \sum_{i=1}^{n} \left\|\frac{d^m}{dx^m}\Big(f(x) - \Pi_k f(x)\Big)\right\|^2_{L_2(x_{i-1},x_i)} \tag{2.37}$$

$$\leq C h^{2(k-j-m+1)} \sum_{i=1}^{n} \left\|f^{(k-j+1)}\right\|^2_{L_2(x_{i-1},x_i)} \tag{2.38}$$

$$= C h^{2(k-j-m+1)} \left\|f^{(k-j+1)}\right\|^2_{L_2(a,b)} \tag{2.39}$$

where $h = \max\{h_i : i = 1 \ldots m\}$. Hence we have the result

$$\left\|\frac{d^m}{dx^m}\Big(f(x) - \Pi_k f(x)\Big)\right\|_{L_2} \leq C h^{k-j-m+1} \left\|f^{(k-j+1)}\right\|_{L_2}, \qquad \forall\, j, m \geq 0 : m + j \leq k. \tag{2.40}$$

This result is used in Chapters 3 and 7 for analysing the error in one-dimensional finite element solutions.

Chapter 3

Finite Element Methods

3.1 Derivation

In general the finite element method may be applied to any partial differential vector equation of the form

$$L(u) = f, \qquad \text{for } x \in \Omega \tag{3.1}$$

(subject to certain boundary conditions) by taking the inner product of both sides with a test vector v and integrating by parts to give the weak form

$$a(u, v) = F(v). \tag{3.2}$$

We shall denote the space containing u and v by H. The reformulated problem (3.2) has less strict continuity requirements than (3.1).

3.1.1 The test problem

In order to introduce the methodology of the finite element method we shall apply it the scalar partial differential equation in two space dimensions given by

$$-\nabla \cdot (a\nabla u) + bu = f \tag{3.3}$$

where the functions a and b satisfy

$$0 < a_0 \leq \quad a \quad \leq a_1 \tag{3.4}$$
$$0 \leq \quad a' \quad \leq a_2 \tag{3.5}$$
$$0 \leq \quad b \quad \leq b_1. \tag{3.6}$$

It will be seen in Chapter 6 that (3.3) is the time-discretized heat conduction equation.

The function u satisfies (3.3) in the domain Ω. With $\Gamma = \Gamma_N \cup \Gamma_D$ denoting a partition of the boundary Γ, we assume that the boundary conditions are the Neumann condition,

$$a\frac{\partial u}{\partial n} = g, \tag{3.7}$$

on Γ_N and the Dirichlet condition,

$$u = 0, \tag{3.8}$$

on Γ_D.

In the case that $\Omega \subset \mathbb{R}$ and specifically that $\Omega = (0, l)$ the partial differential equation in (3.3) reduces to the ordinary differential equation

$$-\frac{\mathrm{d}}{\mathrm{d}x}\left(a\frac{\mathrm{d}u}{\mathrm{d}x}\right) + bu = f \tag{3.9}$$

and the boundary conditions corresponding to (3.7) and (3.8) reduce to

$$u(0) = 0 \quad \text{or} \quad -a\frac{\mathrm{d}u}{dx}\bigg|_{x=0} = 0, \tag{3.10}$$

$$u(l) = 0 \quad \text{or} \quad a\frac{\mathrm{d}u}{\mathrm{d}x}\bigg|_{x=l} = 0. \tag{3.11}$$

In Chapter 7 it will be seen that, with $b = 0$, the equation (3.9) governs the compression of a beam.

3.1.2 The weak problem

The weak form of (3.3)-(3.8) is obtained by first taking the inner product of both sides of (3.3) with a test function, $v \in H$, where in this case

$$H = \left\{v \in H^1 : v = 0 \text{ on } \Gamma_D\right\}.$$

We then have

$$-\int_{x\in\Omega} v\nabla\left(a\nabla u\right)\,\mathrm{d}\boldsymbol{x} + \int_{x\in\Omega} buv\,\mathrm{d}\boldsymbol{x} = \int_{x\in\Omega} fv\,\mathrm{d}\boldsymbol{x}. \tag{3.12}$$

Using the identity

$$\nabla\cdot(va\nabla u) = a\nabla v\cdot\nabla u + v\nabla\cdot(a\nabla u) \tag{3.13}$$

with the divergence theorem together with (3.7) we obtain

$$\int_{x\in\Omega} a\nabla u\cdot\nabla v\,\mathrm{d}\boldsymbol{x} + \int_{x\in\Omega} buv\mathrm{d}\boldsymbol{x} = \int_{x\in\Omega} fv\,\mathrm{d}\boldsymbol{x} + \int_{x\in\Gamma_N} gv\,\mathrm{d}\boldsymbol{x}. \tag{3.14}$$

We define the following inner products for $u, v \in H$, $f \in L_2(\Omega)$ and $g \in L_2(\Gamma_N)$:

$$\begin{aligned} a(u,v)_\Omega &:= \int_{x\in\Omega} (a\nabla u \cdot \nabla v + buv)\, \mathrm{d}\boldsymbol{x} \\ (f,v)_\Omega &:= \int_{x\in\Omega} fv\, \mathrm{d}\boldsymbol{x} = (f,v)_{L_2(\Omega)} \\ [g,v]_{\Gamma_N} &:= \int_{x\in\Gamma_N} gv\, \mathrm{d}\boldsymbol{x} = (g,v)_{L_2(\Gamma_N)}. \end{aligned} \tag{3.15}$$

The weak problem, then, is to find $u \in H$ that satisfies

$$a(u,v)_\Omega = (f,v)_\Omega + [g,v]_{\Gamma_N} \tag{3.16}$$

for all v in H. In future, where the domains Ω and Γ are clear from the context, the subscripts to the inner products will be omitted.

3.1.3 Discretization

Let V be a finite dimensional subspace of H. This means that V is a subspace of H that is spanned by a finite number of basis functions. It is defined by a discretization of the domain, known as a mesh, and the functions used. In one dimension the mesh consists of a line divided into subintervals, known as elements, and a number of points, known as nodes, that lie on and between the connecting points between elements. In two dimensions the mesh is a tessellation where the elements are polygons. We shall not be considering dimensions higher than two. Functions in V are defined in a piecewise way and have appropriate global continuity properties. Each node has associated with it a degree of freedom and a basis function. Hence any function $v \in V$ can be written in matrix form as

$$v = \boldsymbol{N}\boldsymbol{d} \tag{3.17}$$

where $\boldsymbol{N}$ is a matrix containing the basis functions and $\boldsymbol{d}$ is a vector containing the degrees of freedom. For the model problem $\boldsymbol{N}$ is $1 \times n$ where n is the number of nodes. For problems dealing with vector function spaces there will be more than one degree of freedom and basis function for each node. That is, we typically have that $\boldsymbol{N}$ is $m \times (mn)$ and $\boldsymbol{d}$ is $(mn) \times 1$ where m is the number of degrees of freedom per node. The basis functions are defined such that

$$N_i(x_j) = \delta_{ij} \tag{3.18}$$

where x_j is a node and N_j is its corresponding basis function. Hence the degrees of freedom are the function values at the nodes. The functions used are defined for a standard element. In one dimension this can be taken as the interval $[0,1]$ or sometimes $[0,h]$ where h is the length of the element (in higher dimensions h is a measure of the element size). Usually the basis functions are polynomials, the degree of which is

determined by the number of nodes within the element. The simplest is for a two noded element which is linear and, for the element whose nodes are numbered i and j, the two functions are

$$N_i(\xi) = 1 - \xi \tag{3.19}$$
$$N_j(\xi) = \xi \tag{3.20}$$

in the case where $[0, 1]$ is taken as the *standard interval.* Note that ξ is a local variable in this interval.

For two dimensional problems we shall use triangular elements and the *standard element* will be the right angled triangle with vertices at $(0,0)$, $(1,0)$ and $(0,1)$ in the (ξ, η) plane (see Figure 3.1). For the element with nodes numbered i, j and k the functions are

$$N_i(\xi, \eta) = 1 - \xi - \eta, \tag{3.21}$$
$$N_j(\xi, \eta) = \xi, \tag{3.22}$$
$$N_k(\xi, \eta) = \eta. \tag{3.23}$$

The evaluation of integrals over the discretized domain is performed by summing the contributions from each element. That is, for any integral we have

$$\int_{x \in \Omega} (\cdot)\, \mathrm{d}x = \sum_{i=1}^{ne} \int_{x \in \Omega_i} (\cdot)\, \mathrm{d}x. \tag{3.24}$$

For the inner products defined in (3.15) we write

$$a(u, v)_\Omega = \sum_{i=1}^{ne} a(u, v)_{\Omega_i},$$
$$(f, v)_\Omega = \sum_{i=1}^{ne} (f, v)_{\Omega_i},$$
$$[g, v]_\Gamma = \sum_{i=1}^{ne} [g, v]_{\Gamma_i \cap \Gamma_N},$$

where ne is the number of elements and Γ_i is the boundary of Ω_i. Let nbe be the number of boundary elements that make up the Neumann part of the boundary, Γ_N, and let each boundary element of Γ_N be denoted by $\Gamma_{N,i}$ so that

$$\Gamma_N = \bigcup_{i=1}^{nbe} \Gamma_{N,i}. \tag{3.25}$$

Then we may also write the boundary inner product, $[g, v]$, as

$$[g, v]_\Gamma = \sum_{i=1}^{nbe} [g, v]_{\Gamma_{N,i}}. \tag{3.26}$$

3.1.4 The finite element problem

The finite element problem is to find $u_h \in V$ that satisfies

$$\int_{x\in\Omega} a\nabla u_h \cdot \nabla v \,\mathrm{d}\boldsymbol{x} + \int_{x\in\Omega} b u_h v \,\mathrm{d}\boldsymbol{x} = \int_{x\in\Omega} f v \,\mathrm{d}\boldsymbol{x} + \int_{x\in\Gamma_N} g v \,\mathrm{d}\boldsymbol{x} \tag{3.27}$$

for all v in V. The finite element solution may be written as

$$u_h = \boldsymbol{N}\boldsymbol{U} \tag{3.28}$$

where $\boldsymbol{U}$ is the vector of unknowns. Substituting this into (3.27) gives us

$$\int_{x\in\Omega} a\boldsymbol{B}\boldsymbol{U} \cdot \nabla v \,\mathrm{d}\boldsymbol{x} + \int_{x\in\Omega} b\boldsymbol{N}\boldsymbol{U} v \,\mathrm{d}\boldsymbol{x} = \int_{x\in\Omega} f v \,\mathrm{d}\boldsymbol{x} + \int_{x\in\Gamma_N} g v \,\mathrm{d}\boldsymbol{x} \tag{3.29}$$

where $\boldsymbol{B}$ is known as the strain matrix due to early applications in structures (see Chapter 5). For our specific problem it is defined as

$$\boldsymbol{B} = \begin{pmatrix} \nabla N_1 & \nabla N_2 & \dots & \nabla N_n \end{pmatrix} \tag{3.30}$$

which is of size $2 \times n$ when $\Omega \in \mathbb{R}^2$. Taking v in (3.29) to be each column of $\boldsymbol{N}$ in turn we build

$$\left(\int_{x\in\Omega} a\boldsymbol{B}^T\boldsymbol{B} \,\mathrm{d}\boldsymbol{x} + \int_{x\in\Omega} b\boldsymbol{N}^T\boldsymbol{N} \,\mathrm{d}\boldsymbol{x} \right) \boldsymbol{U} = \int_{x\in\Omega} \boldsymbol{N}^T f \mathrm{d}\boldsymbol{x} + \int_{x\in\Gamma_N} \boldsymbol{N}^T g \,\mathrm{d}\boldsymbol{x}. \tag{3.31}$$

This equation may be written as

$$\boldsymbol{K}\boldsymbol{U} = \boldsymbol{F} + \boldsymbol{G} \tag{3.32}$$

where $\boldsymbol{K}$ is known as the stiffness matrix, $\boldsymbol{F}$ is known as the body load vector and $\boldsymbol{G}$ is known as the boundary load vector. This equation is just a linear system which may be solved using any method. We use the preconditioned conjugate gradient method throughout this thesis.

3.1.5 Construction

The integrals are evaluated element by element so that

$$\boldsymbol{K} = \sum_{i=1}^{ne} \int_{x\in\Omega_i} \left(a\boldsymbol{B}^T\boldsymbol{B} + b\boldsymbol{N}^T\boldsymbol{N} \right) \mathrm{d}\boldsymbol{x} \tag{3.33}$$

$$\boldsymbol{F} = \sum_{i=1}^{ne} \int_{x\in\Omega_i} \boldsymbol{N}^T f \,\mathrm{d}\boldsymbol{x} \tag{3.34}$$

$$\boldsymbol{G} = \sum_{i=1}^{nbe} \int_{x\in\Gamma_{N,i}} \boldsymbol{N}^T g \,\mathrm{d}\boldsymbol{x}. \tag{3.35}$$

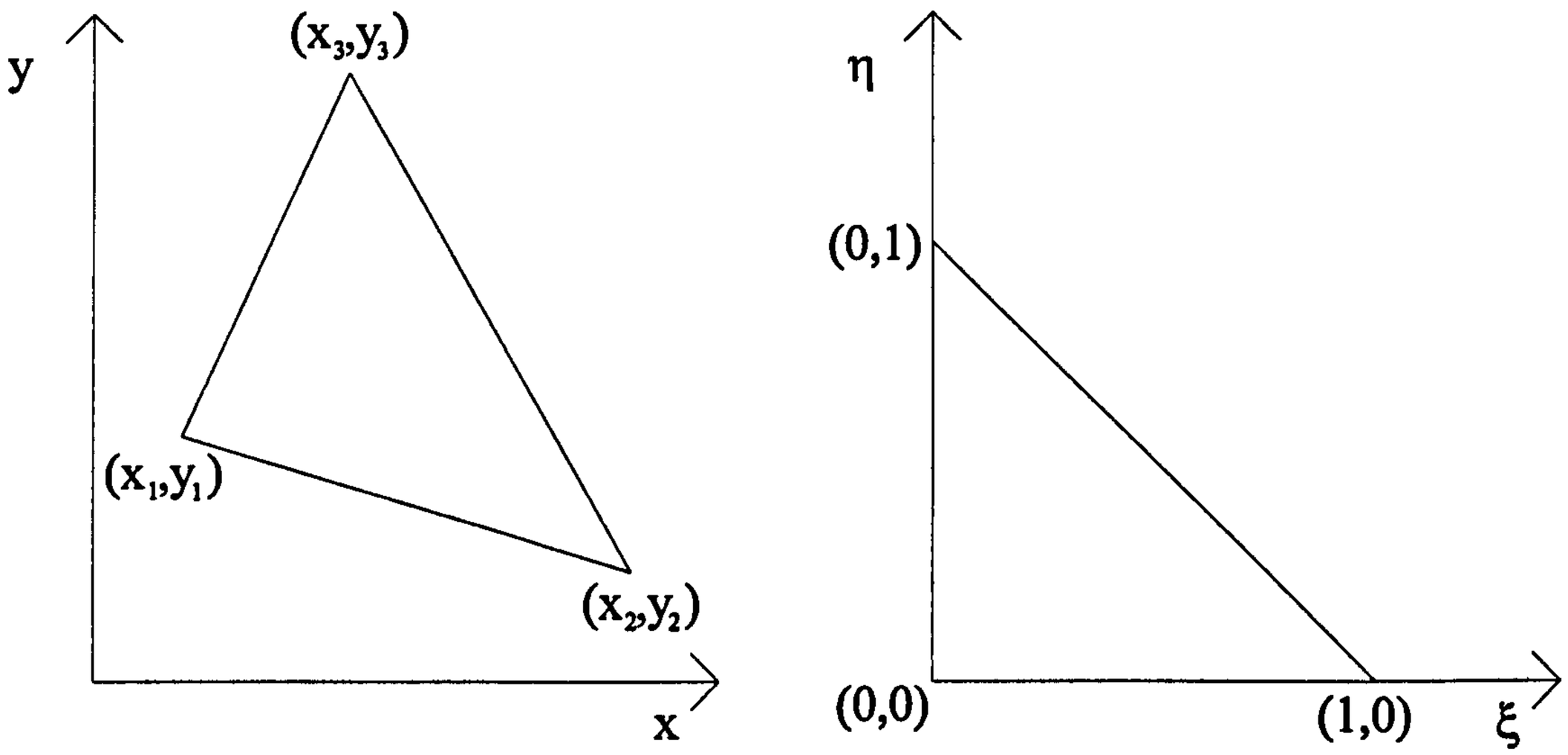

Figure 3.1: General triangular element and standard triangular element

Each element area integral is evaluated by the change in variables from (x, y) to (ξ, η) where ξ and η map x and y onto the standard triangular element (see Figure 3.1). Then we may use the relation

$$\int_{x\in\Omega_i} (\cdot)\,\mathrm{d}\boldsymbol{x} = \int_0^1 \int_0^{1-\eta} (\cdot)\,\mathrm{abs}|\boldsymbol{J}|\,\mathrm{d}\xi\mathrm{d}\eta \tag{3.36}$$

where $\boldsymbol{J}$ is the Jacobian (matrix) of the mapping from (ξ, η) to (x, y). Let the nodes of the element be denoted anticlockwise by (x_1, y_1), (x_2, y_2) and (x_3, y_3). Then the mapping from (ξ, η) to (x, y) is

$$\begin{pmatrix} x \\ y \end{pmatrix} = \begin{pmatrix} x_1 \\ y_1 \end{pmatrix} + \begin{pmatrix} x_2 - x_1 & x_3 - x_1 \\ y_3 - y_1 & y_3 - y_1 \end{pmatrix} \begin{pmatrix} \xi \\ \eta \end{pmatrix}. \tag{3.37}$$

The 2×2 matrix involved in (3.37) is the Jacobian matrix and its determinant is

$$J := |\boldsymbol{J}| = (x_2 - x_1)(y_3 - y_1) - (x_3 - x_1)(y_2 - y_1). \tag{3.38}$$

Given the anticlockwise orientation of (x_1, y_1), (x_2, y_2) and (x_3, y_3) we will always have $J > 0$. Similarly we evaluate the boundary integral by mapping it onto the interval $[0, 1]$ and use

$$\int_{x\in\Gamma_i} (\cdot)\,\mathrm{d}\boldsymbol{x} = \int_0^1 (\cdot)\,l\,\mathrm{d}\xi \tag{3.39}$$

where, if (x_1, y_1) and (x_2, y_2) define the boundary element,

$$l = \sqrt{(x_2 - x_1)^2 + (y_2 - y_1)^2}. \tag{3.40}$$

Hence

$$\boldsymbol{K} = \sum_{i=1}^{ne} \int_0^1 \int_0^{1-\eta} \left(a\boldsymbol{B}^T\boldsymbol{B} + b\boldsymbol{N}^T\boldsymbol{N} \right) J \, \mathrm{d}\xi \mathrm{d}\eta, \tag{3.41}$$

$$\boldsymbol{F} = \sum_{i=1}^{ne} \int_0^1 \int_0^{1-\eta} \boldsymbol{N}^T f \, J \, \mathrm{d}\xi \mathrm{d}\eta, \tag{3.42}$$

$$\boldsymbol{G} = \sum_{i=1}^{nb} \int_0^1 \boldsymbol{N}^T g \, l \, \mathrm{d}\xi. \tag{3.43}$$

When evaluating the element integrals it is helpful to define local vectors and matrices where the nodes are numbered 1, 2 and 3. Let the local stiffness matrix and the local body load vector for the i'th element be denoted by $\boldsymbol{K}_i$ and $\boldsymbol{F}_i$ respectively. These are defined as

$$\boldsymbol{K}_i = \int_0^1 \int_0^{1-\eta} \left(a\boldsymbol{B}_i^T\boldsymbol{B}_i + b\boldsymbol{N}_i^T\boldsymbol{N}_i \right) J \, \mathrm{d}\xi \mathrm{d}\eta, \tag{3.44}$$

$$\boldsymbol{F}_i = \int_0^1 \int_0^{1-\eta} \boldsymbol{N}_i^T f \, J \, \mathrm{d}\xi \mathrm{d}\eta, \tag{3.45}$$

where $\boldsymbol{B}_i$ and $\boldsymbol{N}_i$ are the local strain matrix, of size 2×3, and local basis function vector, of size 1×3, respectively. Similarly let the local boundary load vector for the i'th boundary element be denoted by $\boldsymbol{G}_i$. This is defined as

$$\boldsymbol{G}_i = \int_0^1 \boldsymbol{N}_i^T g \, l \, \mathrm{d}\xi. \tag{3.46}$$

Since the local strain matrix, $\boldsymbol{B}_i$, involves partial derivatives with respect to x and y we must use the chain rule to write them with respect to ξ and η. Hence

$$\boldsymbol{B}_i = \begin{pmatrix} \dfrac{\partial \boldsymbol{N}_i}{\partial x} \\ \dfrac{\partial \boldsymbol{N}_i}{\partial y} \end{pmatrix} = \begin{pmatrix} \dfrac{\partial \xi}{\partial x} & \dfrac{\partial \eta}{\partial x} \\ \dfrac{\partial \xi}{\partial y} & \dfrac{\partial \eta}{\partial y} \end{pmatrix} \begin{pmatrix} \dfrac{\partial \boldsymbol{N}_i}{\partial \xi} \\ \dfrac{\partial \boldsymbol{N}_i}{\partial \eta} \end{pmatrix} = \frac{1}{J} \begin{pmatrix} y_3 - y_1 & y_1 - y_2 \\ \\ x_1 - x_3 & x_2 - x_1 \end{pmatrix} \begin{pmatrix} \dfrac{\partial \boldsymbol{N}_i}{\partial \xi} \\ \dfrac{\partial \boldsymbol{N}_i}{\partial \eta} \end{pmatrix}. \tag{3.47}$$

Using the linear basis functions defined earlier, we evaluate $\boldsymbol{B}_i$ to be

$$\boldsymbol{B}_i = \frac{1}{J} \begin{pmatrix} y_3 - y_1 & y_1 - y_2 \\ x_1 - x_3 & x_2 - x_1 \end{pmatrix} \begin{pmatrix} -1 & 1 & 0 \\ -1 & 0 & 1 \end{pmatrix} = \frac{1}{J} \begin{pmatrix} y_2 - y_3 & y_3 - y_1 & y_1 - y_2 \\ x_3 - x_2 & x_1 - x_3 & x_2 - x_1 \end{pmatrix}. \tag{3.48}$$

The element integrals are usually evaluated numerically for convenience. However, if the form of a, b, f and g are known then the integrals may be evaluated exactly.

3.1.6 Storage

Generally, each node in the finite element mesh connects to only a small number of other nodes. Consequently, the global stiffness matrix is very sparse with the majority of

off-diagonal locations containing zero. It would be very wasteful of computer memory to store the full matrix since most locations would never be addressed. Hence the matrix is stored in a compressed form. The algorithm that has been used stores the matrix elements in a one dimensional array. Another one dimensional array stores the indices where each matrix row begins and another stores the matrix column numbers of each matrix element stored. This is known as compressed row storage.

3.2 Error analysis

3.2.1 Definitions

The error in the finite element solution is denoted by the function e and is defined as

$$e = u - u_h. \tag{3.49}$$

In analysing the error we seek bounds for e in terms of the L_2 and energy norms. The energy norm will be denoted by $\|\cdot\|_\Omega$ and is defined such that

$$\|e\|_\Omega^2 := a(e,e)_\Omega. \tag{3.50}$$

When the meaning of Ω is clear from the context of the text the subscript may be dropped so that the energy norm is denoted simply by $\|\cdot\|$.

The analysis that follows serves as an introduction to some of the techniques used in analysing the error in the finite element method. Attention is made to one-dimensional problems where $g = 0$ since the techniques are required for the frame analysis in Chapter 7. Hence, throughout this section,

$$Lu = -(au')' = f \tag{3.51}$$

$$a(u,v) = (f,v) \tag{3.52}$$

3.2.2 Orthogonality

The weak solution, u, and the finite element solution, u_h, satisfy

$$a(u,v) = (f,v) + [g,v] \,\forall v \in H \tag{3.53}$$

$$a(u_h,v) = (f,v) + [g,v] \,\forall v \in V. \tag{3.54}$$

Restricting v in (3.53) so that $v \in V$ then subtracting (3.54) from (3.53) and substituting (3.49) gives us

$$a(e,v) = 0 \qquad \text{for all } v \in V. \tag{3.55}$$

Hence the error is orthogonal to all functions in the space V with respect to the inner product $a(\cdot,\cdot)$. This result will be used time and time again in subsequent analyses of finite element methods. It implies that we can write

$$a(e,e) = a(e,u-v) \tag{3.56}$$

for any v in V. Applying the Cauchy-Schwarz inequality we have

$$\|e\| \leq \|u-v\| \tag{3.57}$$

for any v in V. Hence, in this norm, u_h is the best approximation to u out of all functions in the space V.

3.2.3 Bound for the energy norm

We may make use of (3.57) to obtain an *a priori* error bound if we let $v = \Pi u$ where Πu is an interpolant to u in V. With this choice we have established, from (3.57), that

$$\|e\| \leq \|u - \Pi u\|. \tag{3.58}$$

In other words, the finite element error, in this norm, is bounded above by the norm of the interpolation error. Now, from (3.15) and the assumptions (3.4) and (3.6),

$$\|u-\Pi u\|^2 \leq a_1 \|(u-\Pi u)'\|_{L_2}^2 + b_1 \|(u-\Pi u)\|_{L_2}^2 . \tag{3.59}$$

By equation (2.40)

$$\left\|(u-\Pi u)^{(n)}\right\|_{L_2} \leq C h^{p+1-n} \left\|u^{(p+1)}\right\|_{L_2}, \qquad n = 0,1,2,\ldots \tag{3.60}$$

where n is the order of differentiation and p is the degree of polynomial used in the interpolation. Hence

$$\|u-\Pi u\|^2 \leq C \left\|u^{(p+1)}\right\|_{L_2} h^{2p}(1+h^2) \tag{3.61}$$

and, by increasing the constant,

$$\|u-\Pi u\| \leq C h^p \left\|u^{(p+1)}\right\|_{L_2} . \tag{3.62}$$

This means that

$$\|e\| \leq C h^p. \tag{3.63}$$

3.2.4 Bound for the L_2 norm

In deriving an upper bound for the L_2 norm of the error we require the following theorem:

Theorem 3.1

Let $u \in H(0,l)$ satisfy (3.51) then

$$\left\| \frac{\mathrm{d}^n u}{\mathrm{d}x^n} \right\|_{L_2} \leq C \left\| f \right\|_{L_2} \tag{3.64}$$

for $n = 0 \ldots 2$ where C is a constant that depends on the operator L and the space H but not the function f.

Proof

From (3.4) and (3.52) and using (2.11) we have

$$a_0 \left\| u' \right\|_{L_2}^2 \leq \left\| u \right\|^2 = (f,u) \leq \left\| f \right\|_{L_2} \left\| u \right\|_{L_2} \leq \sqrt{l} \left\| f \right\|_{L_2} \left\| u' \right\|_{L_2} \tag{3.65}$$

Hence

$$\left\| u' \right\|_{L_2} \leq \frac{\sqrt{l}}{a_0} \left\| f \right\|_{L_2} \tag{3.66}$$

$$\left\| u \right\|_{L_2} \leq \frac{l}{a_0} \left\| f \right\|_{L_2}, \tag{3.67}$$

proving the theorem for $n = 0$ and $n = 1$. To prove the theorem holds for $n = 2$ we use (3.51) to write

$$\left\| au'' \right\|_{L_2} = \left\| f - a'u' \right\|_{L_2} \leq \left\| f \right\|_{L_2} + \left\| a'u' \right\|_{L_2} \tag{3.68}$$

then we use (3.5) to give us

$$a_0 \left\| \frac{\mathrm{d}^2 u}{\mathrm{d}x^2} \right\|_{L_2} \leq \left\| f \right\|_{L_2} + a_2 \left\| \frac{\mathrm{d}u}{\mathrm{d}x} \right\|_{L_2}. \tag{3.69}$$

The proof follows from the fact that the theorem holds for $n = 1$. □

We now use a technique that is known as the Nitsche trick [14, Page 72] to derive a bound for e in the L_2 norm. The trick is to let $\phi \in H$ satisfy

$$L(\phi) = e. \tag{3.70}$$

Now the L_2 norm may be written as

$$\left\| e \right\|_{L_2}^2 = (L(\phi), e) \tag{3.71}$$

$$= a(\phi, e) \tag{3.72}$$

$$= a(\phi - v, e) \tag{3.73}$$

$$\leq \left\| \phi - v \right\| \left\| e \right\| \tag{3.74}$$

for any v in V. Applying (3.63) we have

$$\|e\|_{L_2}^2 \leq C \|\phi - v\| h^p. \tag{3.75}$$

We let $v = \Pi_1 \phi$ be the piecewise linear interpolant to ϕ so that

$$\|e\|_{L_2}^2 \leq C \|\phi - \Pi_1 \phi\| h^p. \tag{3.76}$$

Using (3.60) with $p = 1$ and $n = 1$ gives us

$$\|\phi - \Pi_1 \phi\| \leq Ch \|\phi''\|_{L_2}. \tag{3.77}$$

Using Theorem 3.1 we have

$$\|\phi''\|_{L_2} \leq C \|e\|_{L_2} \tag{3.78}$$

so that, after substituting (3.78) into (3.77),

$$\|\phi - \Pi_1 \phi\| \leq Ch \|e\|_{L_2}. \tag{3.79}$$

Substituting (3.79) into (3.76) and dividing by $\|e\|_{L_2}$ gives us

$$\|e\|_{L_2} \leq Ch^{p+1}. \tag{3.80}$$

3.2.5 Pointwise error bounds and superconvergence

Let $g(x, y)$ belong to $H(0, l) \otimes H(0, l)$ and, with x fixed, let it satisfy the equation

$$Lg(x, y) = -\frac{\partial}{\partial y}\left(a \frac{\partial g}{\partial y}\right) + bg = \delta(y - x) \tag{3.81}$$

where δ is the Dirac delta function. The defining property of δ, that

$$\int_{-\infty}^{\infty} \delta(y - x) f(y) \, \mathrm{d}x = f(x) \tag{3.82}$$

allows us to write

$$e(x) = (\delta(x, \cdot), e) = (Lg(x, \cdot)) = a\,(g(x, \cdot), e)\,. \tag{3.83}$$

The function g is commonly known as a Green's function [14, Page 44]. Due to the orthogonality of the error and the Cauchy-Schwarz inequality we have that

$$|e(x)| \leq \|g(x, \cdot) - \Pi g(x, \cdot)\| \, \|e\| \tag{3.84}$$

where $\Pi g(x, y)$ is the interpolant with respect to the y variable. If x is a connecting node, x_i say, then we may use (3.60) to write

$$|e(x_i)| \leq Ch^p \|e\| . \tag{3.85}$$

With (3.63) we have that

$$|e(x_i)| \leq Ch^{2p}. \tag{3.86}$$

Recall that the global error, measured by the L_2 norm in (3.80), is of order of $h^{(p+1)}$. If the degree of polynomial p is greater than one then the pointwise error at the connecting nodes converges to zero at a faster rate than that globally. This phenomenon is known as superconvergence [14, Page 44].

3.3 Error estimation

The previous section established some results that describe the behaviour of the error in the finite element solution with respect to the discretization parameter h. These *a priori* results in no way attempt to actually quantify the error. This section looks at a variety of post processing techniques that attempt to measure the error in some way based on the calculated finite element solution. Typically, we want to estimate some norm of the error such that the estimator, $\|\hat{e}\|$, and the true norm, $\|e\|$, behave in a similar way asymptotically; i.e. they converge to 0 as h tends to 0 with the same order of h. In other words there exist positive constants C_1 and C_2 such that

$$C_1 \|e\| \leq \|\hat{e}\| \leq C_2 \|e\| . \tag{3.87}$$

To measure this behaviour we define the effectivity index to be the ratio of the estimator to the norm. If the effectivity index converges to a non-zero value as h tends to 0 then the estimator is said to be consistent. Furthermore, if the effectivity index converges to 1 then the estimator is said to be asymptotically exact.

3.3.1 Recovered gradient type estimators

In a piecewise linear finite element method the gradient of the finite element solution is piecewise constant. Hence the gradient function is not defined along element edges and at nodal points. Nodal values of the gradient can only be considered as the limit as one approaches the node from within an element. In this sense the nodal gradient may be considered to be multivalued. A continuous gradient function may be obtained by averaging the limiting nodal values and interpolating these average gradients with piecewise linear basis functions. This average gradient function is an example of a recovered gradient which hopefully is more accurate than the gradient of the finite element solution. We may then make the approximation

$$\|\nabla u - \nabla u_h\| \approx \left\|\nabla u_h^R - \nabla u_h\right\| \tag{3.88}$$

where ∇u_h^R denotes the recovered gradient. Křižek and Neittaanmaki [20] analysed this gradient recovery method in 1984 and showed that, for elliptic problems with a uniform triangular mesh,

$$\|\nabla u - \nabla u_h^R\| \leq Ch^2 \tag{3.89}$$

where C is independent of h.

Averaging the finite element gradient at the nodes is only sensible if that of the true solutions is known to be continuous. In a continuum, physical properties such as heat flux and stress (which involve both material data and gradients) are assumed to be continuous. From the finite element method we usually obtain discontinuous approximations to these quantities. However, because the underlying quantities are continuous, it is intuitively sensible to approximate these by averaging the values generated by the finite element method.

Let us denote by $\boldsymbol{q}_R$ and $\boldsymbol{\sigma}_R$ the averaged/recovered heat flux and stress vectors, respectively. Typically the recovered heat flux has the form

$$\boldsymbol{q}_R = \boldsymbol{N}\boldsymbol{Q} \tag{3.90}$$

where $\boldsymbol{Q}$ contains the recovered flux values at the nodes and $\boldsymbol{N}$ is a matrix of interpolation functions, usually those used as basis functions in the finite element method. Using the averaging recovery method the components of $\boldsymbol{Q}$, $\boldsymbol{Q}_i$ (of length 2 in 2D problems), are given by

$$\boldsymbol{Q}_i = \boldsymbol{q}_R(\boldsymbol{x}_i) = \frac{1}{n}\sum_{k=1}^{n} \boldsymbol{q}_h^{(k)} \tag{3.91}$$

where we are assuming that the node $\boldsymbol{x}_i$ is on n elements and $\boldsymbol{q}_h^{(k)}$ is the finite element heat flux in the k'th of these n elements. A variation of this method is to use a weighted average according to the element area; i.e.

$$\boldsymbol{Q}_i = \boldsymbol{q}_R(\boldsymbol{x}_i) = \frac{\sum_{k=1}^{n} \boldsymbol{q}_h^{(k)} J_k}{\sum_{k=1}^{n} J_k} \tag{3.92}$$

where $J_k > 0$ is the determinant of the Jacobian matrix relating to the k'th element (given by (3.38) for a triangle).

In 1987 [42] Zienkiewicz and Zhu proposed a stress recovery procedure that requires

$$\int_{x\in\Omega} \boldsymbol{N}^T(\boldsymbol{\sigma}_R - \boldsymbol{\sigma}_h)\,\mathrm{d}\boldsymbol{x} = 0 \tag{3.93}$$

where $\boldsymbol{\sigma}_h$ is the stress obtained from u_h. In the context of the heat conduction equation this is equivalent to

$$\int_{x\in\Omega} \boldsymbol{N}^T(\boldsymbol{q}_R - \boldsymbol{q}_h)\,\mathrm{d}\boldsymbol{x} = 0 \tag{3.94}$$

so that, using (3.90), $\boldsymbol{q}_R$ may be obtained from

$$\int_{x\in\Omega} \boldsymbol{N}^T\boldsymbol{N}\,\mathrm{d}\boldsymbol{x}\boldsymbol{Q} = \int_{x\in\Omega} \boldsymbol{N}^T\boldsymbol{q}_h\,\mathrm{d}\boldsymbol{x}. \tag{3.95}$$

To obtain $\boldsymbol{Q}$ would require the solution of the global system given in (3.95) which is a computation as expensive as computing the finite element solution. To simplify things and to reduce significantly the computational cost, Zienkiewicz and Zhu used the lumped local matrix replacement, for the k'th element say,

$$\int_0^1\int_0^{1-\eta} \boldsymbol{N}_k^T\boldsymbol{N}_k\,J_k\,\mathrm{d}\xi\mathrm{d}\eta = \frac{1}{24}\begin{pmatrix}2&1&1\\1&2&1\\1&1&2\end{pmatrix} \rightarrow \frac{1}{6}\begin{pmatrix}1&0&0\\0&1&0\\0&0&1\end{pmatrix}. \tag{3.96}$$

Consequently, the global matrix is diagonal and $\boldsymbol{Q}$ becomes the vector of weighted average fluxes given in (3.92). This error estimator, known as the Z^2 Error Estimator, has been widely used and analysed. The paper by Ainsworth et al. in 1989 [4] concluded that, while the estimator performs well, it is not necessarily asymptotically exact. Rodriguez, in 1994, [28] analysed the estimator for the piecewise linear finite element solution of elliptic problems. He proved that, for any regular triangular mesh, the estimator is equivalent to the error for the Poisson equation with a homogeneous Dirichlet boundary condition. He also proved that the estimator is asymptotically exact on subdomains where the solution is smooth and when parallel meshes are used.

The Z^2 method has been found to be accurate mainly for linear triangular and quadratic quadrilateral elements. For other types of element the Z^2 method is often poor with the effectivity index converging to zero in some cases [6]. For this reason the authors proposed, in 1991, another stress recovery procedure that fits a polynomial by the least squares method to a number of sampling points over a patch of neighbouring elements [41]. The stress is then calculated from the resulting polynomial at the nodal point. This process is sometimes known as Superconvergent Patch Recovery since, for many types of element, the recovered stress values converge at a rate of at least one order higher than $\boldsymbol{\sigma}_h$. Generally the estimator is known as the SPR Error Estimator. Let the patch be denoted by Ω_p and the stress over the patch be denoted by $\boldsymbol{\sigma}_p$. This has the form

$$\boldsymbol{\sigma}_p = \boldsymbol{P}\boldsymbol{a} \tag{3.97}$$

where $\boldsymbol{P}$ is a vector of polynomials and $\boldsymbol{a}$ contains the degrees of freedom which are found by minimising

$$F(\boldsymbol{a}) = \sum_{j=1}^{np}\left(\boldsymbol{\sigma}_h^{(j)} - \boldsymbol{P}\boldsymbol{a}\right)^2. \tag{3.98}$$

where np is the number of sampling points. The minimisation of $F(\boldsymbol{a})$ requires that

$$\sum_{j=1}^{np}\boldsymbol{P}^T\boldsymbol{P}\boldsymbol{a} = \sum_{j=1}^{np}\boldsymbol{P}^T\boldsymbol{\sigma}_h^{(j)}. \tag{3.99}$$

The recovered stress is then given by

$$\boldsymbol{\sigma}_h^R(\boldsymbol{x}_i) = \boldsymbol{\sigma}_p(\boldsymbol{x}_i). \tag{3.100}$$

In 1992 Zienkiewicz and Zhu [43] presented an integral form of their new method in which $\boldsymbol{\sigma}_p$ is found by minimising

$$F(\boldsymbol{a}) = \int_{x \in \Omega_p} (\boldsymbol{\sigma}_h - \boldsymbol{P}\boldsymbol{a})^2 \, d\boldsymbol{x}. \tag{3.101}$$

This requires that

$$\int_{x \in \Omega_p} \boldsymbol{P}^T \boldsymbol{P} \, \mathrm{d}\boldsymbol{x}\boldsymbol{a} = \int_{x \in \Omega_p} \boldsymbol{P}^T \boldsymbol{\sigma}_h \mathrm{d}\boldsymbol{x} \tag{3.102}$$

which, with $\boldsymbol{P} = \boldsymbol{N}$, is the same as (3.95) except that the integration is performed over the patch rather than the whole domain.

3.3.2 The Bank-Weiser error estimator

In 1985 Bank and Weiser [9] proposed the following method for obtaining an error estimator for the finite element solution of problems in the form of (3.3). The idea is to expand $a(e, v)$ in terms of known quantities derived from the data and the finite element solution hence obtaining a weak problem in the finite element error, e. The aim is to derive a local problem for each element, Ω_i, so that the estimator can be calculated element-wise. Let V be the finite element space and $\overline{V}$ be a space containing higher degree polynomials in which we will approximate the error. Using (3.14) with Ω replaced by Ω_i and integration by parts we can write, for any v in $\overline{V}$,

$$a(\boldsymbol{e}, \boldsymbol{v})_{\Omega_i} = (r, v)_{\Omega_i} + [r_B, v]_{\Gamma_i \cap \Gamma_N} - \left[a \frac{\partial u_h}{\partial n}, v \right]_{\Gamma_i \cap \Gamma_I} \tag{3.103}$$

where Γ_i is the set of edges belonging to the i'th element, Γ_I is the set of all interior element edges and the residual quantities, r and r_B, are defined as

$$r = f - L(u_h), \quad \text{elementwise in } \Omega \tag{3.104}$$

$$r_N = g - a \frac{\partial u_h}{\partial n}, \quad \text{edgewise on } \Gamma_N. \tag{3.105}$$

The right hand side is denoted by the functional $F(v)$ so that the error satisfies

$$a(e, v)_{\Omega_i} = F(v)_{\Omega_i}. \tag{3.106}$$

The local problem is obtained by sharing the jumps in the flux along interior edges between the two connecting elements. For each interior edge choose one of the connecting elements to be *in* and the other to be *out*. The jump in flux along the edge is

then defined as

$$\left(a\frac{\partial u_h}{\partial n}\right)_J = \left(a\frac{\partial u_h}{\partial n}\right)_{\Gamma_{\text{out}}} - \left(a\frac{\partial u_h}{\partial n}\right)_{\Gamma_{\text{in}}} \tag{3.107}$$

and we have

$$-\sum_{i=1}^{ne}\left[a\frac{\partial u_h}{\partial n}, v\right]_{\Gamma_i\cap\Gamma_I} = \sum_{i=1}^{ne}\left[\left(a\frac{\partial u_h}{\partial n}\right)_J, v\right]_{\Gamma_i\cap\Gamma_I}. \tag{3.108}$$

By sharing equally the flux jumps between the connecting elements the right hand side of (3.106) is

$$F(v)_{\Omega_i} = (r, v)_{\Omega_i} + [r_N, v]_{\Gamma_i\cap\Gamma_I} + \frac{1}{2}\left[\left(a\frac{\partial u_h}{\partial n}\right)_J, v\right]_{\Gamma_i\cap\Gamma_I}. \tag{3.109}$$

An estimate of the error, $\hat{e}$, may now be found by solving the local problem

$$a(\hat{e}, v)_{\Omega_i} = F(v)_{\Omega_i}. \tag{3.110}$$

Bank and Weiser proved that

$$(1-\beta^2)(1-\gamma^2)\|e\|^2 \leq \|\hat{e}\| \leq (1-C)\|e\| \tag{3.111}$$

where β tends to zero with h and γ and C are constants less than one. They also give a numerical example where the estimator appears to be asymptotically exact in the energy norm. Duran and Rodriguez analysed the estimator in 1991 [13]. They proved the estimator to be asymptotically exact in the energy norm for regular solutions and parallel meshes but showed that it was not so in general. Ainsworth [5] analysed the estimator for finite element approximations on quadrilateral meshes and proved that it is asymptotically exact in the energy norm for regular solutions provided that the degree of approximation is of odd order and that the elements are rectangles.

3.3.3 The Bank-Weiser error estimator for 1D problems

For one dimensional finite element problems it is comparatively easier to derive and implement the Bank-Weiser error estimator than for two dimensional problems. Let $\overline{V}$ be a finite element subspace of H that contains higher degree polynomials than V. Then, for the element $\Omega_i = (x_{i-1}, x_i)$,

$$a(e, v)_{\Omega_i} = \int_{x_{i-1}}^{x_i} (ae'v' + bev)\,\mathrm{d}x \tag{3.112}$$

$$= [ae'v]_{x_{i-1}}^{x_i} + \int_{x_{i-1}}^{x_i} (-(ae')'v + bev)\,\mathrm{d}x \tag{3.113}$$

$$= [ae'v]_{x_{i-1}}^{x_i} + (r, v)_{\Omega_i} \tag{3.114}$$

for all v in $\overline{V}$. If we choose v to belong to $\hat{V}$, the subspace of $\overline{V}$ in which all functions are zero at x_{i-1} and x_i, then we have

$$a(e,v)_{\Omega_i} = (r,v)_{\Omega_i} \tag{3.115}$$

for all v in $\hat{V}$. Hence we can find an approximation to e in $\hat{V}$, denoted by $\hat{e}$, by solving

$$a(\hat{e},v)_{\Omega_i} = (r,v)_{\Omega_i} \tag{3.116}$$

for all v in $\hat{V}$. Then, for each element, the error is found by putting $\hat{e} = \hat{\boldsymbol{N}}\hat{\boldsymbol{E}}$ and solving

$$\hat{\boldsymbol{K}}\hat{\boldsymbol{E}} = \hat{\boldsymbol{F}} \tag{3.117}$$

where

$$\hat{\boldsymbol{K}} = \int_{x_{i-1}}^{x_i} a\hat{\boldsymbol{B}}^T\hat{\boldsymbol{B}} + b\hat{\boldsymbol{N}}^T\hat{\boldsymbol{N}}\,\mathrm{d}x \tag{3.118}$$

$$\hat{\boldsymbol{F}} = \int_{x_{i-1}}^{x_i} r\hat{\boldsymbol{N}}^T\,\mathrm{d}x \tag{3.119}$$

$$\hat{\boldsymbol{B}} = \frac{\mathrm{d}\hat{\boldsymbol{N}}}{\mathrm{d}x}. \tag{3.120}$$

If V is cubic, for example, it may be spanned locally by

$$\hat{N}_1(x) = (x - x_{i-1})(x_i - x) \tag{3.121}$$

$$\hat{N}_2(x) = (x - x_{i-1})(x_i - x)(2x - x_{i-1} - x_i). \tag{3.122}$$

Let us consider the simplest case where $\hat{V}$ is quadratic. Then it may be spanned locally over the i'th element by

$$\hat{N} = (x - x_{i-1})(x_i - x) \tag{3.123}$$

and $\hat{\boldsymbol{K}}$ and $\hat{\boldsymbol{F}}$ become scalars. If a, b and f are constant then

$$\hat{K} = \frac{h^3}{3}\left(a + \frac{bh^2}{10}\right) \tag{3.124}$$

$$\hat{F} = \frac{h^3}{6}\left(f - \frac{b}{2}(U_{i-1} + U_i)\right). \tag{3.125}$$

Hence

$$\hat{E} = \frac{\hat{F}}{\hat{K}} \tag{3.126}$$

and

$$\|\hat{e}\|^2 = \hat{K}\hat{E}^2 = \hat{F}\hat{E} = \frac{h^3\left(f - \frac{b}{2}(U_{i-1} + U_i)\right)^2}{12\left(a + \frac{bh^2}{10}\right)}. \tag{3.127}$$

3.3.4 Implementation of the Bank-Weiser error estimator for 2D problems

For the linear triangular element we may minimally consider, as the higher order approximation of the error, a bilinear function. As basis functions for $\hat{V}$, over the standard triangular element, we may use

$$\hat{N}_1(x,y) = \xi(1-\xi-\eta) \tag{3.128}$$
$$\hat{N}_2(x,y) = \xi\eta \tag{3.129}$$
$$\hat{N}_3(x,y) = \eta(1-\xi-\eta) \tag{3.130}$$

where ξ and η are related to x and y by (3.37). To solve (3.110) for all $v \in \hat{V}$ we construct

$$\hat{\boldsymbol{K}}\hat{\boldsymbol{E}} = \hat{\boldsymbol{F}} \tag{3.131}$$

where

$$\hat{\boldsymbol{K}} := \int_{x\in\Omega_i} \left(a\hat{\boldsymbol{B}}^T\hat{\boldsymbol{B}} + b\hat{\boldsymbol{N}}^T\hat{\boldsymbol{N}}\right) \mathrm{d}\boldsymbol{x} \tag{3.132}$$
$$\hat{\boldsymbol{F}} := \int_{x\in\Omega_i} r\hat{\boldsymbol{N}}^T d\boldsymbol{x} + \int_{x\in\Gamma_i\cap\Gamma} s\hat{\boldsymbol{N}}^T \mathrm{d}\boldsymbol{x} \tag{3.133}$$

where

$$s := \begin{cases} r_B, & \text{if } \boldsymbol{x}\in\Gamma \\ \frac{1}{2}\left(a\frac{\partial u_h}{\partial n}\right)_J, & \text{if } \boldsymbol{x}\in\Gamma_I \end{cases}. \tag{3.134}$$

3.4 Numerical experiment

To investigate the effectiveness of the error estimators discussed we shall apply them to the finite element solution to the test problem (3.3) with

$$f(x,y) = -2a(1-x-y) + \frac{b}{6}\left(x^2(3-2x) + y^2(3-2y)\right) \tag{3.135}$$
$$g(x,y) = 0 \tag{3.136}$$

to which the exact solution is

$$u(x,y) = \frac{1}{6}x^2(3-2x) + \frac{1}{6}y^2(3-2y). \tag{3.137}$$

This is plotted in Figure 3.2. A succession of 7 uniform triangular meshes are used, ranging from 2 to 8192 elements. These are shown in Figure 3.3. We consider three cases with $a = 1$ and $b = 1$, 100 and 10000. The L_2 norms of the true error gradient and the gradients of the three error estimates are given in Table 3.1 where the estimating functions are denoted by ZZ, SPR and BW. They show that the gradient of the true

error is converging at a rate of $O(h)$ as expected. The gradient of the Zienkiewicz-Zhu estimates, ZZ and SPR, are practically the same as each other and also show $O(h)$ convergence. In fact, for the $a = b$ case, the estimates appear to be asymptotically exact in the L_2 norm. The Bank-Weiser estimate is at least consistent for the $b = 1$ and $b = 100$ cases but shows no sign of converging for the $b = 10000$ case with the mesh tried. This suggests a limitation of the Bank-Weiser estimator.

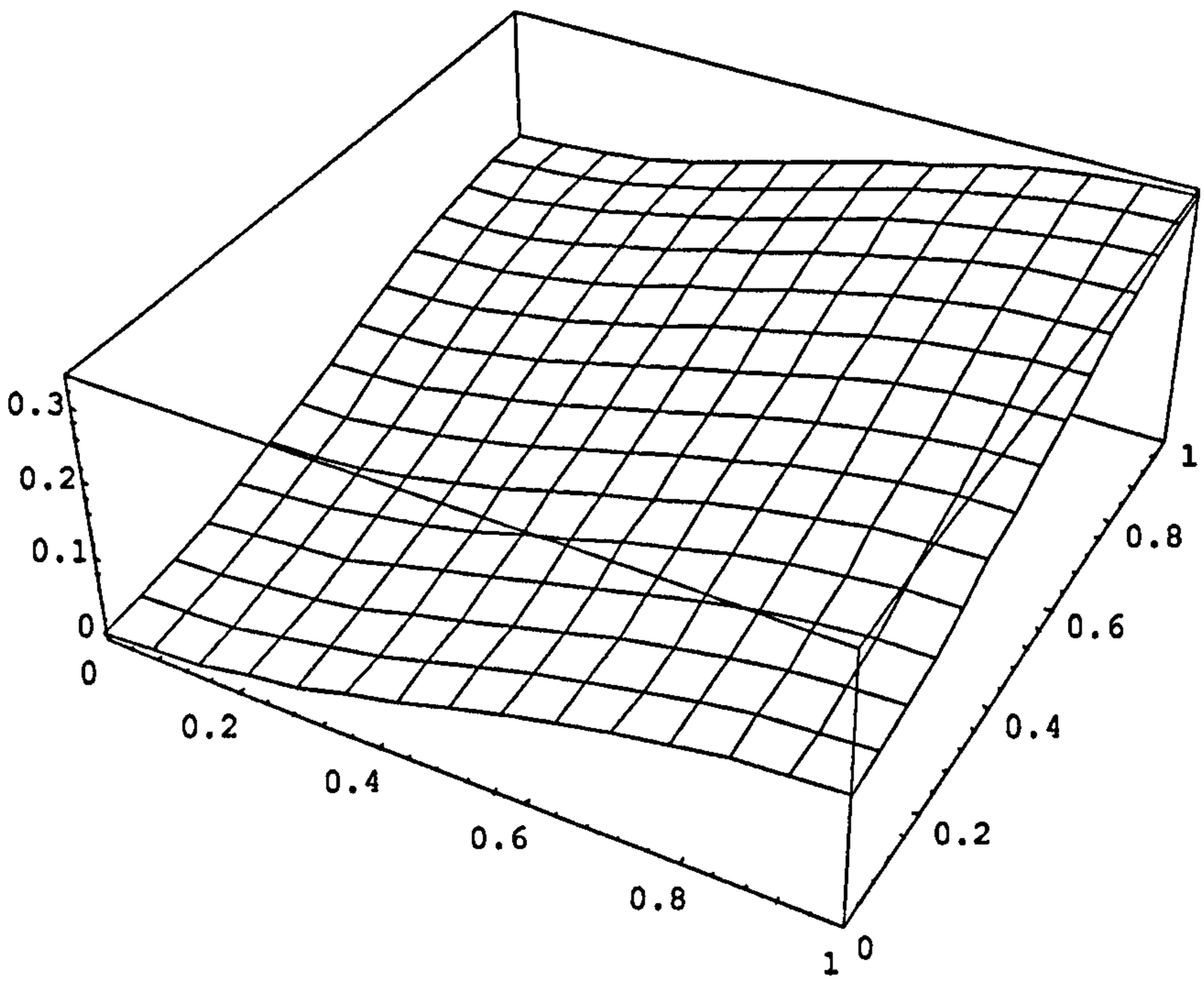

Figure 3.2 : 3D plot of the solution to the test problem.

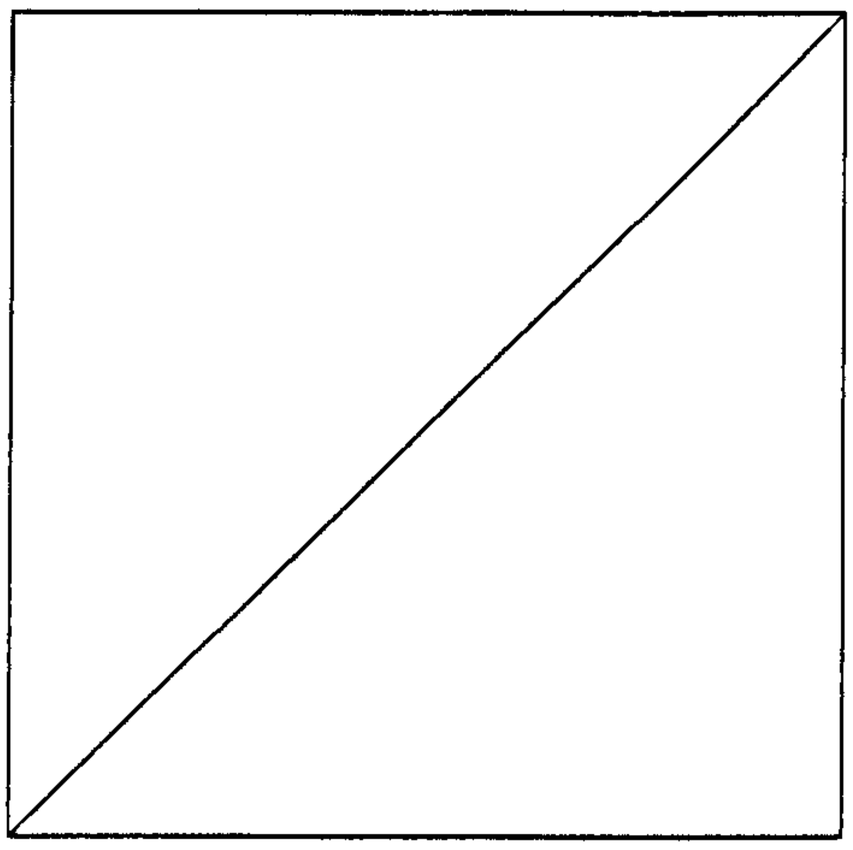

ne=2

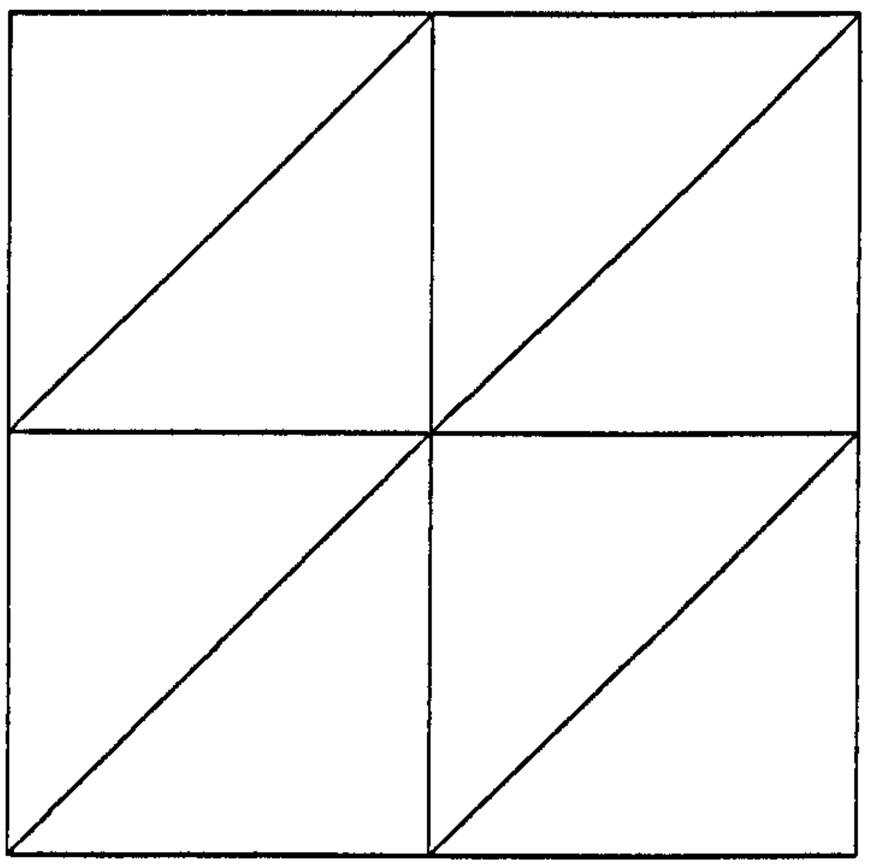

ne=4

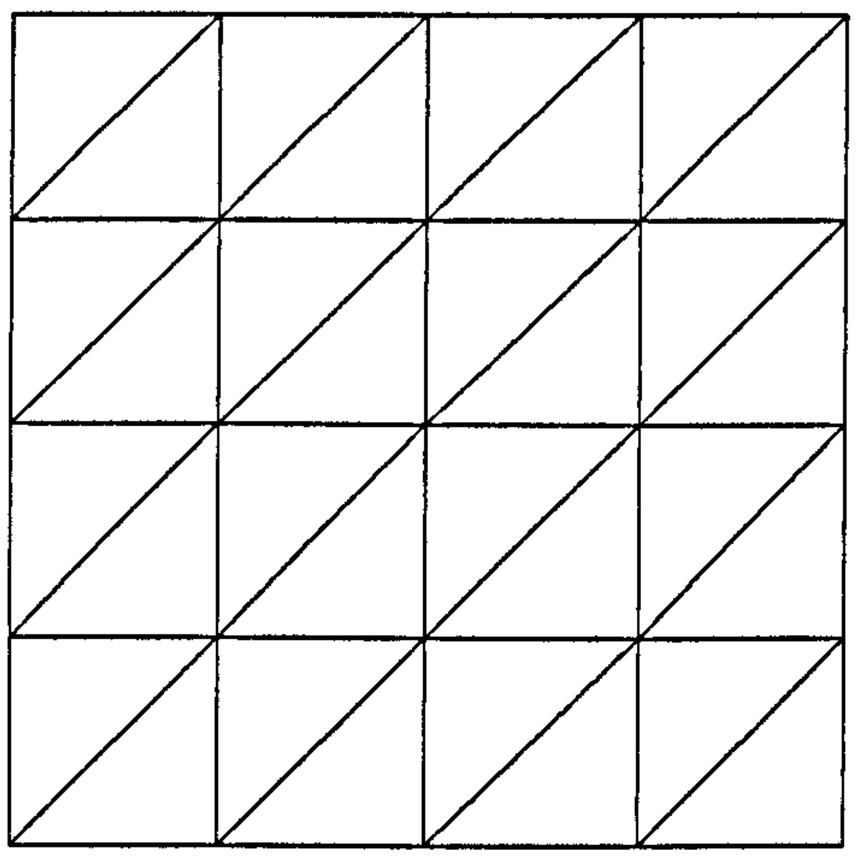

ne=32

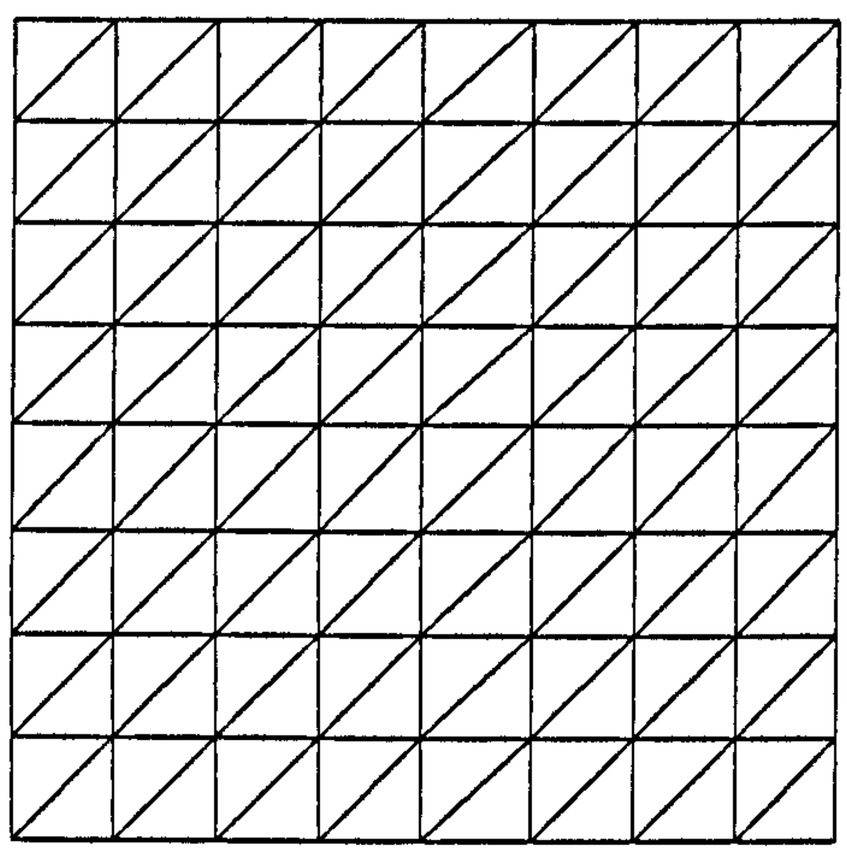

ne=128

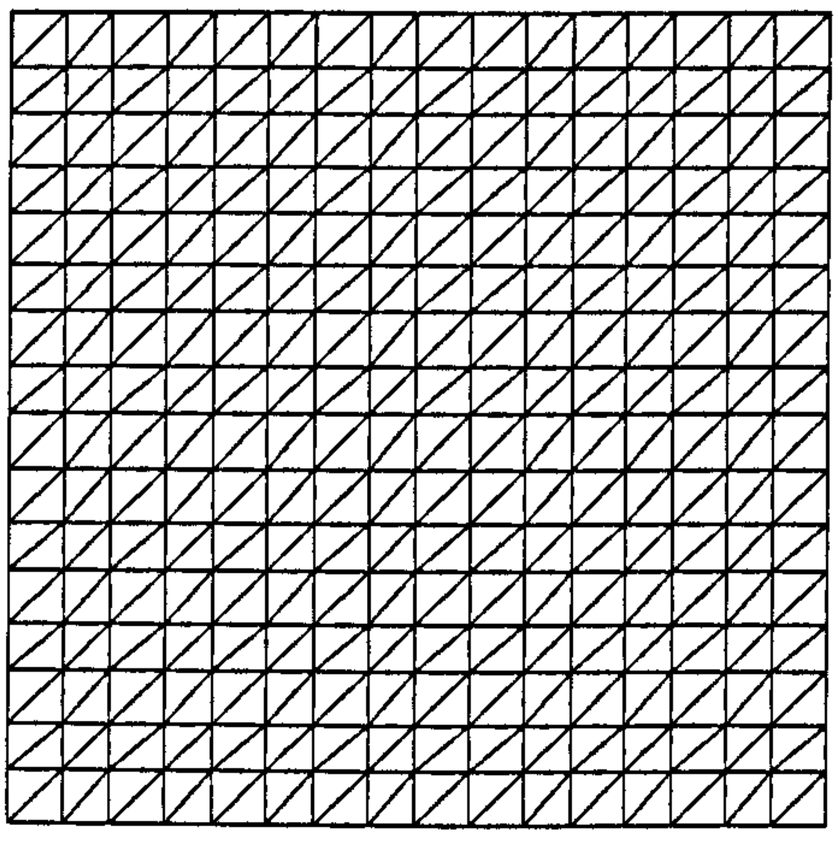

ne=512

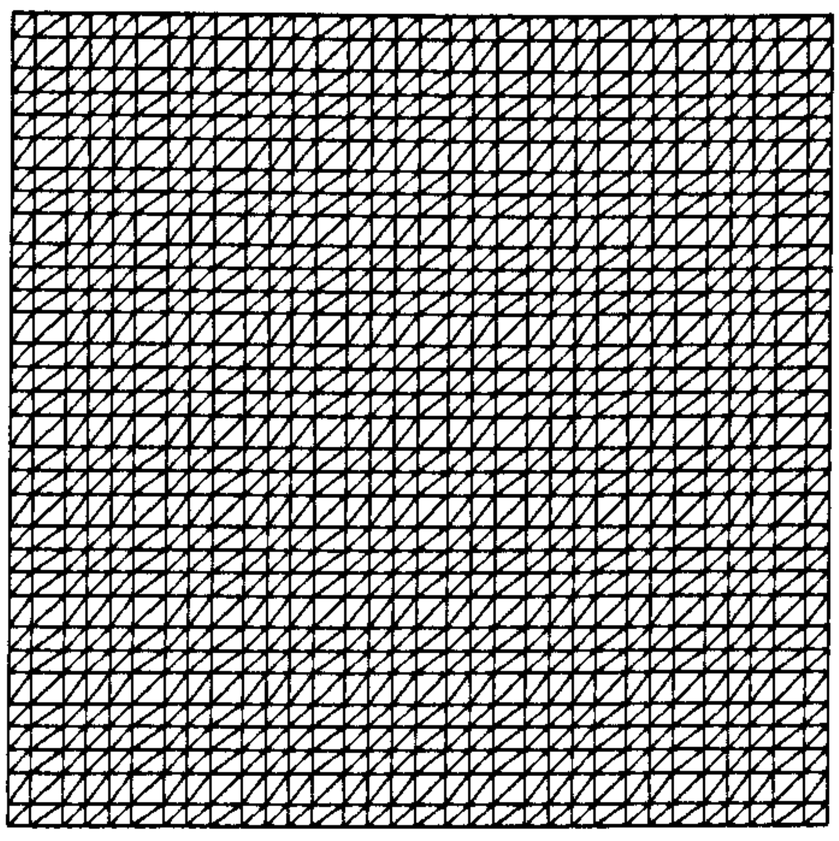

ne=2048

Figure 3.3 : Mesh used to calculate finite element solution to test problem.

Table 3.1 : Numerical results comparing three error estimators.

Case 1 : $\frac{b}{a} = 1$

ne	h	$\|\nabla e\|^2_{L_2}$	$\|\nabla ZZ\|^2_{L_2}$	$\|\nabla SPR\|^2_{L_2}$	$\|\nabla BW\|^2_{L_2}$
2	1.000000	4.09300E-2	1.98868E-3	1.98868E-3	2.31421E-2
4	0.500000	1.15664E-2	8.88582E-4	9.24959E-4	1.32317E-2
32	0.250000	3.23021E-3	2.40735E-3	2.41513E-3	3.55155E-3
128	0.125000	8.46949E-4	7.96819E-4	7.96333E-4	9.03527E-4
512	0.062500	2.15339E-4	2.13155E-4	2.13083E-4	2.28062E-4
2048	0.031250	5.41305E-5	5.41482E-5	5.41423E-5	5.72685E-5
8192	0.015625	1.35555E-5	1.35772E-5	1.35768E-5	1.43417E-5

Case 2 : $\frac{b}{a} = 100$

ne	h	$\|\nabla e\|^2_{L_2}$	$\|\nabla ZZ\|^2_{L_2}$	$\|\nabla SPR\|^2_{L_2}$	$\|\nabla BW\|^2_{L_2}$
2	1.000000	6.74905E-2	1.47194E-2	1.47194E-2	5.40213E-2
4	0.500000	1.36366E-2	1.88117E-3	1.91838E-3	3.14193E-2
32	0.250000	3.78229E-3	2.71821E-3	2.71778E-3	2.07138E-2
128	0.125000	9.65352E-4	8.24879E-4	8.24059E-4	1.10374E-2
512	0.062500	2.41431E-4	2.15121E-4	2.15038E-4	3.65515E-3
2048	0.031250	6.03682E-5	5.42752E-5	5.42690E-5	9.69251E-4
8192	0.015625	1.50958E-5	1.35852E-5	1.35848E-5	2.42867E-4

Case 3 : $\frac{b}{a} = 10000$

ne	h	$\|\nabla e\|^2_{L_2}$	$\|\nabla ZZ\|^2_{L_2}$	$\|\nabla SPR\|^2_{L_2}$	$\|\nabla BW\|^2_{L_2}$
2	1.000000	8.30971E-2	2.23836E-2	2.23836E-2	1.12878E-1
4	0.500000	1.84569E-2	3.92410E-3	3.95596E-3	1.74191E-1
32	0.250000	5.32167E-3	3.21553E-3	3.20666E-3	6.48174E-1
128	0.125000	1.63707E-3	1.00957E-3	1.00925E-3	1.51177E-0
512	0.062500	4.81329E-4	2.72085E-4	2.72066E-4	1.74764E-0
2048	0.031250	1.15714E-4	6.35947E-5	6.35912E-5	1.56037E-0
8192	0.015625	2.29018E-5	1.41625E-5	1.41621E-5	1.19302E-0

Chapter 4

Mesh Generation

4.1 Introduction

Although this thesis is concerned with the finite element solutions to frame problems, which use one-dimensional elements, two-dimensional meshes are required to discretize the beam cross-sections. Since we wish to deal with cross-sections of arbitrary shape we require a general method of 2D mesh generation.

For one dimensional problems generating the mesh is relatively straightforward; one has just to decide on the number of elements and then to divide the domain into that many intervals. For two dimensional problems the situation is quite complex. However, for geometrically simple domains, such as a rectangle, generating a mesh is not much more difficult than in one dimension. For example a triangular mesh for a rectangular domain may be generated using the following algorithms:

Generate the nodes

```
dx:= w/nx;
dy:= h/ny;
for i:= 0 to ny-1 do
begin
  for j:= 0 to nx-1 do
  begin
    x:= i*dx;
    y:= j*dy;
    Node:= CreateNode(x,y);
    Mesh.AddNode(Node);
  end;
end;
```

Generate the elements

```
for i:= 0 to ny-1 do
begin
  for j:= 0 to nx-1 do
  begin
    n1:= i*(nx+1)+j;
    n2:= n1+1;
    n3:= n1+nx+1;
    n4:= n3+1;
    Element:= CreateElement(n1,n2,n4);
    Mesh.AddElement(Element);
    Element:= CreateElement(n1,n2,n3);
    Mesh.AddElement(Element);
  end;
end;
```

where nx and ny are the number of elements along the base and height, respectively,

and `w` and `h` are the dimensions of the rectangle. In the algorithm listing object oriented notation has been used in which `Mesh` is an object containing lists of nodes and elements. The methods `AddNode` and `AddElement` add new nodes and elements to the mesh. Nodes and elements are created with the functions `CreateNode` and `CreateElement`, respectively.

For more complex geometries some techniques have been developed to map the rectangular mesh onto the more complicated domain. This approach is difficult to generalise for use with arbitrary polygonal domains. The technique that has been adopted here is to first define a coarse mesh with nodes only along the polygon sides and then to refine each element until some criterion is satisfied. This may be that the number of refinements reaches a limit or that the maximum element width is less than a specified number. In the later example only elements failing the criterion need to be refined. This method is particularly well suited for use with error estimates (Chapter 3) in which case the criterion is for the estimated error in the element to be less than a given tolerance. Obviously, the finite element solution must be calculated for each mesh which may seem wasteful. However, if an iterative solver is used, such as the Conjugate Gradient Method, then the solution from each stage may be used as the solver's starting vector for the next. This may not be a great saving but, as it is easy to implement, it is better to do so than not.

4.2 The mesh generation algorithm

The algorithm for generating a 2D mesh is presented here. To illustrate the algorithm it is applied to the domain in Figure 4.1a.

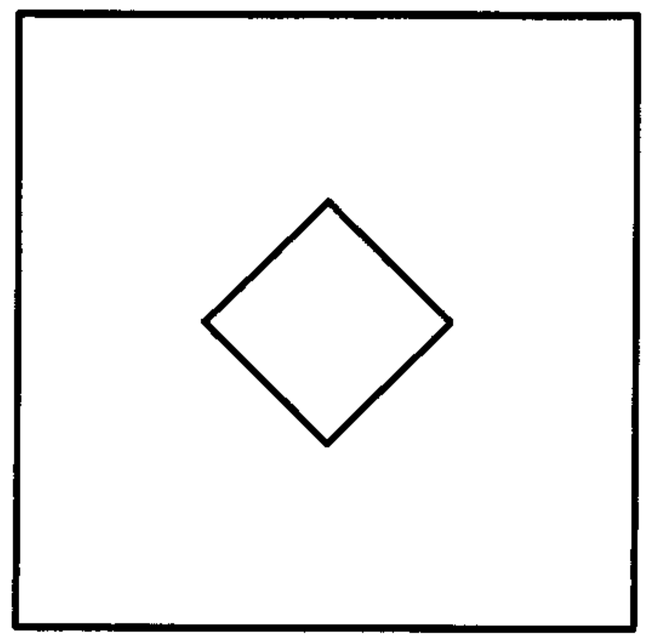

a) Example domain to be meshed.

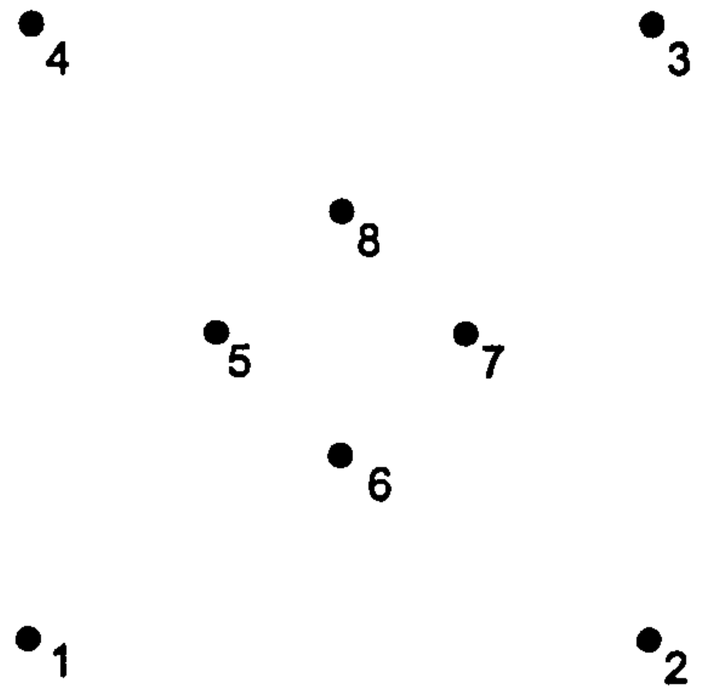

b) Domain nodes.

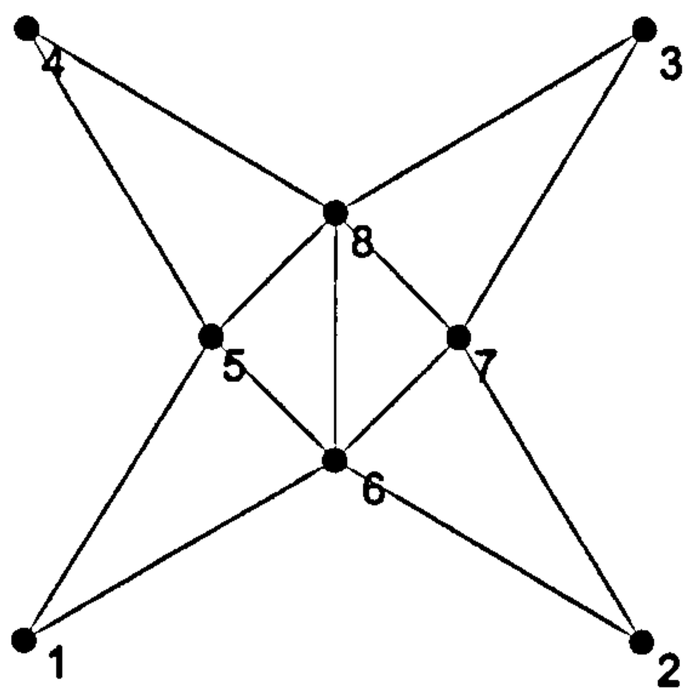

c) Delaunay triangulated nodes.

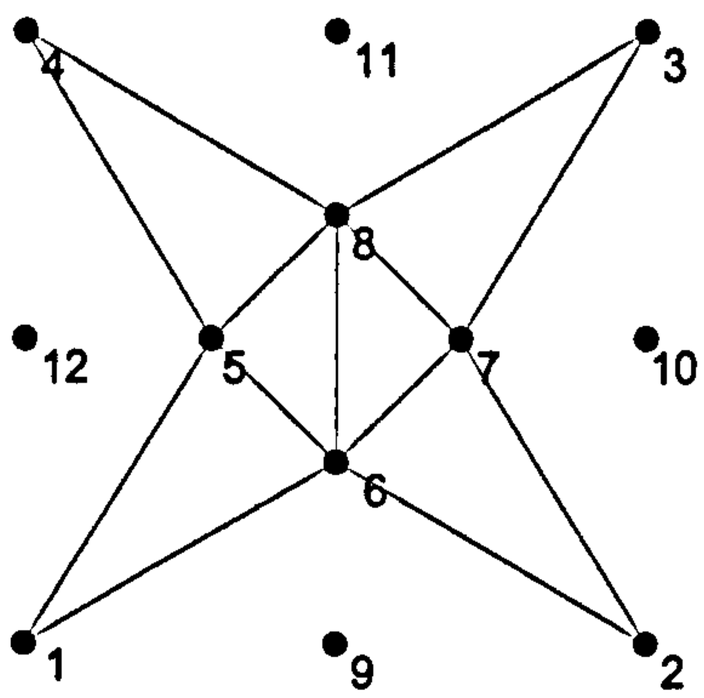

d) Add new domain nodes.

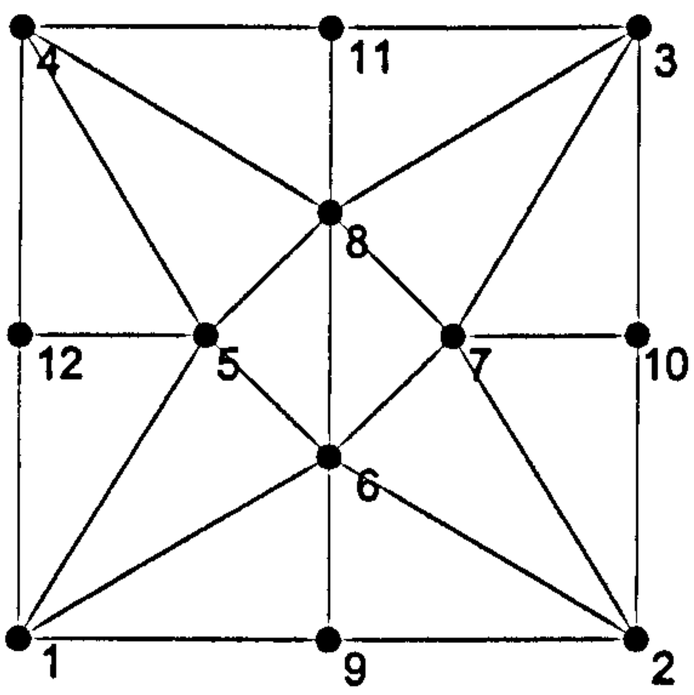

e) Final Delaunay triangulation.

Figure 4.1 - Example illustrating the mesh generation algorithm.

Step 1

Define the domain and subdomains in terms of polygons. The subdomains define areas of different material properties, i.e. the functions a, b, f and g in Section 3.1. Define a data structure to store the polygons indexed such that any subdomain has a higher index than the domain that surrounds it. The data structure for Figure 4.1a is

Polygon Index	Vertices
1	(0,0), (100, 0), (100, 100), (0, 100)
2	(30, 50), (50, 30), (70, 50), (50, 70)

Step 2

Define the nodes as the vertices of the polygons. Store the nodes in a data structure being sure not to include duplicates. Define a data structure that represents the polygons in terms of node numbers. The data structures for Figure 4.1a are

Node Index	x	y
1	0	0
2	100	0
3	100	100
4	0	100
5	30	50
6	50	30
7	70	50
8	50	70

Polygon Index	Nodes
1	1,2,3,4
2	5,6,7,8

and these are illustrated in Figure 4.1b.

Step 3

Triangulate the nodes. This requires four sub-steps:

3.1: Apply the Delaunay triangulation algorithm to the nodes. This is explained in the next section. The Delaunay triangulation of the nodes listed in Step 2 is

Triangle Index	Node Indices		
1	1	6	5
2	2	7	6
3	3	8	7
4	4	5	8
5	5	6	8
6	6	7	8

which is illustrated in Figure 4.1c.

3.2: Check that the triangle edges are consistent with the polygon sides. This is done using the polygon nodes data structure defined in Step 2. The triangle edges are consistent with the polygons if every polygon side is a triangle edge. If the test fails then create new nodes at the midpoint of every polygon side that is not an edge in the Delaunay triangulation. Update the polygon nodes data structure. In the example none of the sides of polygon 1 are triangle edges therefore nodes are added at (50, 0), (100, 50), (50, 100) and (0, 50). Hence the data structures in Step 2 are modified to

Node Index	x	y
1	0	0
2	100	0
3	100	100
4	0	100
5	30	50
6	50	30
7	70	50
8	50	70
9	50	0
10	100	50
11	50	100
12	0	50

Polygon Index	Nodes
1	1,9,2,10,3,11,4,12
2	5,6,7,8

3.3: Add the new nodes to the Delaunay data structure if needed as a result of 3.2. In the case of the example, when nodes 9, 10, 11 and 12 have been added, the new data structure is as follows.

Triangle Index	Node Indices		
1	1	9	6
2	1	6	5
3	1	5	12
4	2	10	7
5	2	7	6
6	2	6	9
7	3	11	8
8	3	8	7
9	3	7	10
10	4	12	5
11	4	5	8
12	4	8	11
13	5	6	8
14	6	7	7

3.4: Repeat steps 3.2 and 3.3 until the polygons are consistent with the Delaunay

triangulation. In the example all polygon sides match triangle edges and so no more nodes are needed. The triangulation is complete.

Step 4

Identify the elements that need refining and create new nodes along their edges. Add the nodes to the Delaunay data structure as in step 3.3 then repeat steps 3.2 to 3.4. For the example we will not refine any elements.

Step 5

Assign the correct polygon index to each triangle. Each triangle is initially assigned a null polygon index (say 0). Starting with the polygon with the highest index a test is made on each element (with a null polygon index) to see if it lies inside the current polygon. If it does then the element's polygon index is set and the remaining elements are tested with the next polygon (in descending order). After the elements have been tested with polygon 2 all remaining elements (whose polygon index is null) have their polygon index set to 1.

The test to determine whether an element lies inside a polygon is performed by triangulating the polygon (using step 3) then testing to see if the centroid of the element lies inside any of the polygon's triangles.

For the example we first triangulate polygon 2:

Triangle index	vertices		
1	(30, 50)	(50, 30)	(50, 70)
2	(50, 30)	(70, 50)	(50, 70)

Then we test each element to see if it's centroid lies inside one of the elements:

Element index	Lies inside triangle
1	no
2	no
3	no
4	no
5	no
6	no
7	no
8	no
9	no
10	no
11	no
12	no
13	1
14	2

Elements 13 and 14 lie inside polygon 2 and so their polygon indices are set to 2. Elements 1 to 12 have their polygon indices set to 1:

Element index	Polygon Index
1	1
2	1
3	1
4	1
5	1
6	1
7	1
8	1
9	1
10	1
11	1
12	1
13	2
14	2

That completes the mesh generation. The next section describes the Delaunay triangulation process that is used in Step 3.

4.3 Delaunay triangulation

In 1850 Dirichlet proposed a systematic method for the decomposition of a given domain into a set of packed convex polygons. Given a set of points the Dirichlet tesselation assigns to each a region that is closer to that point than any other in the set. This results in a set of non-overlapping convex polygons covering the entire domain. Another name for this structure, which comes from computational geometry, is a Voronoi diagram and the convex polygons are known as Voronoi regions. Let the set of points be denoted by $\{p_i : i = 1, \ldots, n\}$ then the Voronoi region V_i is defined as

$$V_i = \{p : |p - p_i| < |p - p_j|, j \neq i\} \tag{4.1}$$

Let us consider the two dimensional case. If there are only two points in the set then the Voronoi diagram is just a line dividing the plane equally between the points (Figure 4.2a). If another point is added then the diagram consists of three lines dividing the plane between the three points as shown in Figure 4.2b. The lines meet a point called a Voronoi vertex. The three points define a triangle whose sides bisect the Voronoi lines at right angles. As more points are added (see Figure 4.2c) more triangles are defined with this relation to the Voronoi diagram. The resulting triangulation is known as a Delaunay triangulation. It has the property that no defining point of any one triangle lies in the circle circumscribing the defining points of any other triangle.

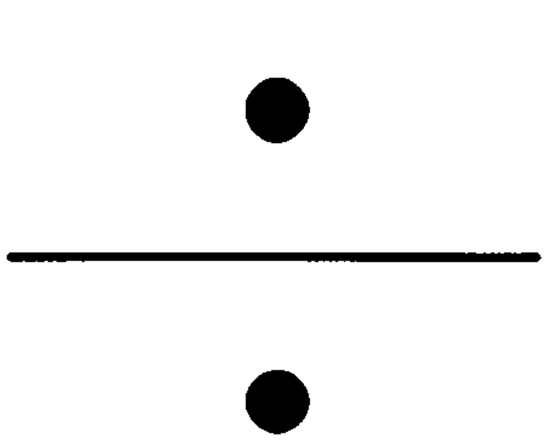

Figure 4.2a

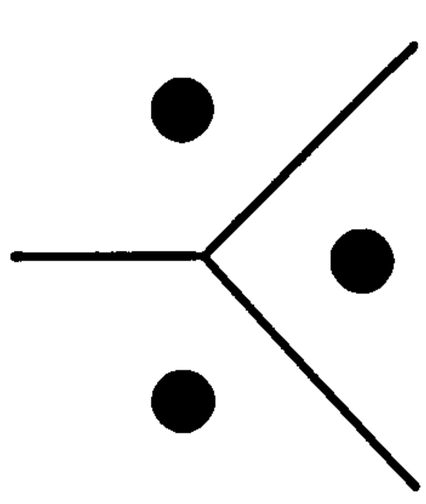

Figure 4.2b

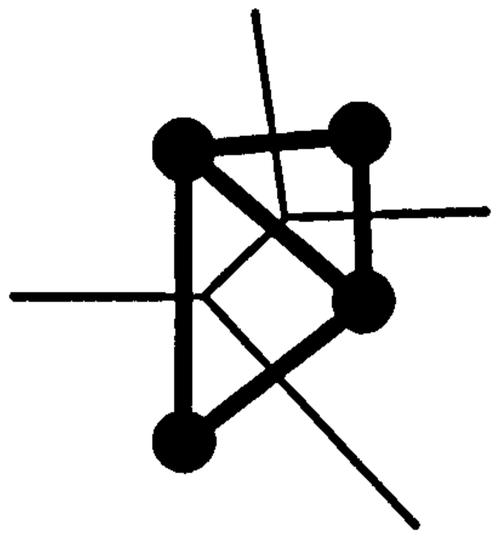

Figure 4.2c

The structure of the Voronoi diagram and Delaunay triangulation may be completely described by two lists for each Voronoi vertex; a list of forming points which define the Delaunay triangle and a list of the neighbouring vertices. In n dimensions each vertex will have $n + 1$ forming points and the same number of neighbouring vertices.

The algorithm for constructing a Delaunay triangulation for any given set of points is a sequential one. Each point is added, one by one, to an existing structure in which some Voronoi vertices are destroyed and new ones created to form the new Voronoi diagram and Delaunay triangulation. Initially one must create a structure such that the Delaunay triangulation encloses all the points of the set. After all points have been added to the structure the exterior triangles are removed. As an example consider the square in Figure 4.3a. Initially we create a simple Voronoi diagram that surrounds the points (Figure 4.3b). We enter the points one by one into the Voronoi diagram (Figures 4.3c and 4.3d). Finally the outer hull is removed to leave the triangulation of the square (Figure 4.3e).

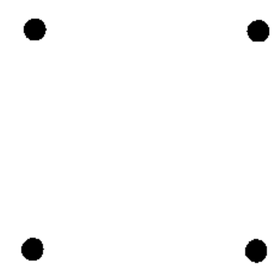

a) Points to be triangulated.

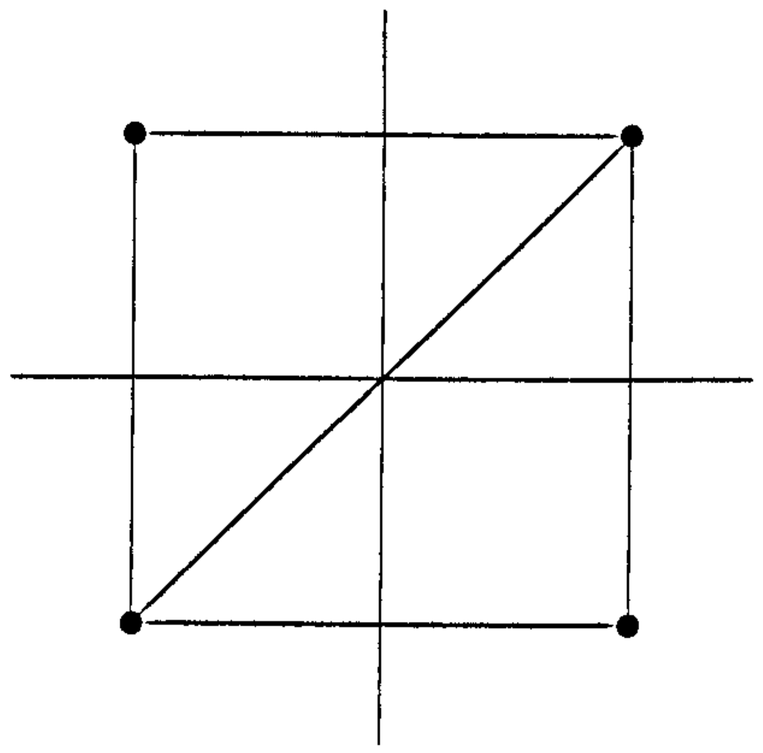

b) Initial Voronoi diagram.

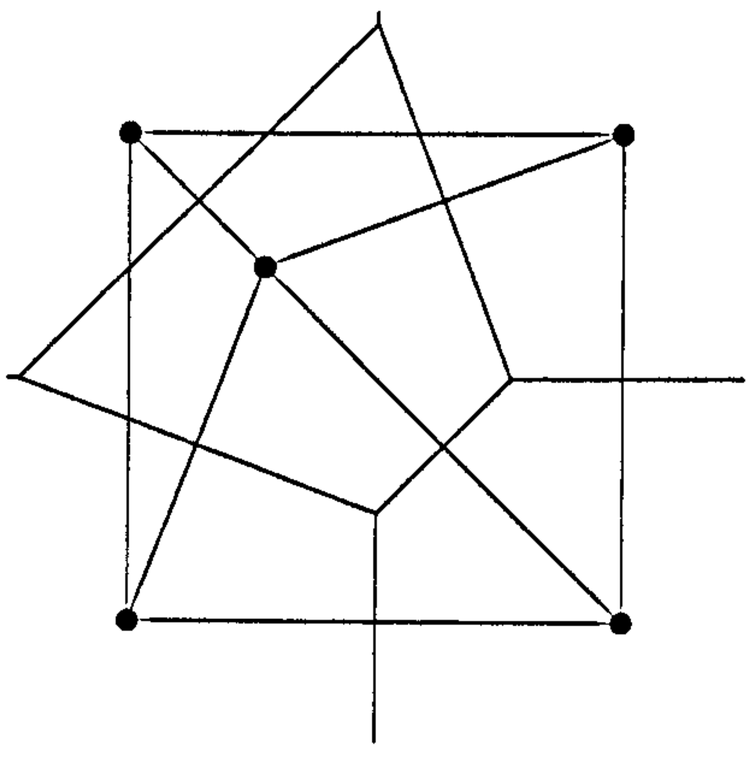

c) Voronoi diagram after adding first point.

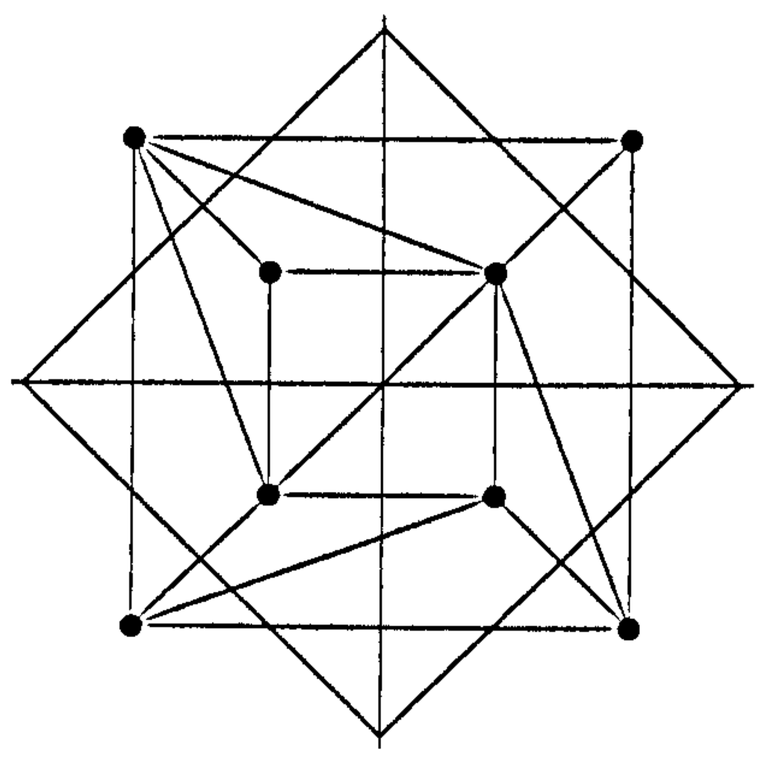

d) Voronoi diagram after adding all points.

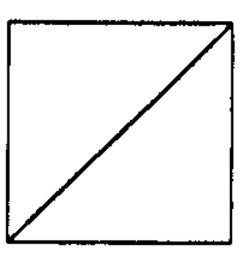

e) Voronoi diagram with outer hull and Voronoi vertices removed.

Figure 4.3 - Illustration of how the Voronoi algorithm triangulates a square.

The details of the algorithm are now presented in six steps. Where necessary object oriented pseudo-code shall be used with the following data structures:

```
VoronoiPoint
  x :  float
  y :  float

VoronoiVertex
  FormingPoints :  array[1..3] of integer
  Neighbours :  array[1..3] of integer
  x :  float
  y :  float
  SquareRadius :  float
  Tag :  integer
  DistanceFrom(px, py) = Sqr(x-px) + Sqr(x-py)
  TestPoint(px,py) = DistanceFrom(px, py) <= SquareRadius

Triangle
  p1 :  integer
  p2 :  integer
  p3 :  integer

Points :  array of VoronoiPoint
Vertices :  array of VoronoiVertex
  Triangles :  array of Triangle
```

Notes

The `Voronoi vertex` property `FormingPoints` stores the point indices of the three forming points.

The `Voronoi vertex` property `Neighbours` stores the vertex indices of the three neighbouring vertices.

The `VoronoiVertex` property `SquareRadius` stores the square of the radius of the circle that circumscribes the three forming points.

The `VoronoiVertex` property `Tag` provides a way of tagging a vertex. It is used in the search routine in Step 3 to prevent a vertex being tested more than once.

Step 1

Define the initial structure. This may be defined by four points forming a rectangle that encloses all the points that are to be added.

Voronoi Diagram

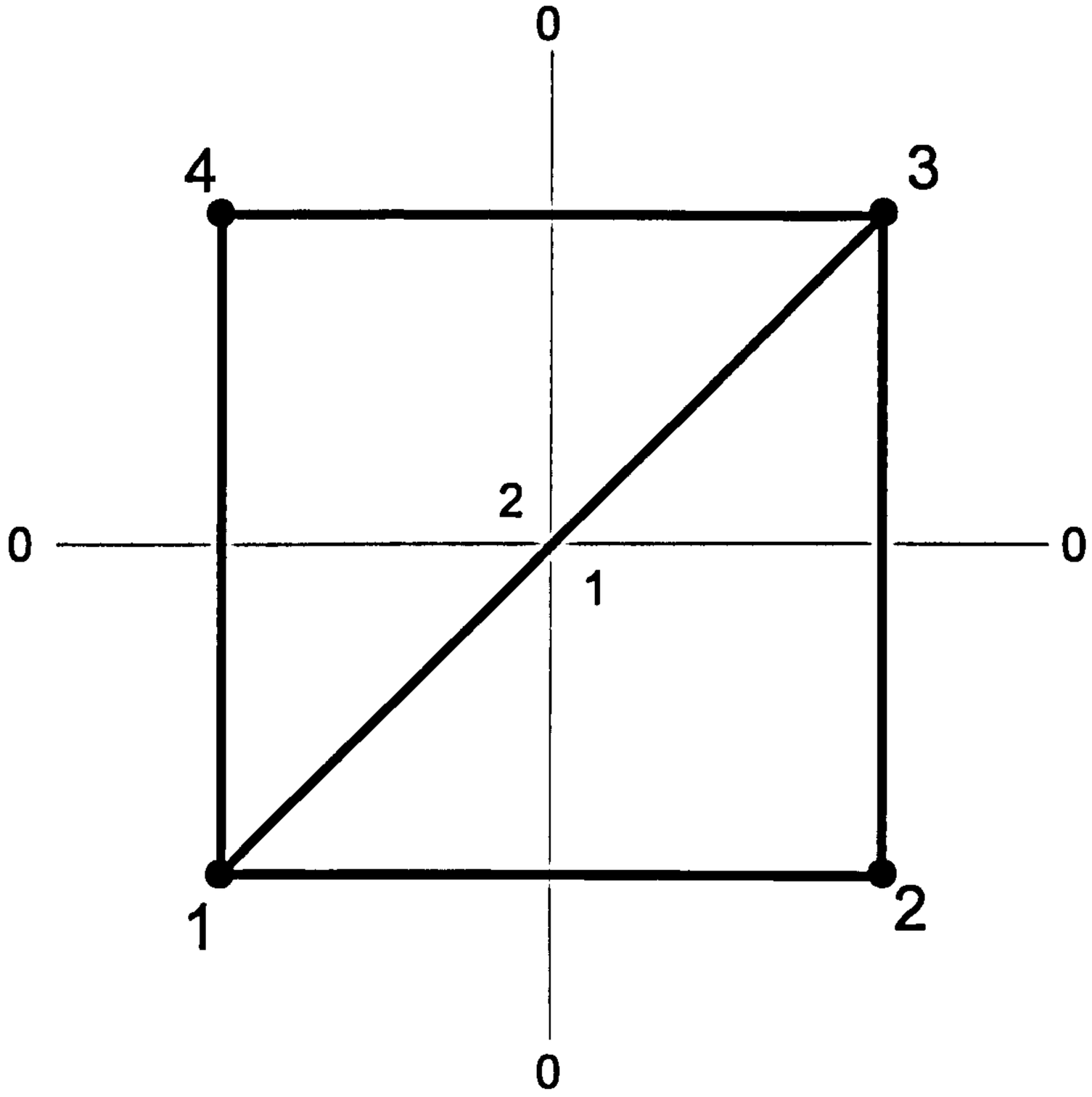

Voronoi Data Structure

Vertex	Forming Points			Neighbouring Vertices		
1	1	2	3	0	0	1
2	1	3	4	1	0	0

where 0 denotes a null index; i.e. points to no defined vertex. Each triangle edge bisects a Voronoi edge that leads to a neighbouring Vertex. For example, vertex 1 and vertex 2 are neighbours joined by a Voronoi polygon edge. Their forming point triangles share a triangle edge from point 1 to point 3 which bisects the Voronoi edge at right angles. This is not immediately clear from the diagram as the Voronoi edge has zero length.

Step 2

Add the new point anywhere within the outer rectangle. In the example below point number 6 is being added to the data structure after point number 5 has already been added.

Voronoi Diagram

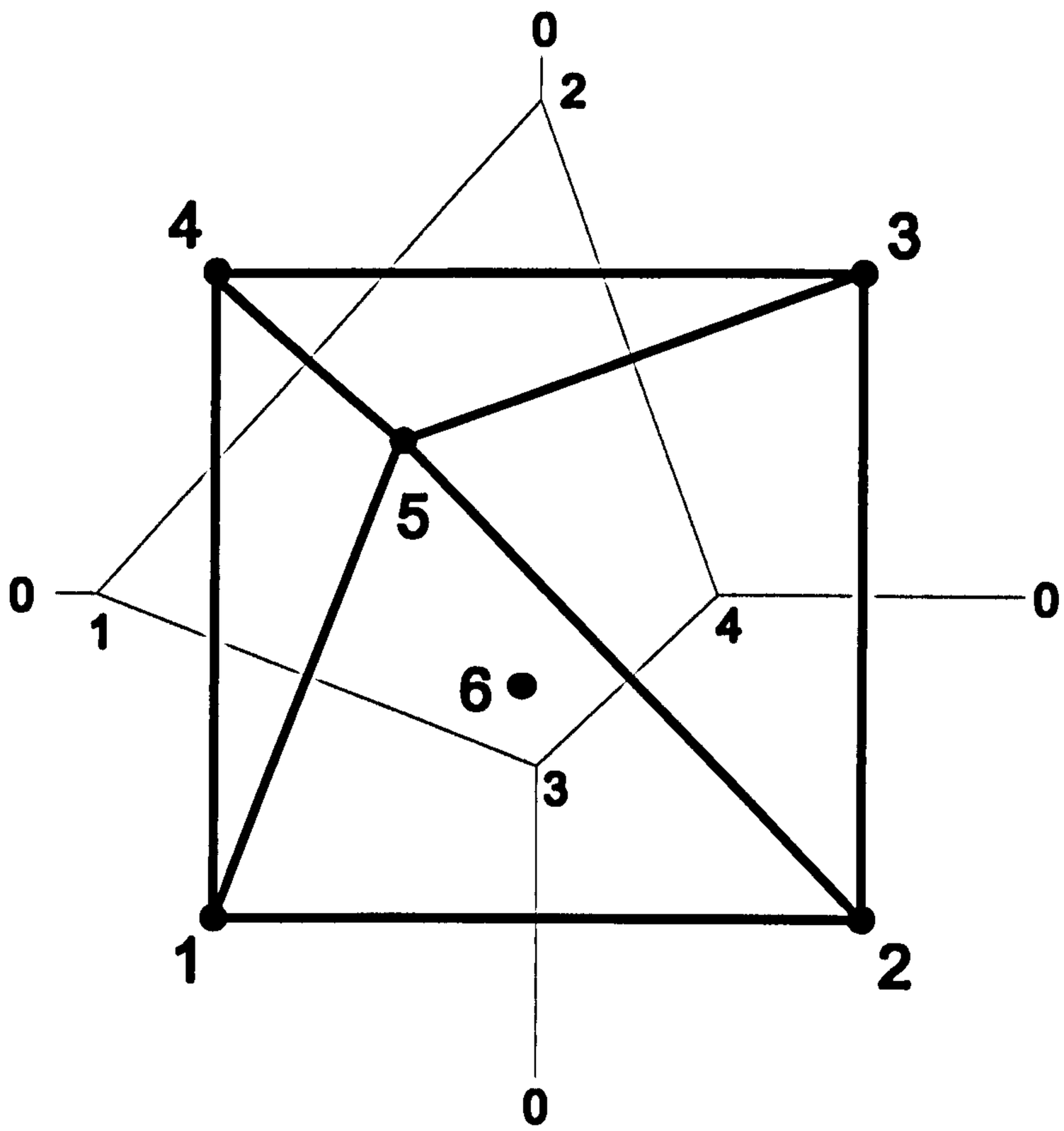

Voronoi Data Structure

Vertex	Forming Points			Neighbouring Vertices		
1	4	1	5	0	3	2
2	3	4	5	0	1	4
3	1	2	5	0	4	1
4	2	3	5	0	2	3

Note that this is the Voronoi structure prior to the addition of point 6.

Step 3

Determine all vertices of the Voronoi diagram that must be deleted. These are the vertices whose forming points define a circle (passing through each forming point) that encloses the new point. In the example illustrated in Step 2 vertex numbers 3 and 4 are to be deleted. This step involves a search process to identify a starting vertex whose circle encloses the new point. Once a starting vertex has been found all the other vertices to be deleted can be found by following the neighbouring vertex links. The search process to locate the starting vertex follows the neighbouring vertex links from an initial vertex, the particular path depending on which neighbouring vertex is closer to the new point.

Pseudo-code

This is a simple bubble sort routine to sort an array of vertices indices, v, into the order of their distance from the new point :

```
procedure Swap(a, i, j)
begin
   temp := a[i]
   a[i] := a[j]
   a[j] := temp
end
```

```
procedure SortVertices(v)
begin
   for i := 1 to 3 do
      d[i] := Vertices[v[i]].DistanceFrom(NewPoint.x, NewPoint.y)
   for i := 1 to 3 do
   begin
      if v[i] > 0 then
      begin
         for j := 1 to 3 do
         begin
            if v[j] > 0 and d[j] < d[i] then
            begin
               Swap(v, i, j)
               Swap(d, i, j)
            end
         end
      end
   end
end
```

Continued...

Starting with the last vertex to be created follow the neighbouring vertex links until a vertex is found that needs to be deleted. The algorithm recursively calls the procedure `Search`. To ensure a vertex is not searched more than once the `Tag` property of each vertex is set to the current point index :

```
global variables
  p :  integer
  found :  boolean

procedure Search(v)
begin
  if not found and v > 0 then
  begin
    if Vertices[v].Tag <> p then
    begin
      Vertices[v].Tag := p
      found := Vertices[v].TestPoint(NewPoint.x, NewPoint.y)
      if found then
        StartingVertex := v
      else
      begin
        for i := 1 to 3 do nv[i] := Vertices[v].Neighbours[i]
        SortVertices(nv)
        for i := 1 to 3 do Search(nv[i])
      end
    end
  end
end

p := Length(Points)
found := False
Search(Length(Vertices))
```

Continued...

Find the other vertices to be deleted by testing every neighbouring vertex and every neighbour's neighbouring vertices. To ensure against repeated testing set the Tag property of each vertex tested to the current point index :

```
SetLength(VerticesToBeDeleted, 1)
VerticesToBeDeleted[1] := v
TestVertexNeighbours(v)

p := Length(Points)
i := 1
while i <= Length(VerticesToBeDeleted) do
begin
  v := VerticesToBeDeleted[n]
  for j := 1 to 3 do
  begin
    nv := Vertices.Neighbours[j]
    if Vertices[nv].Tag <> p then
    begin
      Vertices[nv].Tag := p
      if Vertices[nv].TestPoint(Points[p].x, Points[p].y) then
      begin
        n := Length(VerticesToBeDeleted) + 1
        VerticesToBeDeleted[n] := nv
      end
    end
  end
  inc(i)
end
```

Step 4

Create a list of the new vertices including their forming points and one neighbouring vertex. Removing the triangle edges that bisect the lines joining neighbouring vertices that have been marked for deletion leaves a convex polygon enclosing those vertices. The list of new vertices is created by listing the sides of the convex polygon. Each side is defined by two points which will be the first two forming points of a new vertex. The remaining forming point will be the new one added in step 2. Each side connects to a neighbouring vertex. This will be the first neighbour of the new vertex.

Data for new vertices

Side	Forming Points		Neighbouring Vertex
1	1	2	0
2	2	3	0
3	3	5	2
4	5	1	1

Pseudo-code

Test the neighbours of each vertex in `VerticesToBeDeleted` to see if they themselves are marked for deletion. If a neighbour is not in `VerticesToBeDeleted` then create a new vertex. The first two forming points are those common to the vertex and the neighbour. The other is the new point. The first neighbour of the new vertex is the neighbour of the deleted vertex. The new vertex is created and stored in `NewVertices`:

```
For i := 1 to Length(VerticesToBeDeleted) do
begin
  for j := 1 to 3 do
  begin
    v := VerticesToBeDeleted[i]
    if not (Vertices[v].Neighbours[j] in VerticesToBeDeleted) then
    begin
      n := Length(NewVertices) + 1
      SetLength(NewVertices, n)
      NewVertices[n].FormingPoints[1] := Vertices[v].FormingPoints[j]
      if j=3 then
        NewVertices[n].FormingPoints[2] := Vertices[v].FormingPoints[1]
      else
        NewVertices[n].FormingPoints[2] := Vertices[v].FormingPoints[j+
      NewVertices[n].Neighbours[1] := Vertices[v].Neighbours[j]
      p := Length(Points)
      NewVertices[n].FormingPoints[3] := p
    end
  end
end
```

Step 5

Add the new vertices to the vertex list overwriting deleted entries.

Voronoi Data Structure

Vertex	Forming Points			Neighbouring Vertices		
1	4	1	5	0	3	2
2	3	4	5	0	1	4
3	3	5	6	2	?	?
4	2	3	6	0	?	?
5	1	2	6	0	?	?
6	5	1	6	1	?	?

Pseudo-code

We will want to know where the new vertices have been stored in `Vertices` so we will store the mapping from `NewVertices` to `Vertices` in `NewVertexIndices` :

```
SetLength(NewVertexIndices, Length(NewVertices))
```

First overwrite deleted vertices :

```
for i := 1 to Length(VerticesToBeDeleted) do
begin
  v := VerticesToBeDeleted[i]
  Vertices[v] := NewVertices[i]
  NewVertexIndices[i] := v
end
```

Now create new vertices if necessary :

```
for i := Length(VerticesToBeDeleted) + 1 to Length(NewVertices) do
begin
  v := Length(Vertices) + 1
  SetLength(Vertices, v)
  Vertices[v] := NewVertices[i]
  NewVertexIndices[i] := v
end
```

Step 6

Update the neighbour links of the new vertices and the vertices that surround them by searching for common forming points.

Voronoi Diagram

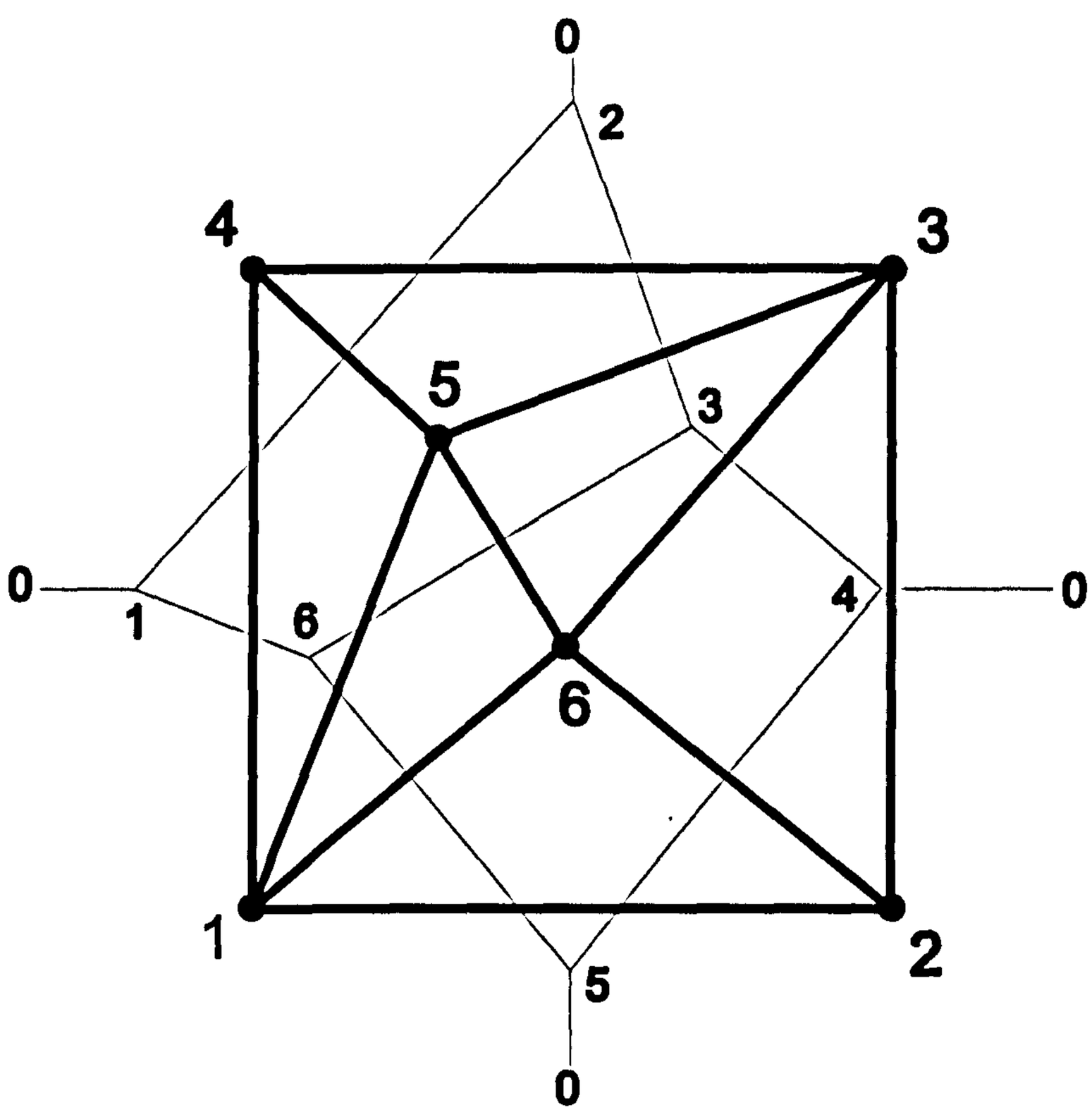

Voronoi Data Structure

Vertex	Forming Points			Neighbouring Vertices		
1	4	1	5	0	6	2
2	3	4	5	0	1	3
3	3	5	6	3	6	4
4	2	3	6	0	3	5
5	1	2	6	0	4	6
6	5	1	6	4	5	3

Pseudo-code

Update the neighbours of the surrounding vertices :

```
for i := 0 to Length(NewVertices) do
begin
  v := NewVertexIndices[i]
  p1 := Vertices[v].FormingPoints[1]
  p2 := Vertices[v].FormingPoints[2]
  w := Vertices[v].Neighbours[1]
  if w > 0 then
  begin
    if Vertices[w].FormingPoints[1] = p1 then
      Vertices[w].Neighbours[3] := v
    else if Vertices[w].FormingPoints[2] = p1 then
      Vertices[w].Neighbours[1] := v
    else
      Vertices[w].Neighbours[2] := v
  end
end
```

Complete the neighbours of the new vertices :

```
for i := 1 to Length(NewVertices) do
begin
v := NewVertexIndices[i]
p1 := Vertices[v].FormingPoints[2]
p2 := Vertices[v].FormingPoints[3]
j := 1
while j <= Length(NewVertices) do
begin
  if (j <> i) then
  begin
    w := NewVertexInices[j]
    q1 := Vertices[w].FormingPoints[2]
    q2 := Vertices[w].FormingPoints[3]
    if (p1 = q2) and (p2 = q1) then
    begin
      Vertices[v].Neighbours[2] := w
      Vertices[w].Neighbours[3] := v
    end
  end
  inc(j)
 end
end
```

Step 7

Calculate the coordinates and square radius for each new vertex.

Pseudo-code

```
Function VoronoiVertex.CalculateValues
begin
  x1 := Points[FormingPoints[1]].x
  x2 := Points[FormingPoints[2]].x
  x3 := Points[FormingPoints[3]].x
  y1 := Points[FormingPoints[1]].y
  y2 := Points[FormingPoints[2]].y
  y3 := Points[FormingPoints[3]].y
  x12 := x1 - x2
  x23 := x2 - x3
  y12 := y1 - y2
  y23 := y2 - y3
  c1 := Sqr(x1) - Sqr(x2) + Sqr(y1) - Sqr(y2)
  c2 := Sqr(x2) - Sqr(x3) + Sqr(y2) - Sqr(y3)
  x := 0.5 * (c1 * y23 - c2 * y12) / (x12 * y23 - x23 * y12)
  y := 0.5 * (c1 * x23 - c2 * x12) / (y12 * x23 - y23 * x12)
  SquareRadius := Sqr(x1-x) + Sqr(y1-y)
end
```

```
for i := 1 to Length(NewVertices) do
begin
  v := NewVertexIndices[i]
  Vertices[v].CalculateValues
end
```

Step 8

Repeat steps 2 to 7 until all points have been added.

Step 9

Remove triangles connected to the initial structure. This may be achieved with a function that returns the triangulation of points from the Voronoi Structure. In the following example a list of points has been added to a voronoi structure that initially has 4 points. Hence a point that has index i has index $i + 4$ in the Voronoi diagram.

Pseudo-code

```
Function GetTriangles
begin
  For i:= 1 to Length(Vertices) do
  begin
    p1:= Vertices[i].FormingPoints[1]-4
    p2:= Vertices[i].FormingPoints[2]-4
    p3:= Vertices[i].FormingPoints[3]-4
    if p1 > 0 and p2 > 0 and p3 > 0 then
    begin
      n := Length(Triangles) + 1
      SetLength(Triangles, n)
      Triangles[n].p1 := p1
      Triangles[n].p2 := p2
      Triangles[n].p3 := p3
    end;
  end;
end;
```

For applications in finite element modelling we only want triangles inside the polygonal boundary. An example of how the Delaunay algorithm may result in unwanted triangles outside the boundary is illustrated in Figure 4.4. Here, the boundary is given, anticlockwise, by nodes 1, 2, 3, 4, 5 and 6 but the Delaunay algorithm has created a triangle with nodes 5, 1 and 6. Fortunately it is easy to test whether or not a triangle lies inside the boundary since the nodal order is always anticlockwise. In this particular example the first triangle node is 5 and the next is 1. If the triangle was inside the boundary then the next boundary node that is also in the triangle would be 1. The next boundary node is actually 6 so the triangle does not lie inside the boundary.

Pseudo-code

Let Boundary denoted the list of node numbers on the boundary ordered anticlockwise. Let p1, p2 and p3 be the indices of the triangle points. The function returns true if the triangle lies inside the polygon boundary :

```
function TestTriangle(p1, p2, p3)
begin
  j := IndexOf(Boundary, p1)
  repeat
    if j = Length(Boundary) then
      j := 1
    else
      j := j + 1
    p:= Boundary[j]
  until p=p2 or p=p3
  Result := p = p2
end
```

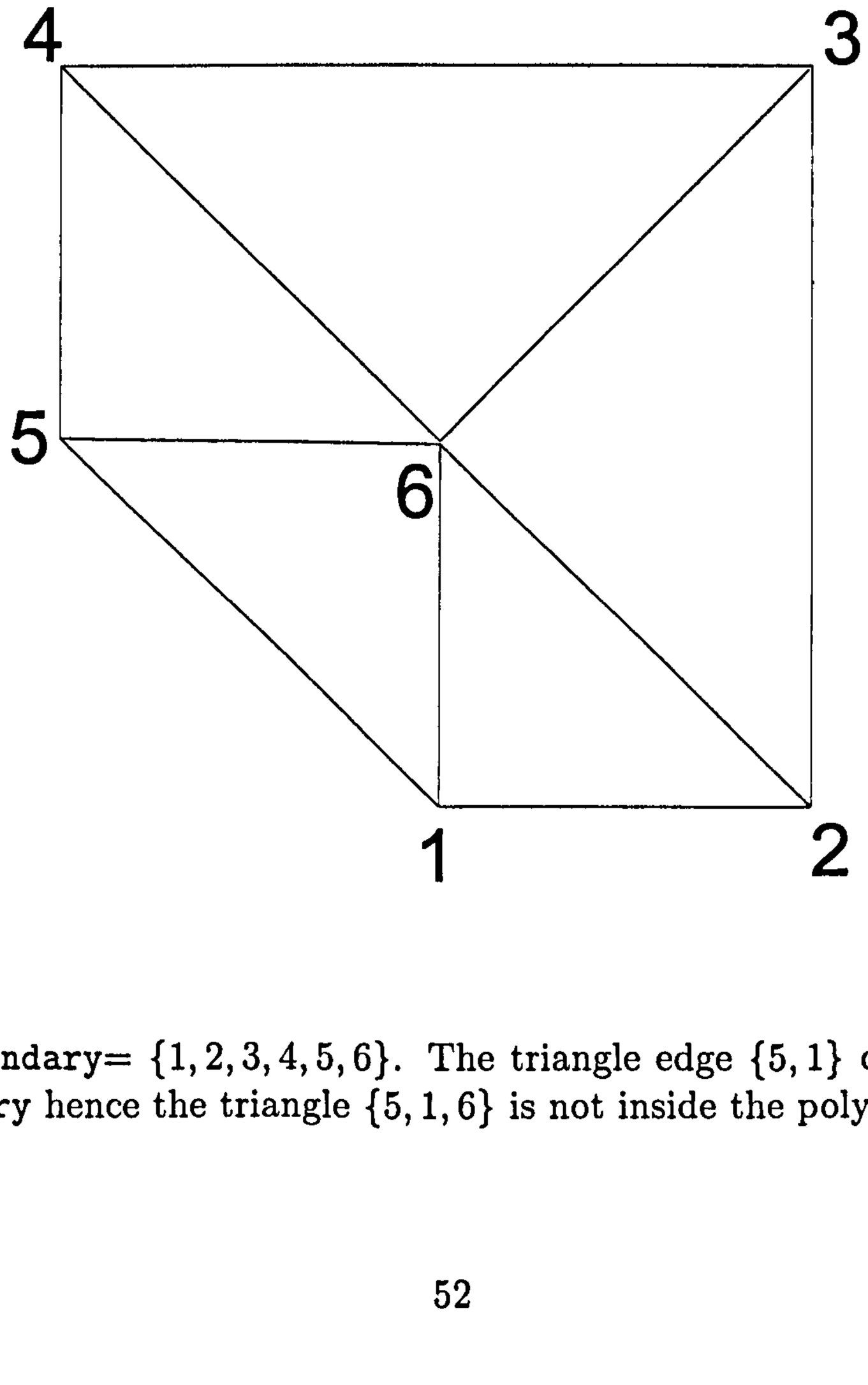

Figure 4.4 - Boundary= $\{1, 2, 3, 4, 5, 6\}$. The triangle edge $\{5, 1\}$ does not appear in order in Boundary hence the triangle $\{5, 1, 6\}$ is not inside the polygon.

4.4 A note about refining a Delaunay triangulation

In the mesh generation algorithm a mesh is generated by adding nodes within elements of a coarser mesh. Hence, with respect to the Voronoi diagram of the coarser mesh, a starting vertex (determined in step 3) is already known for every point to be added. This potentially removes the search process which is of order $n^{\frac{1}{2}}$ where n is the current number of points. However, since the vertices change after the addition of each point, extra work would be required to keep the list of starting vertices consistent with the current Voronoi Diagram. This has not been attempted by the author.

Chapter 5

Structural Modelling

5.1 Introduction

This chapter serves as an introduction to structural modelling. The physical concepts described here are needed in subsequent chapters. In particular, the general integral form of the equilibrium equations in (5.31) and (5.32) will be used, in Chapter 7, to derive the equilibrium equations governing a beam. Everything contained in this chapter is standard and may be found in texts such as Spencer [30], Hunter [16] or Oden [25]. The theory presented here gathers together the relevant parts of these texts to make this thesis self-contained.

5.2 Stress

5.2.1 The stress tensor

Consider a body, $\Omega \in \mathbb{R}^3$, whose surface, Γ, is subjected to a force vector, $\boldsymbol{P}(\boldsymbol{x})$, where $\boldsymbol{x} \in \Gamma$. We define the surface traction vector, $\boldsymbol{t}(\boldsymbol{x})$, at $\boldsymbol{x} = \boldsymbol{p} \in \Gamma$ to be

$$\boldsymbol{t}(\boldsymbol{p}) = \left.\frac{\mathrm{d}\boldsymbol{P}}{\mathrm{d}\Gamma}\right|_{\boldsymbol{x}=\boldsymbol{p}}. \tag{5.1}$$

Let $\boldsymbol{e}_1$, $\boldsymbol{e}_2$ and $\boldsymbol{e}_3$ be the base vectors of a rectangular cartesian coordinate system and let $\boldsymbol{t}_1$, $\boldsymbol{t}_2$ and $\boldsymbol{t}_3$ be the traction vectors on surfaces that are normal to $\boldsymbol{e}_1$, $\boldsymbol{e}_2$ and $\boldsymbol{e}_3$ respectively. We may then write

$$\boldsymbol{t}_1 = \sigma_{11}\boldsymbol{e}_1 + \sigma_{12}\boldsymbol{e}_2 + \sigma_{13}\boldsymbol{e}_3 \tag{5.2}$$

$$\boldsymbol{t}_2 = \sigma_{21}\boldsymbol{e}_1 + \sigma_{22}\boldsymbol{e}_2 + \sigma_{23}\boldsymbol{e}_3 \tag{5.3}$$

$$\boldsymbol{t}_3 = \sigma_{31}\boldsymbol{e}_1 + \sigma_{32}\boldsymbol{e}_2 + \sigma_{33}\boldsymbol{e}_3 \tag{5.4}$$

where the σ_{ij}'s are known as stress components. For a general surface, Γ, whose normal vector at the point $\boldsymbol{p}$ is $\boldsymbol{n}$ the traction is given by

$$\boldsymbol{t} = \boldsymbol{t}_1 \cdot \boldsymbol{n}\boldsymbol{e}_1 + \boldsymbol{t}_2 \cdot \boldsymbol{n}\boldsymbol{e}_2 + \boldsymbol{t}_3 \cdot \boldsymbol{n}\boldsymbol{e}_3 \tag{5.5}$$

or, in matrix form,

$$\boldsymbol{t} = \boldsymbol{\sigma}^T \boldsymbol{n} \tag{5.6}$$

where $\boldsymbol{\sigma}$ is known as the Cauchy stress tensor. Later we will show that $\boldsymbol{\sigma}$ is symmetric so that

$$\boldsymbol{t} = \boldsymbol{\sigma}\boldsymbol{n}. \tag{5.7}$$

5.2.2 Principal stresses

The components of $\boldsymbol{\sigma}$ depend on the chosen coordinate system. Generally, $\boldsymbol{t}$ does not act in the same direction as $\boldsymbol{n}$. When $\boldsymbol{t}$ and $\boldsymbol{n}$ do have the same direction then we can write

$$\boldsymbol{t} = \sigma\boldsymbol{n} \tag{5.8}$$

where σ is the magnitude of $\boldsymbol{t}$. Hence

$$\boldsymbol{\sigma}\boldsymbol{n} = \sigma\boldsymbol{n} \tag{5.9}$$

so that σ is an eigenvalue of $\boldsymbol{\sigma}$. The three eigenvalues, call them σ_1, σ_2 and σ_3, are found from

$$|\boldsymbol{\sigma} - \sigma\boldsymbol{I}| = 0. \tag{5.10}$$

They are called the principal stresses and are each associated with a principal stress direction. In another coordinate system $\boldsymbol{\sigma}$ would become $\boldsymbol{R}^T\boldsymbol{\sigma}\boldsymbol{R}$ where $\boldsymbol{R}$ is a proper orthogonal tensor. That means that $\boldsymbol{R}^T\boldsymbol{R} = \boldsymbol{I}$ and $|\boldsymbol{R}| = 1$ which imply that

$$|\boldsymbol{R}^T\boldsymbol{\sigma}\boldsymbol{R} - \sigma\boldsymbol{I}| = |\boldsymbol{R}||\boldsymbol{\sigma} - \sigma\boldsymbol{I}||\boldsymbol{R}| = |\boldsymbol{\sigma} - \sigma\boldsymbol{I}|. \tag{5.11}$$

This means that the principal stresses are independent of the coordinate system. Expanding (5.10) we find that the principal stresses are the solutions of

$$\sigma^3 - I_1\sigma^2 + I_2\sigma - I_3 = 0 \tag{5.12}$$

where

$$I_1 = \mathrm{tr}(\boldsymbol{\sigma}) = \sigma_{11} + \sigma_{22} + \sigma_{33}, \tag{5.13}$$

$$I_2 = \frac{1}{2}\left(\mathrm{tr}(\boldsymbol{\sigma})^2 - \mathrm{tr}(\boldsymbol{\sigma}^2)\right) = \sigma_{11}\sigma_{22} + \sigma_{22}\sigma_{33} + \sigma_{33}\sigma_{11} - \sigma_{12}^2 - \sigma_{23}^2 - \sigma_{13}^2, \tag{5.14}$$

$$I_3 = |\boldsymbol{\sigma}| = \sigma_{11}\sigma_{22}\sigma_{33} + 2\sigma_{12}\sigma_{23}\sigma_{13} - \sigma_{11}\sigma_{23}^2 - \sigma_{22}\sigma_{13}^2 - \sigma_{33}\sigma_{12}^2. \tag{5.15}$$

The quantities I_1, I_2 and I_3, like the principal stresses, are independent of the coordinate system and are called invariants of the stress tensor. Since they are independent of the coordinate system we can choose the coordinate axes to correspond with the principal directions from which the relations can be written in terms of the principal stresses. Hence we have

$$I_1 = \sigma_1 + \sigma_2 + \sigma_3, \tag{5.16}$$

$$I_2 = \sigma_1\sigma_2 + \sigma_2\sigma_3 + \sigma_3\sigma_1, \tag{5.17}$$

$$I_3 = \sigma_1\sigma_2\sigma_3. \tag{5.18}$$

5.2.3 Spherical and deviatoric stress tensors

The stress tensor may be written as

$$\boldsymbol{\sigma} = \boldsymbol{\sigma}' + \boldsymbol{\sigma}'' \tag{5.19}$$

where

$$\boldsymbol{\sigma}' := \begin{pmatrix} \frac{2\sigma_{11} - \sigma_{22} - \sigma_{33}}{3} & \sigma_{12} & \sigma_{13} \\ \sigma_{12} & \frac{2\sigma_{22} - \sigma_{33} - \sigma_{11}}{3} & \sigma_{23} \\ \sigma_{13} & \sigma_{23} & \frac{2\sigma_{33} - \sigma_{11} - \sigma_{22}}{3} \end{pmatrix}, \tag{5.20}$$

$$\boldsymbol{\sigma}'' := \begin{pmatrix} \frac{\sigma_{11} + \sigma_{22} + \sigma_{33}}{3} & 0 & 0 \\ 0 & \frac{\sigma_{11} + \sigma_{22} + \sigma_{33}}{3} & 0 \\ 0 & 0 & \frac{\sigma_{11} + \sigma_{22} + \sigma_{33}}{3} \end{pmatrix}. \tag{5.21}$$

When the coordinate directions coincide with the principal directions of stress this decomposition simplifies to

$$\boldsymbol{\sigma}' := \begin{pmatrix} \frac{2\sigma_1 - \sigma_2 - \sigma_3}{3} & 0 & 0 \\ 0 & \frac{2\sigma_2 - \sigma_3 - \sigma_1}{3} & 0 \\ 0 & 0 & \frac{2\sigma_3 - \sigma_1 - \sigma_2}{3} \end{pmatrix}, \tag{5.22}$$

$$\boldsymbol{\sigma}'' := \begin{pmatrix} \frac{\sigma_1 + \sigma_2 + \sigma_3}{3} & 0 & 0 \\ 0 & \frac{\sigma_1 + \sigma_2 + \sigma_3}{3} & 0 \\ 0 & 0 & \frac{\sigma_1 + \sigma_2 + \sigma_3}{3} \end{pmatrix}. \tag{5.23}$$

The tensor $\boldsymbol{\sigma}''$ is known as the spherical stress tensor and $\boldsymbol{\sigma}'$ is known as the deviatoric stress tensor. The invariants of the spherical stress tensor are denoted by I_1'', I_2'' and I_3'' and work out to be

$$I_1'' = \sigma_1 + \sigma_2 + \sigma_3 = I_1 \tag{5.24}$$

$$I_2'' = \frac{(\sigma_1 + \sigma_2 + \sigma_3)^2}{3} = \frac{I_1^2}{3} \tag{5.25}$$

$$I_3'' = \frac{(\sigma_1 + \sigma_2 + \sigma_3)^3}{27} = \frac{I_3^3}{27}. \tag{5.26}$$

Similarly the invariants of the deviatoric stress tensor are denoted by I_1', I_2' and I_3' and are

$$I_1' = 0 \tag{5.27}$$

$$I_2' = -\frac{(\sigma_1-\sigma_2)^2+(\sigma_2-\sigma_3)^2+(\sigma_3-\sigma_1)^2}{6} = I_2 - \frac{I_1^2}{3} \tag{5.28}$$

$$I_3' = \frac{(2\sigma_1-\sigma_2-\sigma_3)(2\sigma_2-\sigma_3-\sigma_1)(2\sigma_3-\sigma_1-\sigma_2)}{27} = I_3 - \frac{I_1 I_2}{3} + \frac{2I_1^2}{27}. \tag{5.29}$$

Clearly I_2' is non-positive. Some authors define the second deviatoric stress invariant to be non-negative since it is proportional to the distortion energy. Let us define the invariant J_2 as

$$J_2 := -I_2' = \frac{(\sigma_1-\sigma_2)^2+(\sigma_2-\sigma_3)^2+(\sigma_3-\sigma_1)^2}{6}. \tag{5.30}$$

The stress invariants I_1 and J_2 will be used in Chapter 8, the theory of Plasticity.

5.3 Equilibrium

We assume that, for the body to be in equilibrium, the resultant force and the resultant couple acting within Ω are zero. There are two kinds of force under consideration. They are the surface forces, $\boldsymbol{t}$, acting through Γ and the body forces, $\boldsymbol{f}$, acting throughout Ω. For the resultant force to be zero

$$\int_{x\in\Gamma} \boldsymbol{t}(\boldsymbol{x})\mathrm{d}\boldsymbol{x} + \int_{x\in\Omega} \boldsymbol{f}(\boldsymbol{x})\mathrm{d}\boldsymbol{x} = \boldsymbol{0} \tag{5.31}$$

For the resultant couple to be zero about an arbitrarily chosen origin, $\boldsymbol{o}$, we require that

$$\int_{x\in\Gamma} (\boldsymbol{x}-\boldsymbol{o})\times\boldsymbol{t}(\boldsymbol{x})\mathrm{d}\boldsymbol{x} + \int_{x\in\Omega} (\boldsymbol{x}-\boldsymbol{o})\times\boldsymbol{f}(\boldsymbol{x})\mathrm{d}\boldsymbol{x} \tag{5.32}$$

Using the divergence theorem (5.31) and (5.32) may be written, in component form, as

$$\int_{x\in\Omega} \left(\frac{\partial\sigma_{ij}}{\partial x_i} + f_j\right)\mathrm{d}\boldsymbol{x} = 0 \tag{5.33}$$

$$\int_{x\in\Omega} e_{jpq}\left\{(x_p-o_p)\left(\frac{\partial\sigma_{rq}}{\partial x_r}+f_q\right)+\sigma_{pq}\right\}\mathrm{d}\boldsymbol{x} = 0 \tag{5.34}$$

where e_{ijk} denotes the alternating symbol. These equations must hold for any volume Ω including any of its subregions and so, for equilibrium throughout Ω,

$$\frac{\partial\sigma_{ij}}{\partial x_i} + f_j = 0 \tag{5.35}$$

$$\sigma_{pq} = \sigma_{qp} \tag{5.36}$$

for all $\boldsymbol{x} \in \Omega$. If can be shown [30] that (5.36) also holds for a body in motion and so, in general, $\boldsymbol{\sigma}$ is symmetric. Equations (5.35) and (5.36) are usually combined so that the equations of equilibrium are stated as

$$\frac{\partial \sigma_{ij}}{\partial x_i} + f_i = 0 \tag{5.37}$$

where it is assumed that $\boldsymbol{\sigma}$ is symmetric.

5.4 Strain

When a body is subjected to forces whilst being partly restrained it is seen to change shape. This process is known as deformation. A measure of the deformation is called a strain. Physics teaches us that there are two categories of strain: longitudinal and shear. Consider the body in question as a cube resting on a smooth surface with a force applied evenly over the top face. The cube, which has height h, becomes squashed into a cuboid of height $h - \Delta h$. The longitudinal strain is defined as $-\frac{\Delta h}{h}$. Suppose instead that the cube is fixed to the surface so that is cannot slide and that a force is applied over one of the vertical sides. This time the cube deforms to a parallelopiped; the top face having moved a distance u. The shear stain is defined as $\frac{u}{h}$. We refer to these strains as engineering strains. They serve as sufficient measures of the deformation of a body under particular loading and restraining conditions. In mathematical modelling we require a more general definition of strain describing the way a body deforms from one configuration to another. Let us denote by X_i, $i = 1, 2, 3$, the Cartesian coordinate system of the undeformed body and by x_i the coordinate system of the deformed body. The displacements u_i are defined as

$$u_i = x_i - X_i. \tag{5.38}$$

A possible measure of deformation is the deformation gradient tensor, $\boldsymbol{F}$, given by

$$F_{ij} = \frac{\partial x_i}{\partial X_j} = \frac{\partial u_i}{\partial X_j} + \delta_{ij} \tag{5.39}$$

which gives the unit tensor, $\boldsymbol{I}$, if all displacements are constant. Since we are concerned with the change in the body's shape we should look for a measure that gives $\boldsymbol{I}$ for a rigid body motion. This is when the deformation consists of a constant displacement and a rotation; i.e.

$$\boldsymbol{x} = \boldsymbol{c} + \boldsymbol{R}\boldsymbol{X} \tag{5.40}$$

where $\boldsymbol{c}$ is a constant vector and $\boldsymbol{R}$ is a proper orthogonal tensor (i.e. $\boldsymbol{R}^T\boldsymbol{R} = \boldsymbol{I}$ and $det\boldsymbol{R} = 1$). For a deformation of the form (5.40) $\boldsymbol{F} = \boldsymbol{Q}$ and so $\boldsymbol{F}$ is not a suitable measure. Related to $\boldsymbol{F}$ are the symmetric tensors

$$\boldsymbol{C} = \boldsymbol{F}^T\boldsymbol{F} \tag{5.41}$$

$$\boldsymbol{B} = \boldsymbol{F}\boldsymbol{F}^T \tag{5.42}$$

known as the right and left Cauchy-Green deformation tensors, respectively. These are both suitable measures of deformation since $\boldsymbol{C} = \boldsymbol{B} = \boldsymbol{I}$ when $\boldsymbol{x}$ has the form in (5.40); i.e. they measure the stretching of the material. A material line segment $\Delta \boldsymbol{X}$ deforms to a line segment $\Delta \boldsymbol{x} = \boldsymbol{F}\Delta \boldsymbol{X}$ which can have a different orientation and a different length. The stretching is concerned with the change of length of such line segments and for this we note that

$$|\Delta \boldsymbol{x}|^2 = \Delta \boldsymbol{x}^T \Delta \boldsymbol{x} = \Delta \boldsymbol{X}^T \boldsymbol{F}^T \boldsymbol{F} \Delta \boldsymbol{X} = \Delta \boldsymbol{X}^T \boldsymbol{C} \Delta \boldsymbol{X}. \tag{5.43}$$

For the change in length we have

$$|\Delta \boldsymbol{x}|^2 - |\Delta \boldsymbol{X}|^2 = \Delta \boldsymbol{X}(\boldsymbol{C} - \boldsymbol{I}))\Delta \boldsymbol{X}^T = 2\Delta \boldsymbol{X}^T \boldsymbol{E} \Delta \boldsymbol{X} \tag{5.44}$$

where

$$E_{ij} = \frac{1}{2}\left(\frac{\partial u_i}{\partial X_j} + \frac{\partial u_j}{\partial X_i} + \frac{\partial u_k}{\partial X_i}\frac{\partial u_k}{\partial X_j}\right) \tag{5.45}$$

is known as the Lagrangian strain tensor. It measures the deformation of a body with respect to the initial coordinate system. In the case of small deformation, where $\boldsymbol{F} \approx \boldsymbol{I}$ and $|\Delta \boldsymbol{x}| \approx |\Delta \boldsymbol{X}|$, we have

$$E_{ij} \approx \frac{1}{2}\left(\frac{\partial u_i}{\partial X_j} + \frac{\partial u_j}{\partial X_i}\right) = \epsilon_{ij} \tag{5.46}$$

where ϵ_{ij} is the infinitesimal strain tensor. Both (5.45) and (5.46) are widely used in structural modelling.

5.5 Constitutive equations for linear elastic isotropic materials

The behaviour of a particular material is governed by its constitutive equations. Such equations relate physical properties such as stress, strain and temperature with one another. In structural analysis we need a constitutive equation to relate stress and strain. The structural behaviour of real materials is very complex and it would be difficult to formulate equations capable of determining the stress under any given circumstance. We content ourselves by using equations that describe ideal materials whose behaviour approximate that of real materials.

Many common engineering materials have the property that they undergo small changes of shape when subjected to forces that they normally encounter. They also have a natural shape to which they return after forces, that are not too large, are applied and then removed. Such material are classed as linear elastic. An ideal linear elastic material is one whose stress components may be expressed, using Einstein summation convention, as

$$\sigma_{ij} = C_{ijkl}\epsilon_{kl} \tag{5.47}$$

where C_{ijkl} are components of a fourth order tensor known as the tensor of elastic coefficients. Equation (5.47) is the constitutive equation for a linear elastic material. If the material is also isotropic, meaning it has the same properties in all directions, the elastic coefficients may be expressed in the general form

$$C_{ijkl} = \lambda\delta_{ij}\delta_{kl} + \mu\delta_{ik}\delta_{jl} + \nu\delta_{il}\delta_{jk} \tag{5.48}$$

where λ, μ and ν are scalars. Substituting (5.48) into (5.47) gives

$$\sigma_{ij} = \lambda\delta_{ij}\epsilon_{kk} + \mu\epsilon_{ij} + \nu\epsilon_{ji}. \tag{5.49}$$

Since ϵ is symmetric no generality is lost by writing $\mu = \nu$ so that

$$\sigma_{ij} = \lambda\delta_{ij}\epsilon_{kk} + 2\mu\epsilon_{ij}. \tag{5.50}$$

Equation (5.50) is the constitutive equation for an isotropic linear elastic material. The coefficients λ and μ are known as the Lamé coefficients and are material properties. This equation is an alternative statement of Hooke's law [34, Page 8]:

$$\begin{aligned}
\sigma_{11} &= E\epsilon_{11} + \nu(\sigma_{22} + \sigma_{33}) && (5.51)\\
\sigma_{22} &= E\epsilon_{22} + \nu(\sigma_{11} + \sigma_{33}) && (5.52)\\
\sigma_{33} &= E\epsilon_{33} + \nu(\sigma_{11} + \sigma_{22}) && (5.53)\\
\sigma_{12} &= 2G\epsilon_{12} && (5.54)\\
\sigma_{13} &= 2G\epsilon_{13} && (5.55)\\
\sigma_{23} &= 2G\epsilon_{23} && (5.56)
\end{aligned}$$

where E is the elastic or Youngs modulus and ν is the Poisson ratio of the material. Solving the first three equations for σ_{11}, σ_{22} and σ_{33} we have

$$\begin{pmatrix}\sigma_{11}\\ \sigma_{22}\\ \sigma_{33}\end{pmatrix} = \frac{E}{(1+\nu)(1-2\nu)}\begin{pmatrix}1-\nu & \nu & \nu\\ \nu & 1-\nu & \nu\\ \nu & \nu & 1-\nu\end{pmatrix}\begin{pmatrix}\epsilon_{11}\\ \epsilon_{22}\\ \epsilon_{33}\end{pmatrix} \tag{5.57}$$

so that the general form of Hooke's law is, in subscript notation,

$$\sigma_{ij} = \frac{\nu E}{(1+\nu)(1-2\nu)}\delta_{ij}\epsilon_{kk} + \frac{1}{1+\nu}\epsilon_{ij}. \tag{5.58}$$

Comparing with (5.50) we see that

$$\begin{aligned}
\lambda &= \frac{\nu E}{(1+\nu)(1-2\nu)} && (5.59)\\
\mu &= G = \frac{E}{2(1+\nu)}. && (5.60)
\end{aligned}$$

Hence, E and ν are related to the Lamé coefficients by

$$\begin{aligned}
E &= \frac{3\lambda + 2\mu^2}{\lambda + \mu} && (5.61)\\
\nu &= \frac{\lambda}{2(\lambda + \mu)}. && (5.62)
\end{aligned}$$

5.6 Lamé equations for equilibrium in a linear elastic isotropic material

The Lamé Equilibrium Equations are derived by substituting (5.46) and (5.50) into (5.37). Using Einstein summation convention they are

$$\frac{\partial}{\partial x_i}\left((\lambda+\mu)\frac{\partial u_k}{\partial x_k}\right)+\frac{\partial}{\partial x_j}\left(\mu\frac{\partial u_i}{\partial x_j}\right)+f_i=0 \tag{5.63}$$

for all $\boldsymbol{x}\in\Omega$. If λ and μ are constant then (5.63) may be written in vector notation as

$$(\lambda+\mu)\nabla\nabla\cdot\boldsymbol{u}+\mu\nabla^2\boldsymbol{u}+\boldsymbol{f}=\boldsymbol{0}. \tag{5.64}$$

Boundary conditions for (5.63) and (5.64) are of the type

$$\boldsymbol{u}(\boldsymbol{x}) = \boldsymbol{0}, \quad \boldsymbol{x}\in\Gamma_C \tag{5.65}$$

$$\boldsymbol{t}(\boldsymbol{x}) = \boldsymbol{g}(\boldsymbol{x}), \quad \boldsymbol{x}\in\Gamma_T \tag{5.66}$$

where $\Gamma_C\cup\Gamma_T=\Gamma$ and $\Gamma_C\cap\Gamma_T=\emptyset$. Solutions to the Lamé equations are generally hard to find but we may apply the equations to some simple problems. In the following examples all displacements are assumed to occur in the x_1x_2 plane so that $u_3=0$.

An example of pure shear

Consider a body of height h that is rigidly fixed at each end so that all displacements are zero at $x_3=0$ and $x_2=h$. For simplicity we assume that $u_2=0$ and that u_1 is only a function of x_2. Hence $\nabla\cdot\boldsymbol{u}=0$ and we have, from (5.63),

$$\frac{\mathrm{d}^2u_1}{\mathrm{d}x_2^2}+\frac{f_1}{\mu}=0 \tag{5.67}$$

for $0<x_2<h$ with the boundary conditions

$$u_2(0)=u_2(h)=0. \tag{5.68}$$

If f_1 is constant then this problem has the solution

$$u_1(x_2)=\frac{f_1}{2\mu}x_2(h-x_2) \tag{5.69}$$

which is an example of pure shear. Remember that $\mu=G$ is the shear modulus. The shear stress is given by

$$\sigma_{12}=\mu\frac{\mathrm{d}u_1}{\mathrm{d}x_2}=f_1\left(\frac{h}{2}-x_2\right). \tag{5.70}$$

An example of pure tension

We will assume that the tension is due to the constant body force f_2 and that there are no applied surface forces. For simplicity we assume that $u_1 = 0$ and u_2 is only a function of x_2. Then $\nabla(\nabla \cdot \boldsymbol{u}) = \mathbf{0}$ and we have, from (5.63),

$$\frac{\mathrm{d}^2 u_2}{\mathrm{d}x_2} + \frac{f_2}{\lambda + 2\mu} = 0 \tag{5.71}$$

for $0 < x_2 < h$ with the boundary conditions

$$u_2(0) = 0 \tag{5.72}$$

$$\left.\frac{\mathrm{d}u_2}{\mathrm{d}x_2}\right|_{x_2=h} = 0. \tag{5.73}$$

This has the solution

$$u_2(x_2) = \frac{f_2 x_2(2h - x_2)}{2(\lambda + 2\mu)}. \tag{5.74}$$

The stress is given by

$$\sigma_{22} = (\lambda + 2\mu)\frac{du_2}{dx_2} = f_2(h - x_2). \tag{5.75}$$

If f_2 is positive then the stress is positive and the body is in tension. If it is negative then the stress is negative and the body is in compression. If the tension had not been caused by a body force but instead by a force applied at $x_2 = h$ then the Lamé equations would reduce to

$$\frac{\mathrm{d}^2 u_2}{\mathrm{d}x_2^2} = 0 \tag{5.76}$$

so that u_2 is linear and the stress is constant.

5.7 Energy in structural systems

When forces act within a system and cause components of the system to change, the forces are said to have done work. When work is done energy is exchanged between the system's components. In a structural system, body (i.e. gravitational) forces act throughout the structure and traction forces act on the structure's surface. The result is that the structure deforms; i.e. the strain components are altered. Some of the energy of this process is stored inside the structure as strain energy. If the forces were removed then the strain energy would be used to (at least partly) reverse the deformation. The stored energy in a system is known as the potential energy. This includes both the strain energy and the energy used to fuel the forces. The work done by the forces is equal to a loss in the system's potential energy. In a structural system the forces are usually gravitational and work done results in a loss of gravitational

potential energy. Hence, in a structural system, the deformation process results in a loss of potential energy equal to the gain in strain energy minus the loss of gravitational potential energy. For elastic materials the strain energy, U is given by [30]

$$U = \frac{1}{2} \int_{x \in \Omega} \sigma_{ij} \epsilon_{ij} \, \mathrm{d}\boldsymbol{x} \tag{5.77}$$

and the loss in potential energy, V, due to the work done by the surface traction, $\boldsymbol{g}$, and body force, $\boldsymbol{F}$, is given by

$$V = \int_{x \in \Gamma_T} \boldsymbol{g}^T \boldsymbol{u} \, \mathrm{d}\boldsymbol{x} + \int_{x \in \Omega} \boldsymbol{f}^T \boldsymbol{u} \, \mathrm{d}\boldsymbol{x}. \tag{5.78}$$

The overall loss of potential energy, PE, during the deformation process is

$$PE = U - V. \tag{5.79}$$

5.8 Finite element solutions to the linear elasticity equilibrium equations

We may obtain a finite element approximation to the Lamé equations by first finding a weak formulation of (5.63) with the boundary conditions (5.65) and (5.66). This is derived by first taking the inner product of (5.63) with a vector function $\boldsymbol{v}(\boldsymbol{x}) \in H$ where

$$H = \left\{ \boldsymbol{v} : \boldsymbol{v} \in (H^1(\Omega))^3, \boldsymbol{v}|_{\Gamma_C} = \boldsymbol{0} \right\}. \tag{5.80}$$

This gives us

$$\int_{x \in \Omega} v_i \frac{\partial \sigma_{ij}}{\partial x_j} \, \mathrm{d}\boldsymbol{x} + \int_{x \in \Omega} v_i f_i \, \mathrm{d}\boldsymbol{x} = 0. \tag{5.81}$$

Using the Green formula

$$\int_{x \in \Omega} \frac{\partial \phi}{\partial x_j} \psi \, \mathrm{d}\boldsymbol{x} + \int_{x \in \Omega} \phi \frac{\partial \psi}{\partial x_j} \, \mathrm{d}\boldsymbol{x} = \int_{x \in \Gamma} \phi \psi n_j \, \mathrm{d}\boldsymbol{x} \tag{5.82}$$

and the fact that, since $\sigma_{ij} = \sigma_{ji}$,

$$\sigma_{ij} \frac{\partial v_i}{\partial x_j} = \frac{1}{2} \sigma_{ij} \left(\frac{\partial v_i}{\partial x_j} + \frac{\partial v_i}{\partial x_j} \right) = \frac{1}{2} \sigma_{ij} \left(\frac{\partial v_i}{\partial x_j} + \frac{\partial v_j}{\partial x_i} \right) = \sigma_{ij} \epsilon_{ij}, \tag{5.83}$$

equation (5.81) may be written as

$$\int_{x \in \Omega} \sigma_{ij} \epsilon_{ij}(\boldsymbol{v}) \, \mathrm{d}\boldsymbol{x} = \int_{x \in \Omega} f_i v_i \, \mathrm{d}\boldsymbol{x} + \int_{x \in \Gamma_T} g_i v_i \, \mathrm{d}\boldsymbol{x}. \tag{5.84}$$

This may be written in vector notation if we let

$$\boldsymbol{\sigma} = (\sigma_{11}, \sigma_{22}, \sigma_{33}, \sigma_{12}, \sigma_{23}, \sigma_{31})^T \tag{5.85}$$

$$\boldsymbol{\epsilon} = (\epsilon_{11}, \epsilon_{22}, \epsilon_{33}, 2\epsilon_{12}, 2\epsilon_{23}, 2\epsilon_{31})^T. \tag{5.86}$$

Hence equation (5.84) may be written as

$$\int_{x \in \Omega} \boldsymbol{\sigma}^T(\boldsymbol{u}) \boldsymbol{\epsilon}(\boldsymbol{v}) \, \mathrm{d}\boldsymbol{x} = \int_{x \in \Omega} \boldsymbol{f}^T \boldsymbol{v} \, \mathrm{d}\boldsymbol{x} + \int_{x \in \Gamma_T} \boldsymbol{g}^T \boldsymbol{v} \, \mathrm{d}\boldsymbol{x}. \tag{5.87}$$

The weak problem is to find a $\boldsymbol{u}$ in H that satisfies (5.87) for all $\boldsymbol{v}$ in H. Remember that $\boldsymbol{u}$ is involved through $\boldsymbol{\sigma}$ using (5.50). Using (5.85) and (5.86) the constitutive equation may be written as

$$\boldsymbol{\sigma}(\boldsymbol{u}) = \boldsymbol{D}\boldsymbol{\epsilon}(\boldsymbol{u}) \tag{5.88}$$

where $\boldsymbol{D}$ is the material matrix. Substituting (5.88) into (5.87) gives us

$$\int_{x \in \Omega} \boldsymbol{\epsilon}^T(\boldsymbol{u}) \boldsymbol{D} \boldsymbol{\epsilon}(\boldsymbol{v}) \, \mathrm{d}\boldsymbol{x} = \int_{x \in \Omega} \boldsymbol{f}^T \boldsymbol{v} \, \mathrm{d}\boldsymbol{x} + \int_{x \in \Gamma_T} \boldsymbol{g}^T \boldsymbol{v} \, \mathrm{d}\boldsymbol{x} \tag{5.89}$$

which is in the general form stated in (3.2). Hence the finite element problem is to find $\boldsymbol{u}_h$ in V such that

$$\int_{x \in \Omega} \boldsymbol{\epsilon}^T(\boldsymbol{u}_h) \boldsymbol{D} \boldsymbol{\epsilon}(\boldsymbol{v}) \, \mathrm{d}\boldsymbol{x} = \int_{x \in \Omega} \boldsymbol{f} \boldsymbol{v} \, \mathrm{d}\boldsymbol{x} + \int_{x \in \Gamma_T} \boldsymbol{g} \boldsymbol{v} \, \mathrm{d}\boldsymbol{x} \tag{5.90}$$

for all $\boldsymbol{v}_h$ in V where V is a finite dimensional subset of H. Any vector in V may be written as

$$\boldsymbol{v}_h(\boldsymbol{x}) = \boldsymbol{N}(\boldsymbol{x}) \boldsymbol{U} \tag{5.91}$$

where $\boldsymbol{U}$ is the vector containing the degrees of freedom and $\boldsymbol{N}$ has the form

$$\boldsymbol{N}(\boldsymbol{x}) = [\boldsymbol{N}_1, \boldsymbol{N}_2, .., \boldsymbol{N}_n] \tag{5.92}$$

with

$$\boldsymbol{N}_k(\boldsymbol{x}) = N_k(\boldsymbol{x}) \begin{pmatrix} 1 & 0 \\ 0 & 1 \end{pmatrix} \tag{5.93}$$

where n is the number of nodes and the N_k's are the basis functions of V.

To illustrate the finite element method applied to problems of linear elasticity we will consider a two dimensional implementation using linear triangular elements. We assume that the stress components σ_{33}, σ_{13} and σ_{23} are zero so that the non-zero stress components are given by

$$\sigma_{11} = E\epsilon_{11} + \nu\sigma_{22} \tag{5.94}$$

$$\sigma_{22} = E\epsilon_{22} + \nu\sigma_{11} \tag{5.95}$$

$$\sigma_{33} = 2G\epsilon_{23}. \tag{5.96}$$

Solving for σ_{11} and σ_{22} we have

$$\boldsymbol{\sigma} := \begin{pmatrix} \sigma_{11} \\ \sigma_{22} \\ \sigma_{12} \end{pmatrix} = \frac{E}{1-\nu^2} \begin{pmatrix} 1 & \nu & 0 \\ \nu & 1 & 0 \\ 0 & 0 & \frac{1-\nu}{2} \end{pmatrix} \begin{pmatrix} \epsilon_{11} \\ \epsilon_{22} \\ 2\epsilon_{12} \end{pmatrix} =: \boldsymbol{D}\boldsymbol{\epsilon} \tag{5.97}$$

where we have redefined the vectors $\boldsymbol{\sigma}$ and $\boldsymbol{\epsilon}$ and the material matrix $\boldsymbol{D}$ for the special case of plane stress. For the rest of this chapter the global coordinate variables will be denoted by x and y and, within the standard triangular element, the local coordinate variables will be denoted by ξ and η. Subscripts will denote node numbers. We will use a triangular mesh with linear basis functions. In local coordinates, for the i'th element, these are given by

$$N_1 = 1 - \xi - \eta \tag{5.98}$$
$$N_2 = \xi \tag{5.99}$$
$$N_3 = \eta. \tag{5.100}$$

With the nodes numbered locally $1 \ldots 3$ the mapping from local to global coordinates is given by

$$x = (1-\xi-\eta)x_1 + \xi x_2 + \eta x_3 \tag{5.101}$$
$$y = (1-\xi-\eta)y_1 + \xi y_2 + \eta y_3 \tag{5.102}$$

so that the Jacobian determinant, J_i, is given by

$$J_i = (x_2 - x_1)(y_3 - y_1) - (x_3 - x_1)(y_2 - y_1). \tag{5.103}$$

After making the change of variables we evaluate the local strain matrix to be

$$\boldsymbol{B}_i = \frac{1}{J_i} \begin{pmatrix} y_2 - y_3 & 0 & y_3 - y_1 & 0 & y_1 - y_2 & 0 \\ 0 & x_3 - x_2 & 0 & x_1 - x_3 & 0 & x_2 - x_1 \\ x_3 - x_2 & y_2 - y_3 & x_1 - x_3 & y_3 - y_1 & x_2 - x_1 & y_1 - y_2 \end{pmatrix}. \tag{5.104}$$

We are now able to evaluate the local element stiffness matrix and force vectors. For simplicity let us assume that the material matrix $\boldsymbol{D}$ and the body force vector $\boldsymbol{f}$ are constant over each triangular element. For the local stiffness matrix and force vector we have

$$\boldsymbol{K}_i = \int_0^1 \int_0^{1-\eta} \boldsymbol{B}_i^T \boldsymbol{D} \boldsymbol{B}_i J_i \, \mathrm{d}\xi \mathrm{d}\eta = \frac{J_i}{2} \boldsymbol{B}_i^T \boldsymbol{D} \boldsymbol{B}_i \tag{5.105}$$

$$\boldsymbol{F}_i = \int_0^1 \int_0^{1-\eta} \boldsymbol{N}_i^T \boldsymbol{f} J_i \, \mathrm{d}\xi \mathrm{d}\eta = \frac{J_i}{6} \begin{pmatrix} \boldsymbol{f} \\ \boldsymbol{f} \\ \boldsymbol{f} \end{pmatrix}. \tag{5.106}$$

On the boundary the basis functions reduce to

$$N_j = 1 - \xi \tag{5.107}$$
$$N_k = \xi. \tag{5.108}$$

Hence the local traction vector (with nodes numbered 1 and 2) is evaluated, assuming g is constant over the boundary element, to be

$$\boldsymbol{G}_i = \int_0^1 \begin{pmatrix} 1-\xi & 0 \\ 0 & 1-\xi \\ \xi & 0 \\ 0 & \xi \end{pmatrix} g|x_2 - x_1| \mathrm{d}\xi = \frac{|x_2 - x_1|}{2} \begin{pmatrix} g \\ g \end{pmatrix}. \tag{5.109}$$

All that remains is to apply the boundary conditions on Γ_C. For the 2D finite element solution this is stated as

$$\begin{pmatrix} U_{2i-1} \\ U_{2i} \end{pmatrix} = \begin{pmatrix} 0 \\ 0 \end{pmatrix} \tag{5.110}$$

for all points (x_i, y_i) that lie on Γ_C. This is applied by setting

$$\begin{aligned} K_{2i-1,2i-1} &= 1 && (5.111)\\ K_{2i,2i} &= 1 && (5.112)\\ K_{2i-1,p} &= 0, \quad p \in \{1..2n\} - \{2i-1\} && (5.113)\\ K_{2i,p} &= 0, \quad p \in \{1..2n\} - \{2i\} && (5.114)\\ F_{2i-1} &= 0 && (5.115)\\ F_{2i} &= 0 && (5.116) \end{aligned}$$

for all (x_i, y_i) in Γ_C. In order to preserve the symmetry of $\boldsymbol{K}$ it is also necessary to set

$$\begin{aligned} K_{p,i-1} &= 0, \quad p \in \{1 \ldots 2n\} - \{2i-1\} && (5.117)\\ K_{p,i} &= 0, \quad p \in \{1 \ldots 2n\} - \{2i\}. && (5.118) \end{aligned}$$

5.9 Numerical example

Presented here is a numerical example to illustrate the performance of the finite element method in solving the Lamé equations.

Consider a rectangular body of width a and height $b = 1$ with $a \geq b$ (See Figure 5.1). The body has an elastic modulus of $E = 1000$ and is fixed at $x = 0$ and $x = a$. A body force vector of $(0, -1)$ is applied uniformly. The finite element solution was obtained using uniform triangular mesh of varying densities for values of a ranging from $a = 1$ to $a = 64$ (See Figure 5.2). As an error indicator the L_2 norm of the difference between the recovered stress vector and finite element stress vector was calculated. The recovered stress vector was obtained using the weighted averaging technique. The results are presented in Tables 5.1 - 5.7. For each mesh the central vertical displacement, $u_h(\frac{a}{2})$, is shown along with the percentage difference from that obtained with the previous mesh. The variables nx and ny are the number of elements along the x and y axes, respectively, so that the number of triangular elements, ne is given by $2 \times nx \times ny$.

The error indicator appears to show the expected $O(h)$ behaviour for $nx > 64$. Convergence of the $u_h(\frac{a}{2})$ value is fairly slow, requiring more than 4000 elements to obtain

the first significant figure in the $a = 64$ case. This particular example may be better solved using the beam theory described in Chapter 7.

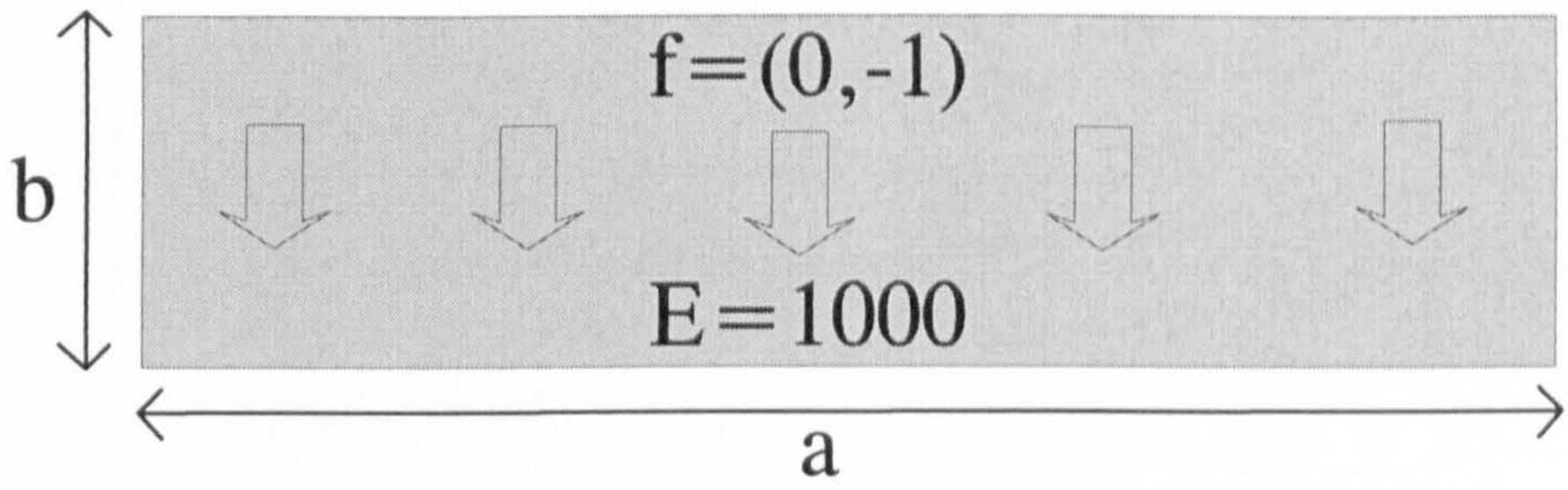

Figure 5.1 : Rectangular body (beam) analysed in numerical example.

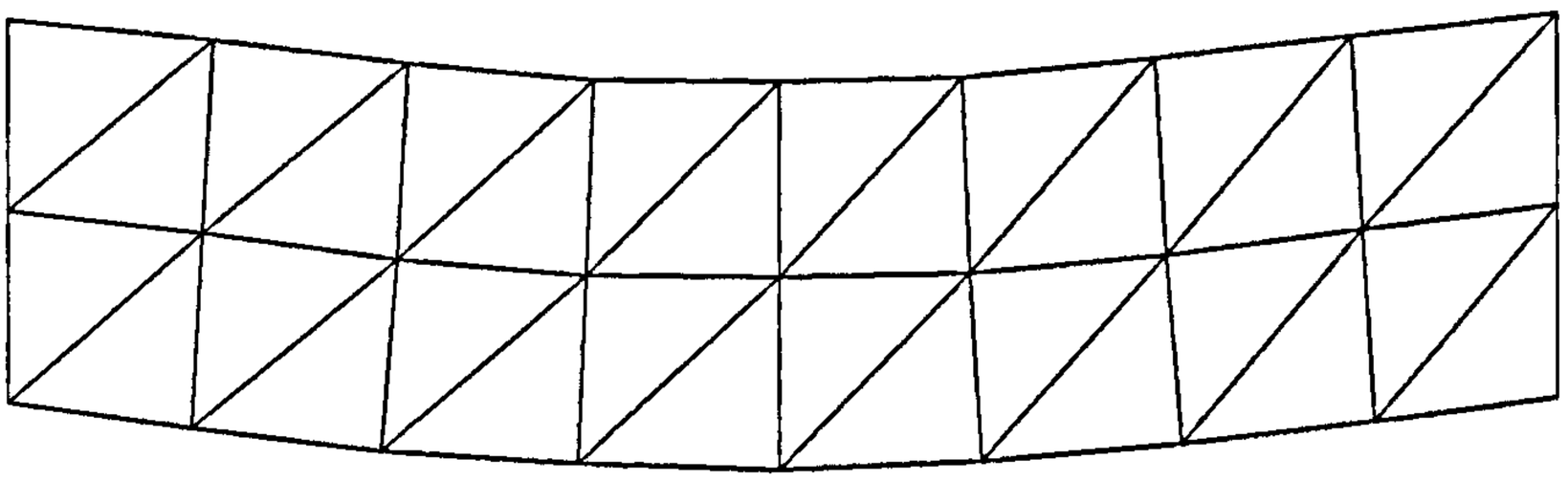

$nx = 8, ny = 2, ne = 32$

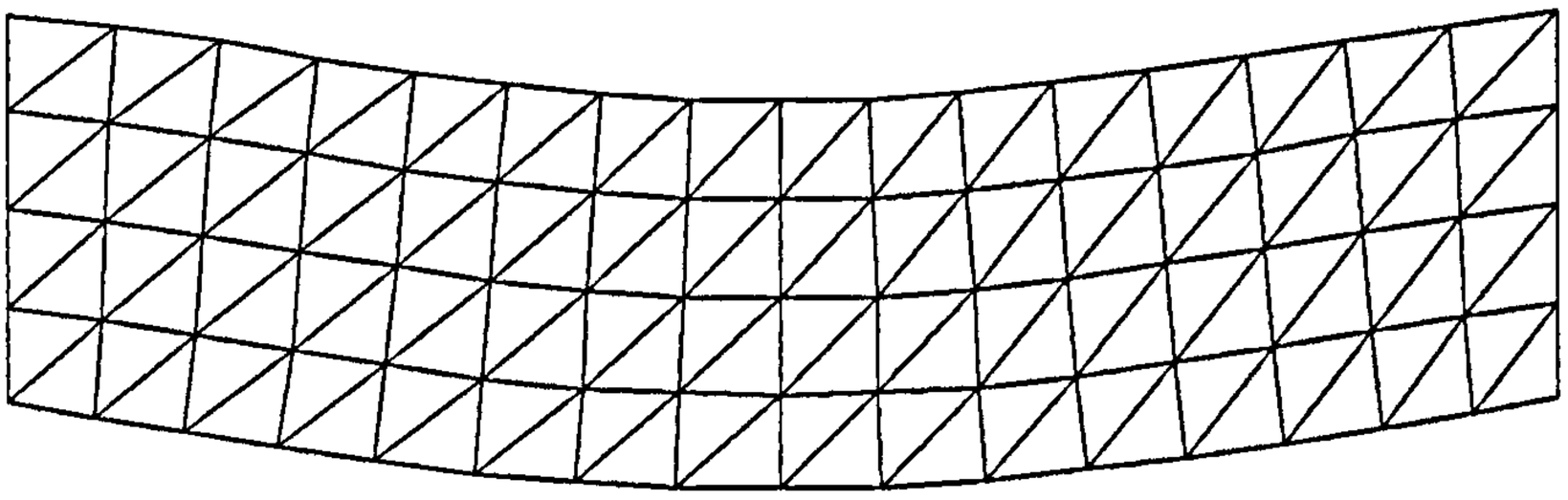

$nx = 16, ny = 4, ne = 128$

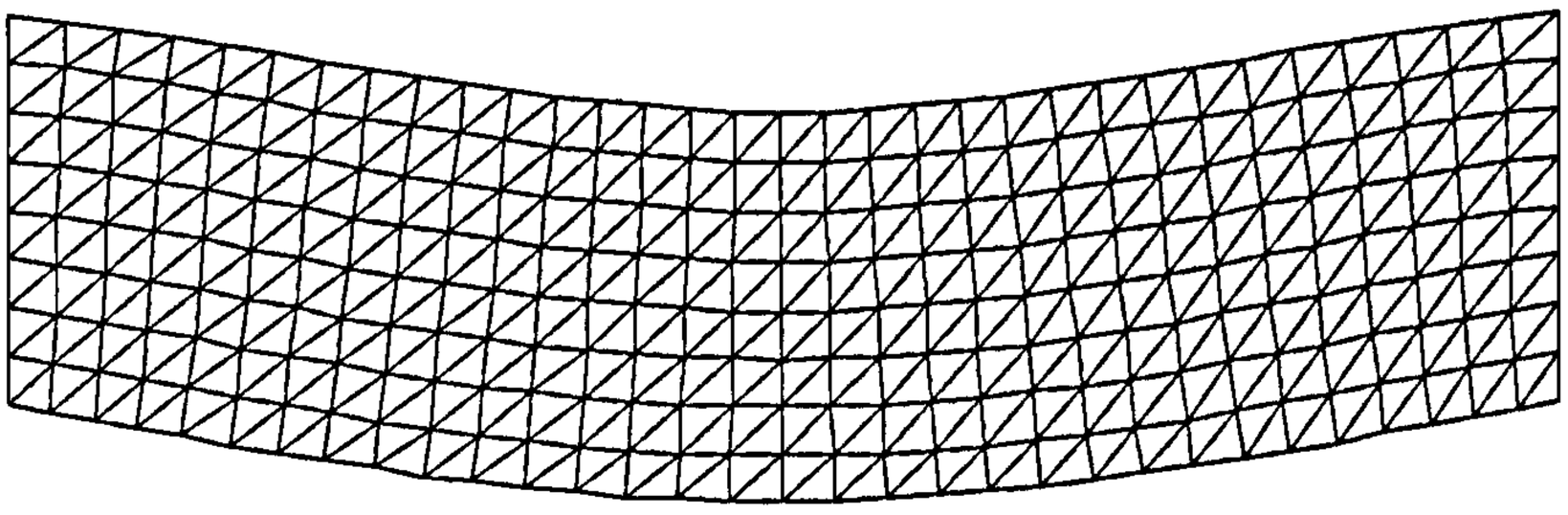

$nx = 32, ny = 8, ne = 512$

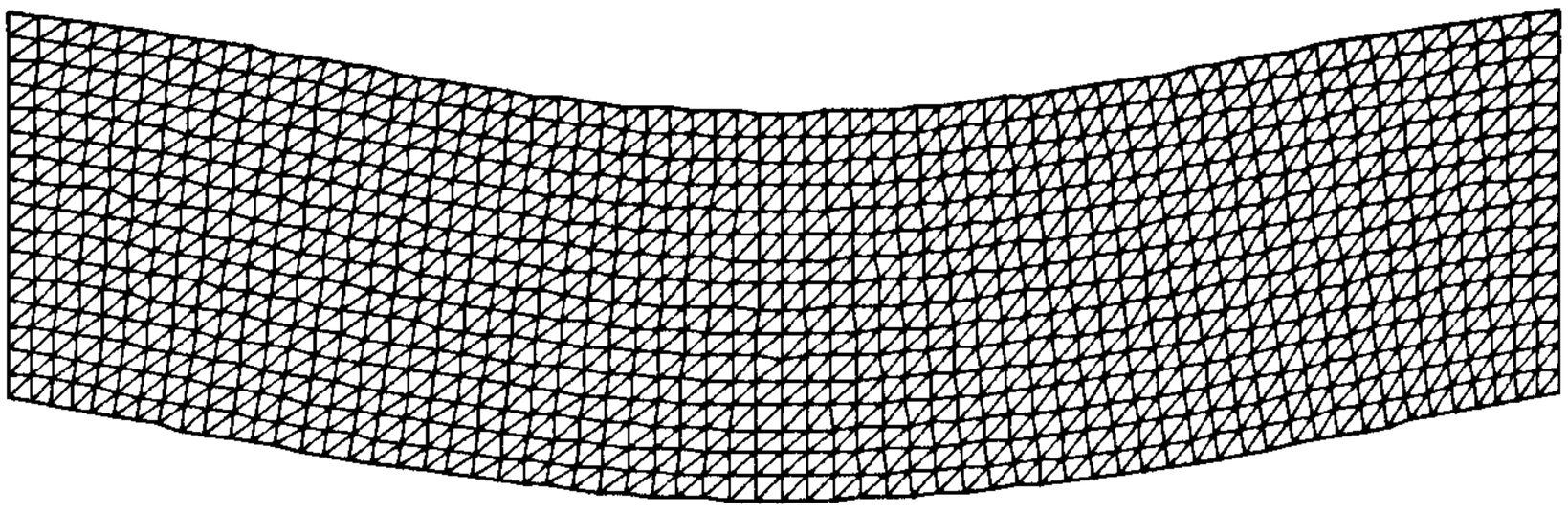

$nx = 64, ny = 16, ne = 2048$

Figure 5.2: Mesh used for the case $a = 4$ showing displacements scaled by 20

Table 5.1: $a = 1$

nx	ny	ne	$u_h(0.5)$	% change	$\|\sigma_R - \sigma_h\|_{L_2}$
2	2	8	-3.12500E-4		0.1412990
4	4	32	-3.36081E-4	7.54592	0.1092530
8	8	128	-3.54122E-4	5.36805	0.0846692
16	16	512	-3.64604E-4	2.96000	0.0572916
32	32	2048	-3.68890E-4	1.17552	0.0344721

Table 5.2: $a = 2$

nx	ny	ne	$u_2(1)$	% change	$\|\sigma_R - \sigma_h\|_{L_2}$
4	2	16	-1.47604E-3		0.4032210
8	4	64	-1.69420E-3	14.78010	0.3735500
16	8	256	-1.83988E-3	8.59875	0.2656750
32	16	1024	-1.89998E-3	3.26652	0.1611320
64	32	4096	-1.91965E-3	1.03527	0.0916544

Table 5.3: $a = 4$

nx	ny	ne	$u_2(2)$	% change	$\|\sigma_R - \sigma_h\|_{L_2}$
8	2	32	-0.917039E-2		1.981260
16	4	128	-1.180780E-2	28.760100	1.668130
32	8	512	-1.316920E-2	11.529700	1.042520
64	16	2048	-1.362870E-2	3.489200	0.578713
128	32	8192	-1.376230E-2	0.980284	0.311657

Table 5.4: $a = 8$

nx	ny	ne	$u_2(4)$	% change	$\|\sigma_R - \sigma_h\|_{L_2}$
16	2	64	-0.884218E-1		11.19020
32	4	256	-1.262250E-1	42.747600	8.72099
64	8	1024	-1.437480E-1	13.882400	5.12059
128	16	4096	-1.492030E-1	3.794840	2.71448
256	32	16384	-1.506940E-1	0.999310	1.40654

Table 5.5: $a = 16$

nx	ny	ne	$u_2(8)$	% change	$\|\sigma_R - \sigma_h\|_{L_2}$
32	2	128	-1.18210		64.18900
64	4	512	-1.76900	49.64890	48.48530
128	8	2048	-2.03113	14.81800	27.84990
256	16	8192	-2.11073	3.91900	14.51540
512	32	32768	-2.13197	1.00629	7.39222

Table 5.6: $a = 32$

nx	ny	ne	$u_2(16)$	% change	$\|\sigma_R - \sigma_h\|_{L_2}$
64	2	256	-1.79966E+1		366.9110
128	4	1024	-2.73195E+1	51.80370	273.8450
256	8	4096	-3.14387E+1	15.07680	156.0470
512	16	16384	-3.26785E+1	2.98931	80.8208

Table 5.7: $a = 64$

nx	ny	ne	$u_2(32)$	% change	$\|\sigma_R - \sigma_h\|_{L_2}$
64	2	256	-2.84404E+2		2088.180
128	4	1024	-4.33372E+2	52.37900	1550.850
256	8	4096	-4.98952E+2	15.13250	880.851
512	16	16384	-5.18624E+2	3.94266	455.011

Chapter 6

Thermal Modelling

6.1 Introduction

The important consequence of fire exposure to the building frame is the increase in temperature. As a result, the beams in the frame expand causing additional loading if the expansion is resisted. Additionally, the beams weaken causing further deformation. This chapter introduces the concept of thermal strain and shows that, in a beam, this causes both a thermal force and thermal moments. The main part of this chapter derives a finite element method for calculating the temperature in the cross-section of a fire-exposed beam taking into account the exchange of radiation between internal cavity walls. This method, accompanied by the mesh generation algorithm in Chapter 4, completes the theoretical background for a computer program to solve the thermal part of the fire-exposed frame problem.

6.2 Thermal expansion

Most building materials experience some change in shape when their temperature is raised. This phenomenon is generally known as thermal expansion since a rise in temperature usually causes a positive thermal strain. If the material is isotropic then the effect is uniform in all directions and so there are no thermal shear strains. Hence thermal strain is hydrostatic for isotropic materials. The common building materials, steel and concrete, are assumed to be thermally isotropic.

When we consider the constitutive equation of a material we relate the stress components, σ_{ij}, to the strains, ϵ_{ij}. For an elastic material experiencing no thermal strain we have, in terms of Lamé coefficients,

$$\sigma_{ij} = \lambda\delta_{ij}(\epsilon_{11} + \epsilon_{22} + \epsilon_{33}) + 2\mu\epsilon_{ij}. \tag{6.1}$$

If the material's temperature is raised then it experiences a thermal strain, ϵ_{th}, in each direction. This alters the equilibrium state of the material so that the elastic strain

components, to which the constitutive equation applies, are found by subtracting the thermal strain from the total strain. Hence the thermoelastic constitutive equation is

$$\sigma_{ij} = \lambda(\epsilon_{11} + \epsilon_{22} + \epsilon_{33}) + 2\mu\epsilon_{ij} - (3\lambda + 2\mu)\delta_{ij}\epsilon_{th}. \tag{6.2}$$

In the vector form used in Chapter 5 we have

$$\boldsymbol{\sigma}(\boldsymbol{u}) = \boldsymbol{D}\boldsymbol{\epsilon}(\boldsymbol{u}) - \boldsymbol{\sigma}_{th} \tag{6.3}$$

where $\boldsymbol{\sigma}_{th}$, known as the thermal load vector, is

$$\boldsymbol{\sigma}_{th} = (3\lambda + 2\mu)\epsilon_{th}\begin{pmatrix}1\\1\\1\\0\\0\\0\end{pmatrix} = \frac{E\epsilon_{th}}{1-2\nu}\begin{pmatrix}1\\1\\1\\0\\0\\0\end{pmatrix}. \tag{6.4}$$

From Chapter 5 we have that

$$\int_{x\in\Omega} \boldsymbol{\sigma}(\boldsymbol{u})^T\boldsymbol{\epsilon}(\boldsymbol{v})\,\mathrm{d}\boldsymbol{x} = \int_{x\in\Omega} \boldsymbol{f}^T\boldsymbol{v}\,\mathrm{d}\boldsymbol{x} + \int_{x\in\Gamma_1} \boldsymbol{g}^T\boldsymbol{v}\,\mathrm{d}\boldsymbol{x}. \tag{6.5}$$

Substituting for $\boldsymbol{\sigma}$ we have

$$\int_{x\in\Omega} \boldsymbol{\epsilon}(\boldsymbol{u})^T\boldsymbol{D}\boldsymbol{\epsilon}(\boldsymbol{v})\,\mathrm{d}\boldsymbol{x} = \int_{x\in\Omega} \boldsymbol{f}^T\boldsymbol{v}\,\mathrm{d}\boldsymbol{x} + \int_{x\in\Gamma_1} \boldsymbol{g}^T\boldsymbol{v}\,\mathrm{d}\boldsymbol{x} + \int_{x\in\Omega} \boldsymbol{\sigma}_{th}^T\boldsymbol{\epsilon}(\boldsymbol{v})\,\mathrm{d}\boldsymbol{x}. \tag{6.6}$$

Hence the weak form of the thermoelastic equilibrium equations is

$$a(\boldsymbol{u},\boldsymbol{v}) = (\boldsymbol{f},\boldsymbol{v}) + [\boldsymbol{g},\boldsymbol{v}] + (\boldsymbol{\epsilon}(\boldsymbol{v}),\boldsymbol{\sigma}_{th}). \tag{6.7}$$

In the 2D finite element solution procedure the local thermal load vector is given by

$$\boldsymbol{Q}_i = \int_0^1 \int_0^{1-\eta} \boldsymbol{B}_i^T\boldsymbol{\sigma}_{th}J_i\,\mathrm{d}\xi\mathrm{d}\eta \tag{6.8}$$

where

$$\boldsymbol{\sigma}_{th} = \frac{E\epsilon_{th}}{1-2\nu}\begin{pmatrix}1\\1\\0\end{pmatrix}. \tag{6.9}$$

If $\boldsymbol{\sigma}_{th}$ is an element constant then

$$\boldsymbol{Q}_i = \frac{J_i}{2}\boldsymbol{B}_i^T\boldsymbol{\sigma}_{th}. \tag{6.10}$$

The finite element solution is then found by solving the system

$$\boldsymbol{K}\boldsymbol{U} = \boldsymbol{F} + \boldsymbol{G} + \boldsymbol{Q} \tag{6.11}$$

where $\boldsymbol{Q}$ is the global thermal load vector found by summing the contributions from $\boldsymbol{Q}_i$ for each element.

6.3 Heat conduction

Fourier's law for the conduction of heat in a solid, isotropic material is

$$\boldsymbol{q} = -k\,(\nabla T) \tag{6.12}$$

where $\boldsymbol{q}$ is the heat flux vector (rate of heat energy flow), k is the thermal conductivity and T is the temperature. The rate of change of heat energy, Q, within a body, Ω, balances the flow of heat through the surface, Γ, so that

$$\int_{\boldsymbol{x}\in\Omega} \frac{\partial Q}{\partial t}\,\mathrm{d}\boldsymbol{x} + \int_{\boldsymbol{x}\in\Gamma} \boldsymbol{q}\cdot\boldsymbol{n}\,\mathrm{d}\boldsymbol{x} = 0, \tag{6.13}$$

where $\boldsymbol{n}$ is the outward-pointing unit vector normal to the surface. Application of the divergence theorem and substitution of (6.3) leads to

$$\frac{\partial Q}{\partial t} = \nabla\cdot(k\nabla T)\,. \tag{6.14}$$

We assume that the heat energy used for thermal expansion is negligible compared with that used to raise the temperature so that

$$\frac{\partial Q}{\partial t} = \frac{\mathrm{d}Q}{\mathrm{d}T}\frac{\partial T}{\partial t}. \tag{6.15}$$

From physics[7] we have that

$$\frac{\mathrm{d}Q}{\mathrm{d}T} = \rho c \tag{6.16}$$

where ρ is the material mass density and c is the specific heat capacity. Hence we have the heat conduction equation

$$\nabla\cdot(k\nabla T) = \rho c\frac{\partial T}{\partial t}. \tag{6.17}$$

A more rigorous derivation of (6.17) is found in Whitaker [38, Chapter 4].

To justify the assumption that the thermal strain energy may be neglected consider this equation presented by Johns [17] for heat conduction with linear thermal expansion:

$$\nabla\cdot(k\nabla T) = (\rho c)_0\frac{\partial T}{\partial t} + \frac{E\alpha T_0}{1-2\nu}\frac{\partial}{\partial t}\left(\epsilon_{11}+\epsilon_{22}+\epsilon_{33}\right) \tag{6.18}$$

where $(\rho c)_0$ is ρc evaluated when there is no thermal strain and T_0 is the initial uniform temperature. For beams, $\epsilon_{22} = \epsilon_{33} = -\nu\epsilon_{11}$ with $\epsilon_{11} = E\alpha(T - T_0)$ so we have

$$\nabla\cdot(k\nabla T) = \left((\rho c)_0 + E^2\alpha^2 T\right)\frac{\partial T}{\partial t}. \tag{6.19}$$

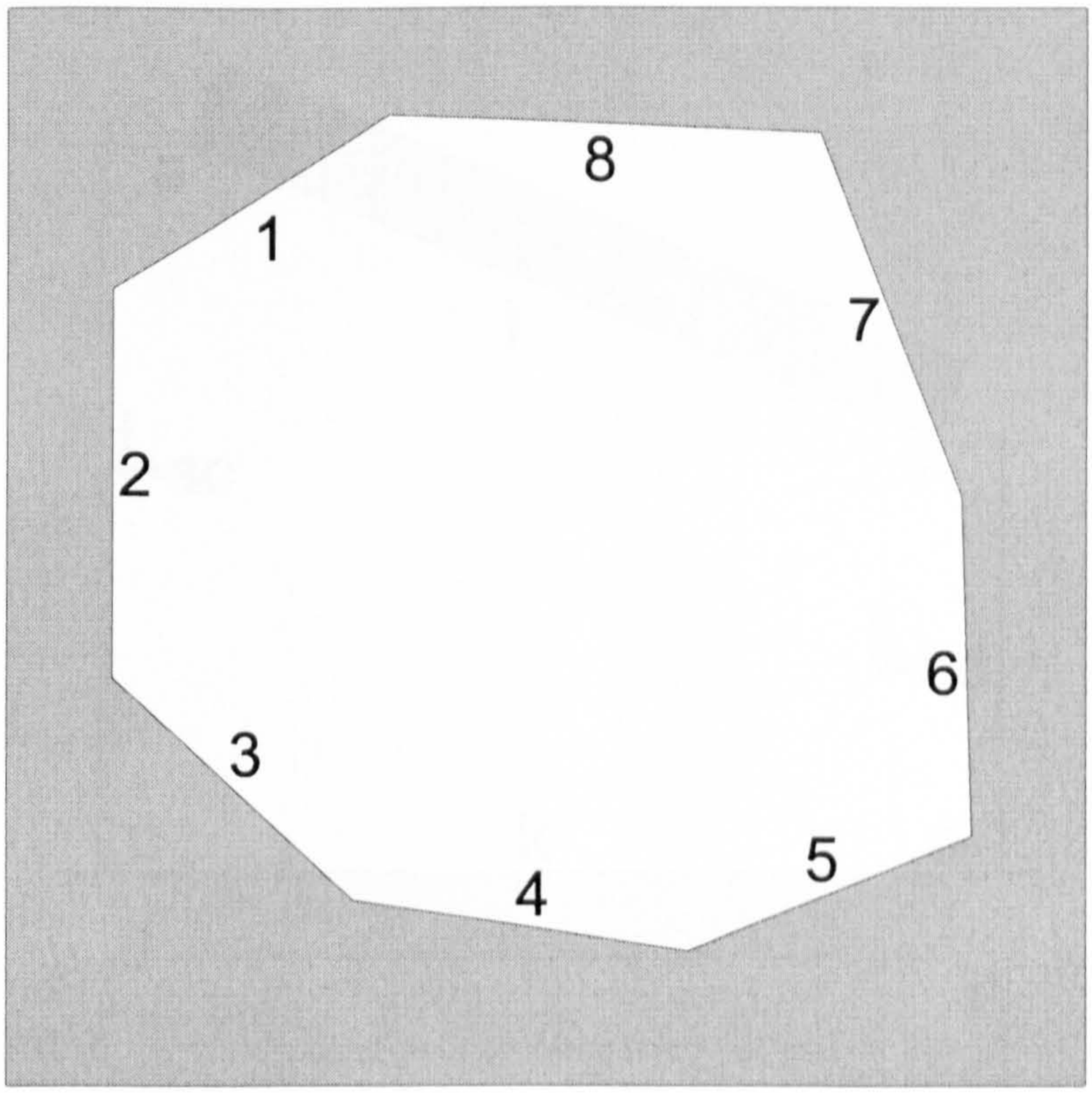

Figure 6.1: Convex cavity

In a typical practical application the quantity ρc will be of the order of 10^6 whereas $E^2\alpha^2 T$ will be of the order of 10^{-1}. Hence the initial assumption is justified. Consequently the temperature distribution is independent of the strain. The solution of the heat conduction equation requires the specification of boundary conditions. For practical problems these are expressions for the heat flux, $\boldsymbol{q}(\boldsymbol{x}, t)$, normal to the surface of the beam. An expression of the form

$$\boldsymbol{q} \cdot \boldsymbol{n} = h_c(T - T_g) + \epsilon\sigma(T^4 - T_g^4) \tag{6.20}$$

is used to model exposure to a post-flashover fire [33]. In (6.20) h_c is the convection coefficient, ϵ is the resultant emissivity, σ is the Stefan-Bolzman constant ($5.67 \times 10^{-8} W m^{-2} K^{-4}$) and T_g is the temperature of the hot gas in Kelvin. Typical values for h_c and ϵ, used to model furnace tests, are $25 W m^{-2} K^{-1}$ and 0.3 respectively.

Treatment of cavities

Some beam designs include cavity regions which require special consideration in the solid thermal model. For simplicity we will ignore the effects of conduction and convection and assume that the only heat exchange is that of radiation between the cavity walls. In fact, Wickstrom[39] only uses a convection model to estimate the average gas temperature inside the cavity. Whitaker [38, Pages 445–450] shows that, for a 2D convex polygonal gray body enclosure where the temperature is uniform on each wall

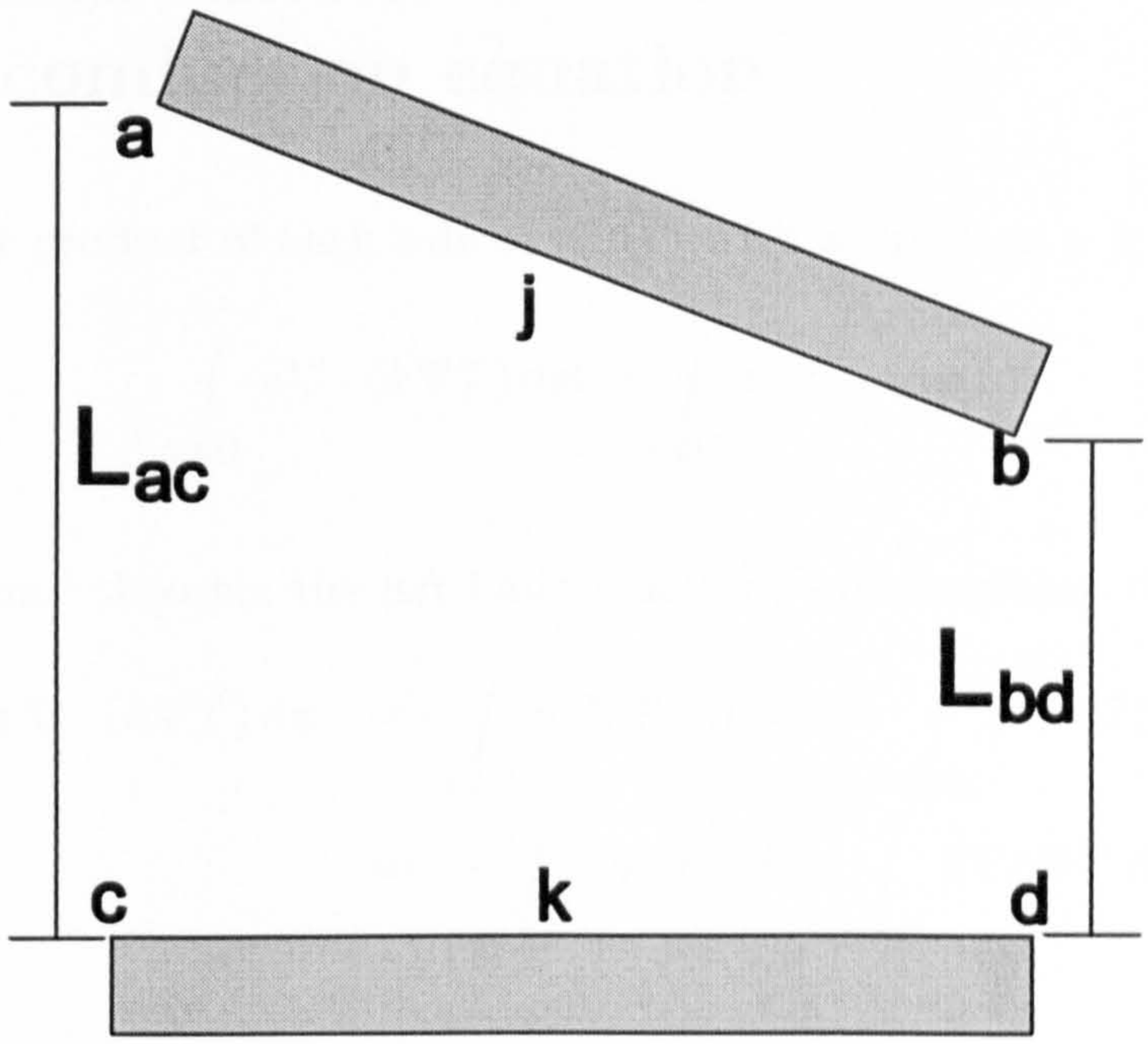

Figure 6.2: Calculation of configuration factor between cavity walls

(see Figure 6.1), the heat flux through the j'th wall is given by

$$\boldsymbol{q} \cdot \boldsymbol{n} = \left(\frac{\epsilon_j}{1 - \epsilon_j} \right) \left(\sigma T_j^t + \sum_{k=1}^{N} M_{jk}^{-1} \left(\frac{\epsilon_k}{1 - \epsilon_k} \right) \sigma T_k^4 \right) \tag{6.21}$$

where ϵ_j is the emissivity of the j'th wall, T_j is the temperature of the j'th wall and M_{jk}^{-1} is the jk'th element of the inverse of the matrix $\boldsymbol{M}$ given by

$$M_{jk} = F_{jk} - \delta_{jk}(1 - \epsilon_k)^{-1} \tag{6.22}$$

where F_{jk} is the configuration factor given by

$$F_{jk} = \frac{L_{ad} + L_{bc} - L_{ac} - L_{bd}}{2L_{ab}}. \tag{6.23}$$

The quantity L_{ab} is the distance between points a and b as illustrated in Figure 6.2. Although the assumption of uniform wall temperature is restrictive we can approximate the non-uniform case by partitioning the wall. This is naturally achieved in the finite element method.

6.4 Galerkin finite element method for solving the heat conduction equation

We take the inner product of each side of (6.17) with a function $v \in H$ to give us

$$\int_{x\in\Omega} v\nabla\cdot(k\nabla T)\,\mathrm{d}\boldsymbol{x} = \int_{x\in\Omega} v\rho c\frac{\partial T}{\partial t}\,\mathrm{d}\boldsymbol{x}. \tag{6.24}$$

Using the divergence theorem the left hand side may be integrated to give

$$\begin{aligned}\int_{x\in\Omega} v\nabla\cdot(k\nabla T)\,\mathrm{d}\boldsymbol{x} &= \int_{x\in\Gamma} vk\nabla T\cdot\boldsymbol{n})\,\mathrm{d}\boldsymbol{x} - \int_{x\in\Omega} k\nabla v\nabla T\,\mathrm{d}\boldsymbol{x} &(6.25)\\ &= -\int_{x\in\Gamma} v\boldsymbol{q}\cdot\boldsymbol{n}\,\mathrm{d}\boldsymbol{x} - \int_{x\in\Omega} k\nabla v\nabla T\,\mathrm{d}\boldsymbol{x}. &(6.26)\end{aligned}$$

Hence (6.24) may be written as

$$\int_{x\in\Omega} k\nabla v\nabla T\,\mathrm{d}\boldsymbol{x} + \int_{x\in\Omega} v\rho c\frac{\partial T}{\partial t}\,\mathrm{d}\boldsymbol{x} + \int_{x\in\Gamma} v\boldsymbol{q}\cdot\boldsymbol{n}\,\mathrm{d}\boldsymbol{x} = 0. \tag{6.27}$$

Let V be a finite dimensional subspace of H. This is a space of piecewise polynomials with nodes at $\boldsymbol{x}_i$, $i = 1\ldots n$. For the finite element method we choose $v \in V$ and approximate T with $T_h \in V$. The approximation T_h may be written as

$$T_h(\boldsymbol{x},t) = \boldsymbol{N}(\boldsymbol{x})\boldsymbol{T}(t) \tag{6.28}$$

where $\boldsymbol{N} = (N_1, N_2, \ldots, N_n)$ is a vector of basis functions and $\boldsymbol{T}$ is the vector containing the time-dependent degrees of freedom. We choose v to be each of the components of $\boldsymbol{N}$ in turn so that, after substituting (6.28) in (6.27), we have

$$\left(\int_{x\in\Omega} k\boldsymbol{B}^T\boldsymbol{B}\,\mathrm{d}\boldsymbol{x}\right)\boldsymbol{T}(t) + \left(\int_{x\in\Omega} \rho c\boldsymbol{N}^T\boldsymbol{N}\,d\boldsymbol{x}\right)\frac{\mathrm{d}\boldsymbol{T}}{\mathrm{d}t} + \int_{x\in\Gamma} \boldsymbol{N}^T\boldsymbol{q}\cdot\boldsymbol{n}\,\mathrm{d}\boldsymbol{x} = 0 \tag{6.29}$$

where, in 2D,

$$\boldsymbol{B} = \begin{pmatrix} \frac{\partial N_1}{\partial x_1} & \frac{\partial N_2}{\partial x_1} & \cdots & \frac{\partial N_n}{\partial x_1} \\ \frac{\partial N_1}{\partial x_2} & \frac{\partial N_2}{\partial x_2} & \cdots & \frac{\partial N_n}{\partial x_2} \end{pmatrix}. \tag{6.30}$$

We define the conductivity matrix, $\boldsymbol{K}_k$, as

$$\boldsymbol{K}_k = \int_{x\in\Omega} k\boldsymbol{B}^T\boldsymbol{B}\,\mathrm{d}\boldsymbol{x} \tag{6.31}$$

and the capacitance matrix, $\boldsymbol{C}$, as

$$\boldsymbol{C} = \int_{x \in \Omega} \rho c \boldsymbol{N}^T \boldsymbol{N} \, \mathrm{d}\boldsymbol{x}. \tag{6.32}$$

Hence (6.29) is written as

$$\boldsymbol{K}\boldsymbol{T} + \boldsymbol{C}\frac{\mathrm{d}\boldsymbol{T}}{\mathrm{d}t} + \int_{x \in \Gamma} \boldsymbol{N}^T \boldsymbol{q} \cdot \boldsymbol{n} \, \mathrm{d}\boldsymbol{x} = 0. \tag{6.33}$$

The boundary, Γ, comprises the external surface, Γ_{ex}, and the cavity walls, Γ_c. Hence the boundary integral may be written as

$$\int_{x \in \Gamma} \boldsymbol{N}^T \boldsymbol{q} \cdot \boldsymbol{n} \, \mathrm{d}\boldsymbol{x} = \int_{x \in \Gamma_{ex}} \boldsymbol{N}^T \boldsymbol{q} \cdot \boldsymbol{n} \, \mathrm{d}\boldsymbol{x} + \int_{x \in \Gamma_c} \boldsymbol{N}^T \boldsymbol{q} \cdot \boldsymbol{n} \, \mathrm{d}\boldsymbol{x}. \tag{6.34}$$

Using (6.20) the integral over Γ_{ex} becomes

$$\int_{x \in \Gamma_{ex}} \boldsymbol{N}^T \boldsymbol{q} \cdot \boldsymbol{n} \, \mathrm{d}\boldsymbol{x} = \int_{x \in \Gamma_{ex}} \boldsymbol{N}^T \left(h_c(T - T_g) + \epsilon\sigma(T^4 - T_g^4) \right) \mathrm{d}\boldsymbol{x} \tag{6.35}$$

$$= \int_{x \in \Gamma_{ex}} \boldsymbol{N}^T h_t (T - T_g) \, \mathrm{d}\boldsymbol{x} \tag{6.36}$$

where

$$h_t = h_c + \epsilon\sigma(T + T_g)(T^2 + T_g^2) \tag{6.37}$$

will be referred to as the total heat transfer coefficient. Replacing T with the approximation T_h we have, in terms of the degree of freedom vector $\boldsymbol{T}$,

$$\int_{x \in \Gamma_{ex}} \boldsymbol{N}^T \boldsymbol{q} \cdot \boldsymbol{n} \, \mathrm{d}\boldsymbol{x} = \left(\int_{x \in \Gamma_{ex}} h_t \boldsymbol{N}^T \boldsymbol{N} \, \mathrm{d}\boldsymbol{x} \right) \boldsymbol{T} - \int_{x \in \Gamma_{ex}} \boldsymbol{N}^T T_g \, \mathrm{d}\boldsymbol{x}. \tag{6.38}$$

Let us define the external heat transfer matrix, $\boldsymbol{K}_{ex}$ and the external heat load vector, $\boldsymbol{F}_{ex}$, to be

$$\boldsymbol{K}_{ex} = \int_{x \in \Gamma_{ex}} h_t \boldsymbol{N}^T \boldsymbol{N} \, \mathrm{d}\boldsymbol{x} \tag{6.39}$$

$$\boldsymbol{F}_{ex} = \int_{x \in \Gamma_{ex}} \boldsymbol{N}^T T_g \, \mathrm{d}\boldsymbol{x}. \tag{6.40}$$

The integral over Γ_c may be written as sum of the integrals over each cavity, i.e.

$$\int_{x \in \Gamma_c} \boldsymbol{N}^T \boldsymbol{q} \cdot \boldsymbol{n} \, \mathrm{d}\boldsymbol{x} = \sum_{i=1}^{nc} \int_{x \in \Gamma_{c,i}} \boldsymbol{N}^T \boldsymbol{q} \cdot \boldsymbol{n} \, \mathrm{d}\boldsymbol{x} \tag{6.41}$$

where nc is the number of cavities. The integral over each $\Gamma_{c,i}$ may be written as the sum of the integrals over each wall, i.e.

$$\int_{x\in\Gamma_{c,i}} \boldsymbol{N}^T\boldsymbol{q}\cdot\boldsymbol{n}\,\mathrm{d}\boldsymbol{x} = \sum_{j=1}^{nw(i)} \int_{x\in\Gamma_{c,i,j}} \boldsymbol{N}^T\boldsymbol{q}\cdot\boldsymbol{n}\,\mathrm{d}\boldsymbol{x} \tag{6.42}$$

where $nw(i)$ is the number of walls of the i'th cavity. Using (6.21) the integral over each $\Gamma_{c,i,j}$ may be written as

$$\int_{x\in\Gamma_{c,i,j}} \boldsymbol{N}^T\boldsymbol{q}\cdot\boldsymbol{n}\,\mathrm{d}\boldsymbol{x} = \int_{x\in\Gamma_{c,i,j}} \boldsymbol{N}^T\left(\frac{\epsilon_{ij}}{1-\epsilon_{ij}}\right)\left\{\sigma T_{ij}^4 + \sum_{k=1}^{nw(i)} M_{ijk}^{-1}\left(\frac{\epsilon_{ik}}{1-\epsilon_{ik}}\right)\sigma T_{ik}^4\right\}\mathrm{d}\boldsymbol{x} \tag{6.43}$$

where ϵ_{ij} is the emissivity of the j'th wall of the i'th cavity, T_{ij} is the temperature of the j'th wall of the i'th cavity and $M_i = [M_{ijk}]$ is the i'th coefficient matrix as defined in (6.22). For the purposes of the finite element method we write the above as

$$\int_{x\in\Gamma_{c,i,j}} \boldsymbol{N}^T\boldsymbol{q}\cdot\boldsymbol{n}\,\mathrm{d}\boldsymbol{x} = \int_{x\in\Gamma_{c,i,j}} \boldsymbol{N}^T\gamma_{ij}T_{ij}\,\mathrm{d}\boldsymbol{x} - \int_{x\in\Gamma_{c,i,j}} \boldsymbol{N}^T q_{ij}\,d\boldsymbol{x} \tag{6.44}$$

where

$$\gamma_{ij} = \left(\frac{\epsilon_{ij}}{1-\epsilon_{ij}}\right)\sigma T_{ij}^3, \tag{6.45}$$

$$q_{ij} = \sum_{k=1}^{nw(i)} M_{ijk}^{-1}\left(\frac{\epsilon_{ik}}{1-\epsilon_{ik}}\right)\sigma T_{ik}^4. \tag{6.46}$$

Now we make the finite element approximation

$$T_{ij}(t) = \boldsymbol{N}(\boldsymbol{x})\boldsymbol{T}(t) \tag{6.47}$$

which gives us

$$\int_{x\in\Gamma_{c,i,j}} \boldsymbol{N}^T\boldsymbol{q}\cdot\boldsymbol{n}\,\mathrm{d}\boldsymbol{x} = \left(\int_{x\in\Gamma_{c,i,j}} \gamma_{ij}\boldsymbol{N}^T\boldsymbol{N}\,\mathrm{d}\boldsymbol{x}\right)\boldsymbol{T} - \int_{x\in\Gamma_{c,i,j}} \boldsymbol{N}^T q_{ij}\,\mathrm{d}\boldsymbol{x}. \tag{6.48}$$

Let us define the cavity heat transfer matrix, $\boldsymbol{K}_c$, and the cavity heat load vector, $\boldsymbol{F}_c$, as

$$\boldsymbol{K}_c = \sum_{i=1}^{nc}\sum_{j=1}^{nw(i)} \int_{x\in\Gamma_{c,i,j}} \gamma_{ij}\boldsymbol{N}^T\boldsymbol{N}\,\mathrm{d}\boldsymbol{x}, \tag{6.49}$$

$$\boldsymbol{F}_c = \sum_{i=1}^{nc}\sum_{j=1}^{nw(i)} \int_{x\in\Gamma_{c,i,j}} \boldsymbol{N}^T q_{ij}\,\mathrm{d}\boldsymbol{x}. \tag{6.50}$$

The finite element heat equation may now be written as

$$\boldsymbol{K}\boldsymbol{T} + \boldsymbol{C}\frac{\mathrm{d}\boldsymbol{T}}{\mathrm{d}t} = \boldsymbol{F} \tag{6.51}$$

where

$$\boldsymbol{K} = \boldsymbol{K}_k + \boldsymbol{K}_{ex} + \boldsymbol{K}_c \tag{6.52}$$

$$\boldsymbol{F} = \boldsymbol{F}_{ex} + \boldsymbol{F}_c. \tag{6.53}$$

We now have a system of ordinary differential equations in the degrees of freedom of the finite element solution which are nonlinear because $\boldsymbol{K}$ and $\boldsymbol{C}$ depend on $\boldsymbol{T}$. This may be solved using any time integration scheme. Zienkiewicz [40, Page 570–575] uses a weighted residual approach to derive, for constant $\boldsymbol{K}$ and $\boldsymbol{C}$, the general recurrence scheme

$$\left(\frac{\boldsymbol{C}}{\Delta t} + \boldsymbol{K}\theta\right)\boldsymbol{T}_i = \left(\frac{\boldsymbol{C}}{\Delta t} - \boldsymbol{K}(1-\theta)\right)\boldsymbol{T}_{i-1} + \boldsymbol{F}_i + \boldsymbol{F}_{i-1}(1-\theta) \tag{6.54}$$

where Δt is the time step length and θ is a parameter between 0 and 1 which determines the specific recurrence scheme. To apply this to fire problems we need to approximate the temperature dependent $\boldsymbol{K}$ and $\boldsymbol{C}$ with their averages over the time step. Hence the recurrence scheme becomes

$$\left(\frac{\bar{\boldsymbol{C}}}{\Delta t} + \bar{\boldsymbol{K}}\theta\right)\boldsymbol{T}_i = \left(\frac{\bar{\boldsymbol{C}}}{\Delta t} - \bar{\boldsymbol{K}}(1-\theta)\right)\boldsymbol{T}_{i-1} + \boldsymbol{F}_i + \boldsymbol{F}_{i-1}(1-\theta) \tag{6.55}$$

where

$$\bar{\boldsymbol{C}} = \frac{\boldsymbol{C}(\boldsymbol{T}_i) + \boldsymbol{C}(\boldsymbol{T}_{i-1})}{2} \tag{6.56}$$

$$\bar{\boldsymbol{K}} = \frac{\boldsymbol{K}(\boldsymbol{T}_i) + \boldsymbol{K}(\boldsymbol{T}_{i-1})}{2}. \tag{6.57}$$

Alternatively we could use

$$\bar{\boldsymbol{C}} = \boldsymbol{C}(\bar{\boldsymbol{T}}) \tag{6.58}$$

$$\bar{\boldsymbol{K}} = \boldsymbol{K}(\bar{\boldsymbol{T}}) \tag{6.59}$$

where

$$\bar{\boldsymbol{T}} = \frac{\boldsymbol{T}_i + \boldsymbol{T}_{i-1}}{2} \tag{6.60}$$

which requires less computational effort. In either case we have a nonlinear system which must be solved iteratively. We shall use $\theta = 1$ which corresponds to an Euler backwards difference scheme. Hence, in (6.51), we make the substitution

$$\frac{\mathrm{d}\boldsymbol{T}}{\mathrm{d}t} = \frac{\boldsymbol{T}_i - \boldsymbol{T}_{i-1}}{\Delta t} \tag{6.61}$$

and approximate $\boldsymbol{C}$, $\boldsymbol{K}$ and $\boldsymbol{F}$ with $\bar{\boldsymbol{C}}$, $\bar{\boldsymbol{K}}$ and $\boldsymbol{F}_i$, respectively. Finally, we have

$$\left(\frac{\bar{\boldsymbol{C}}}{\Delta t} + \bar{\boldsymbol{K}}\right) \boldsymbol{T}_i = \frac{\bar{\boldsymbol{C}}}{\Delta t} \boldsymbol{T}_{i-1} + \boldsymbol{F}_i \tag{6.62}$$

or, rearranging in terms of $\Delta \boldsymbol{T} = \boldsymbol{T}_i - \boldsymbol{T}_{i-1}$,

$$\left(\frac{\bar{\boldsymbol{C}}}{\Delta t} + \bar{\boldsymbol{K}}\right) \Delta \boldsymbol{T} = \boldsymbol{F}_i - \bar{\boldsymbol{K}} \boldsymbol{T}_{i-1}. \tag{6.63}$$

6.5 Mesh generation

We shall use the mesh generation procedure described in Chapter 4 based on a measure of the error calculated after the first time step. We may easily implement the Bank-Weiser error estimator by first discretizing the time dimension of (6.17) to give us the equation to solve in the space domain as

$$-\nabla(k \cdot \nabla T) + \frac{\rho c}{\Delta t} T = \frac{\rho c}{\Delta t} T_0 \tag{6.64}$$

where T_0 is the temperature in the previous time step (in this case the initial temperature). This is the form of the equation for which the Bank-Weiser estimator was implemented in Chapter 3 with $a = k$ and $b = \frac{\rho c}{\Delta t}$. Remember, though, that the error estimator behaved poorly for $b >> a$ so that we must not have

$$\frac{\rho c}{\Delta t} >> k. \tag{6.65}$$

In practice ρc is about 10^5 times greater than k and so the Bank-Weiser estimator cannot be expected to perform well. Hence the error measure we shall use is

$$\|q - q_h\|_{L_2} \tag{6.66}$$

in which we approximate $\boldsymbol{q}$ with the recovered flux $\boldsymbol{q}_R$ given by

$$\boldsymbol{q}_R = \boldsymbol{N}\boldsymbol{Q} \tag{6.67}$$

where the components of $\boldsymbol{Q}$ are given in (3.92).

6.5.1 Test problem

To demonstrate the error estimator we shall apply it to a test problem in which the solution is

$$T(x, y, t) = 20 + 100 \sin(\lambda x) \sin(\lambda y) \exp(-2\alpha^2 \lambda^2 t) \tag{6.68}$$

where T is the temperature in degrees Celsius, x and y are between 0 and $l = 0.1$, $\lambda = \frac{\pi}{l}$ and $\alpha^2 = \frac{k}{\rho c} = \frac{10}{1000000}$. The initial temperature distribution is then

$$T(x, y, 0) = 20 + 100 \sin(\lambda x) \sin(\lambda y) \tag{6.69}$$

(illustrated in Figure 6.1) and the boundary conditions are

$$T(0, y, t) = T(l, y, t) = 20 \tag{6.70}$$
$$T(x, 0, t) = T(x, l, t) = 20. \tag{6.71}$$

The finite element solution has been calculated for a duration of 1 minute using 1, 10 and 100 time steps. The initial mesh was refined four times with zero tolerance so that the refinement was uniform. The uniformly refined meshes are shown in Figure 6.2. Table 6.1 shows the norms of the true flux error and that estimated after the first time step. Figure 6.3 shows adapted meshes obtained using non-zero tolerance values for the 10 timestep case. The results illustrate the effectiveness of the recovered flux estimator for the finite element solution to heat conduction problems using irregular meshes. However, no conclusions can be made regarding consistency or asymptotic exactness.

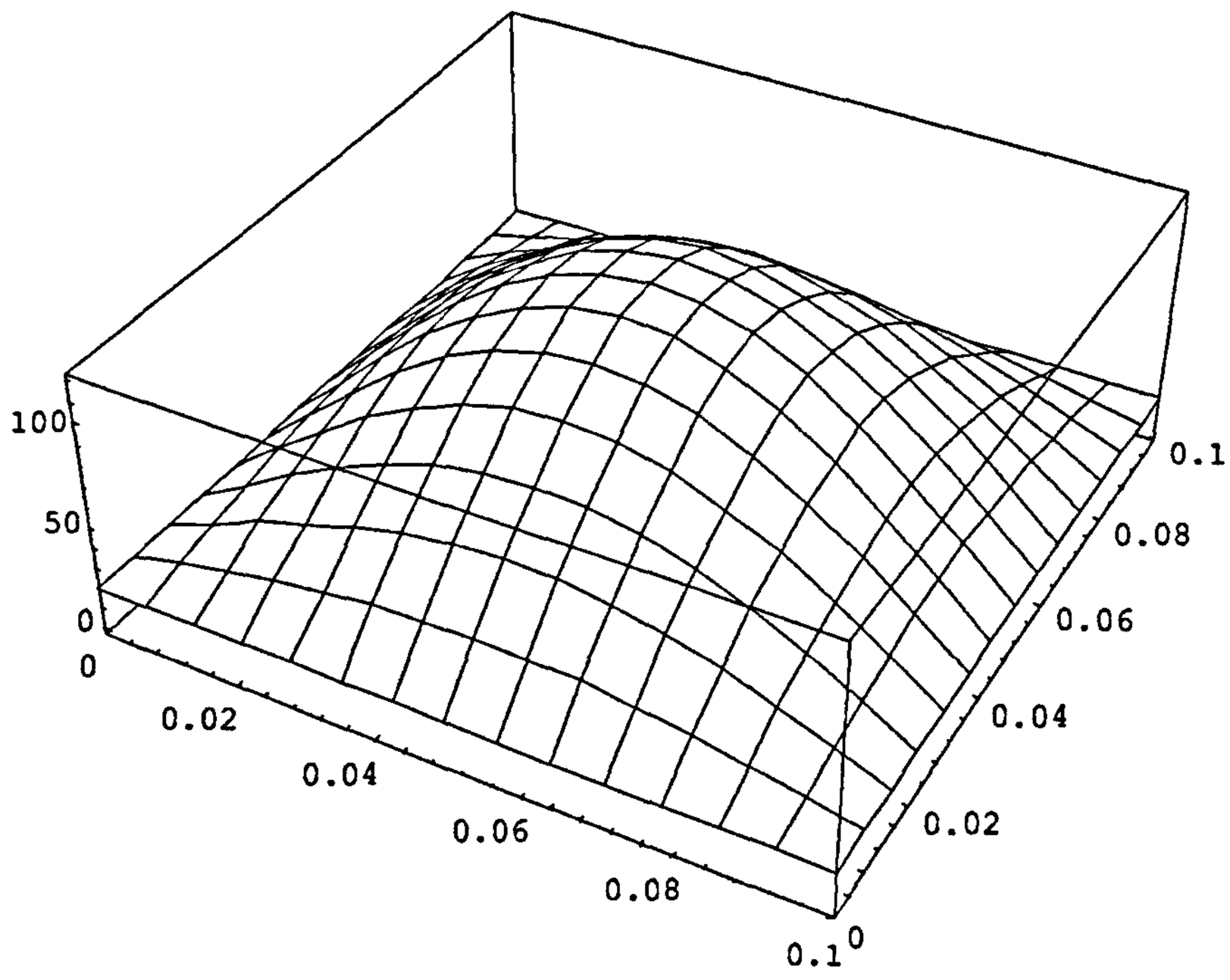

Figure 6.1 : Initial temperature distribution in test problem

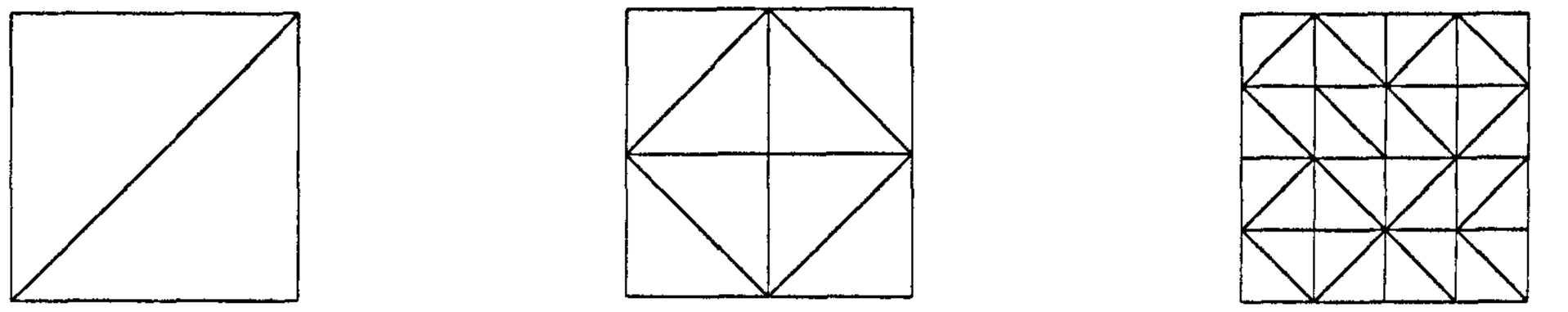

Initial Mesh | First refinement | Second refinement

Third refinement | Fourth refinement

Figure 6.2: Mesh used to analyse the recovered flux error estimator.

Table 6.1: Comparison of true flux errors and recovered flux error estimators.

Elements	$\|q - q_h\|^2_{L_2}$	$\|q_R - q_h\|^2_{L_2}$	Φ^2
8	2.4800E6	1.5100E6	0.609
32	0.4760E6	0.4560E6	0.958
128	0.1360E6	0.1230E6	0.904
512	0.0386E6	0.0300E6	0.789

One time step ($\Delta t = 1$ minute)

Elements	$\|q - q_h\|^2_{L_2}$	$\|q_R - q_h\|^2_{L_2}$	Φ^2
8	3.6000E6	2.7200E6	0.756
32	0.6500E6	0.6590E6	1.010
128	0.1770E6	0.1680E6	0.949
512	0.0589E6	0.0428E6	0.727

Ten time steps ($\Delta t = 0.1$ minute)

Elements	$\|q - q_h\|^2_{L_2}$	$\|q_R - q_h\|^2_{L_2}$	Φ^2
8	3.8000E6	2.9700E6	0.782
32	0.6820E6	0.7110E6	1.040
128	0.1830E6	0.1810E6	0.989
512	0.0472E6	0.0438E6	0.928

One hundred time steps ($\Delta t = 0.01$ minute)

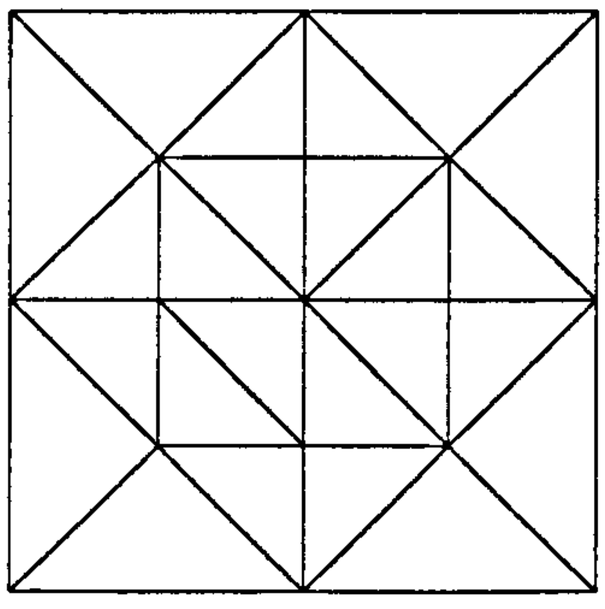

time steps = 10
tolerance = $100000 W/m^2$
nodes = 17
elements = 24
$\|q - q_h\|^2_{L_2}$ = $522E3$
$\|q_R - q_h\|^2_{L_2}$ = $580E3$
Φ^2 = 1.110

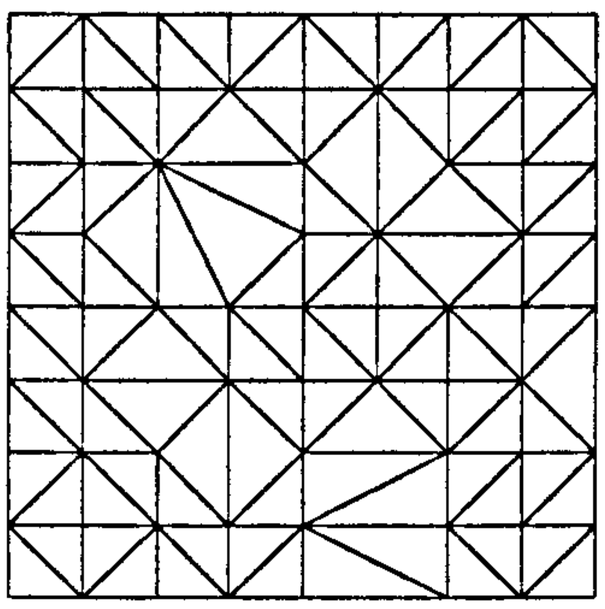

time steps = 10
tolerance = $10000 W/m^2$
nodes = 70
elements = 108
$\|q - q_h\|^2_{L_2}$ = $165E3$
$\|q_R - q_h\|^2_{L_2}$ = $152E3$
Φ^2 = 0.921

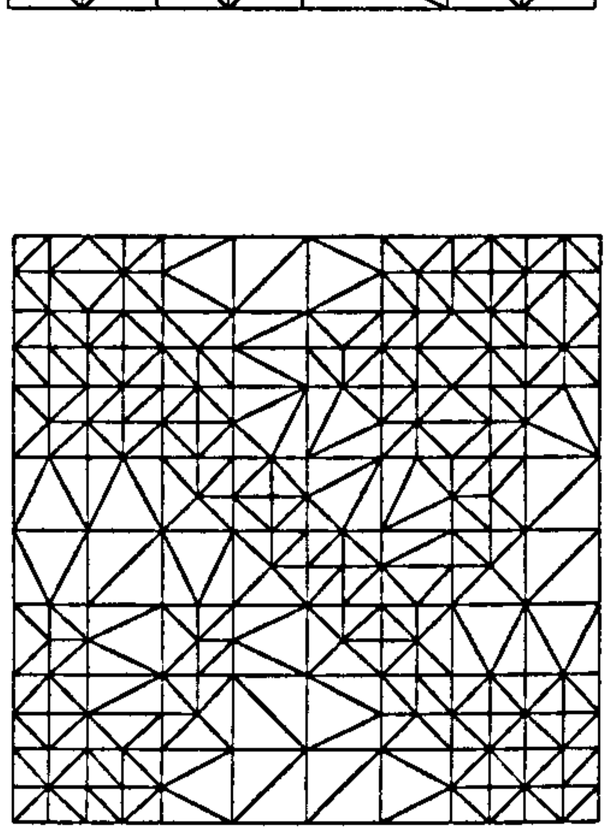

time steps = 10
tolerance = $1000 W/m^2$
nodes = 199
elements = 348
$\|q - q_h\|^2_{L_2}$ = $55.2E3$
$\|q_R - q_h\|^2_{L_2}$ = $50.5E3$
Φ^2 = 0.915

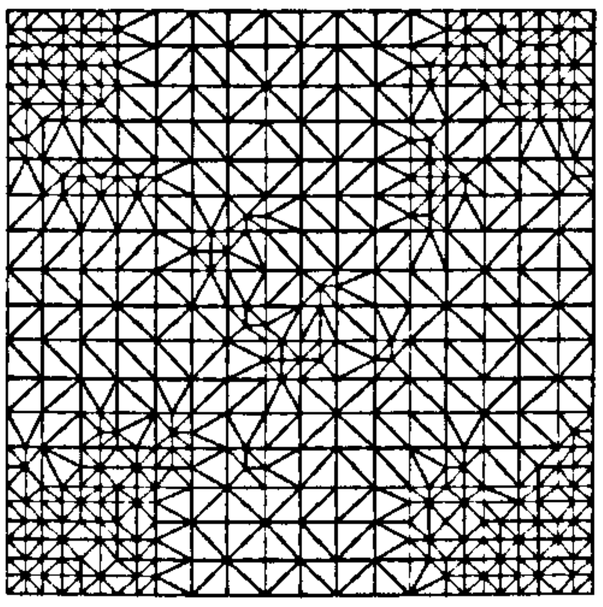

time steps = 10
tolerance = $100 W/m^2$
nodes = 516
elements = 934
$\|q - q_h\|^2_{L_2}$ = $24.9E3$
$\|q_R - q_h\|^2_{L_2}$ = $17.6E3$
Φ^2 = 0.707

Figure 6.3: Adapted mesh that gives convergence to the specified tolerance after the first time step.

Chapter 7

Beam Theory

7.1 Introduction

Having calculated, in the previous chapter, the temperature throughout the frame we now consider the structural consequences. This chapter uses the general theory of Chapter 5 to derive a finite element method for calculating frame deformation. To quantify the error in the method, a new error indicator, based on the 1985 paper by Bank and Weiser [9], is presented.

The most important structural aspect of a building is its frame. Generally, this is an assembly of slender beams which are loaded with the weight of the building's walls and floors. Although a beam is a three dimensional structure its slender nature allows the deformation to be approximated in a one-dimensional way in terms of quantities associated with an interior line. This is the principle behind all beam theories, the most simple of which are based on the Euler-Bernoulli assumption that cross sections remain plane and perpendicular to the line after deformation [25]. In the contexts considered here this provides a reasonable model for the bending of beams although modifications must be added to include the effects of transverse shear (Timoshenko beam theory) and warping should they be deemed significant [25], [11].

The character of a beam's cross section is incorporated into coefficients that influence the beam's resistance to deformation. Under normal conditions a building deforms, when loaded, in a linear elastic way. The modulus of elasticity (Young's modulus) is temperature dependent and an increase in temperature will usually reduce a beam's bending resistance. Furthermore, a heated beam, e.g. in a fire situation, experiences a thermal expansion (thermal strain) causing additional internal stress if this expansion is restricted in any way. If the loading is continually increased or if the structure is continually weakened then a stage will be reached when the internal stresses will exceed a yield point and the deformation will become plastic although in this chapter we shall consider only the linear elastic response.

In the context of the linear elastic deformation of beams and frames the purpose of this chapter is to describe an error estimator of the Bank-Weiser type (see [9]) which

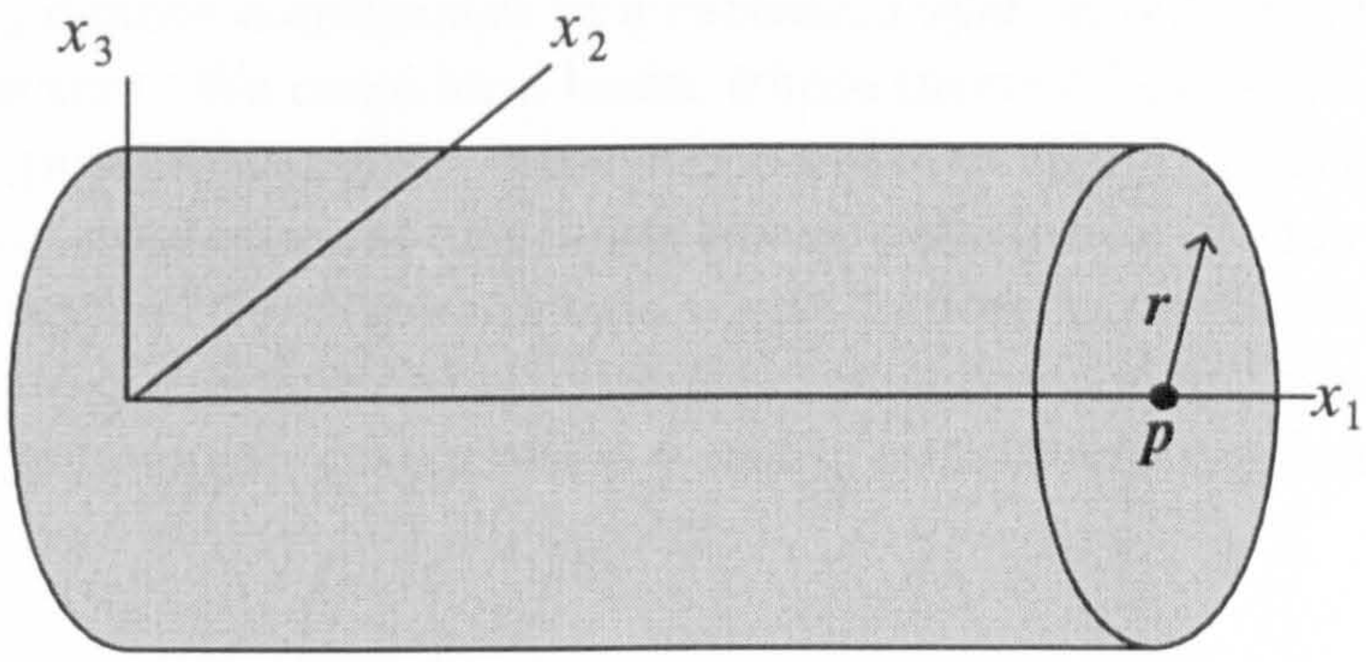

The deformation is approximated in terms of the x_1 coordinate. Any point, $\boldsymbol{x} = (x_1, x_2, x_3)$, may be written as the sum of $\boldsymbol{p} = (x_1, 0, 0)$ and $\boldsymbol{r} = (0, x_2, x_3)$. After deformation $\boldsymbol{p}$ is mapped to $\boldsymbol{p} + \boldsymbol{u}$ and $\boldsymbol{r}$ is mapped to $\boldsymbol{T}\boldsymbol{r}$ where $\boldsymbol{u}$ is the displacement of the interior line and $\boldsymbol{T}$ is a rotation matrix.

Figure 7.1: Beam axes.

can be used to assess the accuracy of the finite element solution to the equations describing the thermoelastic equilibrium of such structures. The main result is to show that the estimator, which can be computed element-by-element, is consistent with the actual error (as measured in the energy norm) and, for higher degrees of the piecewise polynomials used, the estimator is shown to be asymptotically exact. We show that the asymptotically exact cases correspond to cases where the finite element approximation has certain superconvergent properties.

To describe the estimator and our beam and frame model the presentation of the chapter is as follows: In section 7.2 we describe the Euler-Bernoulli beam model and the equilibrium equations in a weak form and we extend this to the case of a frame structure. In section 7.3 we then describe finite element approximations and, in section 7.4 we review the *a priori* estimates of the error considering the situations (involving different orders of the piecewise polynomials used) in which we have superconvergence at identifiable points. The main results of the chapter are then contained in Section 7.5 where we define and analyse the *a priori* error estimator. The performance of the estimator, for different degrees of polynomial approximation, is demonstrated in section 7.6.

7.2 The beam and frame model

7.2.1 Deformation of a beam

We present here the equations which describe the equilibrium of a single beam and we then extend this to describe a frame structure in the case of rigid joints.

Let x_1, x_2 and x_3 denote coordinates in a cartesian system with $\boldsymbol{b}_1$, $\boldsymbol{b}_2$ and $\boldsymbol{b}_3$ denoting the usual base vectors. We consider a beam whose interior line is the part $0 < x_1 < l$ of the x_1-axis with (possibly variable) cross-section of area $A(x_1)$. In Euler-Bernoulli beam theory we have an approximate one-dimensional description of this three-dimensional structure involving just the displacements u_1, u_2 and u_3 in the $\boldsymbol{b}_1$, $\boldsymbol{b}_2$ and $\boldsymbol{b}_3$ directions together with a twist θ about the interior line. It is convenient in what follows in the context of a single beam to gather these 4 scalar quantities together into the vector

$$\boldsymbol{u} := \begin{pmatrix} u_1 \\ u_2 \\ u_3 \\ \theta \end{pmatrix} \quad \text{with } \boldsymbol{u} = \boldsymbol{u}(x_1), 0 < x_1 < l. \tag{7.1}$$

The purpose of this section is to describe the idealised Euler-Bernoulli deformation and to give the system of ordinary differential equations (of length 4)

$$\boldsymbol{L}(\boldsymbol{u}) = \boldsymbol{f} \tag{7.2}$$

that $\boldsymbol{u}$ must satisfy. Since $\boldsymbol{u}$ now denotes the displacement of the interior line, where necessary we shall denote the general displacement vector by $\bar{\boldsymbol{u}}$.

To describe the equations we need to first describe the beam deformation, the strains, the stresses and the forces and moments acting on a cross-section. It is the equilibrium of the forces and moments on the cross-section which generates our system (7.2).

For the deformation of the interior line we have

$$x_1\boldsymbol{b}_1 \to (x_1 + u_1)\boldsymbol{b}_1 + u_2\boldsymbol{b}_2 + u_3\boldsymbol{b}_3. \tag{7.3}$$

The tangent to the deformed interior line is given by

$$\boldsymbol{t}_1 := (1 + u_1')\boldsymbol{b}_1 + u_2'\boldsymbol{b}_2 + u_3'\boldsymbol{b}_3 \tag{7.4}$$

where $'$ denotes differentiation with respect to x_1. With the usual small deformation assumption $\boldsymbol{t}_1$ is approximately unit. Material fibres in the cross-section in the starting state of the beam in the directions $\boldsymbol{b}_2$ and $\boldsymbol{b}_3$ deform in Euler-Bernoulli beam theory to directions in the cross-section perpendicular to the deformed interior line. Hence the cross-section undergoes a transformation equivalent to rotations about the x_2 and x_3 axes of angles θ_2 and θ_3, respectively. Employing the conventional left handed coordinate system with the cork screw rule, these angles are related to the displacement derivatives by

$$\tan\theta_3 = \frac{\mathrm{d}u_2}{ds} = \frac{\mathrm{d}u_2}{\mathrm{d}x_1}\left(1 - \frac{\mathrm{d}u_1}{\mathrm{d}s}\right) \tag{7.5}$$

$$-\tan\theta_2 = \frac{\mathrm{d}u_3}{ds} = \frac{\mathrm{d}u_3}{\mathrm{d}x_1}\left(1 - \frac{\mathrm{d}u_1}{\mathrm{d}s}\right) \tag{7.6}$$

where $s = x_1 + u_1$ (see Figure 7.2). We assume that the angles and displacement derivatives are small so that, to first order,

$$\theta_3 = \frac{\mathrm{d}u_2}{\mathrm{d}x_1} \qquad \text{and} \qquad \theta_2 = -\frac{\mathrm{d}u_3}{\mathrm{d}x_1}. \tag{7.7}$$

Allowing for a twist of small angle θ around the x_1 axis the transformation of the cross-section is given by

$$\begin{pmatrix} 0 \\ x_2 \\ x_3 \end{pmatrix} \rightarrow \begin{pmatrix} 1 & 0 & 0 \\ 0 & 1 & -\theta \\ 0 & \theta & 1 \end{pmatrix} \begin{pmatrix} 1 & 0 & -u_3' \\ 0 & 1 & 0 \\ u_3' & 0 & 1 \end{pmatrix} \begin{pmatrix} 1 & -u_2' & 0 \\ u_2' & 1 & 0 \\ 0 & 0 & 1 \end{pmatrix} \begin{pmatrix} 0 \\ x_2 \\ x_3 \end{pmatrix} \tag{7.8}$$

which, to first order, is

$$\begin{pmatrix} 0 \\ x_2 \\ x_3 \end{pmatrix} \rightarrow \begin{pmatrix} 1 & -u_2' & -u_3' \\ u_2' & 1 & -\theta \\ u_3' & \theta & 1 \end{pmatrix} \begin{pmatrix} 0 \\ x_2 \\ x_3 \end{pmatrix}. \tag{7.9}$$

Hence the transformation matrix is

$$\boldsymbol{T} = (\,\boldsymbol{t}_1 \quad \boldsymbol{t}_2 \quad \boldsymbol{t}_3\,) := \begin{pmatrix} 1 & -u_2' & -u_3' \\ u_2' & 1 & \theta \\ u_3' & -\theta & 1 \end{pmatrix} \tag{7.10}$$

which, to first order, is orthogonal. The (small) deformation of the beam is hence described by

$$\begin{pmatrix} x_1 \\ x_2 \\ x_3 \end{pmatrix} \rightarrow \begin{pmatrix} x_1 + u_1 \\ u_2 \\ u_3 \end{pmatrix} + \begin{pmatrix} 1 & -u_2' & -u_3' \\ u_2' & 1 & -\theta_1 \\ u_3' & \theta_1 & 1 \end{pmatrix} \begin{pmatrix} 0 \\ x_2 \\ x_3 \end{pmatrix} \tag{7.11}$$

and the displacement field is

$$\begin{pmatrix} \bar{u}_1 \\ \bar{u}_2 \\ \bar{u}_3 \end{pmatrix} = \begin{pmatrix} u_1 - x_2 u_2' - x_3 u_3' \\ u_2 - x_3\theta \\ u_3 + x_3\theta \end{pmatrix}. \tag{7.12}$$

This gives the infinitesimal strains

$$\begin{aligned} \epsilon_{11} &= u_1' - x_2 u_2'' - x_3 u_3'' \\ \epsilon_{12} &= -\frac{1}{2} x_3 \theta' \\ \epsilon_{13} &= \frac{1}{2} x_2 \theta'. \end{aligned} \tag{7.13}$$

In Euler-Bernoulli theory it is assumed that $\sigma_{22} = \sigma_{33} = \sigma_{23} = 0$ and, in the case of a linearly elastic beam containing a (hydrostatic) thermal strain ϵ_{th}, the constitutive

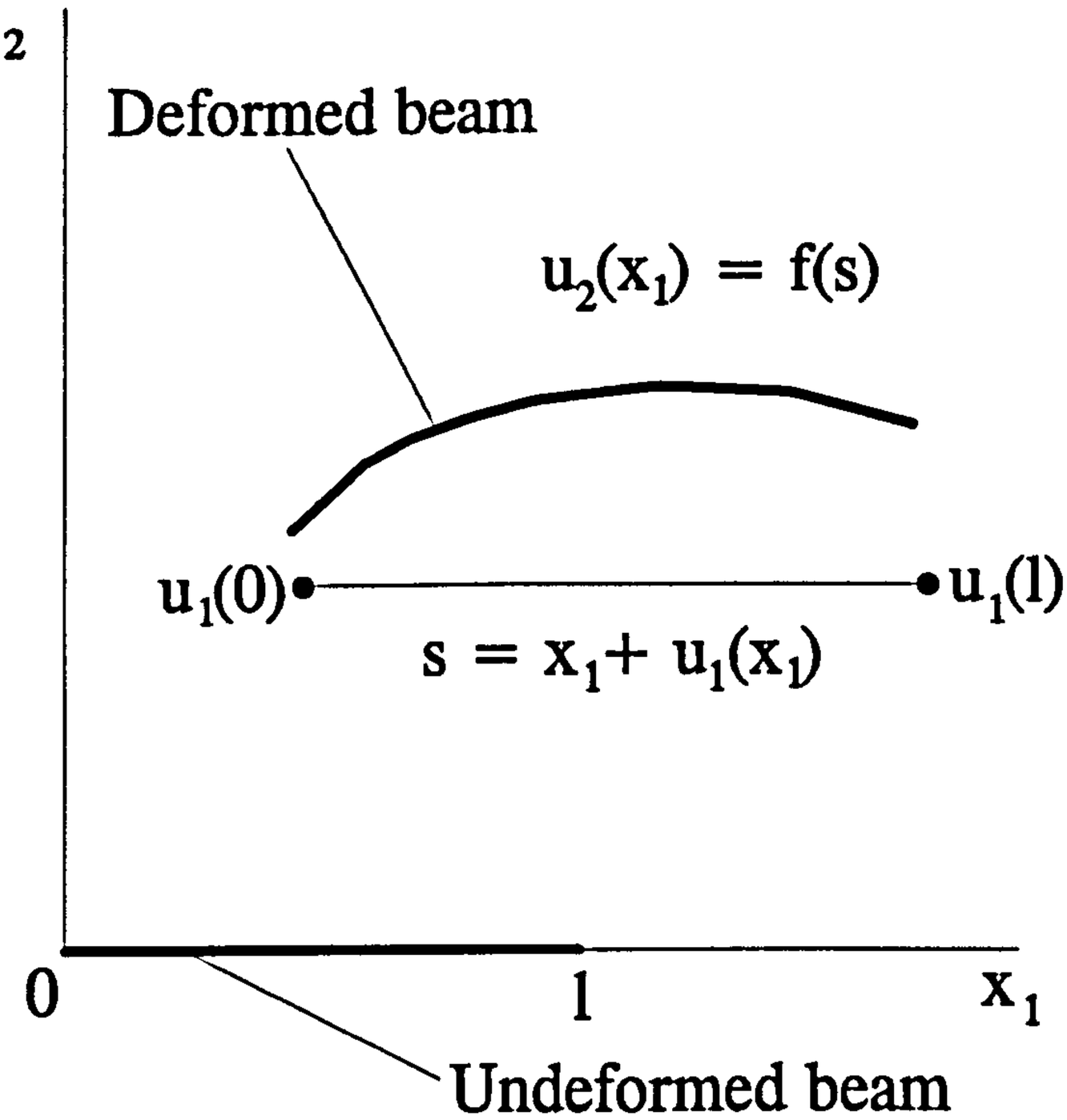

Let s be defined as

$$s := x_1 + u_1(x_1)$$

then the angle between the tangent to the displacement curve and the x_1 axis is given by

$$\begin{aligned} \tan\theta_3 &= \frac{\mathrm{d}u_2}{\mathrm{d}s} \\ &= \frac{\mathrm{d}u_2}{\mathrm{d}x_1}\frac{\mathrm{d}x_1}{\mathrm{d}s} \\ &= \frac{\mathrm{d}u_2}{\mathrm{d}x_1}\left(1 - \frac{\mathrm{d}u_1}{\mathrm{d}s}\right) \end{aligned}$$

Figure 7.2: Relationship between θ_3 and the displacements u_1 and u_2.

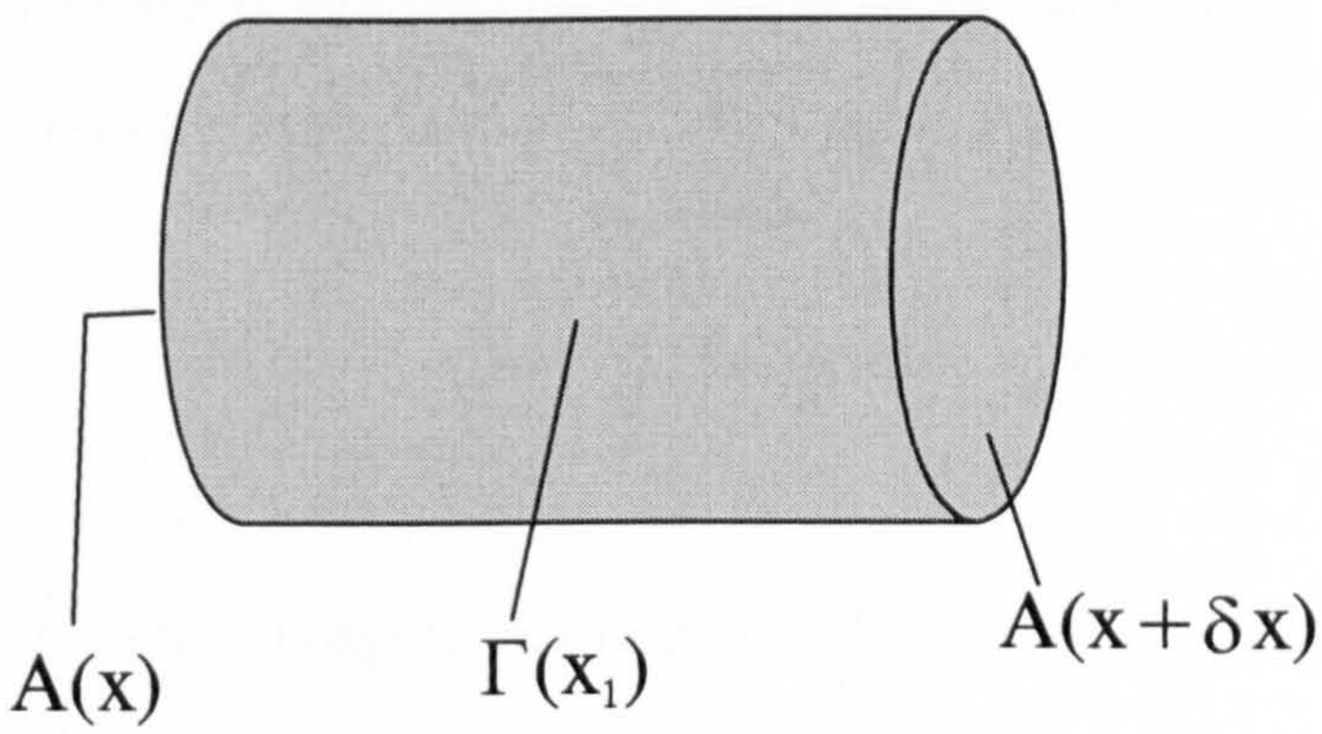

Figure 7.3: Beam slice

equations are

$$\begin{aligned} \sigma_{11} &= E(\epsilon_{11} - \epsilon_{th}) \\ \sigma_{12} &= 2\mu\epsilon_{12} = \left(\frac{E}{1+\nu}\right)\epsilon_{12} \\ \sigma_{13} &= 2\mu\epsilon_{13} = \left(\frac{E}{1+\nu}\right)\epsilon_{13} \end{aligned} \tag{7.14}$$

where as usual E, μ and ν denote Young's modulus, the shear modulus and Poisson's ratio, respectively.

7.2.2 Equilibrium equations

Consider a section of the beam between the points $x_1 = x$ and $x_1 = x + \delta x$. The surface of the section may be divided into the three regions $A(x)$, $A(x+\delta x)$ and $\Gamma(x_1)$ as shown in Figure 7.3. The beam experiences a body force $\boldsymbol{f}$ throughout the section and a surface force $\boldsymbol{g}$ on Γ. Applying the force equilibrium equation (5.31) to this body we have

$$\int_{x\in A(x)} \boldsymbol{t}(\boldsymbol{x})\,\mathrm{d}\boldsymbol{x} + \int_{x\in A(x+\delta x)} \boldsymbol{t}(\boldsymbol{x})\,\mathrm{d}\boldsymbol{x} + \int_{x}^{x+\delta x} \boldsymbol{p}(x_1)\,\mathrm{d}x_1 = 0 \tag{7.15}$$

where

$$\boldsymbol{p}(x_1) = \int_{x\in A(x_1)} \boldsymbol{f}(\boldsymbol{x})\,\mathrm{d}\boldsymbol{x} + \int_{x\in\Gamma(x_1)} \boldsymbol{g}(\boldsymbol{x})\,\mathrm{d}\boldsymbol{x}. \tag{7.16}$$

Application of the moment equilibrium equation (5.32) gives us

$$\int_{x\in A(x)} (x - x_1 e_1) \times t(x)\,\mathrm{d}x \;+\; \int_{x\in A(x+\delta x)} (x - x_1 e_1) \times t(x)\,\mathrm{d}x + \int_{x}^{x+\delta x} (x_1 - x)e_1 \times p(x_1) + m(x_1)\,\mathrm{d}x_1 = 0 \quad (7.17)$$

where

$$m(x_1) = \int_{x\in A(x_1)} (x - x_1 e_1) \times f(x)\,\mathrm{d}x + \int_{x\in\Gamma(x_1)} (x - x_1 e_1) \times g(x)\,\mathrm{d}x. \quad (7.18)$$

We comment on the vector m below. The traction vector is given by (5.7) with the unit normal vector $n(x)$ given by

$$n(x) = \begin{cases} -\begin{pmatrix} 1 \\ u_2' \\ u_3' \end{pmatrix}, & x \in A(x) \\ \\ +\begin{pmatrix} 1 \\ u_2' \\ u_3' \end{pmatrix}, & x \in A(x+\delta x) \end{cases} . \quad (7.19)$$

Substituting (7.19) into (5.7) gives us, to lowest order,

$$t(x) = \begin{cases} -\begin{pmatrix} \sigma_{11} \\ \sigma_{12} \\ \sigma_{13} \end{pmatrix}, & x \in A(x) \\ \\ +\begin{pmatrix} \sigma_{12} \\ \sigma_{12} \\ \sigma_{13} \end{pmatrix}, & x \in A(x+\delta x) \end{cases} . \quad (7.20)$$

Substituting (7.20) into (7.15) and (7.17) we have

$$F(x+\delta x) - F(x) + \int_{x}^{x+\delta x} p(x_1)\,\mathrm{d}x_1 = 0 \quad (7.21)$$

$$M(x+\delta x) - M(x) + \delta x e_1 \times F(x+\delta x) + \int_{x}^{x+\delta x} m(x_1)\,\mathrm{d}x_1 = 0 \quad (7.22)$$

where

$$F = \begin{pmatrix} F_1 \\ F_2 \\ F_3 \end{pmatrix} = \int_{x\in A} \begin{pmatrix} \sigma_{11} \\ \sigma_{12} \\ \sigma_{13} \end{pmatrix} \mathrm{d}x \quad (7.23)$$

$$M = \begin{pmatrix} M_1 \\ M_2 \\ M_3 \end{pmatrix} = \int_{x\in A} \begin{pmatrix} 0 \\ x_2 \\ x_3 \end{pmatrix} \times \begin{pmatrix} \sigma_{11} \\ \sigma_{12} \\ \sigma_{13} \end{pmatrix} dx = \int_{x\in A} \begin{pmatrix} x_2\sigma_{13} - x_3\sigma_{12} \\ x_3\sigma_{11} \\ -x_2\sigma_{11} \end{pmatrix} \mathrm{d}x. \quad (7.24)$$

Taking the limits as δx tends to zero we have

$$\frac{\mathrm{d}\boldsymbol{F}}{\mathrm{d}x} + \boldsymbol{p}(x) = 0 \tag{7.25}$$

$$\frac{\mathrm{d}\boldsymbol{M}}{\mathrm{d}x} + \boldsymbol{e}_1 \times \boldsymbol{F}(x) + \boldsymbol{m}(x) = 0. \tag{7.26}$$

It is not usual to include the moment vector $\boldsymbol{m}$ since its effect on a frame structure is negligible compared to that of the force vector $\boldsymbol{p}$. The inclusion of $\boldsymbol{m}$ would only be justified in single beam problems of pure torsion or frame problems in which secondary effects, such as warping, were being considered. With the assumption that $\boldsymbol{m}$ is zero the full equilibrium equations governing a single beam are

$$\frac{\mathrm{d}F_1}{\mathrm{d}x} + p_1(x) = 0 \tag{7.27}$$

$$\frac{\mathrm{d}F_2}{\mathrm{d}x} + p_2(x) = 0 \tag{7.28}$$

$$\frac{\mathrm{d}F_3}{\mathrm{d}x} + p_3(x) = 0 \tag{7.29}$$

$$\frac{\mathrm{d}M_1}{\mathrm{d}x} = 0 \tag{7.30}$$

$$\frac{\mathrm{d}M_2}{\mathrm{d}x} - F_3(x) = 0 \tag{7.31}$$

$$\frac{\mathrm{d}M_3}{\mathrm{d}x} + F_2(x) = 0. \tag{7.32}$$

The bending equations involving the same force terms are combined to give

$$\frac{\mathrm{d}^2M_2}{\mathrm{d}x^2} + p_3(x) = 0 \tag{7.33}$$

$$\frac{\mathrm{d}^2M_3}{\mathrm{d}x^2} - p_2(x) = 0. \tag{7.34}$$

By defining $S_1 := F_1$, $S_2 := M_3$, $S_3 := -M_2$ and $S_4 := M_1$ we obtain our system

$$\boldsymbol{L}(\boldsymbol{u}) := \begin{pmatrix} -S_1' \\ S_2'' \\ S_3'' \\ -S_4' \end{pmatrix} = \begin{pmatrix} -F_1' \\ -F_2' = M_3'' \\ -F_3' = -M_2'' \\ -M_1' \end{pmatrix} = \begin{pmatrix} p_1 \\ p_2 \\ p_3 \\ 0 \end{pmatrix} =: \boldsymbol{f}. \tag{7.35}$$

To show more explicitly the dependence of $\boldsymbol{L}$ on $\boldsymbol{u}$ it is convenient to define

$$\boldsymbol{B}(\boldsymbol{u}) := \begin{pmatrix} u_1' \\ u_2'' \\ u_3'' \\ \theta' \end{pmatrix}. \tag{7.36}$$

Then, using (7.13), (7.14), (7.23) and (7.24), we have

$$\begin{pmatrix} S_1 \\ S_2 \\ S_3 \\ S_4 \end{pmatrix} = \begin{pmatrix} F_1 \\ M_3 \\ -M_2 \\ M_1 \end{pmatrix} = \boldsymbol{D}\boldsymbol{B}(\boldsymbol{u}) - \boldsymbol{Q} \tag{7.37}$$

where

$$\boldsymbol{D} := \int_{x \in A} E(\boldsymbol{x}) \begin{pmatrix} 1 & -x_2 & -x_3 & 0 \\ -x_2 & x_2^2 & x_2 x_3 & 0 \\ -x_3 & x_2 x_3 & x_3^3 & 0 \\ 0 & 0 & 0 & \dfrac{x_2^2 + x_3^2}{2(1+\nu)} \end{pmatrix} \mathrm{d}\boldsymbol{x} \tag{7.38}$$

$$\boldsymbol{Q} := \int_{x \in A} E(\boldsymbol{x}) \epsilon_{th} \begin{pmatrix} 1 \\ -x_2 \\ -x_3 \\ 0 \end{pmatrix} \mathrm{d}\boldsymbol{x}. \tag{7.39}$$

If the cross-section is symmetric and the interior line corresponds to the elastic centroid then the matrix $\boldsymbol{D}$ is a diagonal matrix. Generally $\boldsymbol{D}$ is not diagonal.

7.2.3 Boundary conditions

Specific solutions of (7.35) depend on the specification of boundary conditions that relate to the degrees of freedom of the beam; i.e. the displacements, u_1, u_2 and u_3, and the rotations, θ_1, θ_2 and θ_3. In most practical problems a particular degree of freedom is either fixed, in which case the displacement or rotation is zero, or unrestricted, in which case its corresponding force or moment is zero. The following table shows the possibilities.

Table 7.1 : Boundary Condition Combinations

D.O.F.	Fixed	Not fixed
u_1	$u_1 = 0$	$F_1 = 0$
u_2	$u_2 = 0$	$F_2 = -M_3' = 0$
u_3	$u_3 = 0$	$F_3 = M_2' = 0$
$\theta_1 = u_4$	$\theta_1 = 0$	$M_1 = 0$
$\theta_2 = -u_3'$	$u_3' = 0$	$M_2 = 0$
$\theta_3 = u_2'$	$u_2' = 0$	$M_3 = 0$

If the displacements are fixed but the rotations are not then the beam is said to be simply supported. If both the displacements and rotations are fixed then the beam is said to be rigidly fixed or clamped.

7.2.4 Frames

A frame structure is an assembly of beams each of which is governed by the beam equations in a local coordinate system; i.e. the beam lies along the x_1 axis in the interval $[0, l]$. A rotation matrix, $\boldsymbol{R}$, maps the local displacements and rotations onto their global orientation. The interaction between the beams is governed by joint conditions that dictate the continuity of the displacements and rotations and relate the forces and moments acting on the joint. Usually it is assumed that the displacements are continuous so that, at a joint,

$$\boldsymbol{R}^{(i)} \begin{pmatrix} u_1^{(i)} \\ u_2^{(i)} \\ u_3^{(i)} \end{pmatrix} = \boldsymbol{R}^{(j)} \begin{pmatrix} u_1^{(j)} \\ u_2^{(j)} \\ u_3^{(j)} \end{pmatrix}, \quad \forall i, j \in \text{ joint} \tag{7.40}$$

where the superscripts denote the beam number. If a joint is rigid then the rotations are also continuous, i.e.

$$\boldsymbol{R}^{(i)} \begin{pmatrix} \theta_1^{(i)} \\ \theta_2^{(i)} \\ \theta_3^{(i)} \end{pmatrix} = \boldsymbol{R}^{(j)} \begin{pmatrix} \theta_1^{(j)} \\ \theta_2^{(j)} \\ \theta_3^{(j)} \end{pmatrix}, \quad \forall i, j \in \quad \text{joint}, \tag{7.41}$$

so that the angles between the beams are preserved. In order for the frame to be in equilibrium the forces and moments acting at a joint must sum to zero. Hence we have

$$\sum_{i \in \text{joint}} \boldsymbol{R}^{(i)} \boldsymbol{F}^{(i)} n^{(i)} = \boldsymbol{0} \tag{7.42}$$

$$\sum_{i \in \text{joint}} \boldsymbol{R}^{(i)} \boldsymbol{M}^{(i)} n^{(i)} = \boldsymbol{0} \tag{7.43}$$

where $n^{(i)}$ is either $+1$ or -1 depending on the direction of the beam as illustrated in Figure 7.4. The rigid joint is a mathematical idealisation that works for most applications to building frameworks. Another idealisation is the pin joint in which the rotations are allowed to be discontinuous and the moments are zero. In a building framework the joints are effectively rigid under normal circumstances. In high temperature conditions, such as a fire, joints may exhibit semi-rigid behaviour in which the rotations are no longer continuous and the moments obey an experimentally derived relationship with the angle differences.

7.2.5 Analytical solutions

Solutions of (7.35) with any combination of boundary conditions from Table 7.1 may be found by direct integration and the solution of a linear system in terms of the beam strains (i.e. u_1', u_2'', u_3'' and θ'). For problems in which the matrix $\boldsymbol{D}$ is diagonal the full vector equation decouples into

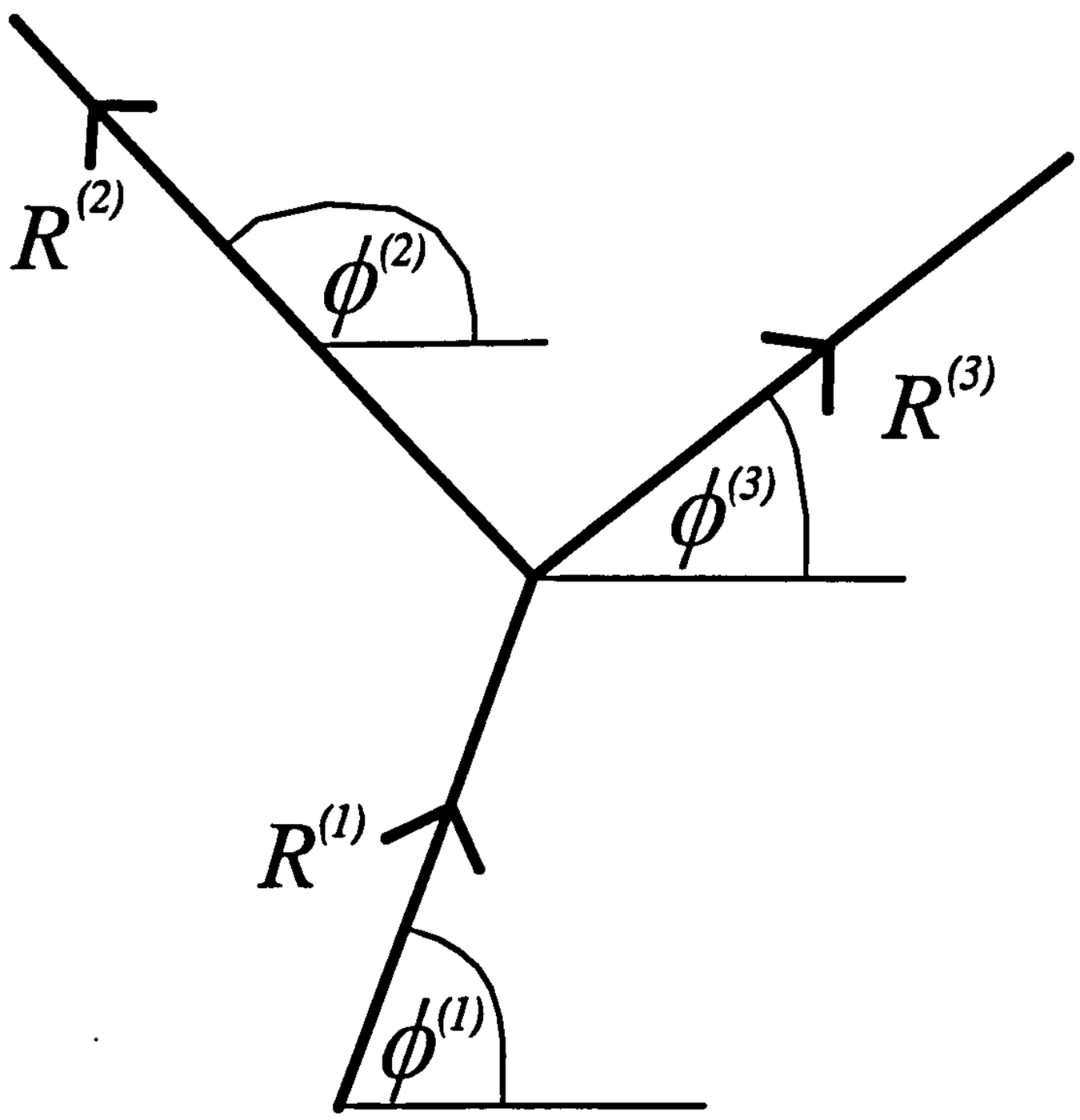

Figure 7.4: Equilibrium of joints. The value of $n^{(i)}$ is $+1$ if the beam is pointing towards the joint and -1 if it is pointing away.

$$-\frac{\mathrm{d}}{\mathrm{d}x}\left(D_{11}\frac{\mathrm{d}u_1}{\mathrm{d}x}\right) = f_1 + \frac{\mathrm{d}Q_1}{\mathrm{d}x} \tag{7.44}$$

$$\frac{\mathrm{d}^2}{\mathrm{d}x^2}\left(D_{22}\frac{\mathrm{d}^2u_2}{\mathrm{d}x^2}\right) = f_2 + \frac{\mathrm{d}^2Q_2}{\mathrm{d}x^2} \tag{7.45}$$

$$\frac{\mathrm{d}^2}{\mathrm{d}x^2}\left(D_{33}\frac{\mathrm{d}^2u_3}{\mathrm{d}x^2}\right) = f_3 + \frac{\mathrm{d}^2Q_3}{\mathrm{d}x^2} \tag{7.46}$$

$$\frac{\mathrm{d}}{\mathrm{d}x}\left(D_{44}\frac{\mathrm{d}\theta}{\mathrm{d}x}\right) = 0. \tag{7.47}$$

Cases where $\boldsymbol{D}$ is constant are relatively easy to solve by direct integration. Three such examples are considered here.

A rigidly fixed beam

Consider the pure bending problem where $f_1 = f_2 = 0$ with f_3 constant and the beam, which is of unit length, rigidly fixed at each end. Integrating (7.46) twice gives

$$D_{33}\frac{\mathrm{d}^2u_3}{\mathrm{d}x^2} = \frac{f_3}{2}x^2 + c_1x + c_2. \tag{7.48}$$

Dividing by D_{33} and integrating twice more gives

$$u_3 = \frac{f_3}{24D_{33}}x^4 + \frac{c_1}{6}x^3 + \frac{c_3}{2}x^2 + c_3x + c_4. \tag{7.49}$$

Using the fact that

$$u_3(0) = u_3'(0) = u_3(1) = u_3'(1) = 0 \tag{7.50}$$

we have the solution

$$u_3 = \frac{f_3}{24D_{33}}x^2(x-1)^2. \tag{7.51}$$

A simply supported beam

Consider the same beam but simply supported at each end. Using the fact that

$$M_2'(0) = M_2(0) = M_2(1) = M_2'(1) = 0 \tag{7.52}$$

and applying it to (7.46) we have that

$$M_2(x) = D_{33}\frac{\mathrm{d}^2u_3}{\mathrm{d}x^2} = \frac{f_3}{2}x(x-1). \tag{7.53}$$

Dividing by D_{33} and using

$$u_3(0) = u_3(1) = 0 \tag{7.54}$$

gives the solution

$$u_3(x) = \frac{f_3}{24D_{33}}x(x-1)(x^2-x-1). \tag{7.55}$$

A simple frame with rigid joints

Consider now an assembly of three beams in the x_1x_3 plane, as illustrated in Figure 7.5, with an applied continuous vertical force along the horizontal beam. Locally, each beam may be mapped onto the $[0, l]$ interval on the x_1 axis and satisfy equations (7.44) and (7.46). If the joints between the beams are rigid then the displacements and rotations at the joints are continuous. Also, since the frame is in equilibrium, the resulting forces acting on the joint and the resulting moments acting on it must be zero. For this plane example this means that, for continuity at the joints,

$$\begin{pmatrix} u_1^{(1)}(1) \\ u_3^{(1)}(1) \\ \theta_2^{(1)}(1) \end{pmatrix} = \begin{pmatrix} 0 & 1 & 0 \\ -1 & 0 & 0 \\ 0 & 0 & 1 \end{pmatrix} \begin{pmatrix} u_1^{(2)}(0) \\ u_3^{(2)}(0) \\ \theta_2^{(2)}(0) \end{pmatrix}, \quad \begin{pmatrix} u_1^{(2)}(1) \\ u_3^{(2)}(1) \\ \theta_2^{(2)}(1) \end{pmatrix} = \begin{pmatrix} 0 & 1 & 0 \\ -1 & 0 & 0 \\ 0 & 0 & 1 \end{pmatrix} \begin{pmatrix} u_1^{(3)}(0) \\ u_3^{(3)}(0) \\ \theta_2^{(3)}(0) \end{pmatrix} \tag{7.56}$$

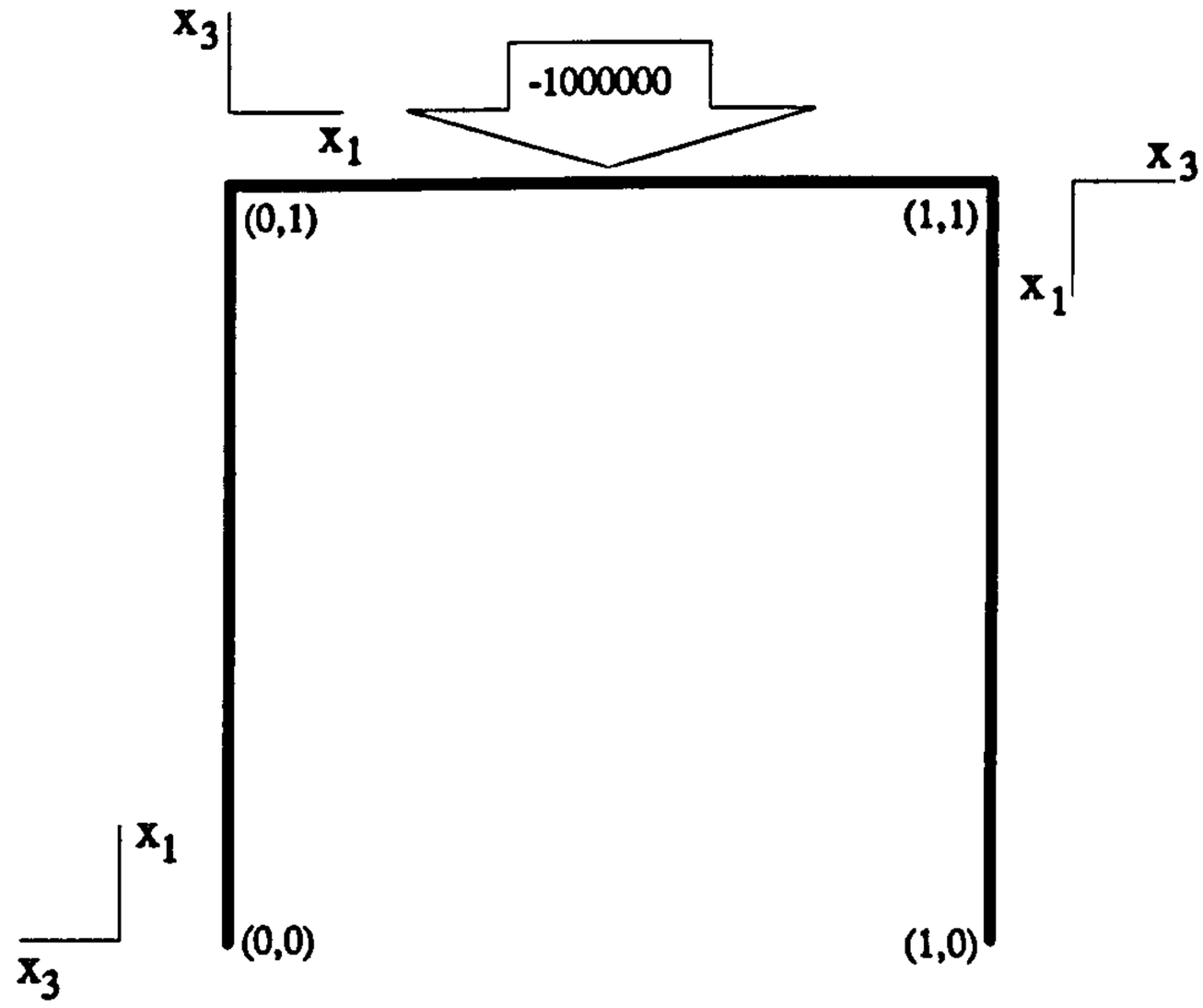

Each beam is modelled by (7.44) and (7.46) in the local co-ordinate systems indicated.

Figure 7.5: Simple frame with rigid joints before deformation

and, for equilibrium at the joints,

$$\begin{pmatrix} F_1(\boldsymbol{u}^{(1)}) \\ F_3(\boldsymbol{u}^{(1)}) \\ M_2(\boldsymbol{u}^{(1)}) \end{pmatrix}_{\text{at } x=1} - \begin{pmatrix} 0 & 1 & 0 \\ -1 & 0 & 0 \\ 0 & 0 & 1 \end{pmatrix} \begin{pmatrix} F_1(\boldsymbol{u}^{(2)}) \\ F_3(\boldsymbol{u}^{(2)}) \\ M_2(\boldsymbol{u}^{(2)}) \end{pmatrix}_{\text{at } x=0} = \begin{pmatrix} 0 \\ 0 \\ 0 \end{pmatrix}$$

$$\begin{pmatrix} F_1(\boldsymbol{u}^{(2)}) \\ F_3(\boldsymbol{u}^{(2)}) \\ M_2(\boldsymbol{u}^{(2)}) \end{pmatrix}_{\text{at } x=1} - \begin{pmatrix} 0 & 1 & 0 \\ -1 & 0 & 0 \\ 0 & 0 & 1 \end{pmatrix} \begin{pmatrix} F_1(\boldsymbol{u}^{(3)}) \\ F_3(\boldsymbol{u}^{(3)}) \\ M_2(\boldsymbol{u}^{(3)}) \end{pmatrix}_{\text{at } x=0} = \begin{pmatrix} 0 \\ 0 \\ 0 \end{pmatrix} \tag{7.57}$$

We assume that the frame is rigidly supported to the ground so that

$$\begin{pmatrix} u_1^{(1)}(0) \\ u_3^{(1)}(0) \\ \theta_2^{(1)}(0) \end{pmatrix} = \begin{pmatrix} 0 \\ 0 \\ 0 \end{pmatrix}, \qquad \begin{pmatrix} u_1^{(3)}(1) \\ u_3^{(3)}(1) \\ \theta_2^{(3)}(1) \end{pmatrix} = \begin{pmatrix} 0 \\ 0 \\ 0 \end{pmatrix}. \tag{7.58}$$

After integrating (7.44) and (7.46) and applying the boundary conditions in (7.58) we have

$$\boldsymbol{u}^{(1)} = \begin{pmatrix} c_1 x \\ c_2 x^3 + c_3 x^2 \end{pmatrix} \tag{7.59}$$

$$\boldsymbol{u}^{(2)} = \begin{pmatrix} c_4 x + c_5 \\ \frac{f_3}{24} x^4 + c_6 x^3 + c_7 x^2 + c_8 x + c_9 \end{pmatrix} \tag{7.60}$$

$$\boldsymbol{u}^{(3)} = \begin{pmatrix} c_{10}(x-l) \\ c_{11}(x-l)^3 + c_{12}(x-l)^2 \end{pmatrix} \tag{7.61}$$

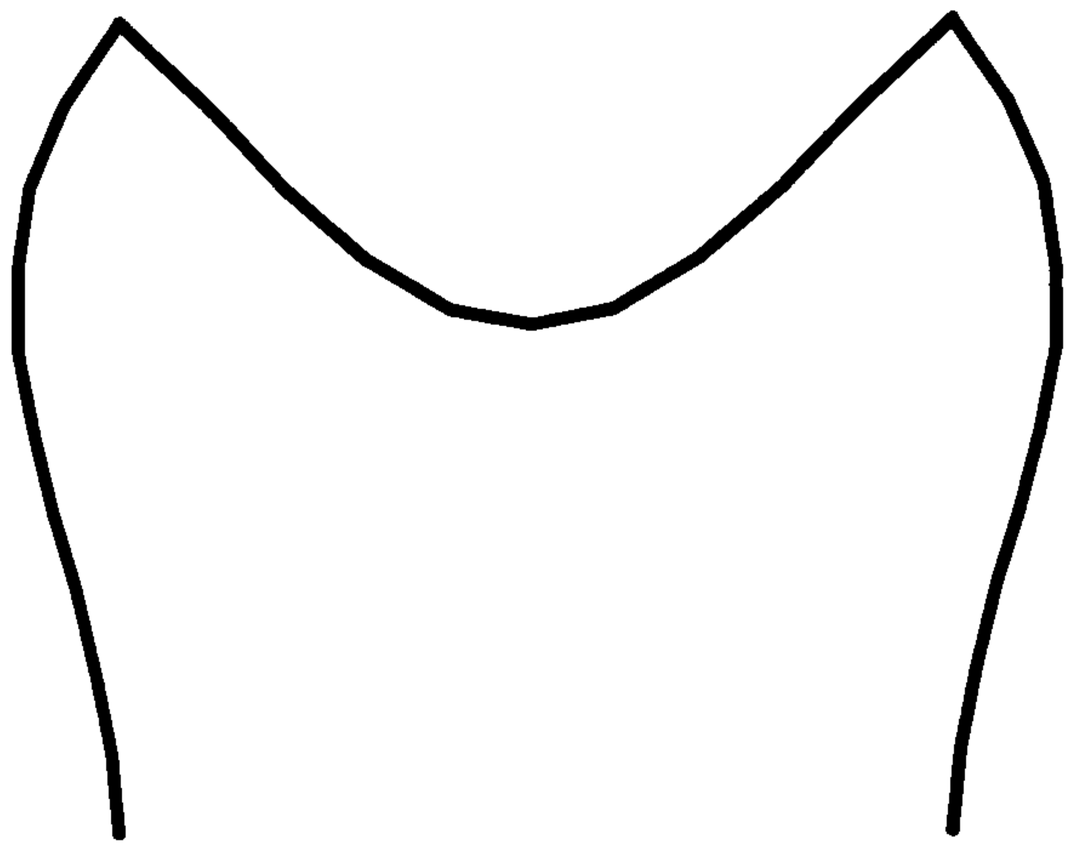

Figure 7.6: Frame after deformation. Displacements scaled by 50.

where $c_1 \ldots c_{12}$ are constants to be determined. Application of (7.56) and (7.57) leads to a system of twelve equations in the twelve unknowns which may be solved using a mathematical computer package, e.g. Mathematica. After obtaining the constant values the solution is found to be

$$\boldsymbol{u}^{(1)} = \begin{pmatrix} \frac{-x}{2000} \\ \frac{(399-400x)x^2}{24060} \end{pmatrix} \tag{7.62}$$

$$\boldsymbol{u}^{(2)} = \begin{pmatrix} \frac{1-2x}{24060} \\ -\frac{1}{2000} - \frac{67x}{4010} - \frac{267x^2}{8020} + \frac{x^3}{10} - \frac{x^4}{20} \end{pmatrix} \tag{7.63}$$

$$\boldsymbol{u}^{(3)} = \begin{pmatrix} \frac{1-x}{2000} \\ \frac{(x-1)^2(400x-1)}{24060} \end{pmatrix} \tag{7.64}$$

and the deformed frame is illustrated in Figure 7.6.

7.2.6 Weak form for a single beam

With the equations in the form $\boldsymbol{L}(\boldsymbol{u}) = \boldsymbol{f}$ we can obtain the weak form for a single beam equation in the usual way. Using vector/matrix notation the weak form is obtained by pre-multiplying by $\boldsymbol{v} \in H = H_1 \otimes H_2 \otimes H_3 \otimes H_4$ and integrating over the length of the beam. We obtain, using integration by parts,

$$\int_0^l \boldsymbol{f}^T \boldsymbol{v} \, \mathrm{d}x = \int_0^l (-S_1' v_1 + S_2'' v_2 + S_3'' v_3 - S_4' v_4) \, \mathrm{d}x \tag{7.65}$$

$$= \int_0^l (S_1 v_1' + S_2 v_2'' + S_3 v_3'' + S_4 v_4') \, \mathrm{d}x + \text{ end terms} \tag{7.66}$$

$$= \int_0^l \boldsymbol{B}(\boldsymbol{v})^T (\boldsymbol{D}\boldsymbol{B}(\boldsymbol{u}) - \boldsymbol{Q}) \, \mathrm{d}x + \text{ end terms} \tag{7.67}$$

where the end terms are given by

$$\text{end terms} = [-S_1 v_1 + S_2' v_2 - S_2 v_2' + S_3' v_3 - S_3 v_3' - S_4 v_4]_0^l \tag{7.68}$$

$$= -[(\, v_1 \quad v_2 \quad v_3 \,)\, \boldsymbol{F} + (\, v_4 \quad -v_3' \quad v_2' \,)\, \boldsymbol{M}]_0^l . \tag{7.69}$$

Thus we have

$$a(\boldsymbol{u},\boldsymbol{v}) = (\boldsymbol{f},\boldsymbol{v}) + (\boldsymbol{Q},\boldsymbol{B}(\boldsymbol{v})) - [(\,v_1 \quad v_2 \quad v_3\,)\,\boldsymbol{F} + (\,v_4 \quad -v_3' \quad v_2'\,)\,\boldsymbol{M}]_0^l \qquad (7.70)$$

where

$$\begin{aligned} a(\boldsymbol{u},\boldsymbol{v}) &= \int_0^l \boldsymbol{B}(\boldsymbol{v})^T \boldsymbol{D}\boldsymbol{B}(\boldsymbol{u})\,\mathrm{d}x_1 \\ (\boldsymbol{f},\boldsymbol{v}) &= \int_0^l \boldsymbol{v}^T\boldsymbol{f}\,\mathrm{d}x_1 \qquad (7.71) \\ (\boldsymbol{Q},\boldsymbol{B}(\boldsymbol{v})) &= \int_0^l \boldsymbol{B}(\boldsymbol{v})^T\boldsymbol{Q}\,\mathrm{d}x_1. \end{aligned}$$

Regarding the test space H, the integration by parts requires that $H_1, H_4 \subset H^1(0,l)$ and $H_2, H_3 \subset H^2(0,l)$. The complete specification of H depends on the boundary conditions of the problem being considered which typically involve $\boldsymbol{u}$, $\boldsymbol{F}$ or $\boldsymbol{M}$ being specified at an end, $x_1 = 0$ or $x_1 = l$. In the case of a single beam we assume that the boundary conditions of the problem and the test space H are such that

$$[(\,v_1 \quad v_2 \quad v_3\,)\,\boldsymbol{F} + (\,v_4 \quad -v_3' \quad v_2'\,)\,\boldsymbol{M}]_0^l = 0. \qquad (7.72)$$

Thus to summarize, we have a test space H and we seek a suitable displacement $\boldsymbol{u}$ satisfying

$$a(\boldsymbol{u},\boldsymbol{v}) = (\boldsymbol{f},\boldsymbol{v}) + (\boldsymbol{Q},\boldsymbol{B}(\boldsymbol{v})) \qquad (7.73)$$

for all $\boldsymbol{v} \in H$.

7.2.7 A rigid frame structure

For a frame structure consisting of nb beams we have nb vectors,

$$\boldsymbol{u}^{(k)} = \boldsymbol{u}^{(k)}(x_1) \text{ for } 0 < x_1 < l^{(k)},$$

and nb equations of the form

$$\boldsymbol{L}^{(k)}(\boldsymbol{u}^{(k)}) = \boldsymbol{f}^{(k)}, \quad 1 \le k \le nb \qquad (7.74)$$

together with boundary conditions and conditions relating to the joints. For a rigid frame the joint conditions are the continuity equations (7.40) and (7.41) and the equilibrium equations (7.42) and (7.43).

With $a(\boldsymbol{u}^{(k)}, \boldsymbol{v}^{(k)})$, $(\boldsymbol{f}^{(k)}, \boldsymbol{v}^{(k)})$ and $(\boldsymbol{Q}^{(k)}, \boldsymbol{B}^{(k)})$ being the quantities corresponding to (7.71) for the kth beam, the weak form is obtained by considering

$$\sum_{k=1}^{nb}(\boldsymbol{L}(\boldsymbol{u}^{(k)}), \boldsymbol{v}^{(k)}) = \sum_{k=1}^{nb}(\boldsymbol{f}^{(k)}, \boldsymbol{v}^{(k)}) \tag{7.75}$$

for test vectors $\boldsymbol{v}^{(k)}, 0 \leq k \leq nb$ which satisfy

$$\boldsymbol{R}^{(k)} \begin{pmatrix} v_1 & v_4 \\ v_2 & -v_3' \\ v_3 & v_2' \end{pmatrix}^{(k)} = \boldsymbol{R}^{(j)} \begin{pmatrix} v_1 & v_4 \\ v_2 & -v_3' \\ v_3 & v_2' \end{pmatrix}^{(j)} \tag{7.76}$$

at the joint between beams k and j. As in the case of a single beam we obtain

$$\sum_{k=1}^{nb} a(\boldsymbol{u}^{(k)}, \boldsymbol{v}^{(k)}) = \sum_{k=1}^{nb}(\boldsymbol{f}^{(k)}, \boldsymbol{v}^{(k)}) + \sum_{k=1}^{nb}(\boldsymbol{Q}^{(k)}, \boldsymbol{v}^{(k)}) \tag{7.77}$$

$$- \sum_{k=1}^{nb} \left[\begin{pmatrix} v_1 & v_2 & v_3 \end{pmatrix}^{(k)} \boldsymbol{F}^{(k)} + \begin{pmatrix} v_4 & -v_3' & v_2' \end{pmatrix}^{(k)} \boldsymbol{M}^{(k)} \right]_0^{l^{(k)}} \tag{7.78}$$

and from the boundary conditions, continuity conditions and joint equilibrium conditions this reduces to

$$\sum_{k=1}^{nb} a(\boldsymbol{u}^{(k)}, \boldsymbol{v}^{(k)}) = \sum_{k=1}^{nb}(\boldsymbol{f}^{(k)}, \boldsymbol{v}^{(k)}) + \sum_{k=1}^{nb}(\boldsymbol{Q}^{(k)}, \boldsymbol{v}^{(k)}). \tag{7.79}$$

Thus, with appropriate re-definition of $\boldsymbol{u}$, $\boldsymbol{v}$, $\boldsymbol{f}$ and $\boldsymbol{Q}$ and for the test space H and with

$$\begin{aligned} a(\boldsymbol{u}, \boldsymbol{v}) &:= \sum_{k=1}^{nb} a(\boldsymbol{u}^{(k)}, \boldsymbol{v}^{(k)}) \\ (\boldsymbol{f}, \boldsymbol{v}) &:= \sum_{k=1}^{nb}(\boldsymbol{f}^{(k)}, \boldsymbol{v}^{(k)}) \\ (\boldsymbol{Q}, \boldsymbol{v}) &:= \sum_{k=1}^{nb}(\boldsymbol{Q}^{(k)}, \boldsymbol{v}^{(k)}) \end{aligned} \tag{7.80}$$

we can again express the weak form in the standard way as

$$a(\boldsymbol{u}, \boldsymbol{v}) = (\boldsymbol{f}, \boldsymbol{v}) + (\boldsymbol{Q}, \boldsymbol{B}(\boldsymbol{v})) \tag{7.81}$$

for all $\boldsymbol{v}$ in H.

7.2.8 A pinned and semi-rigid frame structure

In the previous subsection we considered a frame whose joints were rigid so that the rotations between connecting beams are continuous. This is an idealisation in which the joint resists the moments acting upon it. The other extreme is a pin or ball joint which does not resist the moments so that, at the joint,

$$M^{(k)} = 0 \quad \forall k \in \text{ joint.} \tag{7.82}$$

The rotations are no longer continuous between the beams so that the only continuity condition is

$$R^{(k)} \begin{pmatrix} u_1 \\ u_2 \\ u_3 \end{pmatrix}^{(k)} = R^{(j)} \begin{pmatrix} u_1 \\ u_2 \\ u_3 \end{pmatrix}^{(j)} \tag{7.83}$$

This is also true of a semi-rigid frame. At a semi-rigid joint each moment is governed by an $M - \phi$ relation where ϕ is the difference between the two angles. If the relations are linear then the joint stiffness, $k = \frac{dM}{d\phi}$, is constant and

$$M^{(k)} = \begin{pmatrix} k_1(\theta^{(k)} - \theta^{(j)}) \\ k_2(-u_3^{(k)} + u_3^{(j)})' \\ k_3(u_2^{(k)} - u_2^{(j)})' \end{pmatrix} \tag{7.84}$$

where k_1, k_2 and k_3 are the joint stiffnesses for the rotations about the x_1, x_2 and x_3 axes.

In the case of the pin-jointed frame the weak form is unaltered. However, for semi-rigid frames, the weak form now includes the contribution from each semi-rigid joint. Hence

$$a(u, v) := \sum_{k=1}^{nb} \left(a(u^{(k)}, v^{(k)}) + \left[\begin{pmatrix} v_4^{(k)} & -(v_3^{(k)})' & (v_2^{(k)})' \end{pmatrix} M^{(k)} \right]_0^{l^{(k)}} \right). \tag{7.85}$$

Only solutions to rigid jointed frame problems are considered in this thesis.

7.2.9 Norms

Using (7.80) we define the energy and L_2 norms respectively as

$$\|v\| = a(v, v)^{\frac{1}{2}} \tag{7.86}$$

$$\|v\|_{L_2} = (v, v)^{\frac{1}{2}}. \tag{7.87}$$

The two norms are related by the inequality

$$C_1^2 \|B(v)\|_{L_2} \leq \|v\| \leq C_2^2 \|B(v)\|_{L_2} \tag{7.88}$$

where

$$C_1 = \min_{1\le k\le nb}\left\{\min_{0\le x\le l^{(k)}}\left[\lambda_{\min}\left(\boldsymbol{D}^{(k)}(x)\right)\right]\right\} \tag{7.89}$$

$$C_2 = \max_{1\le k\le nb}\left\{\max_{0\le x\le l^{(k)}}\left[\lambda_{\max}\left(\boldsymbol{D}^{(k)}(x)\right)\right]\right\} \tag{7.90}$$

where $\lambda_{\min}(\boldsymbol{D})$ and $\lambda_{\max}(\boldsymbol{D})$ are the smallest and largest eigenvalue of $\boldsymbol{D}$. Equation (7.88) follows from considering the Rayleigh quotient of $\boldsymbol{D}$ and the fact that $\boldsymbol{D}$ is symmetric [12, Pages 15–18].

For the purpose of bounding the frame displacement vector in the next section we show that

$$\|\boldsymbol{v}\|_{L_2} \le C\,\|\boldsymbol{B}(\boldsymbol{v})\|_{L_2} \tag{7.91}$$

where $C > 0$. Equation (7.91) is analogous to (2.11) and the argument is similar although the details are frame dependent. Consider the case where the frame has just two beams perpendicular to one another. Beam 1 is vertical and beam 2 is horizontal with the joint at $x = l^{(1)}$ for beam 1 and $x = 0$ for beam 2. The base of beam 1 is clamped so that

$$\begin{pmatrix} v_1 \\ v_2 \\ v_3 \end{pmatrix}^{(1)}_{x=0} = \begin{pmatrix} v_4 \\ v_3' \\ v_2' \end{pmatrix}^{(1)}_{x=0} = \begin{pmatrix} 0 \\ 0 \\ 0 \end{pmatrix} \tag{7.92}$$

and the joint between the beams is rigid so that

$$\begin{pmatrix} 0 & 0 & -1 \\ 0 & 1 & 0 \\ 1 & 0 & 0 \end{pmatrix} \begin{pmatrix} v_1 \\ v_2 \\ v_3 \end{pmatrix}^{(1)}_{x=l^{(1)}} = \begin{pmatrix} v_1 \\ v_2 \\ v_3 \end{pmatrix}^{(2)}_{x=0} \tag{7.93}$$

$$\begin{pmatrix} 0 & 0 & -1 \\ 0 & 1 & 0 \\ 1 & 0 & 0 \end{pmatrix} \begin{pmatrix} v_4 \\ -v_3' \\ v_2' \end{pmatrix}^{(1)}_{x=l^{(1)}} = \begin{pmatrix} v_4 \\ -v_3' \\ v_2' \end{pmatrix}^{(2)}_{x=0}. \tag{7.94}$$

For $\boldsymbol{v}^{(1)}$ we have

$$v_1^{(1)}(x) = v_1^{(1)}(0) + \int_0^x (v_1^{(1)})'(y)\,\mathrm{d}y \tag{7.95}$$

$$v_2^{(1)}(x) = v_2^{(1)}(0) + \int_0^x (v_2^{(1)})'(y)\,\mathrm{d}y \tag{7.96}$$

$$v_3^{(1)}(x) = v_3^{(1)}(0) + \int_0^x (v_3^{(1)})'(y)\,\mathrm{d}y \tag{7.97}$$

$$v_4^{(1)}(x) = v_4^{(1)}(0) + \int_0^x (v_4^{(1)})'(y)\,\mathrm{d}y \tag{7.98}$$

$$(v_3^{(1)})'(x) = (v_3^{(1)})'(0) + \int_0^x (v_3^{(1)})''(y)\,\mathrm{d}y \tag{7.99}$$

$$(v_2^{(1)})'(x) = (v_2^{(1)})'(0) + \int_0^x (v_2^{(1)})''(y)\,\mathrm{d}y \tag{7.100}$$

from which we get, using (7.92) and the same argument as for (2.10),

$$|v_1^{(1)}(x)| \leq \sqrt{l^{(1)}} \left\| (v_1^{(1)})' \right\|_{L_2} \tag{7.101}$$

$$|v_2^{(1)}(x)| \leq \sqrt{l^{(1)}} \left\| (v_2^{(1)})' \right\|_{L_2} \tag{7.102}$$

$$|v_3^{(1)}(x)| \leq \sqrt{l^{(1)}} \left\| (v_3^{(1)})' \right\|_{L_2} \tag{7.103}$$

$$|v_4^{(1)}(x)| \leq \sqrt{l^{(1)}} \left\| (v_4^{(1)})' \right\|_{L_2} \tag{7.104}$$

$$|(v_3^{(1)})'(x)| \leq \sqrt{l^{(1)}} \left\| (v_3^{(1)})'' \right\|_{L_2} \tag{7.105}$$

$$|(v_2^{(1)})'(x)| \leq \sqrt{l^{(1)}} \left\| (v_2^{(1)})'' \right\|_{L_2}. \tag{7.106}$$

Now,

$$\left\| v_1^{(1)} \right\|_{L_2}^2 = \int_0^{l^{(1)}} |v_1(y)|^2 \, \mathrm{d}y \tag{7.107}$$

$$\leq \int_0^{l^{(1)}} l^{(1)} \left\| v_1' \right\|_{L_2}^2 \, \mathrm{d}y \tag{7.108}$$

$$= \left(l^{(1)} \right)^2 \left\| v_1' \right\|_{L_2}^2. \tag{7.109}$$

Similarly,

$$\left\| v_2^{(1)} \right\|_{L_2}^2 \leq \left(l^{(1)} \right)^2 \left\| (v_2^{(1)})' \right\|_{L_2}^2 \tag{7.110}$$

$$\left\| v_3^{(1)} \right\|_{L_2}^2 \leq \left(l^{(1)} \right)^2 \left\| (v_3^{(1)})' \right\|_{L_2}^2 \tag{7.111}$$

$$\left\| v_4^{(1)} \right\|_{L_2}^2 \leq \left(l^{(1)} \right)^2 \left\| (v_4^{(1)})' \right\|_{L_2}^2 \tag{7.112}$$

$$\left\| (v_3^{(1)})' \right\|_{L_2}^2 \leq \left(l^{(1)} \right)^2 \left\| (v_3^{(1)})'' \right\|_{L_2}^2 \tag{7.113}$$

$$\left\| (v_2^{(1)})' \right\|_{L_2}^2 \leq \left(l^{(1)} \right)^2 \left\| (v_2^{(1)})'' \right\|_{L_2}^2. \tag{7.114}$$

Furthermore, combining the results for $v_2^{(1)}$ and $(v_2^{(1)})'$ and similarly for $v_3^{(1)}$ and $(v_3^{(1)})'$, we have

$$\left\| v_2^{(1)} \right\|_{L_2}^2 \leq \left(l^{(1)} \right)^4 \left\| (v_2^{(1)})'' \right\|_{L_2}^2 \tag{7.115}$$

$$\left\| v_3^{(1)} \right\|_{L_2}^2 \leq \left(l^{(1)} \right)^4 \left\| (v_3^{(1)})'' \right\|_{L_2}^2. \tag{7.116}$$

Hence we have shown that

$$\left\| v_1^{(1)} \right\|_{L_2} \leq \left(l^{(1)} \right) \left\| (v_1^{(1)})' \right\|_{L_2} \tag{7.117}$$

$$\left\| v_2^{(1)} \right\|_{L_2} \leq \left(l^{(1)} \right)^2 \left\| (v_2^{(1)})'' \right\|_{L_2} \tag{7.118}$$

$$\left\|v_3^{(1)}\right\|_{L_2} \leq \left(l^{(1)}\right)^2 \left\|(v_3^{(1)})''\right\|_{L_2} \tag{7.119}$$
$$\left\|v_4^{(1)}\right\|_{L_2} \leq \left(l^{(1)}\right) \left\|(v_4^{(1)})'\right\|_{L_2} \tag{7.120}$$
$$\left\|(v_3^{(1)})'\right\|_{L_2} \leq \left(l^{(1)}\right) \left\|(v_3^{(1)})''\right\|_{L_2} \tag{7.121}$$
$$\left\|(v_2^{(1)})'\right\|_{L_2} \leq \left(l^{(1)}\right) \left\|(v_2^{(1)})''\right\|_{L_2}. \tag{7.122}$$

Hence, from the definition of $\|\boldsymbol{B}(\boldsymbol{v})\|_{L_2}$, we have

$$\left\|v_1^{(1)}\right\|_{L_2} \leq \left(l^{(1)}\right) \|\boldsymbol{B}(\boldsymbol{v})\|_{L_2} \tag{7.123}$$
$$\left\|v_2^{(1)}\right\|_{L_2} \leq \left(l^{(1)}\right)^2 \|\boldsymbol{B}(\boldsymbol{v})\|_{L_2} \tag{7.124}$$
$$\left\|v_3^{(1)}\right\|_{L_2} \leq \left(l^{(1)}\right)^2 \|\boldsymbol{B}(\boldsymbol{v})\|_{L_2} \tag{7.125}$$
$$\left\|v_4^{(1)}\right\|_{L_2} \leq \left(l^{(1)}\right) \|\boldsymbol{B}(\boldsymbol{v})\|_{L_2} \tag{7.126}$$
$$\left\|(v_3^{(1)})'\right\|_{L_2} \leq \left(l^{(1)}\right) \|\boldsymbol{B}(\boldsymbol{v})\|_{L_2} \tag{7.127}$$
$$\left\|(v_2^{(1)})'\right\|_{L_2} \leq \left(l^{(1)}\right) \|\boldsymbol{B}(\boldsymbol{v})\|_{L_2}. \tag{7.128}$$

For $\boldsymbol{v}^{(2)}$ we have

$$v_1^{(2)}(x) = v_1^{(2)}(0) + \int_0^{(l^{(2)}} (v_1^{(2)})'(y)\,\mathrm{d}y \tag{7.129}$$
$$v_2^{(2)}(x) = v_2^{(2)}(0) + \int_0^{(l^{(2)}} (v_2^{(2)})'(y)\,\mathrm{d}y \tag{7.130}$$
$$v_3^{(2)}(x) = v_3^{(2)}(0) + \int_0^{(l^{(2)}} (v_3^{(2)})'(y)\,\mathrm{d}y \tag{7.131}$$
$$v_4^{(2)}(x) = v_4^{(2)}(0) + \int_0^{(l^{(2)}} (v_4^{(2)})'(y)\,\mathrm{d}y \tag{7.132}$$
$$(v_3^{(2)})'(x) = (v_3^{(2)})'(0) + \int_0^{(l^{(2)}} (v_3^{(2)})''(y)\,\mathrm{d}y \tag{7.133}$$
$$(v_2^{(2)})'(x) = (v_2^{(2)})'(0) + \int_0^{(l^{(2)}} (v_2^{(2)})''(y)\,\mathrm{d}y. \tag{7.134}$$

from which we get

$$|v_1^{(2)}(x)| \leq |v_1^{(2)}(0)| + \sqrt{l^{(2)}} \left\|(v_1^{(2)})'\right\|_{L_2} \tag{7.135}$$
$$|v_2^{(2)}(x)| \leq |v_2^{(2)}(0)| + \sqrt{l^{(2)}} \left\|(v_2^{(2)})'\right\|_{L_2} \tag{7.136}$$
$$|v_3^{(2)}(x)| \leq |v_3^{(2)}(0)| + \sqrt{l^{(2)}} \left\|(v_3^{(2)})'\right\|_{L_2} \tag{7.137}$$
$$|v_4^{(2)}(x)| \leq |v_4^{(2)}(0)| + \sqrt{l^{(2)}} \left\|(v_4^{(2)})'\right\|_{L_2} \tag{7.138}$$
$$|(v_3^{(2)})'(x)| \leq |(v_3^{(2)})'(0)| + \sqrt{l^{(2)}} \left\|(v_3^{(2)})''\right\|_{L_2} \tag{7.139}$$
$$|(v_2^{(2)})'(x)| \leq |(v_2^{(2)})'(0)| + \sqrt{l^{(2)}} \left\|(v_2^{(2)})''\right\|_{L_2}. \tag{7.140}$$

In order to eliminate $|v_1^{(2)}(0)|$, $|v_2^{(2)}(0)|$, $|v_3^{(2)}(0)|$, $|v_4^{(2)}(0)|$, $|(v_3^{(2)})'(0)|$ and $|(v_2^{(2)})'(0)|$ we use the rigid joint conditions (7.93) and (7.94) to write

$$
\begin{aligned}
v_1^{(2)}(0) &= C_{11}v_1^{(1)}(l^{(1)}) + C_{12}v_2^{(1)}(l^{(1)}) + C_{13}v_3^{(1)}(l^{(1)}) && (7.141)\\
v_2^{(2)}(0) &= C_{21}v_1^{(1)}(l^{(1)}) + C_{22}v_2^{(1)}(l^{(1)}) + C_{23}v_3^{(1)}(l^{(1)}) && (7.142)\\
v_3^{(2)}(0) &= C_{31}v_1^{(1)}(l^{(1)}) + C_{32}v_2^{(1)}(l^{(1)}) + C_{33}v_3^{(1)}(l^{(1)}) && (7.143)\\
v_4^{(2)}(0) &= C_{41}v_4^{(1)}(l^{(1)}) + C_{42}(v_3^{(1)})'(l^{(1)}) + C_{43}(v_2^{(1)})'(l^{(1)}) && (7.144)\\
(v_3^{(2)})'(0) &= C_{51}v_4^{(1)}(l^{(1)}) + C_{52}(v_3^{(1)})'(l^{(1)}) + C_{53}(v_2^{(1)})'(l^{(1)}) && (7.145)\\
(v_2^{(2)})'(0) &= C_{61}v_4^{(1)}(l^{(1)}) + C_{62}(v_3^{(1)})'(l^{(1)}) + C_{63}(v_2^{(1)})'(l^{(1)}) && (7.146)
\end{aligned}
$$

where the C_{ij}'s are constants determined from the orientation of the beams. We have shown that

$$
\begin{aligned}
|v_1^{(1)}(l^{(1)})| &\leq C\,\|\boldsymbol{B}(\boldsymbol{v})\|_{L_2} && (7.147)\\
|v_2^{(1)}(l^{(1)})| &\leq C\,\|\boldsymbol{B}(\boldsymbol{v})\|_{L_2} && (7.148)\\
|v_3^{(1)}(l^{(1)})| &\leq C\,\|\boldsymbol{B}(\boldsymbol{v})\|_{L_2} && (7.149)\\
|v_4^{(1)}(l^{(1)})| &\leq C\,\|\boldsymbol{B}(\boldsymbol{v})\|_{L_2} && (7.150)\\
|(v_3^{(1)})'(l^{(1)})| &\leq C\,\|\boldsymbol{B}(\boldsymbol{v})\|_{L_2} && (7.151)\\
|(v_2^{(1)})'(l^{(1)})| &\leq C\,\|\boldsymbol{B}(\boldsymbol{v})\|_{L_2} && (7.152)
\end{aligned}
$$

where C is a generic constant. Therefore,

$$
\begin{aligned}
|v_1^{(2)}(0)| &\leq C\,\|\boldsymbol{B}(\boldsymbol{v})\|_{L_2} && (7.153)\\
|v_2^{(2)}(0)| &\leq C\,\|\boldsymbol{B}(\boldsymbol{v})\|_{L_2} && (7.154)\\
|v_3^{(2)}(0)| &\leq C\,\|\boldsymbol{B}(\boldsymbol{v})\|_{L_2} && (7.155)\\
|v_4^{(2)}(0)| &\leq C\,\|\boldsymbol{B}(\boldsymbol{v})\|_{L_2} && (7.156)\\
|(v_3^{(2)})'(0)| &\leq C\,\|\boldsymbol{B}(\boldsymbol{v})\|_{L_2} && (7.157)\\
|(v_2^{(2)})'(0)| &\leq C\,\|\boldsymbol{B}(\boldsymbol{v})\|_{L_2}\,. && (7.158)
\end{aligned}
$$

Substituting these results into (7.135)...(7.140) we now have

$$
\begin{aligned}
|v_1^{(2)}(x)| &\leq C\,\|\boldsymbol{B}(\boldsymbol{v})\|_{L_2} + \sqrt{l^{(2)}}\,\left\|(v_1^{(2)})'\right\|_{L_2} && (7.159)\\
|v_2^{(2)}(x)| &\leq C\,\|\boldsymbol{B}(\boldsymbol{v})\|_{L_2} + \sqrt{l^{(2)}}\,\left\|(v_2^{(2)})'\right\|_{L_2} && (7.160)\\
|v_3^{(2)}(x)| &\leq C\,\|\boldsymbol{B}(\boldsymbol{v})\|_{L_2} + \sqrt{l^{(2)}}\,\left\|(v_3^{(2)})'\right\|_{L_2} && (7.161)\\
|v_4^{(2)}(x)| &\leq C\,\|\boldsymbol{B}(\boldsymbol{v})\|_{L_2} + \sqrt{l^{(2)}}\,\left\|(v_4^{(2)})'\right\|_{L_2} && (7.162)\\
|(v_3^{(2)})'(x)| &\leq C\,\|\boldsymbol{B}(\boldsymbol{v})\|_{L_2} + \sqrt{l^{(2)}}\,\left\|(v_3^{(2)})''\right\|_{L_2} && (7.163)\\
|(v_2^{(2)})'(x)| &\leq C\,\|\boldsymbol{B}(\boldsymbol{v})\|_{L_2} + \sqrt{l^{(2)}}\,\left\|(v_2^{(2)})''\right\|_{L_2}\,. && (7.164)
\end{aligned}
$$

We know that, from the definition of $\|\boldsymbol{B}(\boldsymbol{v})\|_{L_2}$,

$$\begin{aligned}
\left\|(v_1^{(2)})'\right\|_{L_2} &\leq \|\boldsymbol{B}(\boldsymbol{v})\|_{L_2} && (7.165)\\
\left\|(v_2^{(2)})''\right\|_{L_2} &\leq \|\boldsymbol{B}(\boldsymbol{v})\|_{L_2} && (7.166)\\
\left\|(v_3^{(2)})''\right\|_{L_2} &\leq \|\boldsymbol{B}(\boldsymbol{v})\|_{L_2} && (7.167)\\
\left\|(v_4^{(2)})'\right\|_{L_2} &\leq \|\boldsymbol{B}(\boldsymbol{v})\|_{L_2} && (7.168)
\end{aligned}$$

which may be substituted into (7.159) ... (7.164) to give

$$\begin{aligned}
|v_1^{(2)}(x)| &\leq C\,\|\boldsymbol{B}(\boldsymbol{v})\|_{L_2} && (7.169)\\
|v_2^{(2)}(x)| &\leq C\,\|\boldsymbol{B}(\boldsymbol{v})\|_{L_2} + \sqrt{l^{(2)}}\left\|(v_2^{(2)})'\right\|_{L_2} && (7.170)\\
|v_3^{(2)}(x)| &\leq C\,\|\boldsymbol{B}(\boldsymbol{v})\|_{L_2} + \sqrt{l^{(2)}}\left\|(v_3^{(2)})'\right\|_{L_2} && (7.171)\\
|v_4^{(2)}(x)| &\leq C\,\|\boldsymbol{B}(\boldsymbol{v})\|_{L_2} && (7.172)\\
|(v_3^{(2)})'(x)| &\leq C\,\|\boldsymbol{B}(\boldsymbol{v})\|_{L_2} && (7.173)\\
|(v_2^{(2)})'(x)| &\leq C\,\|\boldsymbol{B}(\boldsymbol{v})\|_{L_2}\,. && (7.174)
\end{aligned}$$

Since

$$\left\|(v_2^{(2)})'\right\|_{L_2}^2 = \int_0^{l^{(2)}} |(v_2^{(2)})'(y)|^2\,\mathrm{d}y \leq \int_0^{l^{(2)}} C^2\,\|\boldsymbol{B}(\boldsymbol{v})\|_{L_2}^2\,\mathrm{d}y \leq l^{(2)}C^2\,\|\boldsymbol{B}(\boldsymbol{v})\|_{L_2}^2\,,$$

implying that $|(v_2^{(2)})'(x)| \leq C\,\|\boldsymbol{B}(\boldsymbol{v})\|_{L_2}$ with a similar result for $|(v_3^{(2)})'(x)|$, we have

$$\begin{aligned}
|v_1^{(2)}(x)| &\leq C\,\|\boldsymbol{B}(\boldsymbol{v})\|_{L_2} && (7.175)\\
|v_2^{(2)}(x)| &\leq C\,\|\boldsymbol{B}(\boldsymbol{v})\|_{L_2} && (7.176)\\
|v_3^{(2)}(x)| &\leq C\,\|\boldsymbol{B}(\boldsymbol{v})\|_{L_2} && (7.177)\\
|v_4^{(2)}(x)| &\leq C\,\|\boldsymbol{B}(\boldsymbol{v})\|_{L_2} && (7.178)\\
|(v_3^{(2)})'(x)| &\leq C\,\|\boldsymbol{B}(\boldsymbol{v})\|_{L_2} && (7.179)\\
|(v_2^{(2)})'(x)| &\leq C\,\|\boldsymbol{B}(\boldsymbol{v})\|_{L_2}\,. && (7.180)
\end{aligned}$$

Finally, upon integrating the above inequalities we have,

$$\begin{aligned}
\left\|v_1^{(2)}\right\|_{L_2} &\leq C\,\|\boldsymbol{B}(\boldsymbol{v})\|_{L_2} && (7.181)\\
\left\|v_2^{(2)}\right\|_{L_2} &\leq C\,\|\boldsymbol{B}(\boldsymbol{v})\|_{L_2} && (7.182)\\
\left\|v_3^{(2)}\right\|_{L_2} &\leq C\,\|\boldsymbol{B}(\boldsymbol{v})\|_{L_2} && (7.183)\\
\left\|v_4^{(2)}\right\|_{L_2} &\leq C\,\|\boldsymbol{B}(\boldsymbol{v})\|_{L_2} && (7.184)\\
\left\|(v_3^{(2)})'\right\|_{L_2} &\leq C\,\|\boldsymbol{B}(\boldsymbol{v})\|_{L_2} && (7.185)\\
\left\|(v_2^{(2)})'\right\|_{L_2} &\leq C\,\|\boldsymbol{B}(\boldsymbol{v})\|_{L_2}\,. && (7.186)
\end{aligned}$$

For each beam we have

$$\left\|v^{(k)}\right\|_{L_2}^2 = \left\|v_1^{(k)}\right\|_{L_2}^2 + \left\|v_2^{(k)}\right\|_{L_2}^2 + \left\|v_3^{(k)}\right\|_{L_2}^2 + \left\|v_4^{(k)}\right\|_{L_2}^2 \leq C \left\|B(v)\right\|_{L_2}^2 \tag{7.187}$$

so that, for the frame,

$$\left\|v\right\|_{L_2}^2 = \left\|v^{(1)}\right\|_{L_2}^2 + \left\|v^{(2)}\right\|_{L_2}^2 \leq C \left\|B(v)\right\|_{L_2}^2 . \tag{7.188}$$

That proves (7.91) for the particular frame. For any rigid-jointed frame, provided at least one point is clamped anywhere in the frame, the same argument may be used to show that there exists a constant C such that

$$|v_j^{(k)}(x)| \leq C \left\|B(v)\right\|_{L_2} . \tag{7.189}$$

for $k = 1 \ldots nb$ and $j = 1 \ldots 4$. Hence (7.91) holds for any rigid-jointed frame. □

7.2.10 Bounds for u in the L_2 norm

We seek bounds for the L_2 norm of u and its derivatives in terms of the load vector f and the thermal load vector Q. From (7.81) with $v = u$ we have

$$\left\|u\right\|^2 \leq \left\|f\right\|_{L_2} \left\|u\right\|_{L_2} + \left\|Q\right\|_{L_2} \left\|B(u)\right\|_{L_2} . \tag{7.190}$$

Using (7.88) and (7.91) we then have

$$C_1 \left\|B(u)\right\|_{L_2}^2 \leq C \left\|f\right\|_{L_2} \left\|B(u)\right\|_{L_2} + \left\|Q\right\|_{L_2} \left\|B(u)\right\|_{L_2} \tag{7.191}$$

so that

$$\left\|B(u)\right\|_{L_2} \leq \frac{C}{C_1} \left\|f\right\|_{L_2} + \frac{1}{C_1} \left\|Q\right\|_{L_2} , \tag{7.192}$$

$$\left\|u\right\|_{L_2} \leq \frac{C^2}{C_1} \left\|f\right\|_{L_2} + \frac{C}{C_1} \left\|Q\right\|_{L_2} . \tag{7.193}$$

7.3 Finite element approximations

7.3.1 Definition

Let $V = V_1 \otimes V_2 \otimes V_3 \otimes V_4$ be a finite dimensional subspace of H. The finite element solution, $u_h \in V$, satisfies

$$a(u_h, v) = (f, v) + (Q, B(v)) \tag{7.194}$$

for all $v \in V$. The error in the finite element solution is defined as

$$e = u - u_h \tag{7.195}$$

or, beam by beam, as

$$e^{(k)} = u^{(k)} - u_h^{(k)}. \tag{7.196}$$

In the next section this will be analysed in both the energy norm and the L_2 norm. The norms are evaluated by summing the integrals over each element of a beam. Let $a(w^{(k)}, v^{(k)})_{\Omega_i}$, $\|w^{(k)}\|_{\Omega_i}$, $(w^{(k)}, v^{(k)})_{\Omega_i}$ and $\|w^{(k)}\|_{L_2(\Omega_i)}$ denote the contribution of the i'th element to $a(w^{(k)}, v^{(k)})$, $\|w^{(k)}\|$, $(w^{(k)}, v^{(k)})$ and $\|w^{(k)}\|_{L_2}$. Then, if $ne(k)$ is the number of elements in the k'th beam,

$$a(w^{(k)}, v^{(k)}) = \sum_{i=1}^{ne(k)} a(w^{(k)}, v^{(k)})_{\Omega_i} \tag{7.197}$$

$$\|w^{(k)}\|^2 = \sum_{i=1}^{ne(k)} \|w^{(k)}\|^2_{\Omega_i} \tag{7.198}$$

$$(w^{(k)}, v^{(k)}) = \sum_{i=1}^{ne(k)} (w^{(k)}, v^{(k)})_{\Omega_i} \tag{7.199}$$

$$\|w^{(k)}\|^2_{L_2} = \sum_{i=1}^{ne(k)} \|w^{(k)}\|^2_{L_2(\Omega_i)} \tag{7.200}$$

where

$$a(w^{(k)}, v^{(k)})_{\Omega_i} = \int_{x_{i-1}}^{x_i} B(w^{(k)})^T D^{(k)} B(v^{(k)})\, \mathrm{d}x \tag{7.201}$$

$$\|w^{(k)}\|^2_{\Omega_i} = \int_{x_{i-1}}^{x_i} B(w^{(k)})^T D^{(k)} B(w^{(k)})\, \mathrm{d}x \tag{7.202}$$

$$(w^{(k)}, v^{(k)})_{\Omega_i} = \int_{x_{i-1}}^{x_i} (w^{(k)})^T v^{(k)}\, \mathrm{d}x \tag{7.203}$$

$$\|w^{(k)}\|^2_{L_2(\Omega_i)} = \int_{x_{i-1}}^{x_i} (w^{(k)})^T w^{(k)}\, \mathrm{d}x. \tag{7.204}$$

7.3.2 Implementation

Using linear and cubic approximations

Each beam element is mapped onto the standard element in the interval $(0, h)$ where h is the element length. The vector $u_h^{(k)}$, over the i'th element, takes the local element form

$$u_h^{(k)} = NU^{(k,i)} \tag{7.205}$$

where the local basis function matrix $\boldsymbol{N}$ has the form

$$\boldsymbol{N} = \begin{pmatrix} N_1 & 0 & 0 & 0 & 0 & 0 & N_2 & 0 & 0 & 0 & 0 & 0 \\ 0 & N_3 & 0 & 0 & 0 & N_5 & 0 & N_4 & 0 & 0 & 0 & N_6 \\ 0 & 0 & N_3 & 0 & -N_5 & 0 & 0 & 0 & N_4 & 0 & -N_6 & 0 \\ 0 & 0 & 0 & N_1 & 0 & 0 & 0 & 0 & 0 & N_2 & 0 & 0 \end{pmatrix} \tag{7.206}$$

and the basis functions are

$$N_1 = 1 - \frac{x}{h}, \tag{7.207}$$

$$N_2 = \frac{x}{h}, \tag{7.208}$$

$$N_3 = \left(1 - \frac{x}{h}\right)^2 \left(1 + \frac{2x}{h}\right), \tag{7.209}$$

$$N_4 = \frac{x^2}{h^2} \left(3 - \frac{2x}{h}\right), \tag{7.210}$$

$$N_5 = x \left(1 - \frac{x}{h}\right)^2, \tag{7.211}$$

$$N_6 = -\frac{x^2}{h} \left(1 - \frac{x}{h}\right). \tag{7.212}$$

The degrees of freedom $U_1^{(k,i)}$, $U_2^{(k,i)}$ and $U_3^{(k,i)}$ are the displacements at $x = 0$ and $U_4^{(k,i)}$, $U_5^{(k,i)}$ and $U_6^{(k,i)}$ are the rotations at $x = 0$ (the negative signs in column 5 and 11 are because $\theta_2 = -u_3'$). Similarly, $U_7^{(k,i)}$ to $U_{12}^{(k,i)}$ are the displacements and rotations at $x = h$. The derivation of a global system of equations proceeds in a similar fashion to that derived in Chapter 3 resulting in a local stiffness matrix $\boldsymbol{K_i}$ and a local force vector $\boldsymbol{F_i}$. An additional consideration here is the orientation of the beam element with respect to that of other elements in the frame. To maintain the physical meaning of the degrees of freedom at the joints and ensure continuity it is necessary to rotate the local degrees of freedom at the joints into a global orientation. In terms of the beam rotation matrix $\boldsymbol{R}^{(k)}$ the local degree of freedom vector, $\boldsymbol{U}^{(k,i)}$, maps to the global degree of freedom vector, $\boldsymbol{U}$, by the relation

$$\begin{pmatrix} \boldsymbol{R}^{(k)} & 0 & 0 & 0 \\ 0 & \boldsymbol{R}^{(k)} & 0 & 0 \\ 0 & 0 & \boldsymbol{R}^{(k)} & 0 \\ 0 & 0 & 0 & \boldsymbol{R}^{(k)} \end{pmatrix} \boldsymbol{U}^{(k,i)} = \begin{pmatrix} \cdots & \boldsymbol{I} & 0 & \cdots & 0 & 0 & \cdots \\ \cdots & 0 & \boldsymbol{I} & \cdots & 0 & 0 & \cdots \\ \cdots & 0 & 0 & \cdots & \boldsymbol{I} & 0 & \cdots \\ \cdots & 0 & 0 & \cdots & 0 & \boldsymbol{I} & \cdots \end{pmatrix} \boldsymbol{U} \tag{7.213}$$

where the position of the $\boldsymbol{I}$'s corresponds to nodes of the i'th element (the other elements, indicated by the $\cdots$, are 3×3 zero matrices). Hence the local stiffness matrix $\boldsymbol{K_i}$ is postmultiplied by the matrix $(\tilde{\boldsymbol{R}}^{(k)})^T$ where

$$\tilde{\boldsymbol{R}}^{(k)} = \begin{pmatrix} \boldsymbol{R}^{(k)} & 0 & 0 & 0 \\ 0 & \boldsymbol{R}^{(k)} & 0 & 0 \\ 0 & 0 & \boldsymbol{R}^{(k)} & 0 \\ 0 & 0 & 0 & \boldsymbol{R}^{(k)} \end{pmatrix}.$$

To assemble the element matrices and element force vectors properly it is also necessary to premultiply the local stiffness matrix and the local force vector by $\tilde{\boldsymbol{R}}^{(k)}$; i.e. the element matrices that are assembled are $\tilde{\boldsymbol{R}}^{(k)}\boldsymbol{K}_i(\tilde{\boldsymbol{R}}^{(k)})^T$.

Using higher-order polynomials

The analysis in Chapter 3 illustrated how the accuracy of the finite element method relates to the degree of polynomial used to represent the finite element space. Analysis in the next section confirms this for finite element frames. It also establishes some other results that depend on using at least quadratic approximations for V_1 and V_4. We consider here such implementations. Three cases are detailed using cubic, quartic and quintic approximations for V_2 and V_3.

Using quadratic and cubic approximations

The degree of polynomial is increased in V_1 and V_4 by adding a node in the centre of each element and increasing the local degrees of freedom by 2. Hence $\boldsymbol{U}^{(k,i)}$ has 14 components and, with the 5th and 6th components of $\boldsymbol{U}^{(k,i)}$ representing the compression and twisting at the central node, $\boldsymbol{N}$ has the form

$$\boldsymbol{N} = \begin{pmatrix} N_1 & 0 & 0 & 0 & 0 & 0 & N_7 & 0 & N_2 & 0 & 0 & 0 & 0 & 0 \\ 0 & N_3 & 0 & 0 & 0 & N_5 & 0 & 0 & 0 & N_4 & 0 & 0 & 0 & N_6 \\ 0 & 0 & N_3 & 0 & -N_5 & 0 & 0 & 0 & 0 & 0 & N_4 & 0 & -N_6 & 0 \\ 0 & 0 & 0 & N_1 & 0 & 0 & 0 & N_7 & 0 & 0 & 0 & N_2 & 0 & 0 \end{pmatrix}. \tag{7.214}$$

The new quadratic basis functions are

$$N_1(x) = \frac{1}{h^2}(2x-h)(x-h), \tag{7.215}$$

$$N_2(x) = \frac{1}{h^2}(2x-h)x, \tag{7.216}$$

$$N_7(x) = -\frac{1}{h^2}4x(x-h). \tag{7.217}$$

The local degree of freedom vector, $\boldsymbol{U}^{(k,i)}$, is related to the global vector, $\boldsymbol{U}$, by

$$\begin{pmatrix} \boldsymbol{R}^{(k)} & \boldsymbol{0} & \boldsymbol{z} & \boldsymbol{z} & \boldsymbol{0} & \boldsymbol{0} \\ \boldsymbol{0} & \boldsymbol{R}^{(k)} & \boldsymbol{z} & \boldsymbol{z} & \boldsymbol{0} & \boldsymbol{0} \\ \boldsymbol{z}^T & \boldsymbol{z}^T & 1 & 0 & \boldsymbol{z}^T & \boldsymbol{z}^T \\ \boldsymbol{z}^T & \boldsymbol{z}^T & 0 & 1 & \boldsymbol{z}^T & \boldsymbol{z}^T \\ \boldsymbol{0} & \boldsymbol{0} & \boldsymbol{z} & \boldsymbol{z} & \boldsymbol{R}^{(k)} & \boldsymbol{0} \\ \boldsymbol{0} & \boldsymbol{0} & \boldsymbol{z} & \boldsymbol{z} & \boldsymbol{0} & \boldsymbol{R}^{(k)} \end{pmatrix} \boldsymbol{U}^{(\mathrm{k,i})} = \begin{pmatrix} \cdots & \boldsymbol{I} & \boldsymbol{0} & \cdot & \boldsymbol{z} & \boldsymbol{z} & \cdot & \boldsymbol{0} & \boldsymbol{0} & \cdots \\ \cdots & \boldsymbol{0} & \boldsymbol{I} & \cdot & \boldsymbol{z} & \boldsymbol{z} & \cdot & \boldsymbol{0} & \boldsymbol{0} & \cdots \\ \cdots & \boldsymbol{z}^T & \boldsymbol{z}^T & \cdot & 1 & 0 & \cdot & \boldsymbol{z}^T & \boldsymbol{z}^T & \cdots \\ \cdots & \boldsymbol{z}^T & \boldsymbol{z}^T & \cdot & 0 & 1 & \cdot & \boldsymbol{z}^T & \boldsymbol{z}^T & \cdots \\ \cdots & \boldsymbol{0} & \boldsymbol{0} & \cdot & \boldsymbol{z} & \boldsymbol{z} & \cdot & \boldsymbol{I} & \boldsymbol{0} & \cdots \\ \cdots & \boldsymbol{0} & \boldsymbol{0} & \cdot & \boldsymbol{z} & \boldsymbol{z} & \cdot & \boldsymbol{0} & \boldsymbol{I} & \cdots \end{pmatrix} \boldsymbol{U} \tag{7.218}$$

where $\boldsymbol{z}$ is a 3×1 zero vector. In this implementation the degrees of freedom stored in $\boldsymbol{U}$ that represent the compression and twisting at the central node are with respect to the local orientation of the beam and have no physical interpretation in the global frame.

Using quadratic and quartic approximations

Increasing the degrees of freedom per element to 16, with the extra 2 representing the bending at the central node, the matrix $\boldsymbol{N}$ has the form

$$\boldsymbol{N} = \begin{pmatrix} N_1 & 0 & 0 & 0 & 0 & 0 & N_7 & 0 & 0 & 0 & N_2 & 0 & 0 & 0 & 0 & 0 \\ 0 & N_3 & 0 & 0 & 0 & N_5 & 0 & N_8 & 0 & 0 & 0 & N_4 & 0 & 0 & 0 & N_6 \\ 0 & 0 & N_3 & 0 & -N_5 & 0 & 0 & 0 & N_8 & 0 & 0 & 0 & N_4 & 0 & -N_6 & 0 \\ 0 & 0 & 0 & N_1 & 0 & 0 & 0 & 0 & 0 & N_7 & 0 & 0 & 0 & N_2 & 0 & 0 \end{pmatrix} \tag{7.219}$$

and the new quartic basis functions are

$$N_3(x) = -\frac{1}{h^4}(x-h)^2(2x-h)(4x+h), \tag{7.220}$$

$$N_4(x) = -\frac{1}{h^4}x^2(2x-h)(4x-5h), \tag{7.221}$$

$$N_5(x) = -\frac{1}{h^3}x(2x-h)(x-h)^2, \tag{7.222}$$

$$N_6(x) = \frac{1}{h^3}x^2(2x-h)(x-h), \tag{7.223}$$

$$N_8(x) = \frac{1}{h^4}16x^2(x-h)^2. \tag{7.224}$$

The local degree of freedom vector, $\boldsymbol{U}^{(k,i)}$, is related to the global vector, $\boldsymbol{U}$, by

$$\begin{pmatrix} R^{(k)} & 0 & 0 & z & 0 & 0 \\ 0 & R^{(k)} & 0 & z & 0 & 0 \\ 0 & 0 & I & z & 0 & 0 \\ z^T & z^T & z^T & 1 & z^T & z^T \\ 0 & 0 & z & z & R^{(k)} & 0 \\ 0 & 0 & z & z & 0 & R^{(k)} \end{pmatrix} U^{(\mathrm{k,i})} = \begin{pmatrix} \cdot & I & 0 & \cdot & 0 & z & \cdot & 0 & 0 & \cdot \\ \cdot & 0 & I & \cdot & 0 & z & \cdot & 0 & 0 & \cdot \\ \cdot & 0 & 0 & \cdot & I & z & \cdot & z^T & z^T & \cdot \\ \cdot & z^T & z^T & \cdot & z^T & 1 & \cdot & z^T & z^T & \cdot \\ \cdot & 0 & 0 & \cdot & 0 & z & \cdot & I & 0 & \cdot \\ \cdot & 0 & 0 & \cdot & 0 & z & \cdot & 0 & I & \cdot \end{pmatrix} U. \tag{7.225}$$

In this implementation all displacements are represented by degrees of freedom at the central node so it would be practical to rotate these onto the global orientation of the frame. Hence, by replacing the $\boldsymbol{I}$ in the left hand side with $\boldsymbol{R}^{(k)}$, the global vector $\boldsymbol{U}$ stores all displacements in terms of the global coordinate system.

Using quadratic and quintic approximations

Increasing the degrees of freedom to 18 per element $\boldsymbol{N}$ has the form

$$\boldsymbol{N} = \begin{pmatrix} N_1 & 0 & 0 & 0 & 0 & 0 & N_7 & 0 & 0 & 0 & 0 & 0 & N_2 & 0 & 0 & 0 & 0 & 0 \\ 0 & N_3 & 0 & 0 & 0 & N_5 & 0 & N_8 & 0 & 0 & 0 & N_9 & 0 & N_4 & 0 & 0 & 0 & N_6 \\ 0 & 0 & N_3 & 0 & -N_5 & 0 & 0 & 0 & N_8 & 0 & -N_9 & 0 & 0 & 0 & N_4 & 0 & -N_6 & 0 \\ 0 & 0 & 0 & N_1 & 0 & 0 & 0 & 0 & 0 & N_7 & 0 & 0 & 0 & 0 & 0 & N_2 & 0 & 0 \end{pmatrix} \tag{7.226}$$

where the new quintic basis functions are

$$N_3(x) = \frac{1}{h^5}(2x-h)^2(x-h)^2(6x+h), \tag{7.227}$$

$$N_4(x) = -\frac{1}{h^5}x^2(2x-h)^2(6x-7h), \tag{7.228}$$

$$N_5(x) = \frac{1}{h^4}x(2x-h)^2(x-h)^2, \tag{7.229}$$

$$N_6(x) = \frac{1}{h^4}x^2(2x-h)^2(x-h), \tag{7.230}$$

$$N_8(x) = \frac{1}{h^4}16x^2(x-h)^2, \tag{7.231}$$

$$N_9(x) = \frac{1}{h^4}8x^2(2x-h)(x-h)^2. \tag{7.232}$$

The local degree of freedom vector, $\boldsymbol{U}^{(k,i)}$, is related to the global vector, $\boldsymbol{U}$, by

$$\begin{pmatrix} \boldsymbol{R}^{(k)} & 0 & 0 & 0 & 0 & 0 \\ 0 & \boldsymbol{R}^{(k)} & 0 & 0 & 0 & 0 \\ 0 & 0 & \boldsymbol{I} & 0 & 0 & 0 \\ 0 & 0 & 0 & \boldsymbol{I} & 0 & 0 \\ 0 & 0 & 0 & 0 & \boldsymbol{R}^{(k)} & 0 \\ 0 & 0 & 0 & 0 & 0 & \boldsymbol{R}^{(k)} \end{pmatrix} \boldsymbol{U}^{(k,i)} = \begin{pmatrix} \cdots & \boldsymbol{I} & 0 & \cdot & 0 & 0 & \cdot & 0 & 0 & \cdots \\ \cdots & 0 & \boldsymbol{I} & \cdot & 0 & 0 & \cdot & 0 & 0 & \cdots \\ \cdots & 0 & 0 & \cdot & \boldsymbol{I} & 0 & \cdot & 0 & 0 & \cdots \\ \cdots & 0 & 0 & \cdot & 0 & \boldsymbol{I} & \cdot & 0 & 0 & \cdots \\ \cdots & 0 & 0 & \cdot & 0 & 0 & \cdot & \boldsymbol{I} & 0 & \cdots \\ \cdots & 0 & 0 & \cdot & 0 & 0 & \cdot & 0 & \boldsymbol{I} & \cdots \end{pmatrix} \boldsymbol{U}. \tag{7.233}$$

In this implementation all displacements and rotations are represented by degrees of freedom at the central node and it would be practical to map these onto the global orientation of the frame. Hence, by replacing the $\boldsymbol{I}$'s in the left hand side with $\boldsymbol{R}^{(k)}$'s, the global vector $\boldsymbol{U}$ stores all degrees of freedom in terms of the global coordinate system.

7.3.3 A note about solving the system

For one dimension problems, a direct method such as Cholesky decomposition is most efficient if the nodes can be numbered so as to give a small band width of the matrix [29]. This is certainly true for a single beam or the frame in Figure 7.5 where the nodes could be numbered consecutively. The Cholesky method may only be implemented if the full band width of the matrix is stored since the decomposition requires the storage of matrix elements between the diagonal and the outer beam which may include entries outside of the compressed matrix structure. For a more complicated frame, where more than two beams meet at a joint, the Cholesky method cannot be used with compressed row storage on the full frame matrix. If a direct solver was to be used then the system would need to be decomposed into direct solvable subsystems, typically one per beam, involving degrees of freedom at internal nodes then coupled by solving another system in the degrees of freedom at the joints. This is difficult to set up in a computer program. However, a partial Cholesky decomposition may be used as a preconditioner to the Conjugate Gradient method [29] which is easy to implement. If the nodes are numbered consecutively along each beam, then the partial Cholesky preconditioner notably reduces the number of iterations in the Conjugate Gradient algorithm.

7.4 *A priori* error estimates

7.4.1 Energy norm estimate

Without actually calculating $\boldsymbol{u}_h$ there are some basic results that can be deduced about the the error, $\boldsymbol{e}$. Firstly, since

$$a(\boldsymbol{u},\boldsymbol{v}) = (\boldsymbol{f},\boldsymbol{v}) + (\boldsymbol{Q},\boldsymbol{B}(\boldsymbol{v})) \tag{7.234}$$

$$a(\boldsymbol{u}_h,\boldsymbol{v}) = (\boldsymbol{f},\boldsymbol{v}) + (\boldsymbol{Q},\boldsymbol{B}(\boldsymbol{v})) \tag{7.235}$$

for all $\boldsymbol{v} \in V$, we have the orthogonality relation,

$$a(\boldsymbol{e},\boldsymbol{v}) = 0. \tag{7.236}$$

This means that we can write

$$\|\boldsymbol{e}\|^2 = a(\boldsymbol{e},\boldsymbol{e}) = a(\boldsymbol{e},\boldsymbol{u}-\boldsymbol{v}) \tag{7.237}$$

for any $\boldsymbol{v} \in V$. Applying the Cauchy Schwarz inequality and dividing by $\|\boldsymbol{e}\|$ gives us

$$\|\boldsymbol{e}\| \leq \|\boldsymbol{u}-\boldsymbol{v}\|. \tag{7.238}$$

In particular we may choose $\boldsymbol{v}$ to be the interpolant to $\boldsymbol{u}$ in V. Let us denote the interpolant by $\Pi\boldsymbol{u}$. Hence we have the familiar result

$$\|\boldsymbol{e}\| \leq \|\boldsymbol{u}-\Pi\boldsymbol{u}\| \tag{7.239}$$

which means $\|\boldsymbol{e}\|$ behaves no worse than the energy norm of the interpolation error. Using (7.88) we have, in terms of the L_2 norm,

$$\|\boldsymbol{e}\| \leq C\|\boldsymbol{B}(\boldsymbol{u}-\Pi\boldsymbol{u})\|_{L_2}. \tag{7.240}$$

Using the Peano kernel theorem [27] it was shown in Chapter 2 that, for a function $f(x)$ interpolated by a piecewise polynomial of degree p, denoted by $\Pi_p f(x)$,

$$\left\| \frac{d^n}{dx^n}\Big(f(x) - \Pi_p f(x)\Big) \right\|_{L_2} \leq C h^{p+1-n} \|f^{(p+1)}\|_{L_2} \tag{7.241}$$

where C is a generic constant and h is the maximum element length. This holds provided $f^{(p+1-n)}$ exists within each element. This is certainly true of $\boldsymbol{u}$ hence we can express $\|\boldsymbol{B}(\boldsymbol{u}-\Pi\boldsymbol{u})\|_{L_2}$ in terms of h. Let p_1 denote the order of polynomials in V_1 and V_4 and let p_2 denote the order of polynomials in V_2 and V_3. Then, using (7.241), we have

$$\|(u_1 - \Pi_{p_1}u_1)'\|_{L_2} \leq C h^{p_1} \|u_1''\|_{L_2} \tag{7.242}$$

$$\|(u_2 - \Pi_{p_2}u_2)''\|_{L_2} \leq C h^{p_2-1} \|u_2''''\|_{L_2} \tag{7.243}$$

$$\|(u_3 - \Pi_{p_2}u_3)''\|_{L_2} \leq C h^{p_2-1} \|u_3''''\|_{L_2} \tag{7.244}$$

$$\|(u_4 - \Pi_{p_1}u_4)'\|_{L_2} \leq C h^{p_1} \|u_4''\|_{L_2}. \tag{7.245}$$

Hence, to leading order of h,

$$\|B(u - \Pi u)\|_{L_2} \leq Ch^t \tag{7.246}$$

where

$$t = \min\{p_1, p_2 - 1\} \tag{7.247}$$

so that

$$\|e\| \leq Ch^t. \tag{7.248}$$

7.4.2 L_2 norm estimate

Using the Nitsche technique [14] we may use (7.246) to obtain an asymptotic estimate of the error in the L_2 norm. The trick is to let $\phi \in H$ satisfy

$$L_0^{(k)}(\phi^{(k)}) = e^{(k)} \tag{7.249}$$

where $L_0^{(k)}$ is defined as the vector operator equivalent to $L^{(k)}$ with $Q^{(k)} = 0$. Then,

$$\|e\|_{L_2}^2 = \sum_{k=1}^{nb}(L_0^{(k)}(\phi^{(k)}), e^{(k)}) \tag{7.250}$$

$$= \sum_{k=1}^{nb} a(\phi^{(k)}, e^{(k)}) \tag{7.251}$$

$$= \sum_{k=1}^{nb} a(\phi^{(k)} - v^{(k)}, e^{(k)}) \tag{7.252}$$

$$\leq \sum_{k=1}^{nb} \left\|\phi^{(k)} - v^{(k)}\right\| \left\|e^{(k)}\right\| \tag{7.253}$$

$$\leq C \sum_{k=1}^{nb} \left\|B(\phi^{(k)} - v^{(k)})\right\|_{L_2} \left\|e^{(k)}\right\| \tag{7.254}$$

$$\leq C \|B(\phi - v)\|_{L_2} \|e\| \tag{7.255}$$

for any $v \in V$. Hence, by equation (7.246),

$$\|e\|_{L_2}^2 \leq Ch^t \|B(\phi - v)\|_{L_2}. \tag{7.256}$$

Now

$$\|B(\phi - v)\|_{L_2}^2 = \|(\phi_1 - v_1)'\|_{L_2}^2 + \|(\phi_2 - v_2)''\|_{L_2}^2 + \|(\phi_3 - v_3)''\|_{L_2}^2 + \|(\phi_4 - v_4)'\|_{L_2}^2. \tag{7.257}$$

Since, within an element, v_1 and v_4 must be at least linear and v_2 and v_3 must be at least cubic we can choose v_1 and v_4 to be the linear interpolants to ϕ_1 and ϕ_4 and

choose v_2 and v_3 to be the Hermite cubic interpolants to ϕ_2 and ϕ_3. With these choices we have, from (2.40), the following bounds

$$\|(\phi_1 - \Pi_1\phi_1)'\|_{L_2} \leq Ch\|\phi_1''\|_{L_2} \tag{7.258}$$
$$\|(\phi_2 - \Pi_3\phi_2)''\|_{L_2} \leq Ch\|\phi_2'''\|_{L_2} \tag{7.259}$$
$$\|(\phi_3 - \Pi_3\phi_3)''\|_{L_2} \leq Ch\|\phi_3'''\|_{L_2} \tag{7.260}$$
$$\|(\phi_4 - \Pi_1\phi_4)'\|_{L_2} \leq Ch\|\phi_4''\|_{L_2}. \tag{7.261}$$

These will be used to deduce the error estimate for the general case. For the special case of pure bending we will use the higher order bounds

$$\|(\phi_2 - \Pi_3\phi_2)''\|_{L_2} \leq Ch^2\|\phi_2''''\|_{L_2} \tag{7.262}$$
$$\|(\phi_3 - \Pi_3\phi_3)''\|_{L_2} \leq Ch^2\|\phi_3''''\|_{L_2}. \tag{7.263}$$

We will show that, for the general case,

$$\|\phi_1''\|_{L_2} \leq C\|e\|_{L_2} \tag{7.264}$$
$$\|\phi_2'''\|_{L_2} \leq C\|e\|_{L_2} \tag{7.265}$$
$$\|\phi_3'''\|_{L_2} \leq C\|e\|_{L_2} \tag{7.266}$$
$$\|\phi_4''\|_{L_2} \leq C\|e\|_{L_2} \tag{7.267}$$

so that

$$\|B(\phi - v)\|_{L_2} \leq Ch\|e\|_{L_2}. \tag{7.268}$$

Then, by equation (7.256),

$$\|e\|_{L_2} \leq Ch^{t+1}. \tag{7.269}$$

For the special case of pure bending where $\phi_1 = \phi_4 = 0$ we will show that

$$\|\phi_2''''\|_{L_2} \leq C\|e\|_{L_2} \tag{7.270}$$
$$\|\phi_3''''\|_{L_2} \leq C\|e\|_{L_2} \tag{7.271}$$

so that

$$\|e\|_{L_2} \leq Ch^{p_2+1}. \tag{7.272}$$

In order to show (7.264) to (7.267) we define the function $\tilde{\phi}$ to be such that

$$B(\tilde{\phi}) = DB(\phi). \tag{7.273}$$

Then

$$\begin{pmatrix} -\tilde{\phi}_1'' \\ \tilde{\phi}_2'''' \\ \tilde{\phi}_3'''' \\ -\tilde{\phi}_4'' \end{pmatrix} = \begin{pmatrix} e_1 \\ e_2 \\ e_3 \\ e_4 \end{pmatrix}. \tag{7.274}$$

Immediately we have

$$\left\|\tilde{\phi}_1''\right\|_{L_2} \leq \|e\|_{L_2} \tag{7.275}$$
$$\left\|\tilde{\phi}_2''''\right\|_{L_2} \leq \|e\|_{L_2} \tag{7.276}$$
$$\left\|\tilde{\phi}_3''''\right\|_{L_2} \leq \|e\|_{L_2} \tag{7.277}$$
$$\left\|\tilde{\phi}_4''\right\|_{L_2} \leq \|e\|_{L_2} \tag{7.278}$$

and, by (7.273),

$$|\tilde{\phi}_1'| \leq C\|e\|_{L_2} \tag{7.279}$$
$$|\tilde{\phi}_2''| \leq C\|e\|_{L_2} \tag{7.280}$$
$$|\tilde{\phi}_3''| \leq C\|e\|_{L_2} \tag{7.281}$$
$$|\tilde{\phi}_4'| \leq C\|e\|_{L_2}. \tag{7.282}$$

From (7.274), (7.280) and (7.281) it follows that

$$|\tilde{\phi}_2'''| \leq C\|e\|_{L_2} \tag{7.283}$$
$$|\tilde{\phi}_3'''| \leq C\|e\|_{L_2} \tag{7.284}$$

since, for $\tilde{\phi}_2'''$,

$$\tilde{\phi}_2''''(x) = e_2 \tag{7.285}$$
$$\tilde{\phi}_2'''(x) = \tilde{\phi}_2'''(0) + \int_0^x e_2(y)\,\mathrm{d}y \tag{7.286}$$
$$\tilde{\phi}_2''(x) = \tilde{\phi}_2''(0) + \tilde{\phi}_2'''(0)x + \int_0^x \int_0^y e_2(z)\,\mathrm{d}z\,\mathrm{d}y. \tag{7.287}$$

Putting $x = l$ into (7.287) gives us

$$|\tilde{\phi}_2'''(0)| \leq \frac{|\tilde{\phi}_2''(0)| + |\tilde{\phi}_2''(l)|}{l} + \|e_2\|_{L_2} \tag{7.288}$$
$$\leq C\|e\|_{L_2} \tag{7.289}$$

then, from (7.286),

$$|\tilde{\phi}_2'''(x)| \leq |\tilde{\phi}_2'''(0)| + \|e_2\|_{L_2} \leq C\|e\|_{L_2}. \tag{7.290}$$

This implies (7.283). An identical argument for $\tilde{\phi}_3$ leads to (7.284). Using (7.273) with the knowledge that $\boldsymbol{D}$ is non-singular we can write

$$\phi_1' = a_{11}\tilde{\phi}_1' + a_{12}\tilde{\phi}_2'' + a_{13}\tilde{\phi}_3'' \tag{7.291}$$
$$\phi_2'' = a_{12}\tilde{\phi}_1' + a_{22}\tilde{\phi}_2'' + a_{23}\tilde{\phi}_3'' \tag{7.292}$$
$$\phi_3'' = a_{13}\tilde{\phi}_1' + a_{23}\tilde{\phi}_2'' + a_{33}\tilde{\phi}_3'' \tag{7.293}$$
$$\phi_4' = a_{44}\tilde{\phi}_4'. \tag{7.294}$$

Differentiating (7.294) gives us

$$\phi_4'' = a_{44}\tilde{\phi}_4'' + a_{44}'\tilde{\phi}_4' \tag{7.295}$$

so that, assuming a_{44} and a_{44}' are bounded,

$$\begin{aligned} |\phi_4''| &\leq C|\tilde{\phi}_4''| + C|\tilde{\phi}_4'| && (7.296)\\ &\leq C\left\|\tilde{\phi}_4''\right\|_{L_2} + C\left\|\tilde{\phi}_4'\right\|_{L_2} && (7.297)\\ &\leq C\left\|e\right\|_{L_2} + C\left\|B(\tilde{\phi})\right\|_{L_2} && (7.298)\\ &\leq C\left\|e\right\|_{L_2} + C\left\|B(\phi)\right\|_{L_2} && (7.299)\\ &\leq C\left\|e\right\|_{L_2} + C\left\|e\right\|_{L_2}. && (7.300) \end{aligned}$$

Hence, we have

$$|\phi_4''| \leq C\left\|e\right\|_{L_2} \tag{7.301}$$

from which we deduce (7.267). Similarly, on differentiating (7.291), we have

$$\begin{aligned} |\phi_1''| &\leq C\left\|\tilde{\phi}_1''\right\|_{L_2} + C\left\|\tilde{\phi}_2'''\right\|_{L_2} + C\left\|\tilde{\phi}_3'''\right\|_{L_2} && (7.302)\\ &\leq C\left\|e\right\|_{L_2}, && (7.303) \end{aligned}$$

due to (7.279), (7.283) and (7.284), which implies (7.267). Differentiating (7.292) gives us

$$\phi_2''' = a_{12}\tilde{\phi}_1'' + a_{12}'\tilde{\phi}_1' + a_{22}\tilde{\phi}_2''' + a_{22}'\tilde{\phi}_2'' + a_{23}\tilde{\phi}_3''' + a_{23}'\tilde{\phi}_3''. \tag{7.304}$$

Using the previous results of this section and assuming that the a_{ij}'s and their required derivatives are bounded we have

$$|\phi_2'''| \leq C\left\|e\right\|_{L_2}. \tag{7.305}$$

Hence, along with a similar result for ϕ_3''', we deduce (7.265) and (7.266).

For the special case of pure bending (7.304) reduces to

$$\phi_2''' = a_{22}\tilde{\phi}_2''' + a_{22}'\tilde{\phi}_2'' + a_{23}\tilde{\phi}_3''' + a_{23}'\tilde{\phi}_3''. \tag{7.306}$$

Differentiating (7.306) gives us

$$\phi_2'''' = a_{22}\tilde{\phi}_2'''' + 2a_{22}'\tilde{\phi}_2''' + a_{22}''\tilde{\phi}_2'' + a_{23}\tilde{\phi}_3'''' + 2a_{23}'\tilde{\phi}_3''' + a_{23}''\tilde{\phi}_3''. \tag{7.307}$$

All the $\tilde{\phi}_2$ and $\tilde{\phi}_3$ terms in (7.307) have been shown to be bounded in terms of $\|e\|_{L_2}$. Therefore, assuming that the a_{ij}'s and their required derivatives are bounded, we may deduce (7.270). Similarly we deduce (7.271).

7.4.3 Pointwise estimates at connecting nodes and joints

The pointwise estimates described in this section rely on the existence of suitably smooth and bounded functions that solve particular frame problems involving the Dirac delta function in the load. These functions are similar in concept to Green's functions (see, for example, the books by Stakgold [31] and Melnikov [23]) and so are referred to as such here.

We consider the pointwise error, $e_j^{(m)}(z)$, which is the j'th component of the error vector in the m'th beam at the point $x = z$. We define global Green's vector functions $\boldsymbol{g}_j^m(z,\cdot)$, for $j = 1\ldots4$ and $z \in (0, l^{(m)})$, such that

$$e_j^{(m)}(z) = a(\boldsymbol{e}, \boldsymbol{g}_j^{(m)}(z,\cdot)) \quad j = 1\ldots4. \tag{7.308}$$

These are specified beam-wise as $\boldsymbol{g}_j^{(m,k)}$ such that

$$\begin{aligned} e_j^{(m)}(z) &= \sum_{k=1}^{nb} a(\boldsymbol{e}^{(k)}, \boldsymbol{g}_j^{(m,k)}(z,\cdot)) \quad j = 1\ldots4 && (7.309)\\ &= \sum_{k=1}^{nb} (\boldsymbol{e}^{(k)}, \boldsymbol{L}_0^{(k)}(\boldsymbol{g}_j^{(m,k)}(z,\cdot)))_{L_2(\Omega_k)} \\ &+ \sum_{k=1}^{nb} \left[\boldsymbol{\varepsilon}(\boldsymbol{e}^{(k)})\boldsymbol{P}^{(k)}\left(\boldsymbol{g}^{(m,k)}(z,\cdot)\right)\right]_0^{l^{(k)}} \quad j = 1\ldots4 && (7.310) \end{aligned}$$

where

$$\boldsymbol{\varepsilon}(\boldsymbol{v}) = \begin{pmatrix} v_1 & v_2 & v_3 & v_4 & -v_3' & v_2' \end{pmatrix}, \tag{7.311}$$

$$\boldsymbol{P}^{(k)}(\boldsymbol{v}) = \begin{pmatrix} \boldsymbol{F}^{(k)}(\boldsymbol{v}) \\ \boldsymbol{M}^{(k)}(\boldsymbol{v}) \end{pmatrix} \tag{7.312}$$

and $\boldsymbol{L}_0^{(k)}$ is the beam differential operator acting on the k'th beam with no thermal load (i.e. $\boldsymbol{Q} = \boldsymbol{0}$). For the case where $z \in (0, l^{(m)})$ (7.308) holds if

$$\boldsymbol{L}_0^{(k)}\boldsymbol{g}_j^{(m,k)}(z,x) = \begin{cases} \boldsymbol{\delta}_j(x-z) & , k = m \\ \boldsymbol{0} & , k \neq m \end{cases} \tag{7.313}$$

with rigid joint conditions where $\boldsymbol{\delta}_j$ is a vector whose j'th component is the Dirac delta function and other components are zero. For the case where z is at a joint, i.e. $z = 0$ or $z = l^{(m)}$, (7.308) holds if

$$\boldsymbol{L}_0^{(k)}\boldsymbol{g}_j^{(m,k)}(z,\cdot) = 0, \quad k = 1,\ldots,nb \tag{7.314}$$

with rigid joint conditions at all joints not corresponding to z. At the z joint we require

that

$$\sum_{k\in\text{joint}} \begin{pmatrix} \boldsymbol{R}^{(k)}\boldsymbol{F}^{(k)}(\boldsymbol{g}_j^{(m,k)})n^{(k)} \\ \boldsymbol{R}^{(k)}\boldsymbol{M}^{(k)}(\boldsymbol{g}_j^{(m,k)})n^{(k)} \end{pmatrix} = \begin{pmatrix} \delta_{1j} \\ \delta_{2j} \\ \delta_{3j} \\ \delta_{4j} \\ 0 \\ 0 \end{pmatrix} \tag{7.315}$$

where δ_{ij} is the Kronecker delta function.

Regarding the form of $\boldsymbol{g}_j^{(m,k)}$ it is straightforward to verify that there are 12 independent solutions to the homogeneous equation (7.314) (which corresponds to $m \neq k$) so that $\boldsymbol{g}_j^{(m,k)}$ may be expressed as

$$\boldsymbol{g}_j^{(m,k)}(z,x) = \sum_{i=1}^{12} c_{ij}^{(m,k)} a_{ij}^{(m,k)}(x) \tag{7.316}$$

where the $c_{ij}^{(m,k)}$'s are constants (depending on z) and the $a_{ij}^{(m,k)}$'s are 12 independent solutions to (7.314). In the m'th beam for the case where $0 < z < l^{(m)}$, $\boldsymbol{g}_j^{(m,m)}$ may be expressed as

$$\boldsymbol{g}_j^{(m,m)}(z,x) = \begin{cases} \sum_{i=1}^{12} c_{ij}^{(m,m)} a_{ij}^{(m,m)}(x), & 0 \leq x < z \\ \sum_{i=1}^{12} d_{ij}^{(m,m)} a_{ij}^{(m,m)}(x), & z < x \leq l^{(m)} \end{cases} \tag{7.317}$$

where the $d_{ij}^{(m,k)}$'s are more constants. For each z all the constants on all the beams are found by applying all the boundary and joint conditions plus jump conditions at $x = z$ which may be found by direct integration of $\boldsymbol{\delta}_j(x - z)$.

Using (7.308) and the orthogonality result in (7.236) we have

$$e_j^{(m)}(z) = a(\boldsymbol{e}, \boldsymbol{g}_j^{(m)}(z,\cdot) - \boldsymbol{v}), \quad j = 1\ldots 4 \tag{7.318}$$

for any $\boldsymbol{v} \in V$. Then, using the Cauchy Schwarz inequality,

$$|e_j^{(m)}(z)| \leq \|\boldsymbol{e}\| \left\|\boldsymbol{g}_j^{(m)}(z,\cdot) - \boldsymbol{v}\right\|. \tag{7.319}$$

We would like to put $\boldsymbol{v}^{(k)} = \Pi \boldsymbol{g}_j^{(m,k)}(z,\cdot)$ so that we may apply the interpolation result to $\boldsymbol{g}_j^{(m,k)}(z,\cdot)$. We can only do this if $\boldsymbol{g}_j(z,\cdot)$ is suitably differentiable within an element. This is the case when z is a connecting node. We may then deduce that $\left\|\boldsymbol{g}_j^{(m)}(z,\cdot) - \boldsymbol{v}\right\|$ is of order h^t. Hence $|e_j(z)|$ is of order h^{2t} at connecting nodes for $j = 1\ldots 4$.

If this convergence rate is faster than the global rate, given by $\|\boldsymbol{e}\|_{L_2}$, then the solution is said to be superconvergent at these points [14, Page 44]. So, for the general case where $\|\boldsymbol{e}\|_{L_2}$ is order h^{t+1}, the finite element method is superconvergent if $t > 1$. Considering each component of $\boldsymbol{e}$ individually it is possible that the second and third

components converge at the higher (pure bending) rate of h^{p_2+1}. Hence we would need $t > 2$ to guarantee superconvergence for e_2 and e_3. However, if it happened that e_1 and e_4 were zero, the convergence rate at connecting nodes would be h^{2p_2-2} and $\|e\|_{L_2}$ would be order h^{p_2+1}. In this case we would need $p_2 > 3$ for superconvergence. To guarantee superconvergence individually for all components of the error in all cases we need $p_1 > 2$ and $p_2 > 3$.

7.4.4 Superconvergent derivatives

We consider here the derivatives of e_2 and e_3 and show that these are superconvergent at the connecting nodes when $t > 1$. We begin by considering, for the $j = 2$ case, the derivative of (7.308) with respect to z in the form

$$\frac{\partial e_2^{(m)}}{\partial z} = \sum_{k=1}^{nb} \int_0^{l^{(k)}} \boldsymbol{B}(\boldsymbol{e}^{(k)})^T \frac{\partial}{\partial z} \left(\boldsymbol{S}^{(k)} \left(\boldsymbol{g}_2^{(m,k)}(z,x) \right) \right) \mathrm{d}x. \tag{7.320}$$

To justify rigorously why (7.320) is valid we would need to consider precisely the properties of $\boldsymbol{g}_2^{(m,m)}(z,x)$ and specifically we would need to consider all the mixed partial derivatives. We do not do this here but instead just note that $\partial \boldsymbol{S}^{(m)}(\boldsymbol{g}_2^{(m,m)}(z,x))/\partial z$, as a function of x, is continuous on the interval $(0, l^{(m)})$ except at $x = z$ where it has a jump discontinuity. That is the integrand is not continuous but it is still integrable. If the evaluation point is a connecting node then the integrand is a 'smooth' function of x within each element. This also applies to $\boldsymbol{S}^{(k)}(\boldsymbol{g}_3^{(m,m)}(z,x))$ and so we have, for $0 < z < l^m$,

$$\frac{\partial e_j^{(m)}}{\partial z} = \sum_{k=1}^{nb} \int_0^{l^{(k)}} \boldsymbol{B}(\boldsymbol{e}^{(k)})^T \frac{\partial}{\partial z} \left(\boldsymbol{S}^{(k)} \left(\boldsymbol{g}_j^{(m,k)}(z,x) \right) \right) \mathrm{d}x, \quad j = 2,3. \tag{7.321}$$

For convenience, let

$$e_5^{(m)}(z) = -\frac{\partial}{\partial z} e_3^{(m)}(z), \quad e_6^{(m)}(z) = \frac{\partial}{\partial z} e_2^{(m)}(z), \tag{7.322}$$

$$g_5^{(m,k)}(z,x) = -\frac{\partial}{\partial z} g_3^{(m,k)}(z,x), \quad g_6^{(m,k)}(z,x) = \frac{\partial}{\partial z} g_2^{(m,k)}(z,x) \tag{7.323}$$

then we may write

$$e_j^{(m)}(z) = a\left(\boldsymbol{e}, \boldsymbol{g}_j(z,\cdot)\right) \quad j = 5,6. \tag{7.324}$$

Hence, in addition to (7.318) we also have

$$e_j^{(m)}(z) = a(\boldsymbol{e}, \boldsymbol{g}_j^{(m)}(z,\cdot) - \boldsymbol{v}), \quad j = 5,6. \tag{7.325}$$

As in the $j = 1 \ldots 4$ case, by letting $\boldsymbol{v}(x)$ be the interpolant to $\boldsymbol{g}_j^{(m,k)}(z,x)$ in the x variable, we arrive at the conclusion that $|e_5^{(m)}|$ and $|e_6^{(m)}|$ are order h^{2t} at the connecting nodes.

The analysis in the next section requires that, in the case of $t = 2$, the order of convergence of e_5 and e_6 is $O(h^4)$ at the mid-points as well as at the connecting nodes. To show this let us consider the mid-point of the m'th element mapped onto the interval $[-\frac{h}{2}, \frac{h}{2}]$. At the mid-point we have

$$e_j^{(m)}(0) = \sum_{k=1}^{nb} a(\boldsymbol{e}, \boldsymbol{g}_j^{(m,k)}(0,\cdot) - \boldsymbol{v}), \qquad j = 5, 6. \tag{7.326}$$

Let $\boldsymbol{v}$ be the linear interpolant to $B(\boldsymbol{g}_j^{(m,m)}(0,x))$ then

$$e_j^{(m)}(0) = \int_{\frac{h}{2}}^{\frac{h}{2}} \left(\boldsymbol{\phi}(x) - \Pi\boldsymbol{\phi}(x)\right)^T \boldsymbol{D}\boldsymbol{B}(\boldsymbol{e}(x))\Big) \, \mathrm{d}x + O(h^4) \tag{7.327}$$

where

$$\boldsymbol{\phi}(x) = \boldsymbol{B}(\boldsymbol{g}_j^{(m,m)}(0,x)) \tag{7.328}$$

and $\boldsymbol{\phi}(x)$ is the linear interpolant to $\boldsymbol{\phi}$. Now,

$$\begin{aligned} \boldsymbol{\phi}(x) - \Pi\boldsymbol{\phi}(x) &= \left(\boldsymbol{\phi}(x) - \boldsymbol{\phi}\left(-\frac{h}{2}\right)\right)\left(\frac{1}{2} - \frac{x}{h}\right) + \left(\boldsymbol{\phi}(x) - \boldsymbol{\phi}\left(\frac{h}{2}\right)\right)\left(\frac{1}{2} + \frac{x}{h}\right) \\ &= \begin{cases} -\left(\frac{1}{2} + \frac{x}{h}\right) J + O(h), & \frac{h}{2} \le x < 0 \\ \left(\frac{1}{2} - \frac{x}{h}\right) J + O(h), & 0 < x \le \frac{h}{2} \end{cases} \end{aligned} \tag{7.329}$$

where

$$\boldsymbol{J} = \boldsymbol{\phi}(0+) - \boldsymbol{\phi}(0-). \tag{7.330}$$

Hence

$$e_j(0) = \int_0^{\frac{h}{2}} \left[\left(\frac{1}{2} - \frac{x}{h}\right) \boldsymbol{J}^T + O(h)\right] \left[\boldsymbol{D}(x)\boldsymbol{B}(\boldsymbol{e}(x)) - \boldsymbol{D}(-x)\boldsymbol{B}(\boldsymbol{e}(-x))\right] \mathrm{d}x + O(h^4). \tag{7.331}$$

Since $\|\boldsymbol{e}\|$ is of order h^2 so is $\boldsymbol{B}(\boldsymbol{e}(x))$ therefore the $O(h)$ term may be taken outside the integral and included in the $O(h^4)$ term. Also

$$\boldsymbol{D}(x) = \boldsymbol{D}(0) + O(h) \tag{7.332}$$

and this $O(h)$ term may also be included in the $O(h^4)$ term. Hence we have

$$e_j(0) = \boldsymbol{J}^T \int_0^{\frac{h}{2}} \left(\frac{1}{2} - \frac{x}{h}\right) \boldsymbol{D}(0)\boldsymbol{B}(\boldsymbol{e}(x) - \boldsymbol{e}(-x)) \, \mathrm{d}x + O(h^4). \tag{7.333}$$

From the definition of g_j it follows that

$$D(0)J = \begin{pmatrix} 0 \\ -1 \\ 0 \\ 0 \end{pmatrix} \tag{7.334}$$

so that

$$e_j(0) = J^T \int_0^{\frac{h}{2}} \left(\frac{1}{2} - \frac{x}{h}\right) (e_j'(x) - e_j'(-x))\,\mathrm{d}x + O(h^4). \tag{7.335}$$

By considering interpolants to e_2 and e_3 we wish to replace the $e_j'(x) - e_j'(-x)$ term with an expression involving $e_j(0)$ and other terms of order no less than h^3. Note that the choice of interpolating polynomial is not necessarily the same as that used in calculating the finite element solution. Considering the Hermite cubic interpolant to $e_2(x)$ we may write

$$e_2(x) = e_2\left(-\frac{h}{2}\right) N_1(x) + e_2\left(\frac{h}{2}\right) N_2(x) + e_2'\left(-\frac{h}{2}\right) N_3(x) + e_2'\left(\frac{h}{2}\right) N_4(x) + f(x) + O(h^5) \tag{7.336}$$

where the basis functions are

$$\begin{aligned} N_1(x) &= 2\left(\tfrac{x}{h} - \tfrac{1}{2}\right)^2 \left(\tfrac{x}{h} + 1\right) & N_2(x) &= -2\left(\tfrac{x}{h} + \tfrac{1}{2}\right)^2 \left(\tfrac{x}{h} - 1\right) \\ N_3(x) &= h\left(\tfrac{x}{h} - \tfrac{1}{2}\right)^2 \left(\tfrac{x}{h} + \tfrac{1}{2}\right) & N_4(x) &= -h\left(\tfrac{x}{h} + \tfrac{1}{2}\right)^2 \left(\tfrac{x}{h} - \tfrac{1}{2}\right) \end{aligned} \tag{7.337}$$

and the first part of the remainder, $f(x)$, is

$$f(x) = \left(\frac{x^2}{h^2} - \frac{1}{4}\right)^2 \tag{7.338}$$

Since $e_2'(-\frac{h}{2})$ and $e_2(\frac{h}{2})$ are order h^4 the N_3 and N_4 terms may be included in the $O(h^5)$ term. Hence we may write

$$e_2(x) = e_2\left(-\frac{h}{2}\right) N_1(x) + e_2\left(\frac{h}{2}\right) N_2(x) + f(x) + O(h^5) \tag{7.339}$$

$$e_2'(x) = e_2\left(-\frac{h}{2}\right) N_1'(x) + e_2\left(\frac{h}{2}\right) N_2'(x) + f'(x) + O(h^4) \tag{7.340}$$

$$e_2''(x) = e_2\left(-\frac{h}{2}\right) N_1''(x) + e_2\left(\frac{h}{2}\right) N_2''(x) + f''(x) + O(h^3) \tag{7.341}$$

so that

$$e_2''(x) - e_2''(-x) = \frac{-24x}{h^3}\left(e_2(\tfrac{h}{2}) - e_2(-\tfrac{h}{2})\right) + f''(x) - f''(-x) + O(h^3) \tag{7.342}$$

$$e_2'(0) = \frac{3}{2h}\left(e_2(\tfrac{h}{2}) - e_2(-\tfrac{h}{2})\right) + f'(0) + O(h^4). \tag{7.343}$$

Combining (7.342) and (7.343) and observing the $f'(0) = 0$ and $f''(x) = f''(-x)$ we have

$$e_2''(x) - e_2''(-x) = \frac{-16x}{h^2} e_2'(0) + O(h^3). \tag{7.344}$$

The same result may be obtained for e_3 and so

$$e_j'(x) - e_j'(-x) = \frac{-16x}{h^2} e_j(0) + O(h^3), \qquad j = 5, 6. \tag{7.345}$$

Substituting this result into (7.335) we have

$$e_j(0) \left[1 - \frac{16}{h} \int_0^{\frac{h}{2}} \left(\frac{1}{2} - \frac{x}{h} \right) \frac{x}{h} \, \mathrm{d}x \right] = O(h^4) \tag{7.346}$$

or

$$\frac{2}{3} e_j(0) = O(h^4). \tag{7.347}$$

Hence we may conclude the mid-point error is also of order h^4.

7.4.5 Zero errors at connecting nodes

If the finite element space V is large enough to contain $g_j(z, \cdot)$, the error component e_j is zero at the connecting nodes. As an example consider the plane single beam problem where the differential operator $\boldsymbol{L}$ is given by

$$\boldsymbol{L}(u) = \begin{pmatrix} -u_1'' - \alpha u_2''' \\ \alpha u_1''' + u_2'''' \end{pmatrix} \tag{7.348}$$

where α is constant and

$$\begin{aligned} u_1(0) = u_2(0) = u_2'(0) &= 0 && (7.349) \\ u_1'(1) + \alpha u_2''(1) &= 0 && (7.350) \\ \alpha u_1'(1) + u_2''(1) &= 0 && (7.351) \\ \alpha u_1''(1) + u_2'''(1) &= 0. && (7.352) \end{aligned}$$

The vectors $\boldsymbol{g}_1 = (g_{11}, g_{12})$, $\boldsymbol{g}_2 = (g_{21}, g_{22})$ and $\boldsymbol{g}_5 = (g_{51}, g_{52})$ satisfy

$$\begin{aligned} -g_{11}''(z,x) - \alpha g_{12}'''(z,x) &= \delta(z,x) && (7.353) \\ \alpha g_{11}'''(z,x) + g_{12}''''(z,x) &= 0 && (7.354) \\ -g_{21}''(z,x) - \alpha g_{22}'''(z,x) &= 0 && (7.355) \\ \alpha g_{21}'''(z,x) + g_{22}''''(z,x) &= \delta(z,x) && (7.356) \\ g_{51}'(z,x) + \alpha g_{52}''(z,x) &= 0 && (7.357) \\ -\alpha g_{51}''(z,x) - g_{52}'''(z,x) &= \delta(z,x) && (7.358) \end{aligned}$$

where $'$ denotes differentiation with respect to x. After integrating and applying (7.350), (7.351) and (7.352) we may combine rows to give us

$$(1-\alpha^2)g'_{11}(z,x) = \text{piecewise constant} \tag{7.359}$$
$$(1-\alpha^2)g''_{12}(z,x) = \text{piecewise constant} \tag{7.360}$$
$$(1-\alpha^2)g'_{21}(z,x) = \text{piecewise linear} \tag{7.361}$$
$$(1-\alpha^2)g''_{22}(z,x) = \text{piecewise linear} \tag{7.362}$$
$$(1-\alpha^2)g'_{51}(z,x) = \text{piecewise constant} \tag{7.363}$$
$$(1-\alpha^2)g''_{52}(z,x) = \text{piecewise constant} \tag{7.364}$$

where the above are discontinuous at $x = z$. If z is a connecting node then, within an element,

$$g_{11} = \text{linear} \tag{7.365}$$
$$g_{12} = \text{quadratic} \tag{7.366}$$
$$g_{21} = \text{quadratic} \tag{7.367}$$
$$g_{22} = \text{cubic} \tag{7.368}$$
$$g_{51} = \text{linear} \tag{7.369}$$
$$g_{52} = \text{quadratic.} \tag{7.370}$$

V_1 and V_2 are minimally linear and cubic, respectively, and so g_1 and g_5 are represented exactly in V. Hence, by (7.318) and (7.325), e_1 and e'_2 are zero at connecting nodes. Furthermore, e_2 is zero at connecting nodes if V_1 is quadratic.

7.5 The *a posteriori* error estimator

7.5.1 The equations satisfied by the error

For the i'th element we have, after integrating (7.201) by parts twice,

$$a(u,v)_{\Omega_i} = (L(u),v)_{\Omega_i} + (Q,B(v))_{\Omega_i} + [P(u)^T\varepsilon(v)]_{x_{i-1}}^{x_i} \qquad \forall v \in H \tag{7.371}$$
$$a(u_h,v)_{\Omega_i} = (L(u_h),v)_{\Omega_i} + (Q,B(v))_{\Omega_i} + [P(u_h)^T\varepsilon(v)]_{x_{i-1}}^{x_i} \qquad \forall v \in H \tag{7.372}$$

where

$$\varepsilon(v)^T := (\, v_1 \quad v_2 \quad v_3 \quad v_4 \quad -v'_3 \quad v'_2 \,). \tag{7.373}$$

Subtracting (7.372) from (7.371) gives us

$$a(e,v)_{\Omega_i} = (r,v)_{\Omega_i} + [P(e)^T\varepsilon(v)]_{x_{i-1}}^{x_i} \qquad \forall v \in H \tag{7.374}$$

where r is the residual,

$$r := L(u) - L(u_h) = f - L(u_h). \tag{7.375}$$

Equation (7.374) gives us a means to calculate, or at least approximate, $\boldsymbol{e}$ since, with suitable choices of $\boldsymbol{v}$ and an approximation of $\boldsymbol{P}(\boldsymbol{e})$, the right hand side may be derived from $\boldsymbol{u}_h$. Furthermore, (7.374) provides a convenient way to evaluate $a(\boldsymbol{e},\boldsymbol{e})_i$. Things are simplified if we choose $\boldsymbol{v}$ such that $\boldsymbol{\varepsilon}(\boldsymbol{v})$ is zero at the connecting nodes. Let $\hat{H} = \hat{H}_1 \otimes \hat{H}_2 \otimes \hat{H}_3 \otimes \hat{H}_4 \subset H$ be the space containing all such functions. Then we have

$$a(\boldsymbol{e},\boldsymbol{v})_{\Omega_i} = (\boldsymbol{r},\boldsymbol{v})_{\Omega_i} \qquad \forall \boldsymbol{v} \in H. \tag{7.376}$$

We will use (7.376) to find an approximation to $\boldsymbol{e}$ in some subspace of $\hat{H}$. We shall denote the approximation by $\hat{\boldsymbol{e}}$. If $\boldsymbol{e}$ is superconvergent at the connecting nodes then restricting $\hat{\boldsymbol{e}}$ to the space $\hat{H}$ would appear justified. Our aim is to bound $\|\hat{\boldsymbol{e}}\|$ in terms of $\|\boldsymbol{e}\|$; i.e. show that the two are equivalent.

7.5.2 Some other finite element spaces

In our analysis we will use other finite subspaces of H which contain higher and possibly lower degree polynomials than V. Let us denote these subspaces by $\overline{V}$ and $\underline{V}$, respectively. The space $\underline{V}$ is the smallest finite element space for solving (7.194); i.e. $\underline{V}_1$ and $\underline{V}_4$ are piecewise linear with C^0 continuity at the connecting nodes and $\underline{V}_2$ and $\underline{V}_3$ are piecewise cubic with C^1 continuity at the connecting nodes. The space $\overline{V}$ contains the finite element solution, $\overline{\boldsymbol{u}}_h \in \overline{V}$, that satisfies

$$a(\overline{\boldsymbol{u}}_h,\boldsymbol{v}) = (\boldsymbol{f},\boldsymbol{\varepsilon}(\boldsymbol{v})) + (\boldsymbol{Q},\boldsymbol{B}(\boldsymbol{v})) \tag{7.377}$$

for all $\boldsymbol{v} \in \overline{V}$. Since $\overline{V}$ contains higher degree polynomials than V there exists a $\beta(h) \leq 1$ that tends to zero with h, such that

$$\|\boldsymbol{u} - \overline{\boldsymbol{u}}_h\| \leq \beta(h) \|\boldsymbol{u} - \boldsymbol{u}_h\| . \tag{7.378}$$

We shall be seeking approximations to $\boldsymbol{e}$ in the space $\overline{V} \cap \hat{H}$. Let us denote this space by

$$\hat{V} = \hat{V}_1 \otimes \hat{V}_2 \otimes \hat{V}_3 \otimes \hat{V}_4. \tag{7.379}$$

Any $\boldsymbol{v} \in \overline{V}$ may be written as the sum of a $\boldsymbol{v}_1 \in \underline{V}$ and a $\boldsymbol{v}_2 \in \hat{V}$ where $\boldsymbol{v}_1$ is the interpolant to $\boldsymbol{v}$ that satisfies

$$\boldsymbol{\varepsilon}(\boldsymbol{v} - \boldsymbol{v}_1) = \boldsymbol{0} \qquad \text{at connecting nodes} \tag{7.380}$$

and $\boldsymbol{v}_2$ is the interpolation error.

7.5.3 Strengthened Cauchy-Schwarz inequality

Let $\boldsymbol{v} \in \hat{V}$ and let $\boldsymbol{v}_p$ be the projection of $\boldsymbol{v}$ in $\underline{V}$ such that

$$a(\boldsymbol{v}_p,\boldsymbol{w}) = a(\boldsymbol{v},\boldsymbol{w}) \tag{7.381}$$

for any $w \in \underline{V}$. By the usual Cauchy-Schwarz inequality we have that

$$|a(v,w)| \leq \|v^p\| \|w\| \tag{7.382}$$

and so we may write

$$|a(v,w)| \leq \gamma(v) \|v\| \|w\| \tag{7.383}$$

where

$$\gamma(v) := \frac{\|v^p\|}{\|v\|}. \tag{7.384}$$

Hence we have the Strengthened Cauchy-Schwarz inequality that, for any $w \in \underline{V}$ and $v \in \hat{V}$,

$$a(w,v) \leq \gamma(h) \|w\| \|v\| \tag{7.385}$$

where

$$\gamma(h) := \sup \{\gamma(v)\} = \sup \left\{ \frac{\|v^p\|}{\|v\|} \right\}. \tag{7.386}$$

Within an element we can find a $v^p \in \underline{V}$ such that

$$a(w,v^p)_{\Omega_i} = a(w,v)_{\Omega_i} \tag{7.387}$$

for all $w \in \underline{V}$ although it is not unique. However, the norm $\|v^p\|_{\Omega_i}$ is defined so that over the i'th element we can say that

$$|a(u,v)_{\Omega_i}| \leq \gamma(h)_i \|u\|_{\Omega_i} \|v\|_{\Omega_i} \tag{7.388}$$

where

$$\gamma(h)_i = \sup \left\{ \frac{\|v^p\|_{\Omega_i}}{\|v\|_{\Omega_i}} \right\} \tag{7.389}$$

and

$$\gamma(v)_i = \frac{\|v^p\|_{\Omega_i}}{\|v\|_{\Omega_i}}. \tag{7.390}$$

Globally,

$$\begin{aligned}
a(w,v) &= \sum a(w,v)_{\Omega_i} && (7.391)\\
&\leq \sum \gamma(h)_i \|w\|_{\Omega_i} \|v\|_{\Omega_i} && (7.392)\\
&\leq \gamma(h)_{\max} \sum \|w\|_{\Omega_i} \|v\|_{\Omega_i} && (7.393)\\
&\leq \gamma(h)_{\max} \left(\sum \|w\|_{\Omega_i}^2 \right)^{\frac{1}{2}} \left(\sum \|v\|_{\Omega_i}^2 \right)^{\frac{1}{2}} && (7.394)\\
&= \gamma(h)_{\max} \|w\| \|v\|. && (7.395)
\end{aligned}$$

So (7.385) holds with

$$\gamma(h) = \max\{\gamma(h)_i\}. \tag{7.396}$$

In equation (7.389) $\gamma(h)_i$ is actually the square root of the largest eigenvalue of the matrix $\hat{K}^{-1}\hat{K}^p$ where, if $\{\hat{N}_j\}, j = 1 \ldots n$, is a basis for $\hat{V}$,

$$\hat{K}_{jk} = a(\hat{N}_j, \hat{N}_k)_{\Omega_i}, \tag{7.397}$$

$$\hat{K}^p_{jk} = a(\hat{N}^p_j, \hat{N}^p_k)_{\Omega_i}. \tag{7.398}$$

This is proven by writing any $v \in \hat{V}$ as

$$v = \sum_{j=1}^{n} c_j \hat{N}_j \tag{7.399}$$

and using the equivalent definition of $\gamma(h)_i$,

$$\gamma(h)_i = \sup_{\|v\|_{\Omega_i}=1} \|\hat{v}^p\|_{\Omega_i}. \tag{7.400}$$

The projection of $\hat{v}$ in $\underline{V}$ is

$$v^p = \sum_{j=1}^{n} c_j \hat{N}^p_j \tag{7.401}$$

so that

$$\|v^p\|^2_{\Omega_i} = \boldsymbol{c}^T \hat{\boldsymbol{K}}^p \boldsymbol{c}. \tag{7.402}$$

We wish to find the supremum of $\|v^p\|^2_{\Omega_i}$ subject to the constraint

$$\|v\|^2_{\Omega_i} = \boldsymbol{c}^T \hat{\boldsymbol{K}} \boldsymbol{c} = 1. \tag{7.403}$$

Hence we define the function $J(\boldsymbol{c}, \mu)$ as

$$J(\boldsymbol{c}, \mu) = \boldsymbol{c}^T \hat{\boldsymbol{K}}^p \boldsymbol{c} - \mu(\boldsymbol{c}^T \hat{\boldsymbol{K}} \boldsymbol{c} - 1) \tag{7.404}$$

where μ is a Lagrange Multiplier [12]. When J is maximized

$$\frac{\partial J}{\partial c_j} = 0 \tag{7.405}$$

for $j = 1 \ldots n$ which leads us to the equation

$$(\hat{\boldsymbol{K}}^p - \mu \hat{\boldsymbol{K}})\boldsymbol{c} = 0 \tag{7.406}$$

or

$$(\hat{\boldsymbol{K}}^{-1}\hat{\boldsymbol{K}}^p - \mu \boldsymbol{I})\boldsymbol{c} = 0. \tag{7.407}$$

Hence μ is one of n eigenvalues of $\hat{\boldsymbol{K}}^{-1}\hat{\boldsymbol{K}}^p$. If $\boldsymbol{c}$ is the corresponding eigenvector then

$$\mu = \frac{\boldsymbol{c}^T \hat{\boldsymbol{K}}^p \boldsymbol{c}}{\boldsymbol{c}^T \hat{\boldsymbol{K}} \boldsymbol{c}} = \frac{\|v^p\|^2_{\Omega_i}}{\|v\|^2_{\Omega_i}} = \gamma(v_i)^2. \tag{7.408}$$

Hence the supremum of $\gamma(v)^2_i$ is the largest value of μ so that

$$\gamma(h)^2_i = \max \mu. \qquad \square \tag{7.409}$$

7.5.4 An intermediate error estimator

In our analysis we will make use of the error estimator, $\overline{e} \in \overline{V}$, defined as

$$\overline{e} = \overline{u}_h - u_h. \tag{7.410}$$

The finite element solutions u_h and $\overline{u}_h$ satisfy

$$a(u_h, v) = (f, \varepsilon(v)) + (Q, B(v)) \tag{7.411}$$

$$a(\overline{u}_h, v) = (f, \varepsilon(v)) + (Q, B(v)) \tag{7.412}$$

for all $v \in V$. Hence

$$a(\overline{e}, v) = a(\overline{u}_h - u_h, v) = 0 \tag{7.413}$$

for all v in V. Furthermore, The true solution u and the finite element solution $\overline{u}_h$ satisfy

$$a(u, v) = (f, \varepsilon(v)) + (Q, B(v) \tag{7.414}$$

$$a(\overline{u}_h, v) = (f, \varepsilon(v)) + (Q, B(v) \tag{7.415}$$

for all $v \in \overline{V}$. Hence

$$a(e - \overline{e}, v) = a(u - \overline{u}_h, v) = 0 \tag{7.416}$$

for all v in $\overline{V}$. It follows from (7.416) that, since $\overline{e} \in \overline{V}$, $a(e, \overline{e}) = a(\overline{e}, \overline{e})$ so that

$$\|\overline{e}\| \leq \|e\| \tag{7.417}$$

and

$$\|e - \overline{e}\|^2 = a(e, e) - 2a(e, \overline{e}) + a(\overline{e}, \overline{e}) = \|e\|^2 - \|\overline{e}\|^2. \tag{7.418}$$

Using (7.378) and (7.417) this gives us

$$\left(1 - \beta(h)^2\right)^{\frac{1}{2}} \|e\| \leq \|\overline{e}\| \leq \|e\|. \tag{7.419}$$

Hence we have shown that $\|\overline{e}\|$ is equivalent to $\|e\|$.

7.5.5 Another intermediate error estimator

Since $\overline{e} \in \overline{V}$ we may write

$$\overline{e} = e_1 + e_2 \tag{7.420}$$

where $e_1 \in \underline{V}$ and $e_2 \in \hat{V}$. Having shown that $\|\overline{e}\|$ is equivalent to $\|e\|$ we will now show that $\|e_2\|$ is equivalent to $\|e\|$. Since $e_1 \in \underline{V}$ and $\underline{V} \subset V$ so that $e_1 \in V$, we may use (7.413) with $v = e_1$. This implies that

$$a(\overline{e}, \overline{e}) = a(\overline{e}, e_2) \tag{7.421}$$

$$a(e_1, e_2) = -a(e_1, e_1). \tag{7.422}$$

From (7.421) we have that

$$\|\overline{e}\| \leq \|e_2\| \tag{7.423}$$

and, from (7.422), we have

$$\|\overline{e}\|^2 = a(e_1 + e_2, e_1 + e_2) \tag{7.424}$$

$$= a(e_2, e_2) - a(e_1, e_1) \tag{7.425}$$

$$= \|e_2\|^2 - \|e_1\|^2. \tag{7.426}$$

Also, from (7.422), we have, using (7.385),

$$a(e_1, e_1) = |a(e_1, e_2)| \leq \gamma(h)\|e_1\|\|e_2\|. \tag{7.427}$$

Combining this with (7.426) we have

$$\|\overline{e}\| \geq \left(1 - \gamma(h)^2\right)^{\frac{1}{2}} \|e_2\|. \tag{7.428}$$

Combining (7.423) and (7.428) we have

$$\|\overline{e}\| \leq \|e_2\| \leq \left(1 - \gamma(h)^2\right)^{-\frac{1}{2}} \|\overline{e}\|. \tag{7.429}$$

Combining (7.429) with (7.419) gives us

$$\left(1 - \beta(h)^2\right)^{\frac{1}{2}} \|e\| \leq \|e_2\| \leq \left(1 - \gamma(h)^2\right)^{-\frac{1}{2}} \|e\|. \tag{7.430}$$

7.5.6 Our error estimator

Definition

So far we have only considered error estimators which, although computable, may not be calculated from the finite element solution, u_h, alone. We now define an estimator that depends only on the residual, r, which was defined in (7.375). Let $\hat{e} \in \hat{V}$ be an approximation to e such that it satisfies

$$a(\hat{e}, v)_{\Omega_i} = (r, v)_{\Omega_i} \tag{7.431}$$

for all $v \in \hat{V}$ and all i. Then, for the energy norm, we have

$$\|\hat{e}\|^2_{\Omega_i} = (r, \hat{e})_{\Omega_i}. \tag{7.432}$$

Implementation

We may calculate $\hat{e}$ within the element by expressing it as a linear combination of basis function vectors for $\hat{V}$. Hence it has the form

$$\hat{e} = \hat{N}E \tag{7.433}$$

where $\hat{N}$ is a matrix whose columns are the basis function vectors and E is a vector containing the degrees of freedom. Choosing v in (7.431) to be each basis function vector in turn will give us a linear system in E.

Before we can evaluate $\hat{e}$ we must choose vectors that span $\hat{V}$. The element basis functions for $\hat{V}_1$ and $\hat{V}_4$ must be of the form

$$x(x-h)f(x) \tag{7.434}$$

and those for $\hat{V}_2$ and $\hat{V}_3$ must be of the form

$$x^2(x-h)^2 f(x) \tag{7.435}$$

where $f(x)$ is an arbitrary function of x. It makes sense to choose $f(x)$ to be symmetric so let us take $f(x)$ to be

$$f(x) = 1, \;\; x - \frac{h}{2}, \;\; \left(x - \frac{h}{2}\right)^2, \ldots. \tag{7.436}$$

Where linear and cubic approximations have been used in V we may use quadratic and quartic functions for $\hat{V}$. Then, within the standard element $(0,h)$, $v \in \hat{V}$ may be written as

$$\begin{pmatrix} v_1 \\ v_2 \\ v_3 \\ v_4 \end{pmatrix} = \begin{pmatrix} \hat{N}_1 & 0 & 0 & 0 \\ 0 & \hat{N}_2 & 0 & 0 \\ 0 & 0 & \hat{N}_2 & 0 \\ 0 & 0 & 0 & \hat{N}_1 \end{pmatrix} \begin{pmatrix} V_1 \\ V_2 \\ V_3 \\ V_4 \end{pmatrix} = \hat{N}_1 V_1 + \hat{N}_2 V_2 + \hat{N}_3 V_3 + \hat{N}_4 V_4 \tag{7.437}$$

where

$$\hat{N}_1 = x(x-h), \tag{7.438}$$

$$\hat{N}_2 = x^2(x-h)^2. \tag{7.439}$$

Where quadratic and cubic functions have been used in V we may use cubic and quartic functions for $\hat{V}$. Then, within the standard element $(0,h)$, $v \in \hat{V}$ may be written as

$$v = \begin{pmatrix} \hat{N}_1 & 0 & 0 & 0 & \hat{N}_3 & 0 \\ 0 & \hat{N}_2 & 0 & 0 & 0 & 0 \\ 0 & 0 & \hat{N}_2 & 0 & 0 & 0 \\ 0 & 0 & 0 & \hat{N}_1 & 0 & \hat{N}_3 \end{pmatrix} \begin{pmatrix} V_1 \\ V_2 \\ \vdots \\ V_6 \end{pmatrix} \tag{7.440}$$

where

$$\hat{N}_1(x) = x(x-h), \tag{7.441}$$
$$\hat{N}_2(x) = x^2(x-h)^2, \tag{7.442}$$
$$\hat{N}_3(x) = x(x-h)\left(x-\frac{h}{2}\right). \tag{7.443}$$

Where quadratic and quartic functions have been used in V we may use cubic and quintic functions for $\hat{V}$. Then, within the standard element $(0,h)$, $v \in \hat{V}$ may be written as

$$v = \begin{pmatrix} \hat{N}_1 & 0 & 0 & 0 & \hat{N}_3 & 0 & 0 & 0 \\ 0 & \hat{N}_2 & 0 & 0 & 0 & \hat{N}_4 & 0 & 0 \\ 0 & 0 & \hat{N}_2 & 0 & 0 & 0 & \hat{N}_4 & 0 \\ 0 & 0 & 0 & \hat{N}_1 & 0 & 0 & 0 & \hat{N}_3 \end{pmatrix} \begin{pmatrix} V_1 \\ V_2 \\ \vdots \\ V_8 \end{pmatrix} \tag{7.444}$$

where

$$\hat{N}_1(x) = x(x-h), \tag{7.445}$$
$$\hat{N}_2(x) = x^2(x-h)^2, \tag{7.446}$$
$$\hat{N}_3(x) = x(x-h)\left(x-\frac{h}{2}\right), \tag{7.447}$$
$$\hat{N}_4(x) = x^2(x-h)^2\left(x-\frac{h}{2}\right). \tag{7.448}$$

Where quadratic and quintic functions have been used in V we may use cubic and sextic functions for $\hat{V}$ although quartic functions are used for $\hat{V}_1$ and $\hat{V}_4$ in the numerical examples. In this case, within the standard element $(0,h)$, $v \in \hat{V}$ may be written as

$$v = \begin{pmatrix} \hat{N}_1 & 0 & 0 & 0 & \hat{N}_3 & 0 & 0 & 0 & \hat{N}_5 & 0 & 0 & 0 \\ 0 & \hat{N}_2 & 0 & 0 & 0 & \hat{N}_4 & 0 & 0 & 0 & \hat{N}_6 & 0 & 0 \\ 0 & 0 & \hat{N}_2 & 0 & 0 & 0 & \hat{N}_4 & 0 & 0 & 0 & \hat{N}_6 & 0 \\ 0 & 0 & 0 & \hat{N}_1 & 0 & 0 & 0 & \hat{N}_3 & 0 & 0 & 0 & \hat{N}_5 \end{pmatrix} \begin{pmatrix} V_1 \\ V_2 \\ \vdots \\ V_{12} \end{pmatrix} \tag{7.449}$$

where

$$\hat{N}_1(x) = x(x-h), \tag{7.450}$$
$$\hat{N}_2(x) = x^2(x-h)^2, \tag{7.451}$$
$$\hat{N}_3(x) = x(x-h)\left(x-\frac{h}{2}\right), \tag{7.452}$$
$$\hat{N}_4(x) = x^2(x-h)^2\left(x-\frac{h}{2}\right), \tag{7.453}$$
$$\hat{N}_5(x) = x(x-h)\left(x-\frac{h}{2}\right)^2, \tag{7.454}$$
$$\hat{N}_6(x) = x^2(x-h)^2\left(x-\frac{h}{2}\right)^2. \tag{7.455}$$

Analysis

The error estimate, $\hat{e}$, is calculated on an element by element basis. Globally, because $\varepsilon(v)$ is zero at the nodes, $\hat{e}$ satisfies

$$a(\hat{e}, v) = (r, v) \tag{7.456}$$
$$\|\hat{e}\|^2 = (r, \hat{e}) \tag{7.457}$$

for all $v \in \hat{V}$. Subtracting (7.431) from (7.376) we have the orthogonality relation

$$a(e - \hat{e}, v)_{\Omega_i} = 0 \tag{7.458}$$

for all $v \in \hat{V}$. Hence we have

$$a(\hat{e}, \hat{e})_{\Omega_i} = a(e, \hat{e})_{\Omega_i} \leq \|e\|_{\Omega_i} \|\hat{e}\|_{\Omega_i} \tag{7.459}$$

so that

$$\|\hat{e}\|_{\Omega_i} \leq \|e\|_{\Omega_i} . \tag{7.460}$$

Hence $\|\hat{e}\|_{\Omega_i}$ is generally an underestimate for $\|e\|_{\Omega_i}$ and, globally, $\|\hat{e}\|$ is an underestimate for $\|e\|$. Now, from (7.458) we have that

$$a(\hat{e}, v) = \sum_{i=1}^{ne} a(\hat{e}, v)_{\Omega_i} = \sum_{i=1}^{ne} a(e, v)_{\Omega_i} = a(e, v) \tag{7.461}$$

for all $v \in \hat{V}$. From (7.413) we have that

$$a(e, v) = a(\overline{e}, v) \tag{7.462}$$

for all $v \in \overline{V}$. Combining the two results gives us

$$a(\hat{e}, v) = a(\overline{e}, v) \tag{7.463}$$

for all $v \in \hat{V}$. Since e_2 is in $\hat{V}$ we have

$$a(\hat{e}, e_2) = a(\overline{e}, e_2). \tag{7.464}$$

Also, since e_1 is in V,

$$\|\overline{e}\|^2 = a(\overline{e}, e_1) + a(\overline{e}, e_2) = a(\overline{e}, e_2) = a(\hat{e}, e_2). \tag{7.465}$$

Using the Cauchy-Schwarz inequality

$$\|\overline{e}\|^2 = a(\hat{e}, e_2) \leq \|\hat{e}\| \|e_2\|. \tag{7.466}$$

Substituting for $\|e_2\|$ using (7.428) and rearranging gives us

$$\left(1-\gamma(h)^2\right)^{\frac{1}{2}} \|\overline{e}\| \leq \|\hat{e}\|. \tag{7.467}$$

Combining (7.467) with (7.419) we have

$$\left(1-\beta(h)^2\right)^{\frac{1}{2}} \left(1-\gamma(h)^2\right)^{\frac{1}{2}} \|e\| \leq \|\hat{e}\| \leq \|e\|. \tag{7.468}$$

Hence $\|\hat{e}\|$ is equivalent to $\|e\|$. □

7.5.7 Consistency and asymptotic exactness

Conditions for asymptotic exactness

The usefulness of $\|\hat{e}\|$ as an approximation to $\|e\|$ depends on the effectivity index, Φ, which is defined as

$$\Phi = \frac{\|\hat{e}\|}{\|e\|}. \tag{7.469}$$

The estimator is said to be asymptotically exact if Φ tends to unity in the limit where h tends to zero [9]. Dividing (7.468) by $\|e\|$ we have

$$\left(1-\beta(h)^2\right)^{\frac{1}{2}} \left(1-\gamma(h)^2\right)^{\frac{1}{2}} \leq \Phi \leq 1. \tag{7.470}$$

Hence asymptotic exactness will be guaranteed if, in addition to $\beta(h)$, we can show that $\gamma(h)$ tends to zero with h.

The superconvergent case

Let us return to equation (7.426) which stated that

$$\|\overline{e}\|^2 = \|e_2\|^2 - \|e_1\|^2. \tag{7.471}$$

We may write $\|e_1\|^2$ as

$$a(e_1, e_1) = \zeta(h) \|e_1\| \|e_2\| \tag{7.472}$$

where

$$\zeta(h) = \frac{\|e_1\|}{\|e_2\|} \tag{7.473}$$

so that

$$\|\overline{e}\| = (1-\zeta(h)^2)^{\frac{1}{2}} \|e_2\|. \tag{7.474}$$

Hence, (7.468) becomes

$$\left(1-\beta(h)^2\right)^{\frac{1}{2}}\left(1-\zeta(h)^2\right)^{\frac{1}{2}}\|\boldsymbol{e}\| \leq \|\hat{\boldsymbol{e}}\| \leq \|\boldsymbol{e}\|. \tag{7.475}$$

Now $\boldsymbol{e}_1$ is defined solely by the values of $\overline{\boldsymbol{e}}$ at the connecting nodes (i.e. where $\boldsymbol{\varepsilon}(\boldsymbol{v}) = 0$ for $\boldsymbol{v} \in \hat{V}$). Hence $\boldsymbol{e}_1$ is order h^{2t} and the first and second derivatives, $\boldsymbol{e}_1'$ and $\boldsymbol{e}_1''$, are order h^{2t-1} and h^{2t-2}. From this fact alone $B(\boldsymbol{e}_1)$ is order h^{2t-2} and so is $\|\boldsymbol{e}_1\|$. Since $\|\boldsymbol{e}_2\|$ is order h^t it may be concluded that $\zeta(h)$ tends to zero as h tends to zero when $t > 2$. Furthermore, when $t = 2$ it has been shown that e_2' and e_3' are order h^4 at both the connecting nodes and the mid-points. It follows that $\overline{e}_2'$ and $\overline{e}_3'$ are also order h^4 at these points. Since $(e_1)_2$ and $(e_1)_3$ are Hermite cubic interpolants of $\overline{e}_2$ and $\overline{e}_3$, the derivatives $(e_1)_2'$ and $(e_1)_3'$ are quadratic interpolants of $\overline{e}_2'$ and $\overline{e}_3'$ at mid-points as well as at connecting nodes. Since $\overline{e}_2$ and $\overline{e}_3$ are order h^4 at these points, $(e_1)_2'$ and $(e_1)_3'$ are order h^4 everywhere and their derivatives are order h^3, the same as $(e_1)_1'$ and $(e_1)_4'$. This leads to the conclusion that $\boldsymbol{B}(\boldsymbol{e}_1)$ and $\|\boldsymbol{e}_1\|$ are order h^3 for $t = 2$. With $t = 2$, $\|\boldsymbol{e}_2\|$ is order h^2 and so $\zeta(h)$ tends to zero as h tends to zero. Hence, for finite element methods where $t \geq 2$, $\|\hat{\boldsymbol{e}}\|$ is asymptotically exact.

It is concluded that, for a general finite element frame, the error estimator is asymptotically exact whenever quadratic functions are used to represent the compression and twisting components of the beams. For special cases where e_1 and e_4 are zero, quartic functions would minimally be needed to represent the bending components to guarantee asymptotic exactness.

The non-superconvergent case

The error estimator $\hat{\boldsymbol{e}} = \hat{\boldsymbol{N}}\boldsymbol{E}$ is found in the i'th element by solving

$$\begin{pmatrix} a(\hat{\boldsymbol{N}}_1,\hat{\boldsymbol{N}}_1)_{\Omega_i} & a(\hat{\boldsymbol{N}}_2,\hat{\boldsymbol{N}}_1)_{\Omega_i} & a(\hat{\boldsymbol{N}}_3,\hat{\boldsymbol{N}}_1)_{\Omega_i} & a(\hat{\boldsymbol{N}}_4,\hat{\boldsymbol{N}}_1)_{\Omega_i} \\ a(\hat{\boldsymbol{N}}_1,\hat{\boldsymbol{N}}_2)_{\Omega_i} & a(\hat{\boldsymbol{N}}_2,\hat{\boldsymbol{N}}_2)_{\Omega_i} & a(\hat{\boldsymbol{N}}_3,\hat{\boldsymbol{N}}_2)_{\Omega_i} & a(\hat{\boldsymbol{N}}_4,\hat{\boldsymbol{N}}_2)_{\Omega_i} \\ a(\hat{\boldsymbol{N}}_1,\hat{\boldsymbol{N}}_3)_{\Omega_i} & a(\hat{\boldsymbol{N}}_2,\hat{\boldsymbol{N}}_3)_{\Omega_i} & a(\hat{\boldsymbol{N}}_3,\hat{\boldsymbol{N}}_3)_{\Omega_i} & a(\hat{\boldsymbol{N}}_4,\hat{\boldsymbol{N}}_3)_{\Omega_i} \\ a(\hat{\boldsymbol{N}}_1,\hat{\boldsymbol{N}}_4)_{\Omega_i} & a(\hat{\boldsymbol{N}}_2,\hat{\boldsymbol{N}}_4)_{\Omega_i} & a(\hat{\boldsymbol{N}}_3,\hat{\boldsymbol{N}}_4)_{\Omega_i} & a(\hat{\boldsymbol{N}}_4,\hat{\boldsymbol{N}}_4)_{\Omega_i} \end{pmatrix} \begin{pmatrix} E_1 \\ E_2 \\ E_3 \\ E_4 \end{pmatrix} = \begin{pmatrix} (r,\hat{\boldsymbol{N}}_1)_{\Omega_i} \\ (r,\hat{\boldsymbol{N}}_2)_{\Omega_i} \\ (r,\hat{\boldsymbol{N}}_3)_{\Omega_i} \\ (r,\hat{\boldsymbol{N}}_4)_{\Omega_i} \end{pmatrix}. \tag{7.476}$$

Obviously, from the definition of $\boldsymbol{D}$, we have that $a(\hat{\boldsymbol{N}}_j,\hat{\boldsymbol{N}}_4) = 0$ for $j \neq 4$ and, since $\boldsymbol{D}$ is symmetric,

$$a(\boldsymbol{N}_j,\boldsymbol{N}_k)_{\Omega_i} = a(\boldsymbol{N}_k,\boldsymbol{N}_j)_{\Omega_i} \tag{7.477}$$

for all j and k. Also we observe that $\hat{N}_2''$ is a Legendre polynomial so that

$$\int_0^h f(x)\hat{N}_2''dx = 0 \tag{7.478}$$

for any linear function $f(x)$. Hence, when $\boldsymbol{D}$ is constant over the element, $a(\hat{\boldsymbol{N}}_j, \hat{\boldsymbol{N}}_2)_{\Omega_i}$ and $a(\hat{\boldsymbol{N}}_j, \hat{\boldsymbol{N}}_3)_{\Omega_i}$ are zero for $j = 1$ and 4. Hence the vector $\boldsymbol{E}$ is found from

$$\begin{pmatrix} a(\hat{\boldsymbol{N}}_1, \hat{\boldsymbol{N}}_1)_{\Omega_i} & 0 \\ 0 & a(\hat{\boldsymbol{N}}_4, \hat{\boldsymbol{N}}_4)_{\Omega_i} \end{pmatrix} \begin{pmatrix} E_1 \\ E_4 \end{pmatrix} = \begin{pmatrix} (r, \hat{\boldsymbol{N}}_1)_{\Omega_i} \\ (r, \hat{\boldsymbol{N}}_4)_{\Omega_i} \end{pmatrix} \tag{7.479}$$

$$\begin{pmatrix} a(\hat{\boldsymbol{N}}_2, \hat{\boldsymbol{N}}_2)_{\Omega_i} & a(\hat{\boldsymbol{N}}_3, \hat{\boldsymbol{N}}_2)_{\Omega_i} \\ a(\hat{\boldsymbol{N}}_2, \hat{\boldsymbol{N}}_3)_{\Omega_i} & a(\hat{\boldsymbol{N}}_3, \hat{\boldsymbol{N}}_3)_{\Omega_i} \end{pmatrix} \begin{pmatrix} E_2 \\ E_3 \end{pmatrix} = \begin{pmatrix} (r, \hat{\boldsymbol{N}}_2)_{\Omega_i} \\ (r, \hat{\boldsymbol{N}}_3)_{\Omega_i} \end{pmatrix}. \tag{7.480}$$

Substituting $E_1, \ldots, E_4$ into equation (7.432) we evaluate

$$\begin{aligned} \|\hat{e}\|^2_{\Omega_i} &= (r, \hat{e})_{\Omega_i} \\ &= \frac{(r, \hat{\boldsymbol{N}}_1)^2_{\Omega_i}}{\|\hat{\boldsymbol{N}}_1\|^2_{\Omega_i}} + \frac{(r, \hat{\boldsymbol{N}}_4)^2_{\Omega_i}}{\|\hat{\boldsymbol{N}}_4\|^2_{\Omega_i}} \\ &+ \frac{(r, \hat{\boldsymbol{N}}_2)^2_{\Omega_i} \|\hat{\boldsymbol{N}}_3\|^2_{\Omega_i} + (r, \hat{\boldsymbol{N}}_3)^2_{\Omega_i} \|\hat{\boldsymbol{N}}_2\|^2_{\Omega_i}}{\|\hat{\boldsymbol{N}}_2\|^2_{\Omega_i} \|\hat{\boldsymbol{N}}_3\|^2_{\Omega_i} - a(\hat{\boldsymbol{N}}_2, \hat{\boldsymbol{N}}_3)^2_{\Omega_i}} \\ &- \frac{2(r, \hat{\boldsymbol{N}}_2)_{\Omega_i}(r, \hat{\boldsymbol{N}}_3)_{\Omega_i} a(\hat{\boldsymbol{N}}_2, \hat{\boldsymbol{N}}_3)_{\Omega_i}}{\|\hat{\boldsymbol{N}}_2\|^2_{\Omega_i} \|\hat{\boldsymbol{N}}_3\|^2_{\Omega_i} - a(\hat{\boldsymbol{N}}_2, \hat{\boldsymbol{N}}_3)^2_{\Omega_i}}. \end{aligned} \tag{7.481}$$

We will now work out the value of $\gamma(h)_i$ in order to determine whether or not we can expect the error estimator to be asymptotically exact. For $\boldsymbol{w} \in V$ and $\boldsymbol{y} \in \overline{V}$ we evaluate $a(\boldsymbol{w}, \boldsymbol{y})_{\Omega_i}$ over an element by writing

$$a(\boldsymbol{w}, \boldsymbol{y})_{\Omega_i} = \boldsymbol{W}^T \int_0^h \boldsymbol{A}(x)\, \mathrm{d}x\, \boldsymbol{Y} \tag{7.482}$$

where

$$\boldsymbol{A}(x) = \begin{pmatrix} N_1' D_{11} \hat{N}_1' & N_1' D_{12} \hat{N}_2'' & N_1' D_{13} \hat{N}_2'' & 0 \\ N_3'' D_{21} \hat{N}_1' & N_3'' D_{22} \hat{N}_2'' & N_3'' D_{23} \hat{N}_2'' & 0 \\ N_3'' D_{31} \hat{N}_1' & N_3'' D_{32} \hat{N}_2'' & N_3'' D_{33} \hat{N}_2'' & 0 \\ 0 & 0 & 0 & N_1' D_{44} \hat{N}_1' \\ N_5'' D_{31} \hat{N}_1' & N_5'' D_{32} \hat{N}_2'' & N_5'' D_{33} \hat{N}_2'' & 0 \\ N_5'' D_{21} \hat{N}_1' & N_5'' D_{22} \hat{N}_2'' & N_5'' D_{23} \hat{N}_2'' & 0 \\ N_2' D_{11} \hat{N}_1' & N_2' D_{12} \hat{N}_2'' & N_2' D_{13} \hat{N}_2'' & 0 \\ N_4'' D_{21} \hat{N}_1' & N_4'' D_{22} \hat{N}_2'' & N_4'' D_{23} \hat{N}_2'' & 0 \\ N_4'' D_{31} \hat{N}_1' & N_4'' D_{32} \hat{N}_2'' & N_4'' D_{33} \hat{N}_2'' & 0 \\ 0 & 0 & 0 & N_2' D_{44} \hat{N}_1' \\ N_6'' D_{31} \hat{N}_1' & N_6'' D_{32} \hat{N}_2'' & N_6'' D_{33} \hat{N}_2'' & 0 \\ N_6'' D_{21} \hat{N}_1' & N_6'' D_{22} \hat{N}_2'' & N_6'' D_{23} \hat{N}_2'' & 0 \end{pmatrix} \tag{7.483}$$

and $\boldsymbol{W}$ and $\boldsymbol{Y}$ are degree of freedom vectors. For the case where $\boldsymbol{D}$ is constant over

the element we may use (7.478) to give us

$$\int_0^h \boldsymbol{A}(x)\,\mathrm{d}x = \begin{pmatrix} 0 & 0 & 0 & 0 \\ 2D_{12} & 0 & 0 & 0 \\ 2D_{13} & 0 & 0 & 0 \\ 0 & 0 & 0 & 0 \\ hD_{31} & 0 & 0 & 0 \\ hD_{21} & 0 & 0 & 0 \\ 0 & 0 & 0 & 0 \\ -2D_{21} & 0 & 0 & 0 \\ -2D_{31} & 0 & 0 & 0 \\ 0 & 0 & 0 & 0 \\ hD_{31} & 0 & 0 & 0 \\ hD_{21} & 0 & 0 & 0 \end{pmatrix}. \tag{7.484}$$

For the case where $\boldsymbol{D}$ is diagonal, D_{21} and D_{31} are both zero so that $a(\boldsymbol{w},\boldsymbol{y})_i$ is always zero and $\gamma(h) = 0$. If $\boldsymbol{D}$ was a function of x then $\gamma(h)$ would tend to zero with h.

For the general case, where $\boldsymbol{D}$ is not diagonal, we need to use (7.386) to evaluate $\gamma(h)$. We see from (7.484) that

$$a(\boldsymbol{w},\boldsymbol{y})_{\Omega_i} = a(\boldsymbol{w},\hat{\boldsymbol{N}}_1 V_1)_{\Omega_i} \leq \gamma(\hat{\boldsymbol{N}}_1)_i \left\|\boldsymbol{w}\right\|_{\Omega_i} \left\|\hat{\boldsymbol{N}}_1 V_1\right\|_{\Omega_i} \tag{7.485}$$

so that $\gamma(h)_i = \gamma(\hat{\boldsymbol{N}}_1)_i$. We find that

$$\left\|(\hat{\boldsymbol{N}}_1)_p\right\|^2_{\Omega_i} = \frac{D_{13}^2 D_{22} - 2D_{12}D_{13}D_{23} + D_{12}^2 D_{33}}{(D_{22}D_{33} - D_{23}^2)} \frac{h^3}{3} \tag{7.486}$$

$$\left\|\hat{\boldsymbol{N}}_1\right\|^2_{\Omega_i} = \frac{D_{11}h^3}{3} \tag{7.487}$$

so that, for constant $\boldsymbol{D}$,

$$\gamma(h)_i^2 = \frac{\left\|(\hat{\boldsymbol{N}}_1)_p\right\|^2_{\Omega_i}}{\left\|\hat{\boldsymbol{N}}_1\right\|^2_{\Omega_i}} = \frac{D_{13}^2 D_{22} - 2D_{12}D_{13}D_{23} + D_{12}^2 D_{33}}{D_{11}(D_{22}D_{33} - D_{23}^2)} = \gamma_i^2. \tag{7.488}$$

When $\boldsymbol{D}$ is not constant $\gamma(h)_i$ tends to γ_i as h tends to zero. We conclude that, in the limit as h tends to zero,

$$\left(1 - \gamma_i^2\right)^{\frac{1}{2}} \leq \Phi \leq 1. \tag{7.489}$$

Since $\gamma(h)_i$ does not tend to zero we cannot say whether or not $\|\hat{\boldsymbol{e}}\|$ is asymptotically exact. The numerical examples in the next section show that it is not.

7.6 Numerical examples

7.6.1 The case of a single beam

Using linear and cubic approximations

A beam of unit length having the material matrix

$$D = \begin{pmatrix} 1 & 0 & \alpha & 0 \\ 0 & 1 & 0 & 0 \\ \alpha & 0 & 1 & 0 \\ 0 & 0 & 0 & 1 \end{pmatrix} \tag{7.490}$$

where $-1 < \alpha < 1$ experiences a load of

$$f = \begin{pmatrix} 0 \\ 0 \\ f(x) \end{pmatrix}. \tag{7.491}$$

This is a 2D problem in the unknown displacements u_1 and u_3 which must satisfy

$$\frac{\mathrm{d}F_1}{\mathrm{d}x} = 0 \tag{7.492}$$

$$-\frac{\mathrm{d}^2 M_2}{\mathrm{d}x^2} = f \tag{7.493}$$

where

$$F_1 = \frac{\mathrm{d}u_1}{\mathrm{d}x} + \alpha \frac{\mathrm{d}^2 u_3}{\mathrm{d}x^2} \tag{7.494}$$

$$M_2 = -\alpha \frac{\mathrm{d}u_1}{\mathrm{d}x} - \frac{\mathrm{d}^2 u_3}{\mathrm{d}x^2} \tag{7.495}$$

The beam is rigidly fixed at $x = 0$ and free from restraint at $x = 1$ so that the boundary conditions are

$$u_1(0) = u_3(0) = u_3'(0) = 0 \tag{7.496}$$

$$F_1(1) = M_2(1) = M_2'(1) = 0. \tag{7.497}$$

We will consider two cases; $f = -1$ and $f = -x$. The first step to finding the solution to this problem is to integrate (7.492) and (7.493) and apply (7.497) to give, for $f = -1$,

$$F_1 = 0 \tag{7.498}$$

$$M_2 = \frac{1}{2}(x-1)^2 \tag{7.499}$$

and, for $f = -x$,

$$F_1 = 0 \tag{7.500}$$

$$M_2 = \frac{1}{6}(x-1)^2(x+2). \tag{7.501}$$

The displacements u_1 and u_3 are then found, for $f = -1$, by solving

$$\frac{\mathrm{d}u_1}{\mathrm{d}x} + \alpha\frac{\mathrm{d}^2u_3}{\mathrm{d}x^2} = 0 \tag{7.502}$$

$$-\alpha\frac{\mathrm{d}u_1}{\mathrm{d}x} - \frac{\mathrm{d}^2u_3}{\mathrm{d}x^2} = \frac{1}{2}(x-1)^2. \tag{7.503}$$

and applying (7.496). This gives us

$$u_1 = \frac{\alpha}{6(1-\alpha^2)}x(x^2-3x+3) \tag{7.504}$$

$$u_3 = \frac{-1}{24(1-\alpha^2)}x^2(x^2-4x+6). \tag{7.505}$$

Similarly, for $f = -x$, the displacements are found by solving

$$\frac{\mathrm{d}u_1}{\mathrm{d}x} + \alpha\frac{\mathrm{d}^2u_3}{\mathrm{d}x^2} = 0 \tag{7.506}$$

$$-\alpha\frac{\mathrm{d}u_1}{\mathrm{d}x} - \frac{\mathrm{d}^2u_3}{\mathrm{d}x^2} = \frac{1}{6}(x-1)^2(x+2) \tag{7.507}$$

and applying (7.496) which gives us

$$u_1 = \frac{\alpha}{24(1-\alpha^2)}x(x^3-6x+8) \tag{7.508}$$

$$u_3 = \frac{-1}{120(1-\alpha^2)}x^2(x^3-10x+20). \tag{7.509}$$

Since this is a plane problem with $u_2 = u_4 = 0$ the residual components r_2 and r_4 will be zero. Hence, from (7.481), we have

$$\|\hat{e}\|^2_{\Omega_i} = \frac{(r,\hat{N}_1)^2_{\Omega_i}}{\|\hat{N}_1\|^2_{\Omega_i}} + \frac{(r,\hat{N}_3)^2_{\Omega_i}}{\|\hat{N}_3\|^2_{\Omega_i}}. \tag{7.510}$$

Since $\boldsymbol{D}$ is the same for every element we have, from (7.488), that

$$\gamma(h)^2 = \gamma_i^2 = \alpha^2. \tag{7.511}$$

Table 7.1 shows values of $\|\hat{e}\|^2$, $\|e\|^2$ and Φ^2 using n elements for $\alpha = 0.5$. They show that Φ^2 tends to $1 - \gamma(h)^2$ which is the lower bound in (7.470). When the load is

Table 7.1: Results with a consistent error estimator

$f = -1$			
n	$\|\hat{e}\|^2$	$\|e\|^2$	Φ^2
1	6.59722E-3	8.79630E-3	0.75000
2	1.71441E-3	2.28588E-3	0.75000
4	4.32671E-4	5.76895E-4	0.75000
8	1.08422E-4	1.44563E-4	0.75000
16	2.71214E-5	3.61619E-5	0.75000
32	6.78135E-6	9.04180E-6	0.75000

$f = -x$			
n	$\|\hat{e}\|^2$	$\|e\|^2$	Φ^2
1	1.89931E-3	3.87897E-3	0.74744
2	6.97354E-4	9.35898E-4	0.74512
4	1.73723E-4	2.32089E-4	0.74852
8	4.34084E-5	5.79081E-5	0.74961
16	1.08510E-5	1.44699E-5	0.74990
32	2.71269E-6	3.61705E-6	0.74997

constant Φ^2 is always $1 - \gamma(h)^2$. This can be explained by observing that, from the differential equations,

$$e_1''(x) = \frac{\alpha}{1-\alpha^2}(x - c_1) \tag{7.512}$$

$$e_3''''(x) = \frac{-1}{1-\alpha^2} \tag{7.513}$$

where c_1 is a constant, independent of the finite element solution. We may integrate these expressions and use the fact that e_1 and e_3' are zero at the nodes to write the local expressions

$$e_1' = \frac{\alpha}{1-\alpha^2}\left[\frac{1}{6}(3x^2 - h^2) - \frac{c_1}{2}(2x - h)\right] \tag{7.514}$$

$$e_3'' = \frac{-1}{1-\alpha^2}\left[\frac{1}{6}(3x^2 - h^2) - \frac{c_2}{2}(2x - h)\right] \tag{7.515}$$

where c_2 is a constant that depends on the finite element solution. This constant is found, using the orthogonality relation $a(e, v) = 0$ for any $v \in V$, to be $\frac{h}{2}$. Hence we may evaluate

$$\|e\|_{\Omega_i}^2 = \frac{1}{1-\alpha^2}\left[\frac{h^5}{720} + \frac{\alpha^2 h^3 (h - 2c_1)^2}{48(1-\alpha^2)}\right]. \tag{7.516}$$

Using (7.510) we have

$$\|\hat{e}\|^2_{\Omega_i} = \frac{h^5}{720} + \frac{\alpha^2 h^3 (h - 2c_1)^2}{48(1-\alpha^2)}. \tag{7.517}$$

Hence the result

$$\|\hat{e}\|^2_{\Omega_i} = (1-\alpha^2)\,\|e\|^2_{\Omega_i}\,. \tag{7.518}$$

Using quadratic and quintic approximations

A beam of unit length has the material matrix

$$\boldsymbol{D} = (1+x)\begin{pmatrix} 1 & 0 & \frac{1}{2} & 0 \\ 0 & 1 & 0 & 0 \\ \frac{1}{2} & 0 & 1 & 0 \\ 0 & 0 & 0 & 1 \end{pmatrix}. \tag{7.519}$$

It is subjected to a load of $f = -1$ and the same restraint as that in the previous example so that the displacement components u_1 and u_3 are found by solving

$$\frac{\mathrm{d}u_1}{\mathrm{d}x} + \frac{1}{2}\frac{\mathrm{d}^2 u_3}{\mathrm{d}x^2} = 0 \tag{7.520}$$

$$-\frac{1}{2}\frac{\mathrm{d}u_1}{\mathrm{d}x} - \frac{\mathrm{d}^2 u_3}{\mathrm{d}x^2} = \frac{(x-1)^2}{2(x+1)}. \tag{7.521}$$

This has the solution

$$u_1 = \frac{x}{6}(x-6) + \frac{4}{3} ln(1+x) \tag{7.522}$$

$$u_3 = -\frac{x}{9}(x^2 - 9x - 24) - \frac{8}{3}(1+x) ln(1+x). \tag{7.523}$$

The finite element solution and the error estimator were calculated using the spaces V and $\hat{V}$ defined earlier in this example. Table 7.2 shows the values of $\|\hat{e}\|^2$, $\|e\|^2$ and Φ^2 for n elements. They confirm the asymptotic exactness of $\|\hat{e}\|$.

7.6.2 Frame examples

A plane frame

The three beams forming the frame in Figure 7.7 each have the non-diagonal beam material matrix

$$\boldsymbol{D} = (x^2 - 2x + 2)\begin{pmatrix} 2 & 1 & 0 & 0 \\ 1 & 2 & 0 & 0 \\ 0 & 0 & 1 & 0 \\ 0 & 0 & 0 & 1 \end{pmatrix} \tag{7.524}$$

Table 7.2: Results with an asymptotically exact error estimator

n	$\|\hat{e}\|^2$	$\|e\|^2$	Φ^2
1	1.11135E-3	1.12237E-3	0.99018
2	9.38276E-5	9.40836E-5	0.99728
4	6.51257E-6	6.51722E-6	0.99929
8	4.19440E-7	4.19516E-7	0.99982
16	2.64211E-8	2.64223E-8	0.99995
32	1.65459E-9	1.65461E-9	0.99999

Table 7.3: Results with a consistent error estimator

n	$\|\hat{e}\|$	$\|e\|$	Φ
1	5.877E-3	6.565E-3	0.895126
2	2.835E-3	3.289E-3	0.862177
4	1.468E-3	1.699E-3	0.863803
8	7.444E-4	8.602E-4	0.865386
16	3.737E-4	4.315E-4	0.865860
32	1.870E-4	2.160E-4	0.865984

and are loaded such that the solutions are

$$u_1^{(k)} = 10^{-3}\exp\left(k(x-1)\right) + \text{a linear function} \tag{7.525}$$
$$u_2^{(k)} = 10^{-3}\exp\left(-k(x-1)\right) + \text{a cubic function.} \tag{7.526}$$

The three linear and cubic functions (18 parameters in total) are determined by the clamping assumptions at the base nodes (three conditions at each), the continuity conditions at the joints (three conditions at each) and the equilibrium conditions at the joints (three conditions at each). These are found by setting up and solving a linear system on a computer.

Table 7.3 shows the calculated values of $\|e\|$, $\|\hat{e}\|$ and the effectivity index, Φ, where linear and cubic approximations are used to calculate the finite element solution and quadratic and quartic functions are used to estimate the error using n elements per beam. The results confirm that the error estimator is consistent with an effectivity index of about 0.8659. This is in agreement with (7.489) since $\gamma_i^2 = 0.25$ giving $\Phi \in [\sqrt{0.75}, 1]$.

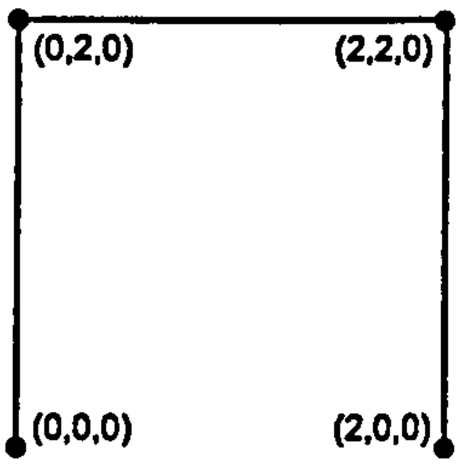

Figure 7.7: A plane frame.

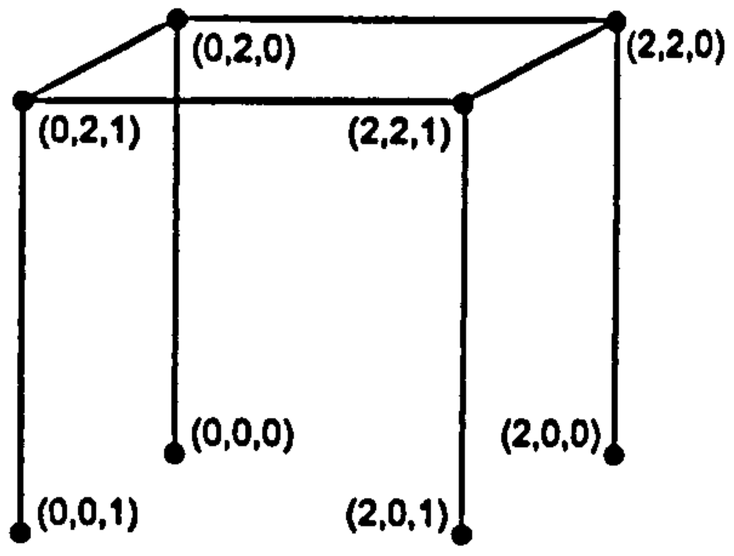

Figure 7.8: A 3D frame.

A 3D frame

The eight beams forming the frame in Figure 7.8 each have the non-diagonal material matrix

$$\boldsymbol{D} = (x^2 - 2x + 2)\begin{pmatrix} 4 & 1 & 4 & 0 \\ 1 & 4 & 1 & 0 \\ 1 & 1 & 4 & 0 \\ 0 & 0 & 0 & 4 \end{pmatrix} \tag{7.527}$$

and are loaded such that the solutions are

$$u_1^{(k)} = 10^{-3}\exp\left(\frac{k}{2}(x-1)\right) + \text{a linear function} \tag{7.528}$$

$$u_2^{(k)} = 10^{-3}\exp\left(-\frac{k}{2}(x-1)\right) + \text{a cubic function} \tag{7.529}$$

$$u_3^{(k)} = 10^{-3}\exp(x-1) + \text{a cubic function} \tag{7.530}$$

$$u_4^{(k)} = 10^{-3}(x-1)^5 + \text{a linear function.} \tag{7.531}$$

The $8 \times 12 = 96$ parameters associated with these linear and cubic approximations are obtained by setting up and solving a system on a computer as in the previous example.

Table 7.4 shows the calculated values of $\|\boldsymbol{e}\|$, $\|\hat{\boldsymbol{e}}\|$ and the effectivity index, Φ, where linear and cubic functions are used to calculate the finite element solution and quadratic and quartic functions are used to estimate the error using n elements per beam. The results confirm that the error estimator is consistent with an effectivity index of about 0.98. This is in agreement with (7.489) since $\gamma_i^2 = 0.1$ giving $\Phi \in [\sqrt{0.9}, 1]$.

Table 7.5 shows the calculated values where quadratic and cubic functions are used to calculate the finite element solution and cubic and quartic functions are used to estimate the error using n elements per beam. The results confirm that the error estimator is asymptotically exact.

Table 7.4: Results with a consistent error estimator

n	$\|\hat{e}\|$	$\|e\|$	Φ
1	5.614E-2	6.290E-2	0.892627
2	3.022E-2	3.279E-2	0.921838
4	1.766E-2	1.838E-2	0.960643
8	9.503E-3	9.722E-3	0.977422
16	4.849E-3	4.939E-3	0.981886
32	2.437E-3	2.479E-3	0.983014

Table 7.5: Results with an asymptotically exact error estimator

n	$\|\hat{e}\|$	$\|e\|$	Φ
1	5.444E-2	5.672E-2	0.959807
2	2.053E-2	2.099E-2	0.978454
4	6.391E-3	6.427E-3	0.994371
8	1.702E-3	1.704E-3	0.998578
16	4.324E-4	4.326E-4	0.999644
32	1.085E-4	1.086E-4	0.999911

Chapter 8

Theory of Plasticity

8.1 Introduction

It was mentioned in Chapter 6 that, as the temperature rises, the resistance of a structure to deformation decreases. In these circumstances the stresses within the structure are more likely to exceed levels within the applicability of the elastic theory described so far. The theory of plasticity, introduced in this chapter, models structural behaviour past the elastic state. The finite element method, described in Chapter 7, is extended to include the plastic response. This chapter completes the theoretical background for solving small-strain, fire-exposed, frame problems.

In a uniaxial tension experiment a material will obey Hooke's law until the stress reaches a critical value. At this point the relationship between stress and strain is no longer linear. The material is said to have yielded. The critical stress value at which yielding occurs is known as the yield stress. Eventually, with increasing strain, the stress reaches a constant value. At this point the material cannot resist any further loading. If the load is maintained the material will continue to deform and never reach equilibrium (until it breaks). This is the plastic state. If the material is unloaded at any time then the stress decreases linearly with decreasing strain. Upon reloading the stress again increases linearly until it reaches the yield value. This may be a higher (or lower) value than before in which case the material has experienced some form of hardening (or softening). The plastic theory presented here is based on Chapter 7 of Hinton and Owen [26] and Hsu [15].

Once a material has yielded its stress state is modelled incrementally; i.e. the increment in stress is a function of the increment in strain. It is assumed that an increment in strain, $d\epsilon$, can be written as the sum of an elastic part, $\mathrm{d}\epsilon_e$, and a plastic part, $\mathrm{d}\epsilon_p$; i.e.

$$\mathrm{d}\epsilon = \mathrm{d}\epsilon_e + \mathrm{d}\epsilon_p. \tag{8.1}$$

The yield criterion for the uniaxial case can be written as

$$\sigma - \sigma_y(\epsilon_p) = 0, \tag{8.2}$$

where σ_y is the yield stress which we have assumed to be a function of the plastic strain, ϵ_p. The increase in σ_y due to ϵ_p is termed as strain hardening. Alternatively, we could assume that σ_y is a function of the work done to plastically deform the material. In this case the increase in σ_y is termed as work hardening. We will use the strain-hardening hypothesis for now and use the work-hardening hypothesis in the next section when we consider the multi-axial stress state.

Under the strain-hardening hypothesis the yield function, Y, is defined as

$$Y(\sigma, \epsilon_p) = \sigma - \sigma_y(\epsilon_p). \tag{8.3}$$

It is negative whenever the material is in an elastic state and zero when the material has yielded. It can never be positive since the stress cannot exceed the yield stress. If the material has yielded then any further increase in strain can only cause a stress increment such that the yield criterion holds; i.e.

$$dY(\mathrm{d}\sigma, \mathrm{d}\epsilon_p) = 0. \tag{8.4}$$

The elastic strain increment, $d\epsilon_e$, is defined as that required to give the equivalent stress if the material was still in a linear elastic state, i.e.

$$\frac{\mathrm{d}\sigma}{\mathrm{d}\epsilon_e} = E. \tag{8.5}$$

Hence, by the chain rule,

$$\mathrm{d}Y = \frac{\partial Y}{\partial \sigma}\mathrm{d}\sigma + \frac{\partial Y}{\partial \epsilon_p}\mathrm{d}\epsilon_p \tag{8.6}$$

$$= \mathrm{d}\sigma - \frac{\mathrm{d}\sigma_y}{\mathrm{d}\epsilon_p}\mathrm{d}\epsilon_p \tag{8.7}$$

$$= E\mathrm{d}\epsilon_e - H\mathrm{d}\epsilon_p \tag{8.8}$$

where we define the hardening value of the material, H, to be

$$H := \frac{\mathrm{d}\sigma_y}{\mathrm{d}\epsilon_p}. \tag{8.9}$$

For the yield criterion to hold,

$$H\mathrm{d}\epsilon_p = E\mathrm{d}\epsilon_e = E(\mathrm{d}\epsilon - \mathrm{d}\epsilon_p) \tag{8.10}$$

and we have that

$$\mathrm{d}\epsilon_p = \frac{E}{E+H}\mathrm{d}\epsilon. \tag{8.11}$$

The incremental stress-strain relationship is thus given by

$$\mathrm{d}\epsilon = \mathrm{d}\epsilon_e + \mathrm{d}\epsilon_p \tag{8.12}$$

$$= \frac{d\sigma}{E} + \frac{E}{E+H}\mathrm{d}\epsilon. \tag{8.13}$$

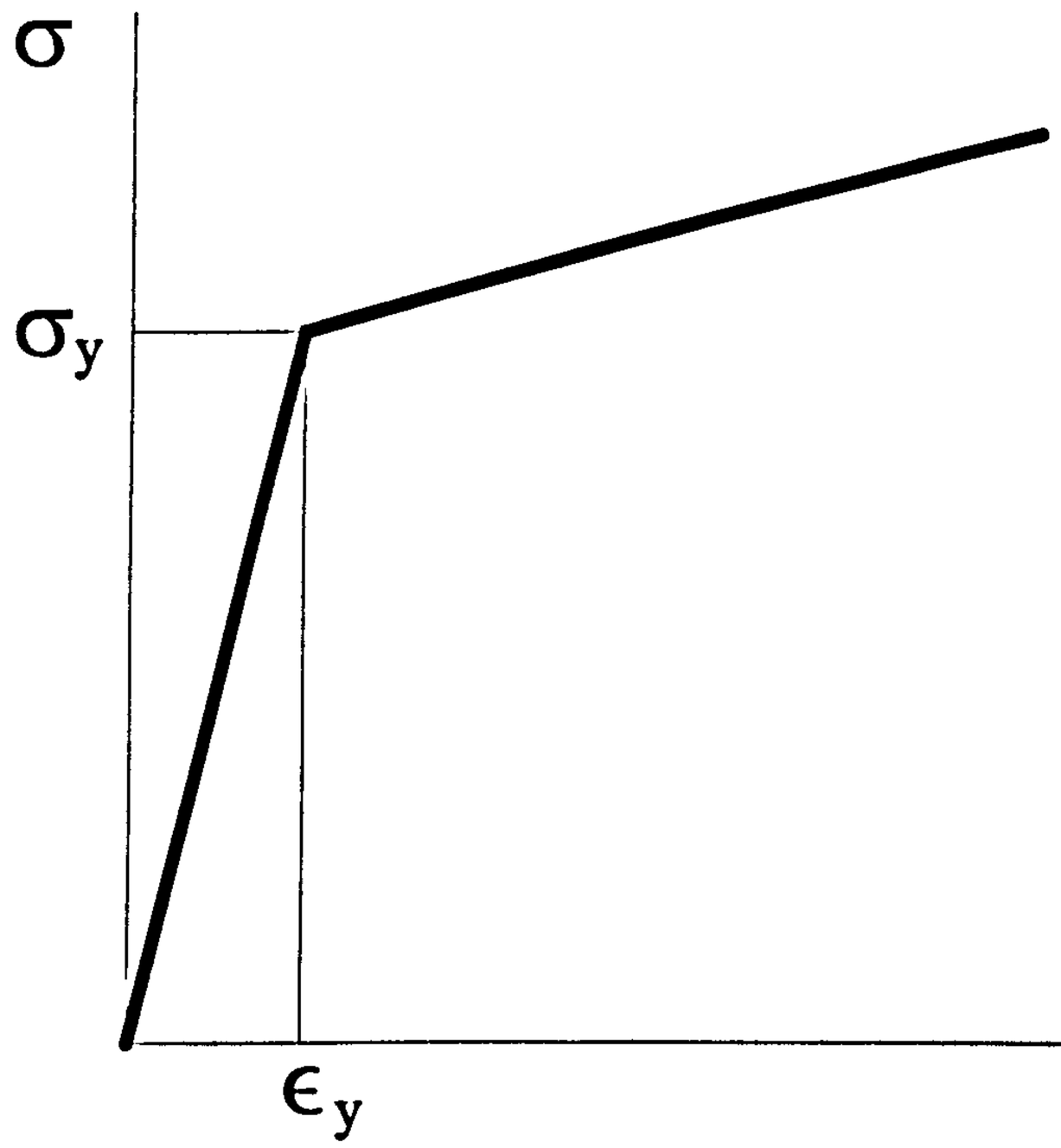

Figure 8.1: Stress-strain curve with strain (or work) hardening.

Re-arranging we have

$$\mathrm{d}\sigma = E\left(1 - \frac{E}{E+H}\right)\mathrm{d}\epsilon. \tag{8.14}$$

As an example, consider an isothermal beam of uniform cross-section subjected to a tensile force P at $x = 1$ while being restrained at $x = 0$. The stress-strain curve is illustrated in Figure 8.1. It is linear elastic until the yield stress, σ_y, is reached. The load may be thought of as being applied in two stages: pre-yield (elastic) and post-yield. During the elastic stage we have

$$F(u) = A\sigma(u) = EA\frac{\mathrm{d}u}{\mathrm{d}x} = P. \tag{8.15}$$

The force required to cause the beam to yield, P_y, is found from

$$P_y = A\sigma_y \tag{8.16}$$

so that, at the yield point,

$$\frac{\mathrm{d}u}{\mathrm{d}x} = \frac{\sigma_y}{E}, \tag{8.17}$$

$$u(x) = x\frac{\sigma_y}{E} \tag{8.18}$$

where A is the cross-sectional area and σ_y is the yield stress of the material. During

the post-yield stage the increment obeys

$$\Delta F = EA\left(1 - \frac{E}{E+H}\right)\frac{d(\Delta u)}{dx} = P - P_y. \tag{8.19}$$

This implies that

$$\frac{\mathrm{d}(\Delta u)}{\mathrm{d}x} = \frac{P - P_y}{EA}\left(1 - \frac{E}{E+H}\right)^{-1} \tag{8.20}$$

$$\Delta u = x\frac{P - P_y}{EA}\left(1 - \frac{E}{E+H}\right)^{-1}. \tag{8.21}$$

The final displacement is found by adding Δu to u_y to give

$$u(x) = x\left[\frac{\sigma_y}{E} + \frac{P - P_y}{EA}\left(1 - \frac{E}{E+H}\right)^{-1}\right]. \tag{8.22}$$

Experimental data provide us with the relationship between stress and total strain. The value of H is derived from this using (8.9) and (8.11); i.e.

$$H = \frac{\mathrm{d}\sigma_y}{\mathrm{d}\epsilon_p} \tag{8.23}$$

$$= \frac{\mathrm{d}\sigma_y}{\mathrm{d}\epsilon}\frac{\mathrm{d}\epsilon}{\mathrm{d}\epsilon_p} \tag{8.24}$$

$$= \left(1 + \frac{H}{E}\right)\frac{\mathrm{d}\sigma_y}{\mathrm{d}\epsilon}. \tag{8.25}$$

Re-arranging we have

$$H = \frac{E\dfrac{\mathrm{d}\sigma_y}{\mathrm{d}\epsilon}}{E - \dfrac{\mathrm{d}\sigma_y}{\mathrm{d}\epsilon}}. \tag{8.26}$$

8.2 General theory

When there is more than one stress under consideration the yield state of the material depends on some function of the stress components. We now employ the work-hardening hypothesis so that the yield stress depends on the plastic work which we denote by κ. It is defined incrementally as

$$\mathrm{d}\kappa := \boldsymbol{\sigma}^T \mathrm{d}\boldsymbol{\epsilon}_p, \tag{8.27}$$

where $\boldsymbol{\sigma}$ is a column vector containing the stress components. The yield function takes the form

$$Y = \bar{\sigma}(\boldsymbol{\sigma}) - \sigma_y(\kappa), \tag{8.28}$$

where $\bar{\sigma}$, known as the effective stress, depends on the particular material model. For metals it is defined to be consistent with the case of uniaxial tension. When a material is in a plastic state an increment in stress produces an increment in the plastic strain which is defined in terms of a plastic potential, ψ. The relation between $d\epsilon_p$ and ψ is the flow rule

$$\mathrm{d}\epsilon_p = \mathrm{d}\lambda \frac{\partial \psi}{\partial \boldsymbol{\sigma}}, \tag{8.29}$$

where $\mathrm{d}\lambda$ is a constant of proportionality to be determined. The Associated Theory of Plasticity states that the plastic potential is the yield function, i.e. $\psi = Y$, so that the flow rule is

$$\mathrm{d}\epsilon_p = \mathrm{d}\lambda \frac{\partial Y}{\partial \boldsymbol{\sigma}}. \tag{8.30}$$

The flow vector, $\boldsymbol{a}$, is defined as

$$\boldsymbol{a} := \frac{\partial Y}{\partial \boldsymbol{\sigma}} \tag{8.31}$$

so that the flow rule is simply

$$\mathrm{d}\epsilon_p = \mathrm{d}\lambda \boldsymbol{a}. \tag{8.32}$$

When the material is in a yielded state any increase in $\boldsymbol{\sigma}$ or κ must cause a zero increment in Y. For the increment in Y we have, from the chain rule,

$$\mathrm{d}Y = \left(\frac{\partial Y}{\partial \boldsymbol{\sigma}}\right)^T \mathrm{d}\boldsymbol{\sigma} + \frac{\mathrm{d}Y}{\mathrm{d}\kappa}\mathrm{d}\kappa. \tag{8.33}$$

From (8.27) and (8.32) we have

$$\mathrm{d}\kappa = \boldsymbol{\sigma}^T \mathrm{d}\epsilon_p = \boldsymbol{\sigma}^T \boldsymbol{a} \mathrm{d}\lambda. \tag{8.34}$$

Euler's theorem on homogeneous functions states that if $f(\boldsymbol{x})$ is homogeneous and of degree n then [26, Page 228]

$$\boldsymbol{x}^T \frac{\partial f}{\partial \boldsymbol{x}} = nf. \tag{8.35}$$

Using this on Y in (8.28) and the fact that $Y = 0$ during plastic deformation we have

$$\boldsymbol{\sigma}^T \boldsymbol{a} = \boldsymbol{\sigma}^T \frac{\partial \bar{\sigma}}{\partial \boldsymbol{\sigma}} = \bar{\sigma}(\boldsymbol{\sigma}) = \sigma_y(\kappa). \tag{8.36}$$

Hence (8.34) becomes

$$\mathrm{d}\kappa = \sigma_y(\kappa)\mathrm{d}\lambda. \tag{8.37}$$

From (8.28) we have

$$\frac{\partial Y}{\partial \kappa} = -\frac{\mathrm{d}\sigma_y}{\mathrm{d}\kappa}. \tag{8.38}$$

Substituting (8.37) and (8.38) into (8.33) we have, during plastic deformation,

$$\mathrm{d}Y = \boldsymbol{a}^T \mathrm{d}\boldsymbol{\sigma} - H \mathrm{d}\lambda = 0 \tag{8.39}$$

where

$$H = \frac{\mathrm{d}\sigma_y}{\mathrm{d}\kappa} \sigma_y. \tag{8.40}$$

The value of H will be discussed later. From Hooke's law

$$\boldsymbol{\sigma} = \boldsymbol{D} \left(\boldsymbol{\epsilon} - \boldsymbol{\epsilon}_p \right) \tag{8.41}$$

which may be rearranged to give

$$\boldsymbol{\epsilon} = \boldsymbol{D}^{-1} \boldsymbol{\sigma} + \boldsymbol{\epsilon}_p. \tag{8.42}$$

The strain increment is obtained using the chain rule with (8.42) to give

$$\mathrm{d}\boldsymbol{\epsilon} = \mathrm{d}\boldsymbol{D}^{-1} \boldsymbol{\sigma} + \boldsymbol{D}^{-1} \mathrm{d}\boldsymbol{\sigma} + \mathrm{d}\boldsymbol{\epsilon}_p. \tag{8.43}$$

For isothermal applications the $\mathrm{d}\boldsymbol{D}^{-1}$ term will always be zero. Hence we may rearrange (8.43) to give

$$\mathrm{d}\boldsymbol{\sigma} = \boldsymbol{D} \left(\mathrm{d}\boldsymbol{\epsilon} - \mathrm{d}\boldsymbol{\epsilon}_p \right). \tag{8.44}$$

Substituting (8.44) into (8.39) gives us

$$\mathrm{d}Y = \boldsymbol{a}^T \boldsymbol{D} \left(\mathrm{d}\boldsymbol{\epsilon} - \boldsymbol{a} \mathrm{d}\lambda \right) - H \mathrm{d}\lambda = 0. \tag{8.45}$$

Solving for $\mathrm{d}\lambda$ we have

$$\mathrm{d}\lambda = \frac{\boldsymbol{a}^T \boldsymbol{D} \mathrm{d}\boldsymbol{\epsilon}}{\boldsymbol{a}^T \boldsymbol{D} \boldsymbol{a} + H}. \tag{8.46}$$

Substituting (8.46) into (8.32) we have

$$\mathrm{d}\boldsymbol{\epsilon}_p = \frac{\boldsymbol{a}\boldsymbol{a}^T \boldsymbol{D} \mathrm{d}\boldsymbol{\epsilon}}{\boldsymbol{a}^T \boldsymbol{D} \boldsymbol{a} + H}. \tag{8.47}$$

Substituting (8.47) into (8.44) gives us

$$\mathrm{d}\boldsymbol{\sigma} = \left(\boldsymbol{D} - \frac{\boldsymbol{D}\boldsymbol{a}\boldsymbol{a}^T \boldsymbol{D}}{\boldsymbol{a}^T \boldsymbol{D} \boldsymbol{a} + H} \right) \mathrm{d}\boldsymbol{\epsilon}. \tag{8.48}$$

We define the elastoplasticity matrix, $\boldsymbol{D}_{ep}$, to be

$$\boldsymbol{D}_{ep} = \boldsymbol{D} - \frac{\boldsymbol{D}\boldsymbol{a}\boldsymbol{a}^T \boldsymbol{D}}{\boldsymbol{a}^T \boldsymbol{D} \boldsymbol{a} + H}. \tag{8.49}$$

The value of H is obtained from uniaxial tests on the material. For the uniaxial case we may write

$$H = \frac{\partial \sigma_y}{\partial \kappa}\sigma_y = \frac{\partial \sigma_y}{\partial \epsilon_p}\frac{\partial \epsilon_p}{\partial \kappa}\sigma_y. \tag{8.50}$$

From (8.27) we have

$$\mathrm{d}\kappa = \sigma_y \, \mathrm{d}\epsilon_p \tag{8.51}$$

so that

$$H = \frac{\partial \sigma_y}{\partial \epsilon_p} \tag{8.52}$$

which is equivalent to (8.9). The value of H can now be obtained from experimental data. For the general case we define an effective plastic strain, $\bar{\epsilon}_p$, and an effective stress, $\bar{\sigma}$, such that

$$\mathrm{d}\kappa = \bar{\sigma}\mathrm{d}\bar{\epsilon}_p. \tag{8.53}$$

Now (8.52) becomes

$$H = \frac{\partial \sigma_y}{\partial \bar{\epsilon}_p}. \tag{8.54}$$

The calculation of $\bar{\sigma}$ depends on the yield condition of the material. This will be discussed later. The calculation of $\bar{\epsilon}_p$ is then performed using

$$\mathrm{d}\bar{\epsilon}_p = \frac{\mathrm{d}\lambda \boldsymbol{a}^T \boldsymbol{\sigma}}{\bar{\sigma}}. \tag{8.55}$$

With every increment in $\bar{\epsilon}_p$ comes an increment in σ_y given by

$$\mathrm{d}\sigma_y = A\mathrm{d}\bar{\epsilon}_p. \tag{8.56}$$

8.3 Thermal effects

The elastic modulus and the yield stress are both functions of temperature. Furthermore, when materials are heated, they experience thermal strain. Hence we must rewrite (8.28) as

$$Y = \bar{\sigma}(\boldsymbol{\sigma}) - \sigma_y(\kappa, T) \tag{8.57}$$

so that (8.39) becomes

$$\mathrm{d}Y = \boldsymbol{a}^T \mathrm{d}\boldsymbol{\sigma} - H\mathrm{d}\lambda - S dT \tag{8.58}$$

where

$$S = \frac{\partial \sigma_y}{\partial T}. \tag{8.59}$$

The strain increment (8.43) becomes

$$\mathrm{d}\boldsymbol{\epsilon} = \mathrm{d}\boldsymbol{D}^{-1}\boldsymbol{\sigma} + \boldsymbol{D}^{-1}\mathrm{d}\boldsymbol{\sigma} + \mathrm{d}\boldsymbol{\epsilon}_p + \mathrm{d}\boldsymbol{\epsilon}_{th} \tag{8.60}$$

where $\boldsymbol{\epsilon}_{th}$ is the thermal strain vector so that

$$\mathrm{d}\boldsymbol{\sigma} = \boldsymbol{D}\left(\mathrm{d}\boldsymbol{\epsilon} - \mathrm{d}\boldsymbol{\epsilon}_p - \mathrm{d}\boldsymbol{\epsilon}_{th} - \mathrm{d}\boldsymbol{D}^{-1}\boldsymbol{\sigma}\right). \tag{8.61}$$

Substituting (8.32) and (8.61) into (8.58) gives us

$$\boldsymbol{a}^T\boldsymbol{D}\left(\mathrm{d}\boldsymbol{\epsilon} - \boldsymbol{a}\mathrm{d}\lambda - \mathrm{d}\boldsymbol{\epsilon}_{th} - \mathrm{d}\boldsymbol{D}^{-1}\boldsymbol{\sigma}\right) - H\mathrm{d}\lambda - S\mathrm{d}T = 0. \tag{8.62}$$

Solving for $\mathrm{d}\lambda$ we have

$$\mathrm{d}\lambda = \frac{\boldsymbol{a}^T\boldsymbol{D}\left(\mathrm{d}\boldsymbol{\epsilon} - \mathrm{d}\boldsymbol{\epsilon}_{th} - \mathrm{d}\boldsymbol{D}^{-1}\boldsymbol{\sigma}\right) - SdT}{\boldsymbol{a}^T\boldsymbol{D}\boldsymbol{a} + H} \tag{8.63}$$

so that

$$\mathrm{d}\boldsymbol{\sigma} = \left(\boldsymbol{D} - \frac{\boldsymbol{D}\boldsymbol{a}\boldsymbol{a}^T\boldsymbol{D}}{\boldsymbol{a}^T\boldsymbol{D}\boldsymbol{a} + \boldsymbol{A}}\right)\left(\mathrm{d}\boldsymbol{\epsilon} - \mathrm{d}\boldsymbol{\epsilon}_{th} - \mathrm{d}\boldsymbol{D}^{-1}\boldsymbol{\sigma}\right) + \frac{\boldsymbol{D}\boldsymbol{a}S\mathrm{d}T}{\boldsymbol{a}^T\boldsymbol{D}\boldsymbol{a} + H}. \tag{8.64}$$

Rearranging and substituting (8.49), we have

$$\mathrm{d}\boldsymbol{\sigma} = \boldsymbol{D}_{ep}\mathrm{d}\boldsymbol{\epsilon} - \mathrm{d}\boldsymbol{Q} \tag{8.65}$$

where

$$\mathrm{d}\boldsymbol{Q} = \boldsymbol{D}_{ep}\left(\mathrm{d}\boldsymbol{\epsilon}_{th} + \mathrm{d}\boldsymbol{D}^{-1}\boldsymbol{\sigma}\right) - \frac{\boldsymbol{D}\boldsymbol{a}S\mathrm{d}T}{\boldsymbol{a}^T\boldsymbol{D}\boldsymbol{a} + H}. \tag{8.66}$$

8.4 Equilibrium equations

Prior to any plastic stress increment the body is in equilibrium. For the body to remain in equilibrium the stress increment, $d\boldsymbol{\sigma}$, must satisfy the weak equation

$$\int_{x\in\Omega} \boldsymbol{\epsilon}(\boldsymbol{v})^T\mathrm{d}\boldsymbol{\sigma}\,\mathrm{d}\boldsymbol{x} = \int_{x\in\Omega} \boldsymbol{v}^T d\boldsymbol{f}\,\mathrm{d}\boldsymbol{x} + \int_{x\in\Gamma_N} \boldsymbol{v}^T d\boldsymbol{g}\,\mathrm{d}\boldsymbol{x} \quad \forall\,\boldsymbol{v}\in H. \tag{8.67}$$

Substituting (8.65) we have

$$\int_{x\in\Omega} \boldsymbol{\epsilon}(\boldsymbol{v})^T\boldsymbol{D}_{ep}\boldsymbol{\epsilon}(\mathrm{d}\boldsymbol{u})\,\mathrm{d}\boldsymbol{x} = \int_{x\in\Omega} \boldsymbol{v}^T\mathrm{d}\boldsymbol{f}\,\mathrm{d}\boldsymbol{x} + \int_{x\in\Gamma_N} \boldsymbol{v}^T\mathrm{d}\boldsymbol{g}\,\mathrm{d}\boldsymbol{x} + \int_{x\in\Omega} \boldsymbol{\epsilon}(\boldsymbol{v})^T\mathrm{d}\boldsymbol{Q}\,\mathrm{d}\boldsymbol{x} \quad \forall\,\boldsymbol{v}\in H. \tag{8.68}$$

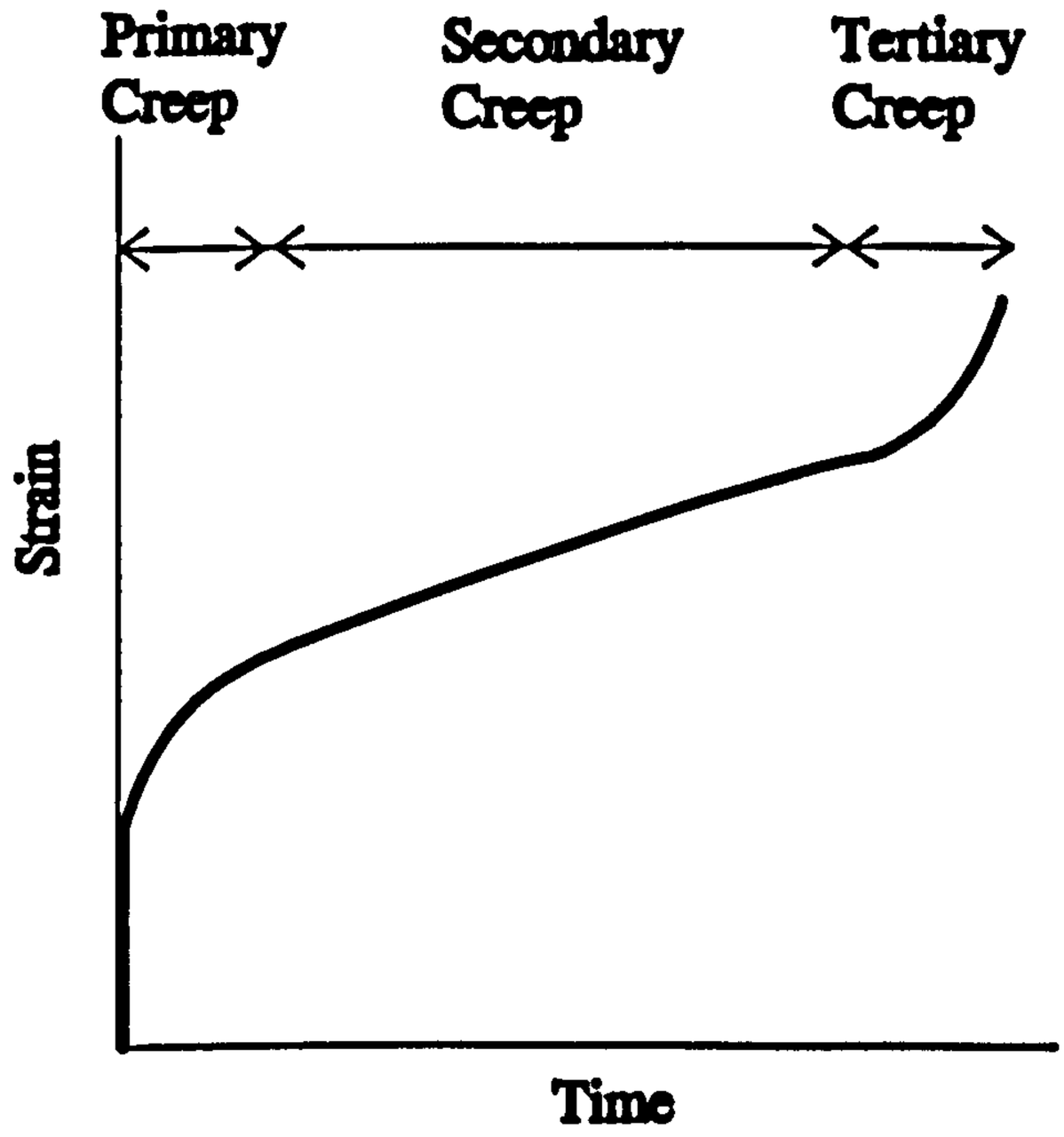

Figure 8.2: Typical creep curve

In practice the infinitesimal increments, $\mathrm{d}\boldsymbol{u}$, $\mathrm{d}\boldsymbol{f}$, $\mathrm{d}\boldsymbol{g}$ and $\mathrm{d}\boldsymbol{Q}$, are replaced by finite ones, $\Delta\boldsymbol{u}$, $\Delta\boldsymbol{f}$, $\Delta\boldsymbol{g}$ and $\Delta\boldsymbol{Q}$ where

$$\Delta\boldsymbol{Q} = \boldsymbol{D}_{ep}\left(\Delta\boldsymbol{\epsilon}_{th} + \Delta\boldsymbol{\sigma}\boldsymbol{d}\boldsymbol{D}^{-1} + \Delta\boldsymbol{\epsilon}_{c}\right) - \frac{\boldsymbol{D}\boldsymbol{a}\boldsymbol{S}\Delta T}{\boldsymbol{a}^{T}\boldsymbol{D}\boldsymbol{a} + H}. \tag{8.69}$$

Hence the weak equilibrium equation governing the finite displacement increment, $\Delta\boldsymbol{u}$, is

$$\int_{x\in\Omega} \boldsymbol{\epsilon}(\boldsymbol{v})^{T}\boldsymbol{D}_{ep}\boldsymbol{\epsilon}(\Delta\boldsymbol{u})\,\mathrm{d}\boldsymbol{x} = \int_{x\in\Omega} \boldsymbol{v}^{T}\Delta\boldsymbol{f}\,\mathrm{d}\boldsymbol{x} + \int_{x\in\Gamma_{N}} \boldsymbol{v}^{T}\Delta\boldsymbol{g}\,\mathrm{d}\boldsymbol{x} + \int_{x\in\Omega} \boldsymbol{\epsilon}(\boldsymbol{v})^{T}\Delta\boldsymbol{Q}\,\mathrm{d}\boldsymbol{x} \quad \forall\,\boldsymbol{v}\in\boldsymbol{H}. \tag{8.70}$$

8.5 Creep

Although the creep theory presented here is not used in this thesis, the possible significance of creep deformation to a fire-exposed frame justifies its inclusion. This section illustrates how creep may be incorporated into the plasticity model.

Under normal conditions (i.e., normal stresses and temperatures) most building materials deform only in response to an applied load. In such circumstances the deformation is instantaneous. However, under exceptional circumstances, like the subjection to a high temperature environment, further deformation may occur if the load is maintained.

Such behaviour is called creep deformation and is regarded as the time-dependent inelastic deformation of solids. It can be generally considered to consist of three stages:

Primary creep period: This has a relatively high deformation rate.

Secondary Creep: This has a much slower and constant growth rate and normally occurs at high temperatures. This is also known as steady-state creep.

Tertiary Creep: This is the most detrimental type of creep deformation as the deformation rate becomes extremely high and usually results in catastrophic rupture of the structure in a very short time.

These are illustrated in Figure 8.2. For steels at fire-exposed temperatures the primary creep period is short compared with the secondary creep period. Hence, for practical purposes, the primary creep period is ignored.

The creep rate of a material depends on the time since loading, the temperature and the stress. A general form for the uniaxial case is

$$\frac{\mathrm{d}\epsilon_c}{\mathrm{d}t} = f(\sigma, t, T) = f_1(\sigma) f_2(t) f_3(T). \tag{8.71}$$

Various forms of $f_1(\sigma)$, $f_2(t)$ and $f_3(T)$ have been proposed by researchers. Some of the commonly used ones are listed in Hsu [15]. For fire applications it is assumed that the creep rate only depends on the stress and the temperature and so we take $f_2 = 1$. Most models use

$$f_3(T) = \exp\left(\frac{-Q}{RT}\right) \tag{8.72}$$

where

$$Q = \text{Activation energy} \tag{8.73}$$
$$R = \text{Universal gas constant } (8.31 J mol^{-1} K) \tag{8.74}$$
$$T = \text{Absolute temperature.} \tag{8.75}$$

The activation energy is, for a given stress, a measure for the temperature at which the creep becomes significant. Hsu [15] uses Norton's law,

$$\frac{\mathrm{d}\epsilon_c}{\mathrm{d}t} = K\sigma^n \exp\left(-\frac{Q}{RT}\right), \tag{8.76}$$

where K and n are are material constants. Lie [21, 153] uses the Zener-Hollomon law,

$$\frac{\mathrm{d}\epsilon_c}{\mathrm{d}t} = Z \exp\left(-\frac{Q}{RT}\right), \tag{8.77}$$

where Z is the Zener-Hollomon parameter which is a measure of the creep rate of a material in the secondary creep period at a given temperature. According to Lie [21],

for mild structural steel (ASTM A36),

$$\frac{Q}{R} = 40000K \tag{8.78}$$

$$Z = 1.23 \times 10^{16} \exp(0.000427\sigma)h^{-1}, \quad 100 < \sigma \leq 300N/mm^2 \tag{8.79}$$

and, for cold drawn pre-stressing steel (ASTM A421),

$$\frac{Q}{R} = 30000K \tag{8.80}$$

$$Z = 8.21 \times 10^{13} \exp(0.000142\sigma)h^{-1}, \quad 135 < \sigma \leq 700N/mm^2. \tag{8.81}$$

For general multi-axial cases the constitutive laws are expressed in terms of effective stress and strain. The two laws become, respectively,

$$\frac{d\bar{\epsilon}_c}{\mathrm{d}t} = K\bar{\sigma}^n \exp\left(-\frac{Q}{RT}\right) \tag{8.82}$$

$$\frac{d\bar{\epsilon}_c}{\mathrm{d}t} = Z(\bar{\sigma}) \exp\left(-\frac{Q}{RT}\right) \tag{8.83}$$

where $\bar{\epsilon}_c$ is the effective creep strain and $\bar{\sigma}$ is the effective stress. Incremental creep strain may be expressed in terms of a plastic creep potential function; i.e

$$\mathrm{d}\boldsymbol{\epsilon}_c = \mathrm{d}\lambda \frac{\partial \psi}{\partial \boldsymbol{\sigma}} \tag{8.84}$$

where $\mathrm{d}\lambda$ is a positive parameter that depends on the loading history and ψ is the creep potential function (analogous to the plastic potential function in the previous section). If $\psi = Y$ as before then

$$\mathrm{d}\boldsymbol{\epsilon}_c = \mathrm{d}\lambda \boldsymbol{a}. \tag{8.85}$$

If we assume that the creep strain is incompressible then the effective creep strain may be defined as [15]

$$\mathrm{d}\bar{\epsilon}_c := \left(\frac{2}{3}\mathrm{d}\boldsymbol{\epsilon}_c^T \mathrm{d}\boldsymbol{\epsilon}_c\right)^{\frac{1}{2}}. \tag{8.86}$$

Substituting (8.85) into (8.86) gives

$$\mathrm{d}\bar{\epsilon}_c = \sqrt{\frac{2}{3}}\mathrm{d}\lambda\sqrt{\boldsymbol{a}^T\boldsymbol{a}} \tag{8.87}$$

so that

$$\mathrm{d}\lambda = \sqrt{\frac{3}{2}}\frac{\mathrm{d}\bar{\epsilon}_c}{\sqrt{\boldsymbol{a}^T\boldsymbol{a}}}. \tag{8.88}$$

The value of $d\bar{\epsilon}_c$ is determined from either Norton's law (8.76) or Zener-Hollomon's law (8.77) by integrating over the time increment; i.e.

$$\begin{aligned} \mathrm{d}\bar{\epsilon}_c &= \int_{t_{n-1}}^{t_n} K\bar{\sigma}^n \exp\left(-\frac{Q}{RT}\right) dt \qquad \text{Norton,} \\ \mathrm{d}\bar{\epsilon}_c &= \int_{t_{n-1}}^{t_n} Z(\bar{\sigma}) \exp\left(-\frac{Q}{RT}\right) dt \quad \text{Zener-Hollomon.} \end{aligned} \tag{8.89}$$

Following on from the thermal elastoplastic analysis earlier we assume that the total strain increment may be expressed by extending (8.60) to

$$\mathrm{d}\epsilon = \sigma \mathrm{d}D^{-1} + D^{-1}\mathrm{d}\sigma + \mathrm{d}\epsilon_p + \mathrm{d}\epsilon_{th} + \mathrm{d}\epsilon_c. \tag{8.90}$$

This modification to the thermal elastoplastic theory only results in changing the $\mathrm{d}Q$ term, given in (8.66), to

$$\mathrm{d}Q = D_{ep}\left(\mathrm{d}\epsilon_{th} + \mathrm{d}D^{-1}\sigma + \mathrm{d}\epsilon_c\right) - \frac{DaB\mathrm{d}T}{a^T Da + A}. \tag{8.91}$$

8.6 Yield conditions

The yield condition should be independent of the co-ordinate system employed. Hence it may be dependent on the principal stresses, σ_1, σ_2 and σ_3, and the stress invariants, I_1, I_2 and I_3. Any combination of these will be independent of the coordinate system and may contribute to the yield condition. For metals, plastic deformation has been shown experimentally to be essentially independent of hydrostatic pressure; i.e. I_1. Hence the yield condition may be assumed to be a function of the deviatoric stress invariants, J_2 and J_3, only.

The Tresca yield criterion

This states that yielding begins when the maximum shear stress reaches a critical value. In terms of principal stresses it may be stated as

$$\tau_{max} = \frac{\sigma_1 - \sigma_3}{2} = k(\kappa), \tag{8.92}$$

where σ_1 and σ_3 are the maximum and minimum principal stresses, respectively, and k is a constant to be determined. For the uniaxial tension case, yielding occurs when

$$\frac{\sigma_y}{2} = k \tag{8.93}$$

so we have that

$$\bar{\sigma} = \sigma_1 - \sigma_3. \tag{8.94}$$

The von Mises yield criterion

This states that yielding begins when the distortion energy equals the distortion energy at yield in uniaxial tension. The distortion energy is proportional to J_2 and so the yield criterion is for J_2 to reach a critical value. When yielding occurs under uniaxial tension

$$J_2 = \frac{\sigma_y^2}{3} \tag{8.95}$$

and so

$$\bar{\sigma} = \sqrt{3} J_2^{\frac{1}{2}}. \tag{8.96}$$

The Mohr-Coulomb yield criterion

Mohr extended the Tresca yield criterion by assuming that yielding depends not only on the shear stress but that it also depends on the normal stress acting on the shearing plane. This is, in fact, a generalisation of the Coulomb friction failure law which may be stated as

$$\tau = c - \sigma_n \tan\phi, \tag{8.97}$$

where τ is the magnitude of the shearing stress, σ_n is the normal stress (tensile stress positive), c is the cohesion and ϕ is the angle of internal friction. Note that both c and ϕ are material properties that are determined experimentally. Mohr demonstrated that, graphically, (8.97) represents a straight line tangent to the largest principal stress circle as shown in Figure 8.3.

From Figure 8.3 equation (8.97) may be rewritten as

$$\frac{\sigma_1 - \sigma_3}{2}\cos\phi = c - \left(\frac{\sigma_1 + \sigma_3}{2} + \frac{\sigma_1 - \sigma_3}{2}\sin\phi\right)\tan\phi \tag{8.98}$$

which simplifies to

$$\sigma_1 - \sigma_3 + (\sigma_1 + \sigma_3)\sin\phi = 2c\cos\phi. \tag{8.99}$$

The key difference between this yield criterion and the previous two is that yielding now depends on the direction of the stress. Let σ_t and σ_c denote the magnitude of the yield stresses for the cases of uniaxial tension and compression, respectively. Then, from (8.99), we have

$$\sigma_t(1 + \sin\phi) = 2c\cos\phi \tag{8.100}$$

$$\sigma_c(1 - \sin\phi) = 2c\cos\phi. \tag{8.101}$$

Solving for ϕ and c we have

$$\phi = \sin^{-1}\left(\frac{\sigma_c - \sigma_t}{\sigma_c + \sigma_t}\right) \tag{8.102}$$

$$c = \frac{\sqrt{\sigma_t \sigma_c}}{2}. \tag{8.103}$$

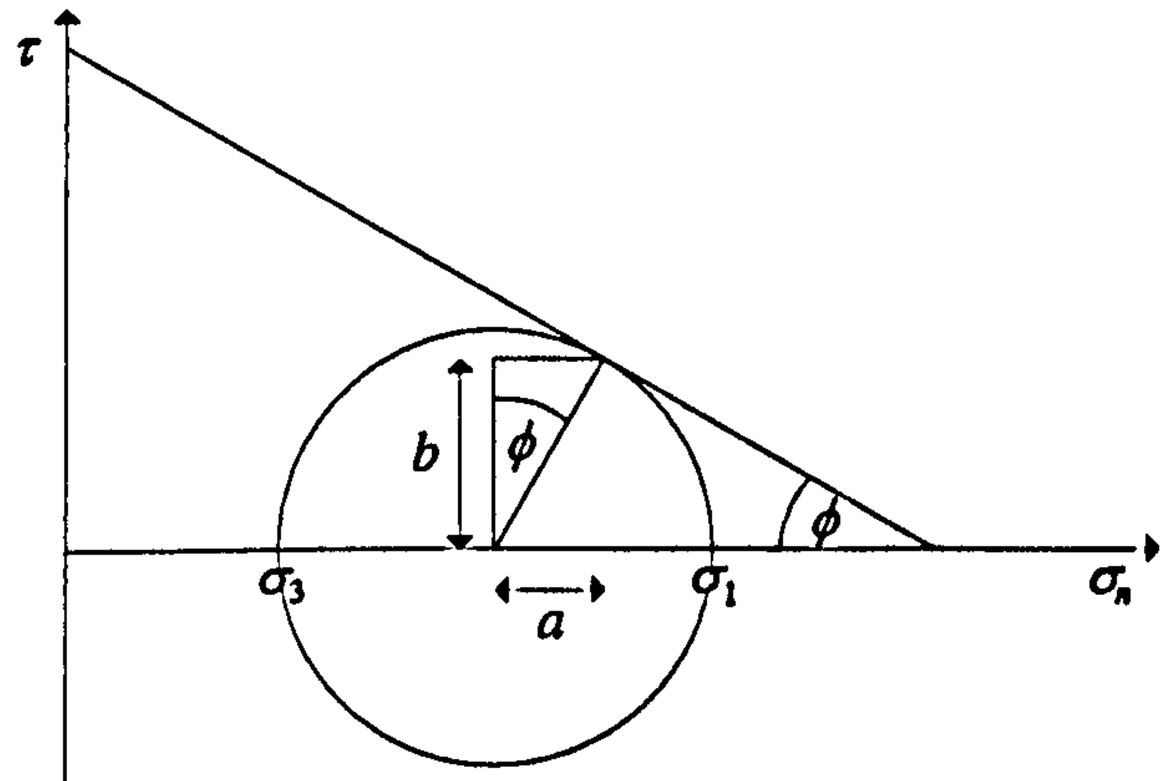

$$a = \frac{\sigma_1 - \sigma_3}{2} \sin\phi$$
$$b = \frac{\sigma_1 - \sigma_3}{2} \cos\phi$$

Figure 8.3: Mohr circle representation of the Mohr-Coulomb yield criterion

Hence (8.99) may be written as

$$\sigma_1 - \sigma_3 + \frac{(\sigma_1 + \sigma_3)}{\sigma_c + \sigma_t} = \frac{2\sigma_c\sigma_t}{\sigma_c + \sigma_t} \tag{8.104}$$

which simplifies to give

$$\sigma_1\sigma_c - \sigma_3\sigma_t = \sigma_c\sigma_t. \tag{8.105}$$

Then, for the case of uniaxial tension, (8.105) reduces to

$$\sigma_1 = \sigma_t \tag{8.106}$$

and, for uniaxial compression,

$$-\sigma_3 = \sigma_c. \tag{8.107}$$

The Drucker-Prager yield criterion

An approximation to the Mohr-Coulomb law was presented by Drucker and Prager in 1952 as a modification of the von Mises yield criterion. The influence of a hydrostatic stress component on yielding was introduced by adding an I_1 term in the von Mises expression so that the yield criterion is

$$\alpha I_1 + \sqrt{3}\,(J_2)^{\frac{1}{2}} = k. \tag{8.108}$$

Now, for uniaxial tension and compression cases, respectively, we have

$$\sigma_t(1+\alpha) = k \tag{8.109}$$
$$\sigma_c(1-\alpha) = k. \tag{8.110}$$

Hence

$$\alpha = \frac{\sigma_c - \sigma_t}{\sigma_c + \sigma_t} \tag{8.111}$$

$$k = \frac{2\sigma_c\sigma_t}{\sigma_c + \sigma_t}. \tag{8.112}$$

Note that these are related to the Mohr-Coulomb parameters by

$$\alpha = \sin\phi \tag{8.113}$$

$$k = 2c\cos\phi. \tag{8.114}$$

8.7 Application to beams

In beam theory the only non-zero stress components are σ_{11}, σ_{12} and σ_{13} so that the deviatoric stress tensor is

$$\boldsymbol{\sigma}' = \begin{pmatrix} \frac{2}{3}\sigma_{11} & \sigma_{12} & \sigma_{13} \\ \sigma_{12} & -\frac{1}{3}\sigma_{11} & 0 \\ \sigma_{13} & 0 & -\frac{1}{3}\sigma_{11} \end{pmatrix}. \tag{8.115}$$

Hence the invariants I_1 and J_2 are

$$I_1 = \sigma_{11} \tag{8.116}$$

$$J_2 = \frac{1}{3}\sigma_{11}^2 + \sigma_{12}^2 + \sigma_{13}^2. \tag{8.117}$$

The flow vector may be written as

$$\boldsymbol{a} = \frac{\partial F}{\partial I_1}\frac{\partial I_1}{\partial \boldsymbol{\sigma}} + \frac{\partial F}{\partial (J_2^{\frac{1}{2}})}\frac{\partial (J_2^{\frac{1}{2}})}{\partial \boldsymbol{\sigma}} \tag{8.118}$$

so that, using (8.108),

$$\boldsymbol{a} = \begin{pmatrix} \alpha \\ 0 \\ 0 \end{pmatrix} + \frac{1}{\sqrt{3}J_2^{\frac{1}{2}}}\begin{pmatrix} \sigma_{11} \\ 3\sigma_{12} \\ 3\sigma_{13} \end{pmatrix}. \tag{8.119}$$

Recall that the linear elastic constitutive relation between the components of stress and strain is

$$\boldsymbol{\sigma} = \begin{pmatrix} \sigma_{11} \\ \sigma_{12} \\ \sigma_{13} \end{pmatrix} = \begin{pmatrix} E & 0 & 0 \\ 0 & G & 0 \\ 0 & 0 & G \end{pmatrix}\begin{pmatrix} \epsilon_{11} \\ \epsilon_{12} \\ \epsilon_{13} \end{pmatrix} = \boldsymbol{D}\boldsymbol{\epsilon} \tag{8.120}$$

and that the relation between beam stresses and beam strains is

$$\boldsymbol{S} = \begin{pmatrix} S_1 \\ S_2 \\ S_3 \\ S_4 \end{pmatrix} = \int_{x \in \boldsymbol{A}} \boldsymbol{X}^T \boldsymbol{\sigma}\, d\boldsymbol{x} \tag{8.121}$$

where

$$\boldsymbol{X} = \begin{pmatrix} 1 & -x_2 & -x_3 & 0 \\ 0 & 0 & 0 & -x_3 \\ 0 & 0 & 0 & x_2 \end{pmatrix}. \tag{8.122}$$

The elastoplastic relation between the stress and strain increments is

$$\Delta\boldsymbol{\sigma} = \boldsymbol{D}_{ep}\Delta\boldsymbol{\epsilon} - \Delta\boldsymbol{Q} \tag{8.123}$$

so that, for the finite increment in beam stresses, $\Delta\boldsymbol{S}$,

$$\Delta\boldsymbol{S} = \int_{x\in\boldsymbol{A}} \boldsymbol{X}^T\Delta\boldsymbol{\sigma}\,\mathrm{d}x - \int_{x\in\boldsymbol{A}} \boldsymbol{X}^T\Delta\boldsymbol{Q}\,\mathrm{d}x \tag{8.124}$$

$$= \int_{x\in\boldsymbol{A}} \boldsymbol{X}^T\boldsymbol{D}_{ep}\Delta\boldsymbol{\epsilon}\,\mathrm{d}x - \int_{x\in\boldsymbol{A}} \boldsymbol{X}^T\Delta\boldsymbol{Q}\,\mathrm{d}x \tag{8.125}$$

$$= \int_{x\in\boldsymbol{A}} \boldsymbol{X}^T\boldsymbol{D}_{ep}\boldsymbol{X}\boldsymbol{B}(\Delta\boldsymbol{u})\,\mathrm{d}x - \int_{x\in\boldsymbol{A}} \boldsymbol{X}^T\Delta\boldsymbol{Q}\,\mathrm{d}x. \tag{8.126}$$

Hence we may write

$$\Delta\boldsymbol{S} = \boldsymbol{D}_{Bep}\boldsymbol{B}(\Delta\boldsymbol{u}) - \boldsymbol{Q}_B, \tag{8.127}$$

where

$$\boldsymbol{D}_{Bep} := \int_{x\in\boldsymbol{A}} \boldsymbol{X}^T\boldsymbol{D}_{ep}\boldsymbol{X}\,\mathrm{d}x \tag{8.128}$$

$$\boldsymbol{Q}_B := \int_{x\in\boldsymbol{A}} \boldsymbol{X}^T\Delta\boldsymbol{Q}\,\mathrm{d}x. \tag{8.129}$$

The weak incremental equilibrium equation governing a thermoelastic-plastic beam is, therefore,

$$\int_0^l \boldsymbol{B}(\boldsymbol{v})^T\boldsymbol{D}_{Bep}\boldsymbol{B}(\Delta\boldsymbol{u})\,\mathrm{d}x = \int_0^l \boldsymbol{v}^T\Delta\boldsymbol{q}\,\mathrm{d}x + \int_0^l \boldsymbol{B}(\boldsymbol{v})^T\boldsymbol{Q}_B\,\mathrm{d}x \quad \forall\,\boldsymbol{v}\in\boldsymbol{H}. \tag{8.130}$$

The finite element solution is obtained by finding the incremental degree of freedom vector, $\Delta\boldsymbol{U}$ that satisfies

$$\boldsymbol{K}\Delta\boldsymbol{U} = \Delta\boldsymbol{F}, \tag{8.131}$$

where

$$\boldsymbol{K} := \int_0^L \boldsymbol{B}^T\boldsymbol{D}_{Bep}\boldsymbol{B}\,\mathrm{d}x \tag{8.132}$$

$$\Delta\boldsymbol{F} := \int_0^L \left(\boldsymbol{N}^T\Delta\boldsymbol{q} + \boldsymbol{B}^T\Delta\boldsymbol{Q}_B\right)\,\mathrm{d}x. \tag{8.133}$$

8.8 Data structures for plastic frame analysis

The evaluation of the plastic beam coefficients matrix involves the numerical integration of stress components over the cross section. Hence the stress components need to be stored at Gauss points within each triangular element of the cross-section. Furthermore, the cross-sectional stresses need to be stored for Gauss points along the beam element. Hence the data structure for storing the stress components is $\texttt{Stresses}(i, j, k, l, m)$ where

$$\begin{aligned} i &= \text{Beam element number}, 1 \leq i \leq nbe && (8.134)\\ j &= \text{Beam element Gauss point number}, 1 \leq j \leq nbgp && (8.135)\\ k &= \text{Cross-section element number}, 1 \leq k \leq ncse && (8.136)\\ l &= \text{Cross-section element Gauss point number}, 1 \leq l \leq ncsgp && (8.137)\\ m &= \text{Stress component number}, 1 \leq m \leq 3, && (8.138) \end{aligned}$$

where

$$\begin{aligned} nbe &= \text{Number of beam elements} && (8.139)\\ nbgp &= \text{Number of beam element Gauss points} && (8.140)\\ ncse &= \text{Number of cross-section elements} && (8.141)\\ nvsgp &= \text{Number of cross-section element Gauss points.} && (8.142) \end{aligned}$$

Similarly we define the data structures $\texttt{PlasticStrains}(i, j, k, l)$ to store the effective strains and $\texttt{YieldStresses}(i, j, k, l)$ to store the yield stresses throughout the frame. Temperatures may be stored at each cross-section element Gauss point so as to use the same data structure type as the stresses and plastic strains. However, since the finite element temperature distribution is piecewise-linear, they only need to be stored at the cross-section nodes. In many fire applications the temperatures in a particular beam only vary across the cross-section and not along the length of the beam. Hence the temperatures only need to be stored once for each beam. Using an object oriented approach the temperature data structure may be regarded as a property of the cross-section and take the form $\texttt{CrossSection.Temperatures}(i, j)$ where

$$\begin{aligned} i &= \text{Cross-section node number}, 1 \leq i \leq ncse && (8.143)\\ j &= \text{Timestep number}, 0 \leq j \leq nts && (8.144) \end{aligned}$$

where nts is the number of timesteps in the finite element temperature calculations.

8.9 Solution procedure

Equation (8.131) may be solved using the Tangent Stiffness Method which solves the non-linear equation

$$\boldsymbol{K}(\boldsymbol{x})\boldsymbol{x} = \boldsymbol{F} \qquad (8.145)$$

using the iteration

$$K(x_i)(\Delta x) = \Psi(x_i) \tag{8.146}$$
$$x_{i+1} = x_i + \Delta x \tag{8.147}$$

where

$$\Psi(x) = F - K(x)x. \tag{8.148}$$

Initially, the elastic finite element solution is obtained resulting in a displacements vector, U. From this the stresses, σ_{ij}, are calculated at each integration (Gauss) points and stored in $\texttt{Stresses}(i,j,k,l,m)$. The maximum effective stress, $\bar{\sigma}_{max}$, is also calculated so that the fraction of F that caused first yield, β, is determined to be

$$\beta = \frac{\sigma_y}{\bar{\sigma}_{max}}. \tag{8.149}$$

The displacements and stresses at yield are then updated to be

$$U = \beta \times U \tag{8.150}$$
$$\texttt{Stresses}(i,j,k,l,m) = \beta \times \texttt{Stresses}(i,j,k,l,m) \quad \forall i,j,k,l,m. \tag{8.151}$$

The effective plastic strains and the yield stresses are set to

$$\texttt{PlasticStrains}(i,j) = 0 \quad \forall i,j \tag{8.152}$$
$$\texttt{YieldStresses}(i,j) = \sigma_y \quad \forall i,j. \tag{8.153}$$

The remaining load, $(1-\beta)F$, is divided into n load steps of size ΔF. For each load step ΔU is calculated using the iteration

$$K(U_i)\Delta\Delta U = \Psi\left[(\Delta U)_i\right] \tag{8.154}$$
$$(\Delta U)_{i+1} = (\Delta U)_i + \Delta\Delta U, \tag{8.155}$$

where

$$\Psi\left[(\Delta U)_i\right] = \Delta F - \int_{x\in\Omega} B^T (\Delta\sigma)_i \, \mathrm{d}x \tag{8.156}$$

and, initially,

$$\Delta U = 0 \tag{8.157}$$
$$\texttt{StressIncrements}(i,j) = 0 \quad \forall i,j. \tag{8.158}$$

The calculation of $\texttt{StressIncrements(i,j)}$ is achieved using (8.65). For the stress increment we have, during plastic deformation,

$$\Delta\sigma = \int \mathrm{d}\sigma = \int D_{ep} \, \mathrm{d}\epsilon \tag{8.159}$$

which is evaluated by dividing the integral into m steps so that

$$\Delta\boldsymbol{\sigma} = \sum_{i=1}^{m} \frac{1}{m} \boldsymbol{D}_{ep} \Delta\boldsymbol{\epsilon} \tag{8.160}$$

where $\Delta\boldsymbol{\epsilon}$ is evaluated from

$$\Delta\boldsymbol{\epsilon} = \begin{pmatrix} \Delta\epsilon_{11} \\ \Delta\epsilon_{12} \\ \Delta\epsilon_{13} \end{pmatrix} = \begin{pmatrix} B_1(\boldsymbol{du}) - x_2 B_2(\mathrm{d}\boldsymbol{u}) - x_3 B_3(\mathrm{d}\boldsymbol{u}) \\ -\frac{x_3}{2} B_2(\mathrm{d}\boldsymbol{u}) \\ \frac{x_2}{2} B_3(\mathrm{d}\boldsymbol{u}) \end{pmatrix}. \tag{8.161}$$

If the material has not yielded at a particular point or it is being unloaded (i.e. $d\lambda < 0$) then $\boldsymbol{D}_{ep}$ reduces to $\boldsymbol{D}$ and

$$\Delta\boldsymbol{\sigma} = \boldsymbol{D}\Delta\boldsymbol{\epsilon}. \tag{8.162}$$

8.10 Error estimation

After a load increment has been applied the increment to the true displacement, $\Delta\boldsymbol{u}$, and the increment to the finite element displacement, $\Delta\boldsymbol{u}_h$, satisfy

$$a(\Delta\boldsymbol{u}, \boldsymbol{v}) = (\Delta\boldsymbol{q}, \boldsymbol{v}) + [\Delta\boldsymbol{Q}, \boldsymbol{v}] \tag{8.163}$$

$$a(\Delta\boldsymbol{u}_h, \boldsymbol{v}) = (\Delta\boldsymbol{q}, \boldsymbol{v}) + [\Delta\boldsymbol{Q}, \boldsymbol{v}] \tag{8.164}$$

to within an iteration tolerance. Assuming that the iteration error is negligible compared with errors due to the finite element mesh the analysis of Chapter 7 may be applied to the plastic case. Hence the error estimator defined in Section 7.5.6 may be applied with confidence. The only difference in the implementation is in the evaluation of the residual vector, $\boldsymbol{r}$. This is defined as

$$\boldsymbol{r} := \begin{pmatrix} q_1 \\ q_2 \\ q_3 \\ 0 \end{pmatrix} - \begin{pmatrix} -S_1'(\boldsymbol{u}_h) \\ S_2''(\boldsymbol{u}_h) \\ S_3''(\boldsymbol{u}_h) \\ -S_4'(\boldsymbol{u}_h) \end{pmatrix} \tag{8.165}$$

which requires the derivatives of the stress components. The stresses are stored discretely and cannot be calculated exactly from the finite element solution. In practise the beam stress vector, $\mathrm{d}\boldsymbol{S}$, is calculated at the gauss points then its derivatives are approximated by differentiating a polynomial that interpolates $\mathrm{d}\boldsymbol{S}$ at the gauss points. Let the interpolation error in $\boldsymbol{r}$ be denoted by $\boldsymbol{\varepsilon}$ and defined as

$$\boldsymbol{\varepsilon} := \begin{pmatrix} (\mathrm{d}S_1 - \Pi\mathrm{d}S_1)' \\ -(\mathrm{d}S_2 - \Pi\mathrm{d}S_2)'' \\ -(\mathrm{d}S_3 - \Pi\mathrm{d}S_3)'' \\ (\mathrm{d}S_4 - \Pi\mathrm{d}S_4)' \end{pmatrix}. \tag{8.166}$$

In the definition of $\hat{e}$, we have

$$a(\hat{e}, v)_{\Omega_i} = (r, v)_{\Omega_i} + (\epsilon, v)_{\Omega_i} \tag{8.167}$$

for all $v \in \hat{V}$. Following through the analysis in section 7.5.6 we have the bounds

$$-C\|\epsilon\|_{L_2} + \left(1-\beta(h)^2\right)^{\frac{1}{2}}\left(1-\gamma(h)^2\right)^{\frac{1}{2}}\|e\| \leq \|\hat{e}\| \leq \|e\| + C\|\epsilon\|_{L_2}. \tag{8.168}$$

Using the interpolation result in section 2 and the fact that dS is differentiated twice we have that, when there are n Gauss points and a corresponding interpolant of degree $\leq n-1$,

$$\|\epsilon\| \leq Ch^{n-2}. \tag{8.169}$$

For $\|de\|$ to be asymptotically exact $\|\epsilon\|$ must converge to zero at a faster rate than $\|de\|$. For the quadratic and cubic finite element method, the fastest that $\|de\|$ can converge is with order h^2. Hence the number of gauss points must be greater than 4 to guarantee asymptotic exactness. When quartic or quintic functions are used for the bending displacements the number of gauss points must be greater than 5 or 6, respectively.

8.11 Numerical examples

Presented here are three applications of the computational method described in this chapter. The first considers a single heated beam which illustrates the combined thermal effects of expansion and material weakening. The second example considers a simple 2D frame loaded at room temperature so that it undergoes elastoplastic deformation. This illustrates how errors occur in the finite element solution due to the plasticity and how adaptivity of the mesh reduces the error. The third example considers a 3D two storey frame where the ground floor beams and columns are exposed to a heating curve. This illustrates the application of the error indicator to fire-exposed frame problems. All three examples use the von Mises yield criterion with values of E, H and S calculated from the data in Table 8.3.

8.11.1 A thermoplastic beam

The simply supported beam of length 1350mm has an applied force of 60810 N at one end and is heated underneath as illustrated in Figure 8.4. The measured temperatures are given in Table 8.1 and are used as boundary conditions to calculate the complete temperature distribution using the thermal properties in Table 8.2. Using the structural properties in Table 8.3 the displacement of the beam was calculated for different exposure times. The vertical displacement of the midpoint is listed in Table 8.4 and plotted in Figure 8.5 for comparison with experimental values [32]. A close match between experimental and computational values is shown up to around 24 minutes which

is about the time the beam first yields. After this time the computed displacement follows a similar path to that in the experiment except that it happens over a shorter time.

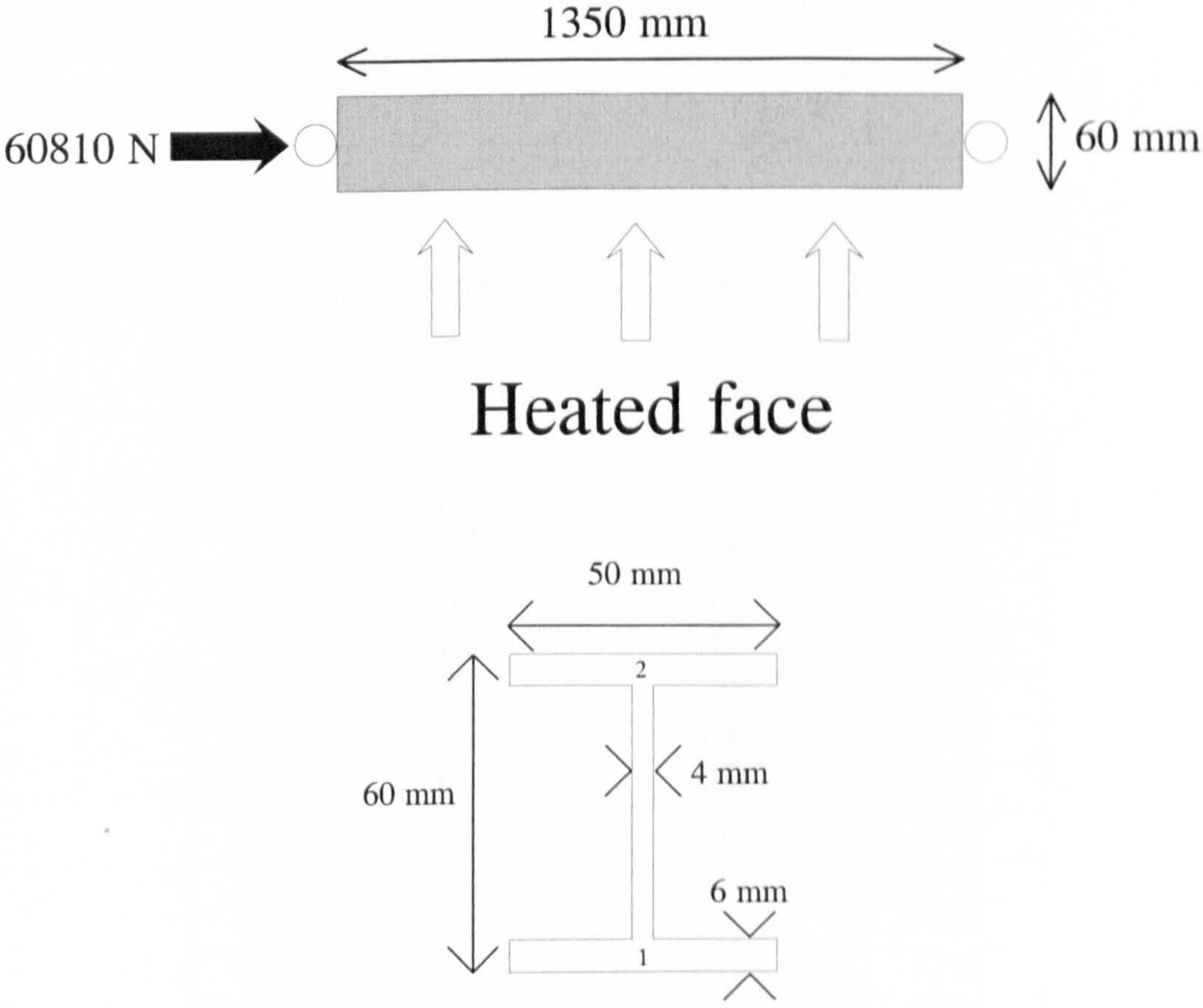

Figure 8.4 : Beam dimensions

Table 8.1 : Measured temperatures

Time (mins)	$T_1(^\circ C)$	$T_2(^\circ C)$
4	40.5	20.4
8	110.3	41.4
12	221.0	93.3
20	395.5	234.0
24	566.7	312.4
28	632.6	377.0
32	675.4	419.0
35	697.7	437.0
46	740.0	461.0

Table 8.2 : Thermal properties of steel [36]

$T(°C)$	$k(Wm^{-1}K^{-1})$	$c(Jkg^{-1}K^{-1})$	$\rho(kgm^{-3})$
0	52.0	440	7850
20	52.0	440	7850
50	51.7	450	7842
100	51.0	480	7827
150	50.0	505	7812
200	48.8	530	7797
250	47.5	550	7781
300	46.0	565	7765
350	44.5	585	7748
400	42.7	610	7731
450	41.0	640	7713
500	39.2	675	7695
550	37.5	715	7675
600	35.5	760	7655
650	33.8	820	7635
700	32.0	1010	7616
725	31.0	1600	7608
735	30.0	5000	7612
750	28.5	1300	7618
775	26.0	1010	7622
800	26.0	810	7626
825	25.8	730	7627
850	26.0	685	7622
875	26.2	660	7611
900	26.5	650	7599
950	27.0	650	7574
1000	27.5	650	7549
1050	28.0	650	7523
1100	28.5	650	7500
1150	29.0	650	7477
1200	29.5	655	7453

Table 8.3a : Structural properties of grade 43A steel for 20°C to 350°C [2]

Strain %	Stress (N/mm^2) for Various Temperatures (°C)							
	20	50	100	150	200	250	300	350
0.00	0.0	0.0	0.0	0.0	0.0	0.0	0.0	0.0
0.01	18.4	18.4	18.4	17.3	16.6	15.8	15.6	14.5
0.02	36.7	36.7	35.7	34.9	33.2	31.9	31.4	29.1
0.03	55.1	54.1	54.1	53.2	49.7	47.7	46.9	43.4
0.04	73.4	72.4	71.7	70.6	66.3	63.5	62.5	57.9
0.05	91.8	89.3	90.0	88.2	82.9	79.3	78.0	72.4
0.06	110.2	109.1	107.4	105.6	99.2	95.4	93.8	87.0
0.07	128.3	126.7	125.7	123.2	115.3	111.2	109.4	101.2
0.08	146.6	144.8	143.3	141.5	132.3	127.0	125.0	115.8
0.09	165.0	163.2	161.7	158.9	148.9	143.1	132.1	124.4
0.10	183.0	181.6	179.0	176.5	165.5	158.9	136.4	129.0
0.12	220.1	217.5	214.7	211.4	198.6	181.8	144.5	138.0
0.14	255.0	247.1	234.1	225.4	208.1	188.2	152.2	145.9
0.16	255.0	247.1	238.4	229.5	213.4	193.8	158.9	152.2
0.18	255.0	247.1	242.3	232.6	217.5	198.4	164.5	157.8
0.20	255.0	247.1	244.8	234.6	221.1	202.2	169.8	163.2
0.25	255.0	247.1	246.1	237.7	229.2	208.8	181.3	174.7
0.30	255.0	247.1	246.1	239.7	233.8	213.9	191.9	184.9
0.35	255.0	247.1	246.1	241.0	237.4	217.3	199.7	192.8
0.40	255.0	247.1	246.1	241.7	239.2	219.8	207.1	199.7
0.50	255.0	247.1	246.1	243.8	241.2	225.4	217.8	210.6
0.60	255.0	247.1	246.1	244.0	241.7	230.0	225.7	218.5
0.70	255.0	247.1	246.1	244.3	242.3	233.6	230.9	225.2
0.80	255.0	247.1	246.1	244.5	242.8	237.4	235.4	231.5
0.90	255.0	247.1	246.1	244.5	243.0	240.7	238.7	235.6
1.00	255.0	247.1	246.1	244.9	243.5	242.8	241.2	239.7

Table 8.3b : Structural properties of grade 43A steel for 400°C to 800°C [2]

Strain %	Stress (N/mm^2) for Various Temperatures (°C)								
	400	450	500	550	600	650	700	750	800
0.00	0.0	0.0	0.0	0.0	0.0	0.0	0.0	0.0	0.0
0.01	13.3	11.7	9.4	6.9	5.6	4.1	2.0	2.0	1.8
0.02	26.8	23.5	19.1	13.5	11.5	8.2	4.1	3.8	3.3
0.03	40.0	35.2	28.6	20.4	17.1	12.2	6.1	5.9	5.6
0.04	53.3	46.9	38.3	27.0	22.7	16.6	8.2	7.9	7.4
0.05	66.8	58.7	47.7	33.9	28.3	20.7	10.5	9.9	9.4
0.06	80.1	70.1	57.1	40.7	34.2	24.7	12.5	11.7	11.2
0.07	93.3	81.9	66.8	47.4	39.3	28.3	14.5	13.8	13.0
0.08	106.6	93.6	76.2	54.3	45.1	32.9	16.6	15.3	14.0
0.09	116.8	105.3	85.7	60.9	48.5	36.0	18.6	16.3	14.0
0.10	121.6	111.7	95.4	67.8	51.3	38.0	20.7	17.3	14.0
0.12	131.6	118.3	102.3	81.3	56.1	41.3	24.7	19.4	14.3
0.14	139.5	124.7	108.6	87.2	60.7	43.9	26.8	20.4	14.3
0.16	145.9	130.8	113.5	92.6	64.3	46.2	28.1	21.4	14.5
0.18	151.2	135.9	118.6	96.9	67.6	48.2	29.6	22.2	14.8
0.20	156.3	140.3	122.9	100.0	70.9	50.0	31.1	23.0	15.0
0.25	167.8	150.2	132.3	105.8	77.3	54.3	34.9	25.0	15.3
0.30	177.7	158.9	140.3	110.7	82.9	58.4	38.3	27.0	15.8
0.35	185.9	166.5	146.4	115.5	87.5	62.5	41.1	28.6	16.3
0.40	192.3	172.9	151.5	119.3	91.3	66.0	43.6	30.1	16.6
0.50	203.5	183.9	158.6	125.5	96.4	72.2	47.4	32.4	17.3
0.60	211.4	192.5	165.5	131.8	100.5	77.3	49.5	33.4	17.9
0.70	219.6	199.9	172.4	137.4	103.8	82.1	50.2	34.2	18.1
0.80	227.5	206.0	177.2	142.0	107.4	85.7	50.5	34.4	18.1
0.90	232.8	210.9	181.3	145.9	110.2	89.0	51.0	34.7	18.6
1.00	238.4	214.7	184.1	148.9	111.7	91.8	51.3	34.9	18.6

Table 8.4 : Tabulated results

Time (mins)	Elastic	ElastoPlastic	Experimental
7.5	-3.2	-3.2	-2.4
20	-10.2	-10.2	-13.2
24	-14.2	-14.3	——
28	-10.7	-10.8	-15.9
36	+9.2	+12.2	-14.3
44	+22.8	+30.1	-4.4
55	+42.4	+60.7	+45.2

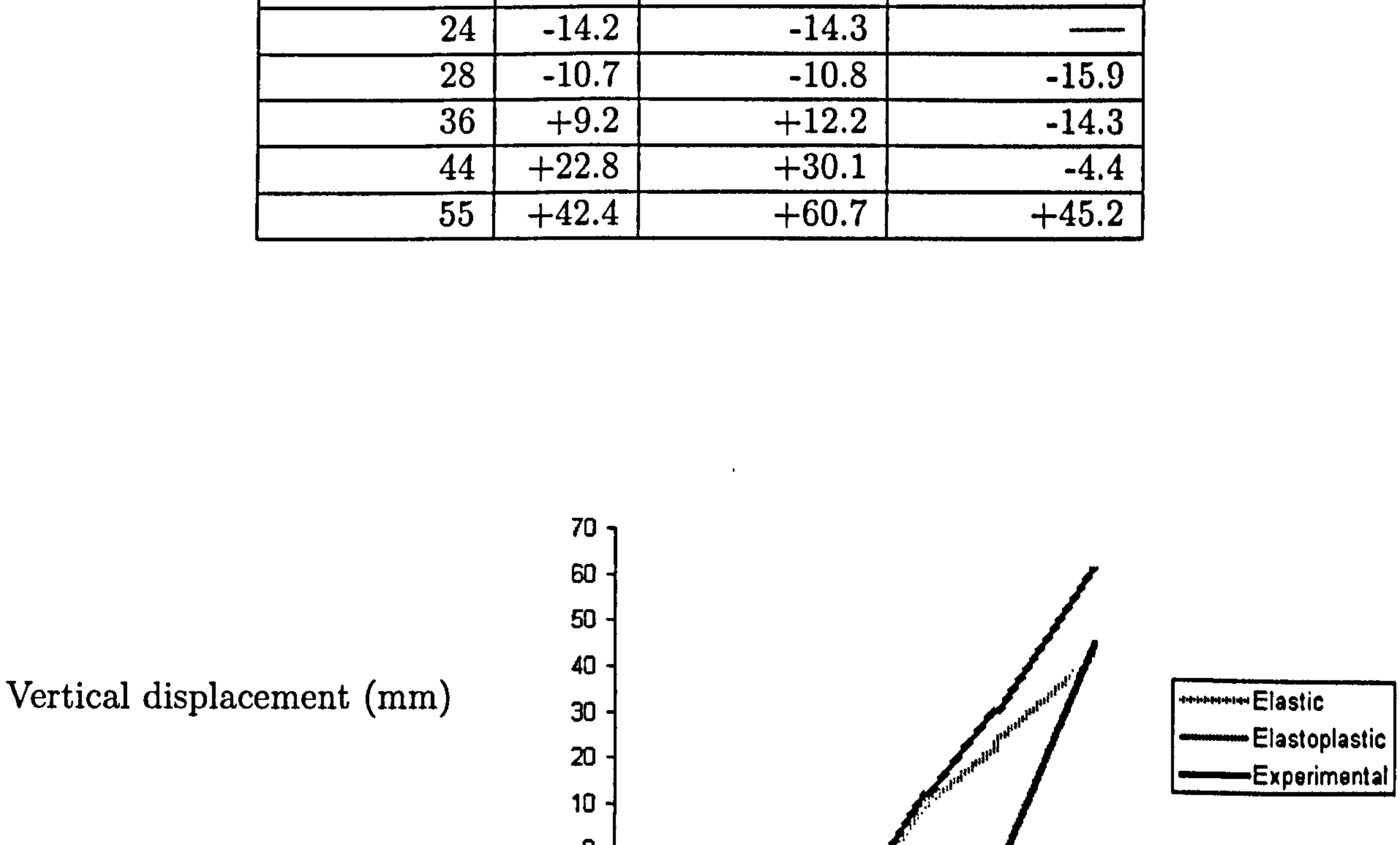

Figure 8.5 : Graphical results

8.11.2 A plastic frame

The frame illustrated in Figure 8.6 is loaded continually along the horizontal beam so that the deformation becomes plastic. Table 8.5 shows the vertical displacements in the horizontal beam calculated with the finite element method using the error estimator to adapt the mesh. These are illustrated in Figure 8.7.

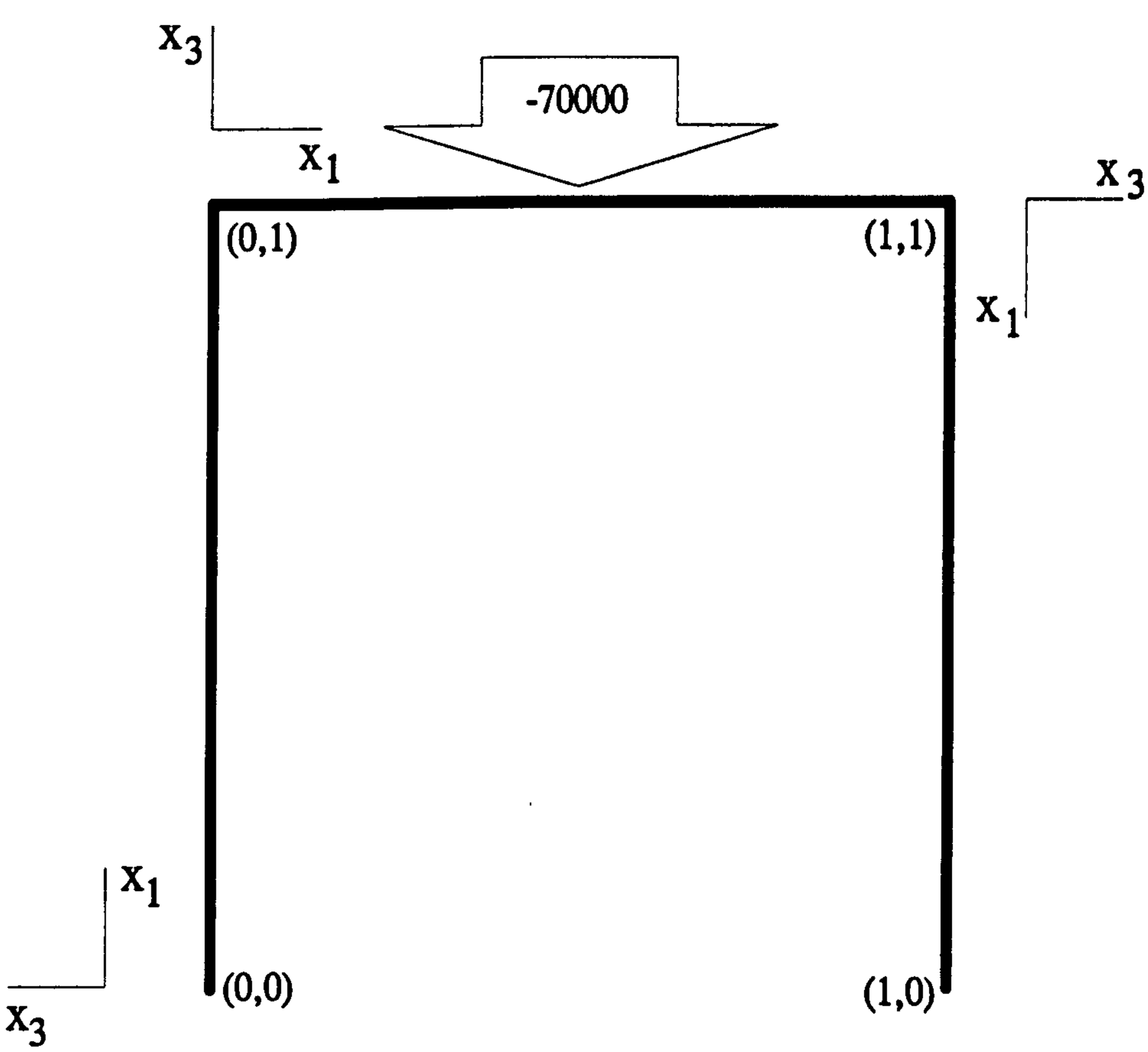

Figure 8.6 : Plastic frame

Table 8.5 : Numerical results for plastic frame.

ne	$u_3^{(2)}(0)$	$u_3^{(2)}(0.5)$	$\|\hat{e}\|^2$
3	-0.241	-5.23	7.75E-2
6	-0.244	-5.61	2.00E-1
10	-0.247	-5.78	1.04E-1
14	-0.251	-5.89	3.92E-2
18	-0.252	-5.91	3.05E-3
24	-0.252	-5.91	2.89E-4

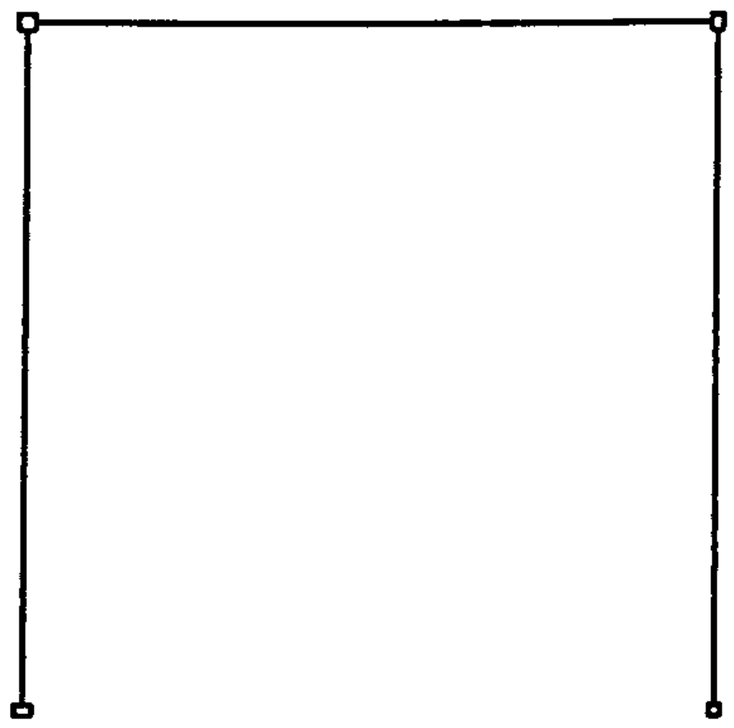

$\|e\|^2 = 7.75\text{E-}2$

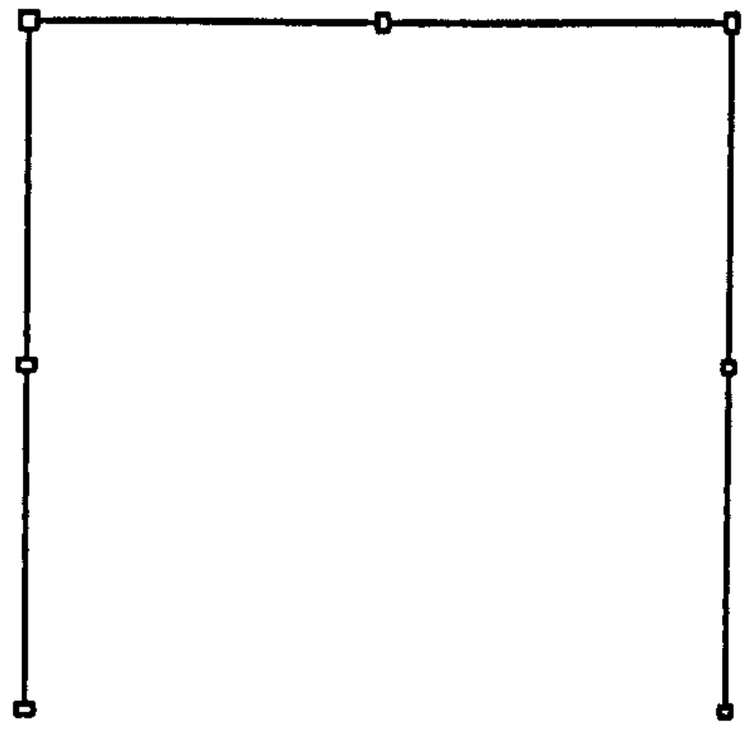

$\|e\|^2 = 2.00\text{E-}1$

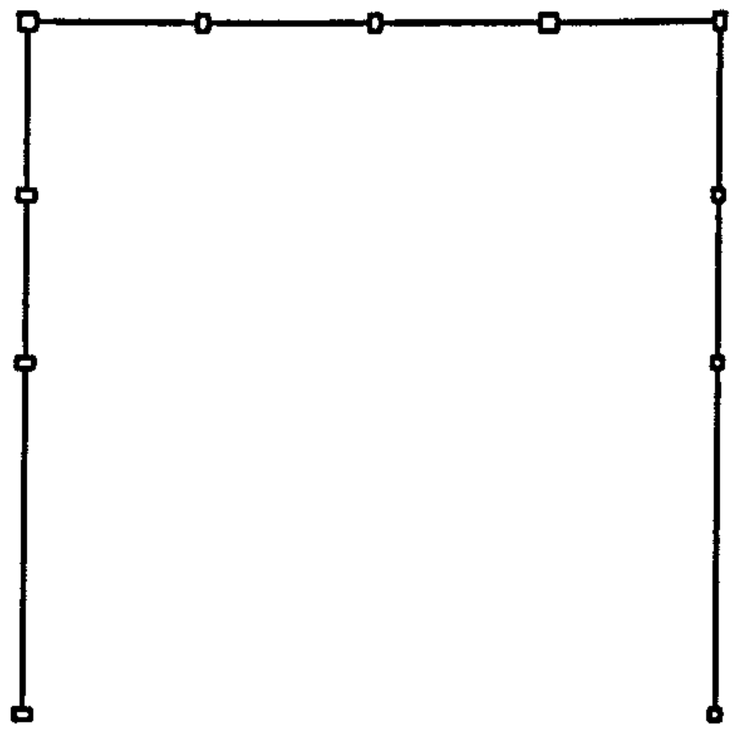

$\|e\|^2 = 1.04\text{E-}1$

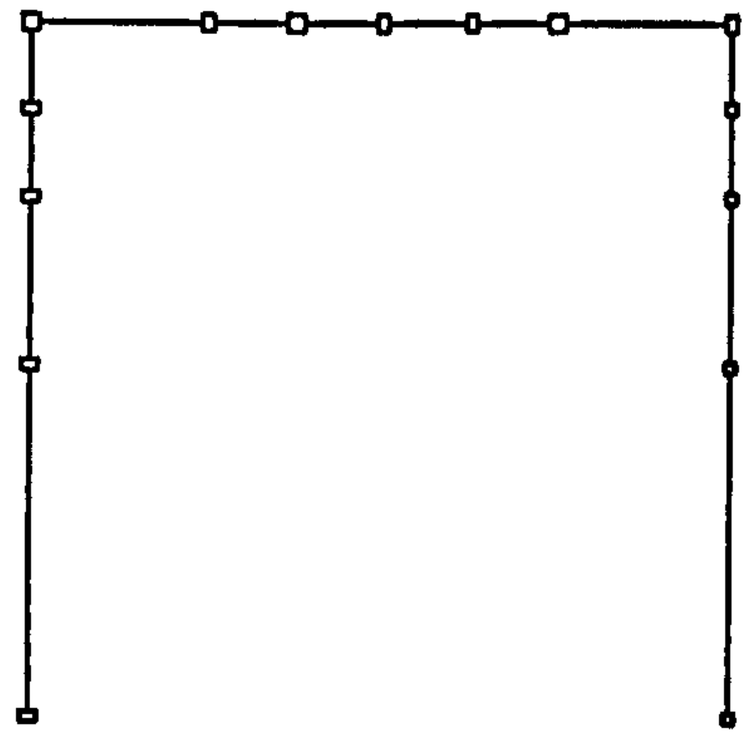

$\|e\|^2 = 3.92\text{E-}2$

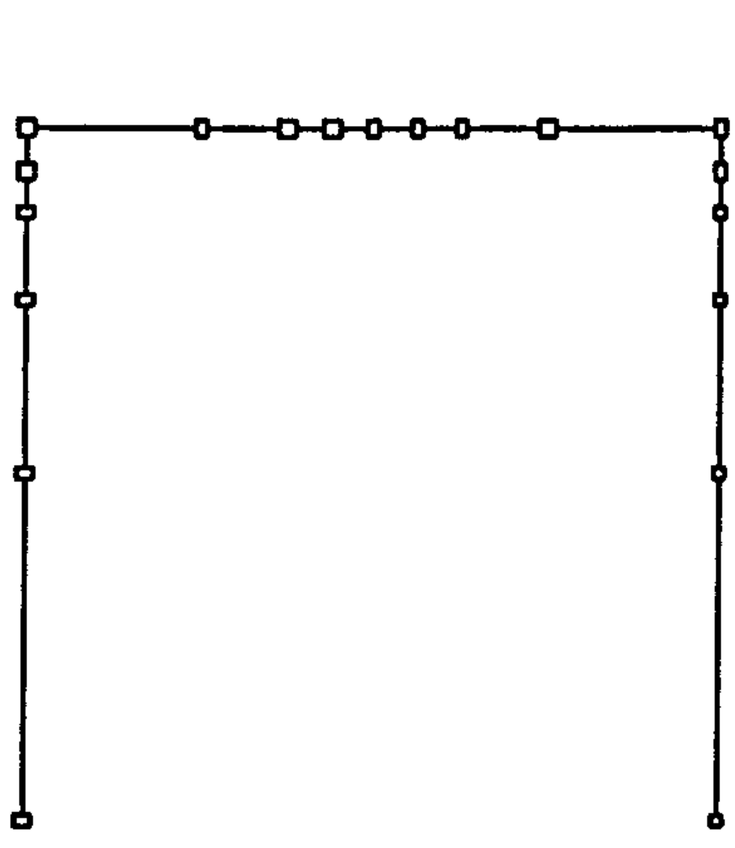

$\|e\|^2 = 3.05\text{E-}3$

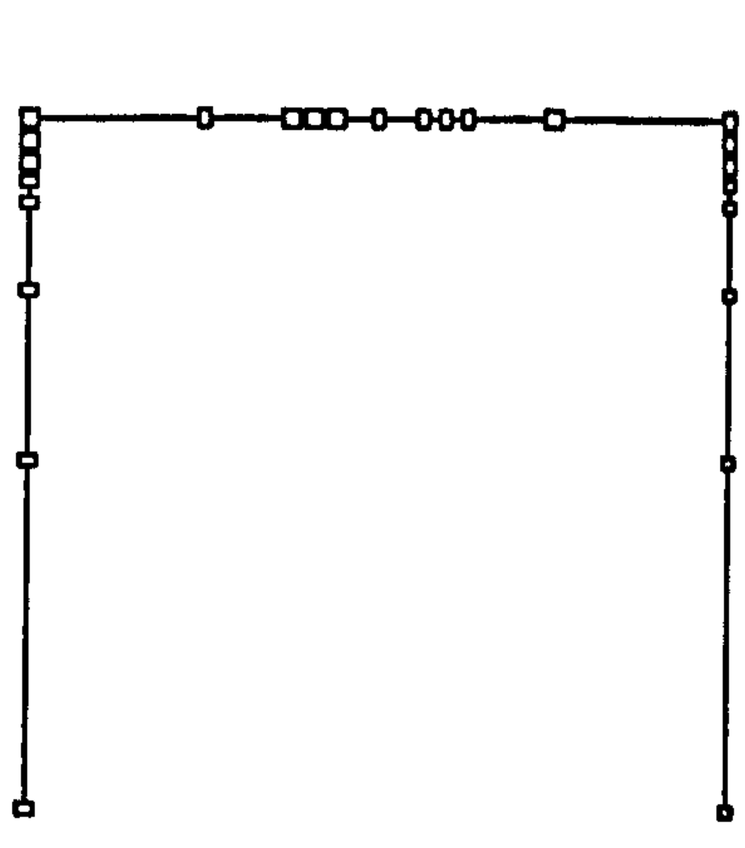

$\|e\|^2 = 2.89\text{E-}4$

Figure 8.7 : Adaptive mesh for plastic frame with error estimates

8.11.3 A thermoplastic two-storey frame

The two storey frame, illustrated in Figure 8.8a, is loaded along each horizontal beam with a force of 100 kN/m. The ground floor is exposed to a fire such that the gas temperature follows the standard BS476 curve [1] so that the ground floor columns and beams are exposed as illustrated in Figure 8.9. The deformation of the frame, illustrated in Figure 8.8b, is calculated after 3 minutes, just after first yield. Table 8.6 shows the estimate of the error for each mesh used in the calculation. The first mesh consists of one element per beam which is refined where the element contribution to $\|\hat{e}\|_{L_2}^2$ is greater than 0.01.

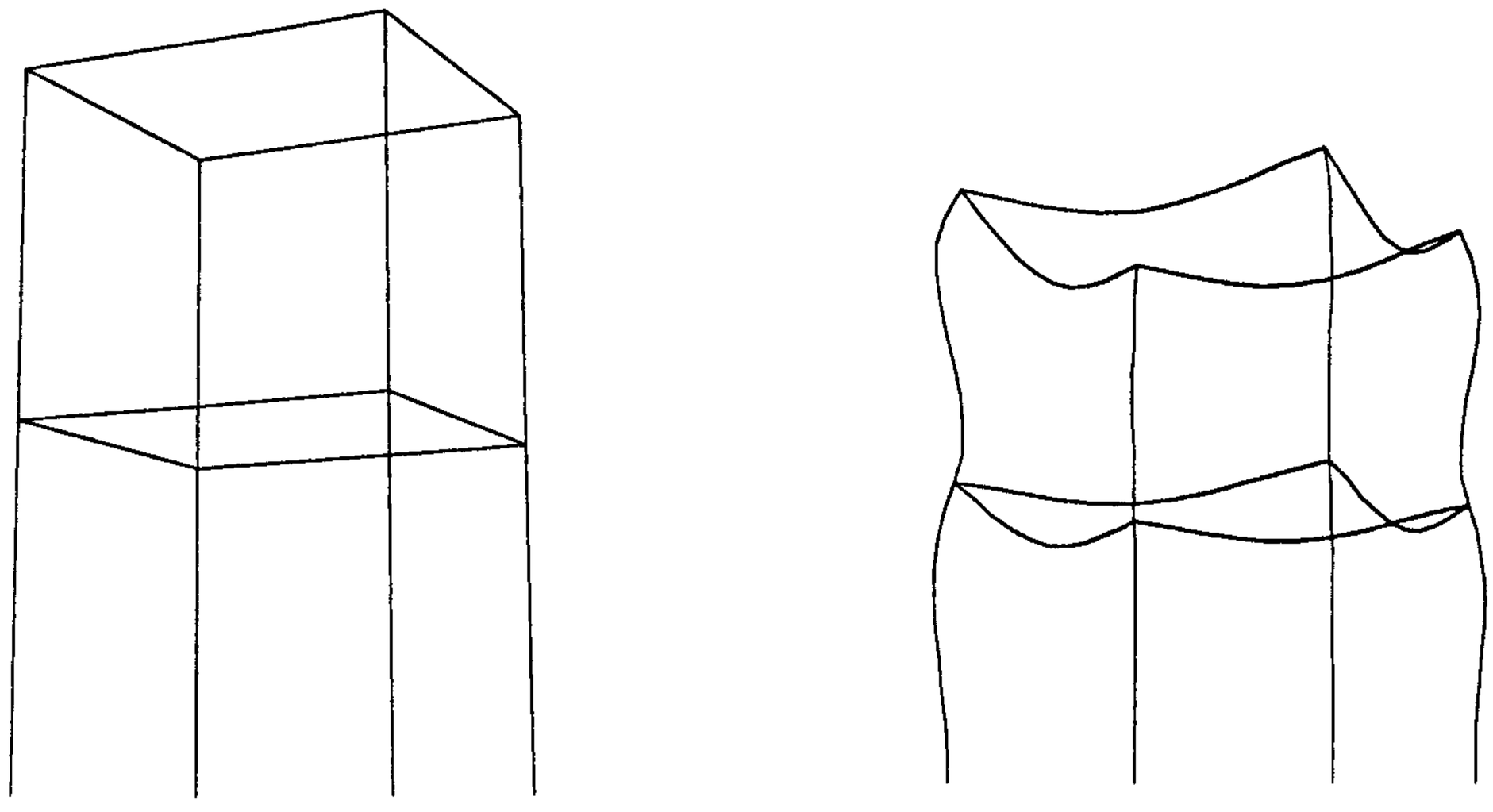

(a) (b)

Figure 8.8 : Undeformed (a) and deformed (b) frame showing connecting nodes for the 24 element mesh.

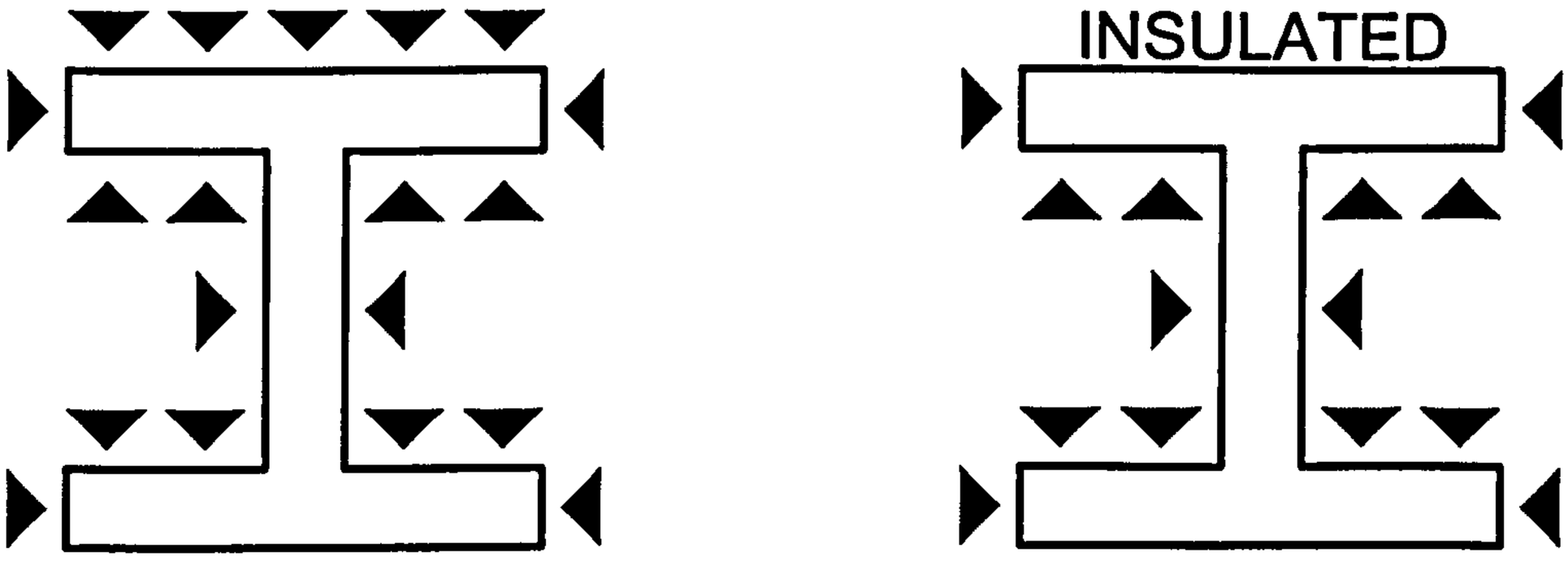

(a) (b)

Figure 8.9 : Exposed column (a) and exposed beam (b) in the ground floor.

Table 8.6 : Estimates of the error for each frame mesh.

Elements	Nodes	DOF	$\|\hat{e}\|^2_{L_2}$
16	28	168	1.38 E+2
24	44	264	8.62 E+0
40	76	456	5.39 E-1
72	140	840	3.37 E-2

Chapter 9

Conclusions

Modelling the fire-exposed frame has been separated into two decoupled problems. The first calculates the temperature throughout the frame then the second calculates the displacements due to mechanical loads and to the rise in temperature. Techniques required to solve the heat conduction equation, derived in Chapter 6, have been described. These include the fully automatic generation of a triangular mesh for any polygonal domain, in Chapter 4, and the calculation of error indicators.

A 3D model for the deformation of a single beam has been derived in Chapter 7 using the assumptions that

i) beam cross-sections remain plane and perpendicular to the neutral line during deformation (Euler-Bernoulli);
ii) warping effects are negligible;
iii) strains are small enough to neglect nonlinear terms.

In the model, the general displacements, $\bar{u}_1$, $\bar{u}_2$, $\bar{u}_3$, and the beam displacements u_1, u_2, u_3 and θ, are related by

$$\begin{pmatrix} \bar{u}_1 \\ \bar{u}_2 \\ \bar{u}_3 \end{pmatrix} = \begin{pmatrix} u_1 - x_2 u_2' - x_3 u_3' \\ u_2 - x_3\theta \\ u_3 + x_2\theta \end{pmatrix} \tag{9.1}$$

and the linear infinitesimal strains, ϵ_{11}, ϵ_{12} and ϵ_{13}, are related to the displacements by

$$\begin{aligned} \epsilon_{11} &= u_1' - x_2 u_2'' - x_3 u_3'', \\ \epsilon_{12} &= -\frac{1}{2} x_3 \theta', \\ \epsilon_{13} &= \frac{1}{2} x_2 \theta'. \end{aligned} \tag{9.2}$$

The behaviour of the beam is determined by the constitutive relation of the material which relates the components of stress, σ_{ij}, with the infinitesimal strains and the thermal strain, ϵ_{th}. The description of the beam model makes use of equivalent properties

that relate to the cross section of the beam. They are the beam displacement vector

$$\boldsymbol{u} = \begin{pmatrix} u_1 \\ u_2 \\ u_3 \\ \theta \end{pmatrix}, \tag{9.3}$$

the beam strain vector

$$\boldsymbol{B}(\boldsymbol{u}) = \begin{pmatrix} u_1' \\ u_2'' \\ u_3'' \\ \theta' \end{pmatrix}, \tag{9.4}$$

the beam thermal load vector

$$\boldsymbol{Q} = \int_{x \in A} E(\boldsymbol{x}, T)\epsilon_{th} \begin{pmatrix} 1 \\ -x_2 \\ -x_3 \\ 0 \end{pmatrix}, \tag{9.5}$$

and the beam stress vector

$$\boldsymbol{S}(\boldsymbol{u}) = \int_{x \in A} \begin{pmatrix} \sigma_{11} \\ -x_2\sigma_{11} \\ -x_3\sigma_{11} \\ x_2\sigma_{13} - x_3\sigma_{12} \end{pmatrix} d\boldsymbol{x}. \tag{9.6}$$

The linear constitutive relation for a beam,

$$\boldsymbol{S}(\boldsymbol{u}) = \boldsymbol{D}\boldsymbol{B}(\boldsymbol{u}) - \boldsymbol{Q}, \tag{9.7}$$

has been derived from Hooke's law where

$$\boldsymbol{D} = \int_{x \in A} E(\boldsymbol{x}) \begin{pmatrix} 1 & -x_2 & -x_3 & 0 \\ -x_2 & x_2^2 & x_2x_3 & 0 \\ -x_3 & x_2x_3 & x_3^3 & 0 \\ 0 & 0 & 0 & \frac{x_2^2 + x_3^2}{2(1+\nu)} \end{pmatrix} \mathrm{d}\boldsymbol{x}. \tag{9.8}$$

The equilibrium equation

$$\boldsymbol{L}(\boldsymbol{u}) = \begin{pmatrix} -S_1' \\ S_2'' \\ S_3'' \\ -S_4' \end{pmatrix} = \begin{pmatrix} f_1 \\ f_2 \\ f_3 \\ 0 \end{pmatrix} = \boldsymbol{f} \tag{9.9}$$

has been derived based on the conservation of linear and angular momentum. The beam model has been extended to a frame by assuming that the joints between beams are rigid; i.e.

i) Displacements and rotations are continuous;
ii) Resultant forces and moments at a joint are zero.

The inner product $(\boldsymbol{u}, \boldsymbol{v})$ has been defined for a frame composed of nb beams to be

$$(\boldsymbol{u}, \boldsymbol{v}) = \sum_{k=1}^{nb} \int_0^{l^{(k)}} \left(\boldsymbol{u}^{(k)}\right)^T \boldsymbol{v}^{(k)} \, \mathrm{d}x. \tag{9.10}$$

Using this definition, the weak form of the equilibrium equations has been derived,

$$a(\boldsymbol{u}, \boldsymbol{v}) = (\boldsymbol{B}(\boldsymbol{u}), \boldsymbol{DB}(\boldsymbol{v}) = (\boldsymbol{f}, \boldsymbol{v}) + (\boldsymbol{Q}, \boldsymbol{B}(\boldsymbol{v})) \qquad \forall \boldsymbol{v} \in H, \tag{9.11}$$

and it has been proven that

$$\|\boldsymbol{u}\|_{L_2} \leq C \, \|\boldsymbol{B}(\boldsymbol{u})\|_{L_2} \leq C_1 \, \|\boldsymbol{f}\|_{L_2} + C_2 \, \|\boldsymbol{Q}\|_{L_2}, \tag{9.12}$$

where C, C_1 and C_2 are constants.

A finite element method has been derived for solving the weak equation in a space of piecewise polynomial vectors, V. This has been shown to be superconvergent at the connecting nodes if quadratic functions are used to approximate the u_1 and $u_4 = \theta$ displacements and polynomials of degree 3 or higher are used to approximate the u_2 and u_3 displacements. An error indicator, $\|\hat{\boldsymbol{e}}\|$ has been derived, based on the work of Bank and Weiser [9], to estimate the error in the energy norm, $\|\boldsymbol{e}\|$. The indicator is found by solving the local problem

$$a(\hat{\boldsymbol{e}}, \boldsymbol{v})_{\Omega_i} = (\boldsymbol{r}, \boldsymbol{v})_{\Omega_i} \qquad \forall \boldsymbol{v} \in \hat{V} \tag{9.13}$$

where $\hat{V}$ contains polynomials of higher order than those in V and on the boundary of Ω_i, i.e. the connecting nodes,

$$v_1 = v_2 = v_3 = v_4 = v_3' = v_2' = 0 \qquad \forall \boldsymbol{v} \in \hat{V}. \tag{9.14}$$

It has been shown that

$$\left(1 - \beta(h)^2\right)^{\frac{1}{2}} \left(1 - \gamma(h)^2\right)^{\frac{1}{2}} \|\boldsymbol{e}\| \leq \|\hat{\boldsymbol{e}}\| \leq \|\boldsymbol{e}\| \tag{9.15}$$

where, as h tends to zero, $\beta(h)$ tends to zero and $\gamma(h)$ tends to a constant so that the indicator is consistent. Furthermore, it has been shown that

$$\left(1 - \beta(h)^2\right)^{\frac{1}{2}} \left(1 - \zeta(h)^2\right)^{\frac{1}{2}} \|\boldsymbol{e}\| \leq \|\hat{\boldsymbol{e}}\| \leq \|\boldsymbol{e}\|, \tag{9.16}$$

where

$$\zeta(h) := \frac{\|\boldsymbol{e}_1\|}{\|\boldsymbol{e}_2\|}, \qquad \boldsymbol{e}_1 \in \underline{V}, \qquad \boldsymbol{e}_2 \in \hat{V} \tag{9.17}$$

and $\overline{e} := e_1 + e_2$ is the projection of e in $\underline{V} \cup \hat{V}$. From the superconvergent properties of certain finite element solutions it has been shown that $\|e_1\|$ tends to zero with a higher order of h than $\|e_2\|$ [19]. Hence, for superconvergent finite element solutions, the error indicator is asymptotically exact in that

$$\frac{\|\hat{e}\|}{\|e\|} \to 1 \qquad \text{as} \qquad h \to 0. \tag{9.18}$$

The contents of this thesis have been intended to serve as an introduction to solving fire-exposed frame problems using finite elements. Future work can build on this by refining the beam model described in Chapter 7 (e.g., see references [25] and [11]) and the material model described in Chapter 8 to accurately predict the structural response using the new error estimator.

References

[1] BS476 : Part 8 : 1972. *Fire tests in building materials and structures. Test methods and criteria for the fire resistance of elements of building construction.* British Standards Institution, London, 1972.

[2] BS4360 : 1979. *Specification for weldable structural steels.* British Standards Institution, London, 1979.

[3] International Standard ISO-834-1975/4 Ammendment 2. *Fire resistance tests-elements of building construction.* International Organization for standardization, Geneva, 1980.

[4] M. Ainsworth, J. Z. Zhu, A. W. Craig, and O. C. Zienkiewicz. Analysis of the Zienkiewicz-Zhu a-posteriori error estimator in the finite element method. *Internation Journal of Numerical Methods in Engineering*, 28:2161–2174, 1989.

[5] Mark Ainsworth. The performance of Bank-Weiser's error estimator for quadrilateral finite elements. *Numerical Methods for Partial Differential Equations*, 10:609–623, 1994.

[6] J. E. Akin. *Finite Elements for Analysis and Design.* Academic Press, 1994.

[7] George B. Arfken, David F. Griffing, Donald C. Kelly, and Joseph Priest. *University Physics.* Academic Press, 1984.

[8] Ivo Babuska and Werner C. Rheinboldt. A posteriori error analysis of finite element solutions for one-dimensional problems. *SIAM Journal of Numerical Analysis*, 18:565–589, 1981.

[9] R. E. Bank and A. Weiser. Some a posteriori error estimators for elliptic partial differential equations. *Mathematics of Computation*, 44(170):283–301, 1985.

[10] G. V. Berg and D. A. Da Deppo. Dynamic analysis of elasto-plastic structures. *ASCE Journal of the Engineering Mechanics Division*, 86, 1960.

[11] W. F. Chen and T. Atsuta. *Theory of Beam-Columns.* Volume 2, McGraw-Hill Inc., 1977.

[12] Philippe G. Ciarlet. *Introduction to Numerical Linear Algebra and Optimisation.* Cambridge Univertisity Press, 1989.

[13] Ricardo Duran, Maria Amelia Muschietti, and Rodolfo Rodriguez. On the asymptotic exactness of error estimators for linear triangular finite elements. *Numerische Mathematik*, 59:107–127, 1991.

[14] Graeme Fairweather. *Finite Element Galerkin Methods for Differential Equations.* Marcel Dekker, 1978.

[15] T.R. Hsu. *The Finite Element Method in Thermomechanics.* Allen & Unwin, Inc., 1986.

[16] S. C. Hunter. *Mechanics of Continuous Media.* John Wiley & Sons, 1976.

[17] D. J. Johns. *Thermal Stress Analyses.* Pergamon Press, 1965.

[18] Claes Johnson. *Numerical Solution of Partial Differential Equations by the Finite Element Method.* Cambridge University Press, 1992.

[19] J. A. Kirby, M. K. Warby, and J. R. Whiteman. Superconvergence and an error estimator for the finite element analysis of beams and frames. *Numerical Methods for Partial Differential Equations*, due for publication in 2001.

[20] M. Krizek and P. Neittaanmaki. Superconvergence phenomenon in the finite element method arising from averaging gradients. *Numerische Mathematik*, 45:105–116, 1984.

[21] T. T. Lie. *Fire and Buildings.* Applied Science Publishers Limited, 1972.

[22] H. L. Malhotra. *Design of Fire-Resisting Structures.* Surrey University Press, 1982.

[23] Yu A. Melnikov. *Green's functions in Applied Mechanics.* Computational Mechanics Publications, Southampton, UK, 1995.

[24] Navin C. Nigam. Yielding in framed structures under dynamic loads. *ASCE Journal of the Engineering Mechanics Division*, 96, 1970.

[25] J. T. Oden. *Mechanics of Elastic Structures.* McGraw-Hill Inc., 1967.

[26] D. R. J. Owen and E. Hinton. *Finite Elements in Plasticity: Theory and Practise.* Pineridge Press Limited, 1980.

[27] M. J. Powell. *Approximation Theory and Methods.* Cambridge University Press, 1989.

[28] Rodolfo Rodriguez. Some remarks on Zienkiewicz-Zhu estimator. *Numerical Methods for Partial Differential Equations*, 10:625–635, 1994.

[29] H. R. Schwarz. *Finite Element Methods.* Academic Press, 1988.

[30] A. J. M. Spencer. *Continuum Mechanics.* Longman Scientific and Technical, 1994.

[31] Ivar Stakgold. *Green's functions and boundary value problems.* John Wiley & Sons, 1979.

[32] Fire Research Station. *Internal report surveying fire-related structural computer software.* Building Research Establishment.

[33] M. J. Terro. *Numerical Modelling of Thermal & Structural Response of Reinforced Concrete Structures in Fire.* PhD thesis, Department of Civil Engineering, Imperial College, 1991.

[34] S. Timoshenko. *Theory of Elasticity.* McGraw-Hill Inc., 1934.

[35] Theodore G. Toridis and K. Khozeimeh. Computer analysis of rigid frames. *Computers and Structures*, 1:193–221, 1971.

[36] B. E. Wainman, B. R. Kirby, L. N. Tomlinson, T. R. Kay, and R. R. Preston. The behaviour of unprotected steel floor beams in the standard fire resistance test - compendium of predicted temperature profiles. *British Steel Technical, Swindon Laboraties, Rotherham*, 1990.

[37] Y. C. Wang. A theoretical investigation into the residual deformation of steel beams after a fire and its design implications. In *International Conference on Fire Research and Engineering*, pages 539–544, 1995.

[38] Stephen Whitaker. *Fundamental Principles of Heat Transfer.* Robert E. Krieger Publishing Company, 1983.

[39] Ulf Wickström. *Report No. 79-3 - A Numerical Procedure for Calculating Temperature in Hollow Structures Exposed to Fire.* Department of Structural Mechanics, Lund Institute of Technology, Sweden.

[40] O. C. Zienkiewicz. *The Finite Element Method (3rd Edition).* McGraw-Hill Inc., 1977.

[41] O. C. Zienkiewicz and J. Z. Zhu. Adaptivity and mesh generation. *Internation Journal of Numerical Methods in Engineering*, 32:783–810, 1991.

[42] O. C. Zienkiewicz and J. Z. Zhu. A simple error estimator and adaptive procedure for practical engineering analysis. *Internation Journal of Numerical Methods in Engineering*, 24:337–357, 1987.

[43] O. C. Zienkiewicz and J. Z. Zhu. Superconvergent derivative recovery techniques and a posteriori error estimation in the finite element method parts i and ii. *Internation Journal of Numerical Methods in Engineering*, 33:1331–1382, 1992.

[44] M. Zlámal. On the finite element method. *Numerische Mathematik*, 12:394–409, 1968.